

UNIVERSITY OF OKLAHOMA

GRADUATE COLLEGE

DESIGN AND SYNTHESIS OF BISTABLE AND TRISTABLE [2]CATENANES AS
PROBES FOR NON-COVALENT MOLECULAR INTERACTIONS

A DISSERTATION

SUBMITTED TO THE GRADUATE FACULTY

in partial fulfillment of the requirements for the

Degree of

DOCTOR OF PHILOSOPHY

By

XINGANG PAN
Norman, Oklahoma
2007

UMI Number: 3273883

Copyright 2007 by
Pan, Xingang

All rights reserved.



UMI Microform 3273883

Copyright 2007 by ProQuest Information and Learning Company.
All rights reserved. This microform edition is protected against
unauthorized copying under Title 17, United States Code.

ProQuest Information and Learning Company
300 North Zeeb Road
P.O. Box 1346
Ann Arbor, MI 48106-1346

DESIGN AND SYNTHESIS OF BISTABLE AND TRISTABLE [2]CATENANES AS
PROBES FOR NON-COVALENT MOLECULAR INTERACTIONS

A DISSERTATION APPROVED FOR THE
DEPARTMENT OF CHEMISTRY AND BIOCHEMISTRY

BY

Ronald L. Halterman, Chair

Kenneth M. Nicholas

Daniel T. Glatzhofer

Robert P. Houser

Edgar A. O'Rear III

ACKNOWLEDGEMENTS

I would like to thank Dr. Ronald L. Halterman for his mentoring for these years. As my major advisor, he taught me not only abundant knowledge but also how to pursue knowledge myself and think independently. Without his help and guidance, I would not be able to get through all the difficulties I have been struggling for these years. I also want to thank Dr. Susan Nimmo for her help in the NMR facility. Her expertise and experience in the NMR facility is a precious treasure in the Department of Chemistry & Biochemistry. Special thanks go to Jason Moore, my best colleague and wonderful friend. He is always supportive and ready to give hands whenever I need. All the former and current members in the Dr. Halterman's group are appreciated. I also want to thank all the faculty and staff in the Department of Chemistry & Biochemistry for their support.

My wife, Katherine, is the woman who always stands with me. She is my best friend and lover. Her optimistic personality teaches me how to face the difficulties and trouble bravely. I would like to thank God to meet her and marry her. I am such a luck guy. I also would like to thank my family in China, my father and my brother. Their support made this possible.

TABLE OF CONTENTS

CHAPTER 1	Molecular Motors and Template Synthesis	1
1.1	Molecular Motors	1
1.1.1	Introduction of Molecular Machines	1
1.1.2	Natural Molecular Motors	3
1.1.3	Artificial Molecular Motors	5
1.1.3.1	Unidirectional Rotation around Single Bond	5
1.1.3.2	Unidirectional Rotation around Double Bond	9
1.1.3.3	Unidirectional Rotation around Interlocked Mechanic Bond	14
1.1.3.4	Reversible Rotation around Interlocked Mechanic Bond	18
1.2	Catenanes and Template synthesis	22
1.2.1	Transition Metal Template Synthesis of [2]catenanes	23
1.2.2	Hydrogen Bonding Template Synthesis of [2]catenanes	24
1.2.3	π - π Stacking Template Synthesis of [2]Catenanes	25
1.3	Exploration of Thermally Driven Molecular Motors	28
CHAPTER 2	Synthesis of Symmetric [2]Catenanes and Path Selection Study	33
2.1	Design of Symmetric [2]Catenanes with Path Selection	33
2.2	Synthesis and Characterization of Building Components and Symmetric [2]Catenanes	37
2.3	Purification of Symmetric [2]Catenanes	43
2.4	Characterization of [2]Catenanes	44
2.4.1	Characterization of [2]Catenane 2.4	46
2.4.2	Characterization of [2]Catenane 2.5	48
2.4.3	Characterization of [2]Catenane 2.6	50
2.5	Variable Temperature ^1H NMR Study of [2]Catenanes	48
2.5.1	Variable Temperature ^1H NMR of [2]Catenane 2.4	52
2.5.2	Variable Temperature ^1H NMR of [2]Catenane 2.5	54
2.5.3	Variable Temperature ^1H NMR of [2]Catenane 2.6	57
2.6	Summary and Conclusions	60
CHAPTER 3	Synthesis and Study of Symmetric [2]Catenanes with Wider Rigid Tethers	66
3.1	Design of [2]Catenanes with Wider Rigid Tethers	66
3.2	Synthesis and Characterization of the Wider Rigid Tethers	69
3.3	Synthesis and Characterization of [2]Catenanes with Wider Rigid Tethers	72
3.3.1	Synthesis and Purification of [2]Catenanes	72

3.3.2 Characterization of [2]Catenane 3.1	75
3.3.3 Characterization of [2]Catenane 3.2	77
3.3.4 Characterization of [2]Catenane 3.3	79
3.3.5 Characterization of [2]Catenane 3.4	82
3.3.6 Unique findings in [2]catenanes 3.1 - 3.4	77
3.4 Variable Temperature ^1H NMR Study of [2]Catenanes	85
3.4.1 Variable Temperature ^1H NMR of [2]Catenane 3.1	85
3.4.2 Variable Temperature ^1H NMR of [2]Catenane 3.2	88
3.4.3 Variable Temperature ^1H NMR of [2]Catenane 3.3	90
3.4.4 Variable Temperature ^1H NMR of [2]Catenane 3.4	92
3.5 Summary and Conclusions	94
 CHAPTER 4 Synthesis and Study of [2]Catenanes with Photoisomerizable Gates	 100
4.1 Design of Model of [2]Catenanes with Photoisomerizable Gates	100
4.2 Synthesis of Symmetric [2]Catenanes with Rigid Top Tether	106
4.2.1 Synthesis and Characterization of the Precursor for Symmetric [2]Catenanes with Rigid Top Tether	106
4.3.2 Synthesis of [2]Catenane with Rigid Top Tether	109
4.3 Synthesis and Characterization of [2]Catenanes with Photoisomerizable Gates	111
4.3.1 Synthesis of the Precursors of [2]Catenanes with Photoisomerizable Gates	111
4.3.2 Synthesis of [2]Catenanes with Photoisomerizable Gates	118
4.3.3 Characterization of [2]Catenanes with Photoisomerizable Gates	120
4.3.3.1 Characterization of [2]Catenane 4.3	120
4.3.3.2 Characterization of [2]Catenane 4.4	122
4.3.3.3 Characterization of [2]Catenane 4.5	124
4.3.3.4 Characterization of [2]Catenane 4.6	126
4.3.3.5 Characterization of [2]Catenane 4.7	128
4.3.3.6 Characterization of [2]Catenane 4.8	129
4.3.4 Variable Temperature ^1H NMR of [2]Catenane	130
4.3.4.1 Variable Temperature ^1H NMR of [2]Catenane 4.3	130
4.3.4.2 Variable Temperature ^1H NMR of [2]Catenane 4.4	131
4.3.4.3 Variable Temperature ^1H NMR of [2]Catenane 4.6	133
4.3.4.4 Variable Temperature ^1H NMR of [2]Catenane 4.8	134
4.3.5 2D-EXSY Spectra of Catenanes 4.2, 4.4, 4.6, 4.8 at 313 K	135
4.3.5.1 2D-EXSY Spectrum of Catenanes 4.6	137

4.3.5.2 2D-EXSY Spectrum of Catenanes 4.2	138
4.3.5.3 2D-EXSY Spectrum of Catenanes 4.4	139
4.3.5.4 2D-EXSY Spectrum of Catenanes 4.8	139
4.4 Summary and Conclusions	139
CHAPTER 5 Towards a Unidirectional Molecular Motor: Synthesis of Tristable [2]Catenanes	142
5.1 Design of Tristable [2]Catenane as a Unidirectional Molecular Motor	142
5.2 Retrosynthesis of the target molecules	145
5.3 Synthesis and Characterization of Intermediates and Precursors	146
5.3.1 Synthesis and Characterization of Intermediates and Monomer 5.1a	146
5.3.2 Synthesis of Tristable [2]Catenane in One Pot	151
5.3.3 Extended Route for Tristable [2]Catenane: Synthesis and Characterization of Intermediates and Precursor 5.2a	152
5.3.4 Attempts in Synthesis of [2]Catenane or [3]Catenanes from the Precursor 5.2a	158
5.3.5 Synthesis of the Monomer 5.1b	162
5.4 Summary and Conclusions	164
CHAPTER 6 Conclusions and Future Perspectives	165
EXPERIMENTAL	170
REFERENCES	293

DESIGN AND SYNTHESIS OF BISTABLE AND TRISTABLE [2]CATENANES AS PROBES FOR NON-COVALENT MOLECULAR INTERACTIONS

ABSTRACT

Making unidirectional molecular motors is a very inspiring topic for scientists since control of molecule-level movements is difficult and rewarding. Unidirectional molecular motors driven by photochemical, chemical with thermal energy were successfully achieved. However, no purely thermally driven molecular motors have been reported since they could violate the well-established theory. In our study, we hoped to utilize random thermal fluctuation to drive unidirectional motion through a thermally-driven modulation of the translational energy potential. Our studies were based on the movements of a interlocked system – [2]catenanes. These catenanes consisted of two interlocked parts: a dibenzo-34-crown-10 ether (BPP34C10) and macrocycle rings containing 4, 4'-dipyridiniums tethered by aryl spacers.

The conformational interconversions of six [2]catenanes containing a dibenzo-34-crown-10 ether (BPP34C10) interlocked with rings containing two 4,4'-dipyridiniums tethered by 1,3-bis(ethyloxy)phenyl and 1,3-xylyl or 1,4-xylyl spacers have been studied. In these symmetric catenanes, we were able to control the path

selection of one ring around another macrocycle with blocked or unblocked tethers. The free energy of activation for passing along the unblocked tethers ranged from 11 to 13 kcal/mol. The 1:1 ratio of two isomers at low temperature indicated that two binding sites are isoenergetic. We demonstrated an ability to control the movements of one ring around another ring along different pathways with different energy barriers in interlocked systems.

With wider bis(p-benzyl)methyl spacers in 4,4'-dipyridinium macrocycles interlocked with the BPP34C10, four symmetric [2]catenanes have been studied. Symmetric blocking groups on tethers enabled either pathway for circumrotation of the BPP34C10 between isoenergetic sites to be blocked. We also found that it is possible to lower the energy barriers for circumrotation of the BPP34C10 along wider tethers. The energy barriers required for passage over the unblocked, wider rigid tethers were about 11.5 kcal/mol. According to the chemical shifts of the BPP34C10, its internal hydroquinone ring could π - π -stack with only one 4,4'-dipyridinium binding site at a time. This study demonstrated an ability to select the pathway in these [2]catenanes containing the rigid bis(p-benzyl)methyl tether and to lower the energy barrier for interconversion through destabilization of the ground state structures.

[2]Catenanes containing the BPP34C10 interlocked with rings of two 4,4'-dipyridiniums tethered by two phenyl rings conjugated with an enone have been

studied. The unsymmetric gates, 4-methylphenyl, 4-n-butylphenyl, 4-isopropylphenyl, 4-biphenyl, were appended in the enone system to modulate energy barriers to drive a preferential circumrotation of the BPP34C10. However, according to their ^1H NMR and 2D-EXSY spectra, the 1:1 ratio of two isomers indicated no biasing gate effect as designed. This ratio indicated equal energy of two ground states of 4,4'-dipyridinium binding sites in these catenanes. We demonstrate that the ground states of two binding sites are not affected by unsymmetric gates in the catenanes with rigid tethers.

Tristable catenanes with three identical binding sites were designed for a unidirectional molecular motor. Interlocked with the BPP34C10, a ring with three 4,4'-dipyridinium sites was designed to be tethered by three identical 3-(2-ethyl)-1-methylphenyl tethers. 4-Methylbenzyl or 4-isopropylbenzyl groups were installed on the phenyl groups to provide conformationally mobile gates. Most of synthesis of this system has been accomplished except the last step.

Through these studies, we demonstrated an ability to control the path selection along different pathways with blocked and unblocked tethers in the interlocked system-[2]catenanes. With wider tethers, we were able to lower the energy barriers by destabilization of the ground state structures. In the catenanes with rigid ethers, we demonstrated an ability to control equal or close energy barriers of two ground states even with unsymmetric gates. No bias for unidirectional motion was observed.

Chapter 1

Molecular Motors and Template Synthesis

1.1 Molecular Motors

1.1.1 Introduction of Molecular Machines

Machines are extremely important in our daily lives. A machine is a device which is composed of components and achieves a specific function.¹ From ancient times, people have been making machines to live a more convenient, more efficient and more enjoyable life. To some extent, the civilization of human kind is dependent on the design and construction of machines. For instance, trains and aircraft make it possible for people to travel a long-distance way in shorter time. Clocks and watches help us master our time and follow our agenda. Machines, natural or artificial, exist in a range of length scales like trains as long as a kilometer, microelectromechanic systems (SEMS) as small as millimeters, protein motor on the micrometer scale.²

Miniaturization is a challenging and very important topic. There are two approaches to perform miniaturization: top-down and bottom-up. The top-down approach, which has been the main philosophy in miniaturization, is reaching its practical and fundamental limits (about 50 nm). On the other hand, the bottom-up approach seems particularly promising for the future development nowadays. “There is plenty of room at the bottom”, said Dr. Richard Feynman, a Noble Prize Laureate in physics, in his famous

talk to American Physical Society in 1959.³ He pointed out the possibility of making the smallest machines in the world, which are based on an atom by atom approach. However, practically, it is hard to imagine that we can manipulate atoms easily. They are not spheres and they prefer to binding strongly with each other except some rare cases. To make atom-based machines, either high energy is required or operation of those machines is extremely difficult let alone the cost they might need. In other words, “atom by atom” bottom-up approach would not be able to convince people, especially chemists. From the 1980s, with the development of supramolecular chemistry, it was realized that appropriate molecules are much more convenient building blocks than atoms in manufacturing nanoscale machines and devices.¹

Compared to atoms, molecules have a lot of advantages:¹

- 1) Molecules are stable species, but atoms always bind strongly with each other and don't exist freely in most cases;
- 2) Most substances in the earth exist as molecules;
- 3) Molecules can be altered in chemical reactions. Atoms don't change in chemical reactions. Chemical reactions have been well studied and understood;
- 4) Molecules can have distinct spheres and device-related properties.

Machines at molecular levels are extremely interesting to scientists in recent years since there are numerous potential applications in materials, medicine, energy,

environments etc. Molecular machines are different from their macroscopic counterparts.⁴ In the macroscopic world, machines don't work unless some directed external energy is introduced. Usually, conventional machines are rigid and are barely affected by the environment, like room temperature. As scales of machines decrease, the mass of machines becomes less and viscous force begins to dominate. Molecules are in incessant, random Brownian motion unless frozen at 0 K.⁵ The control of motion of molecules at will is an inspiring topic for scientists and is necessary if molecular scale machines are to be useful.

1.1.2 Natural Molecular Motors

In biological systems, there are quite a few natural molecular motors which make motions of live system possible, like ATP synthase, myosin and kinesin.⁶ The ATP synthase system⁶ has been well studied in great details and might be one of the most important and well-known biological molecular motors. ATP synthase is an enzyme which is a rotary motor powered by proton gradient to synthesize or hydrolyze ATP molecules, storing or releasing energy needed for living bodies. As described in **Figure 1.1**, it consists of two rotary molecular motors, F_1 and F_0 , which were connected by a common shaft. Each motor tends to rotate in opposite direction. The F_1 motor rotates in one direction by the hydrolysis of ATP while the F_0 motor is driven in the opposite

direction by the energy stored in a transmembrane electrochemical gradient. Whether the synthase rotates clockwise or counterclockwise depends on cellular environments. When F_0 dominates, it drives the F_1 motor in reverse by torque via the shaft whereupon it synthesizes the ATP from ADP and a phosphate. When F_1 dominates, it hydrolyzes the ATP to ADP, releasing energy and driving the F_0 motor in reverse, which pumps the ions through the membrane.

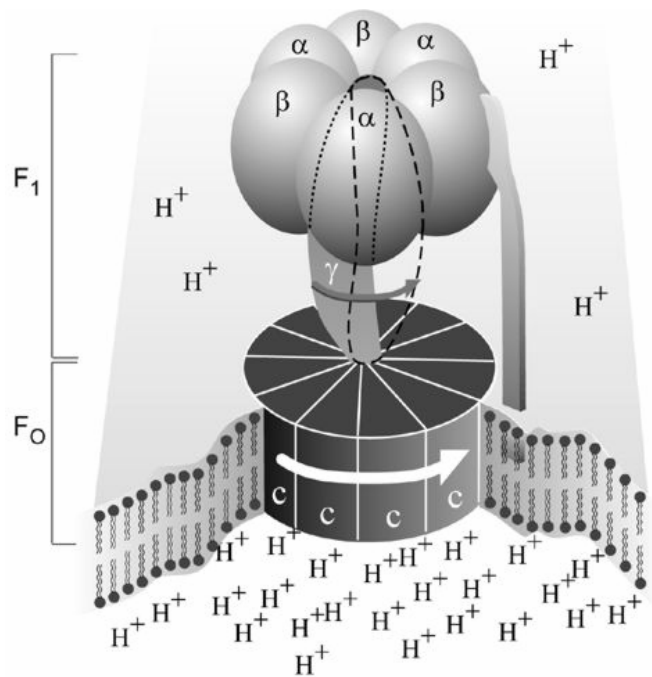


Figure 1.1 Natural molecular motor⁷

More importantly, the rotary motions of the F_1 and F_0 motors are reversible. This biological system doesn't fight Brownian motion but utilizes this random fluctuation.⁴ Although ATP synthase has been the most notable example, other molecular motors have been well studied. Myosin and kinesin are linear motors which help convert the energy of

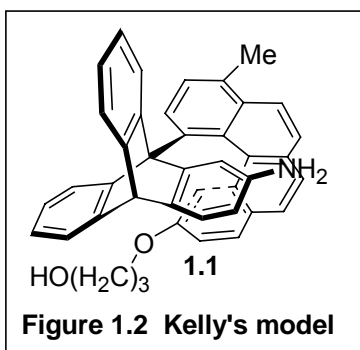
ATP hydrolysis into physical work, like polymer substrate in our muscles.⁸

1.1.3 Artificial Molecular Motors

Any attempt to construct artificial molecular motors as complex as these biological system would be a seemingly impossible mission at present. The design of man-made molecular motors must and can be simplified to perform similar motions. A few groups have made great progress in this field.

1.1.3.1 Unidirectional Rotation around Single Bond

T. Ross Kelly et al^{9,10} developed a unidirectional molecular motor (**Figure 1.2**) which consisted of two components: a triptycene and a [4]helicene. The two components



were connected by a single bond functioning as an axle.

[4]Helicene functioned as a friction brake that prevented the free rotation of triptycene. The energy barrier to rotation of triptycene around the triptycene/helicene single bond is about 25 kcal/mol, which is much higher than the

energy barrier to rotation of a typical single bond. The helicene can be seen as a stiff pawl for a ratchet. If we can imagine, without any functional group (amino group or hydroxypropyl tether) on the triptycene component or helicene, the triptycene would

rotate clockwise or counterclockwise randomly. The designed molecule **1.1** allowed a unidirectional rotary motion with a chemical activation since the amino group and hydroxylpropyl group are proximal to each other.

The energy transformation of the Kelly's design is detailed in **Figure 1.3**. In **a)**, the energy diagram represents a 240° rotation of single bond between triptycene and helicene. In **b)**, a molecule could stay in a low-energy conformation (120°) in which the molecule can be activated to jump freely in either direction to either excited states by thermal energy. Diagram **c)** represents a molecule activated to an excited rotamer which could freely go back to the original ground state. Once this excited

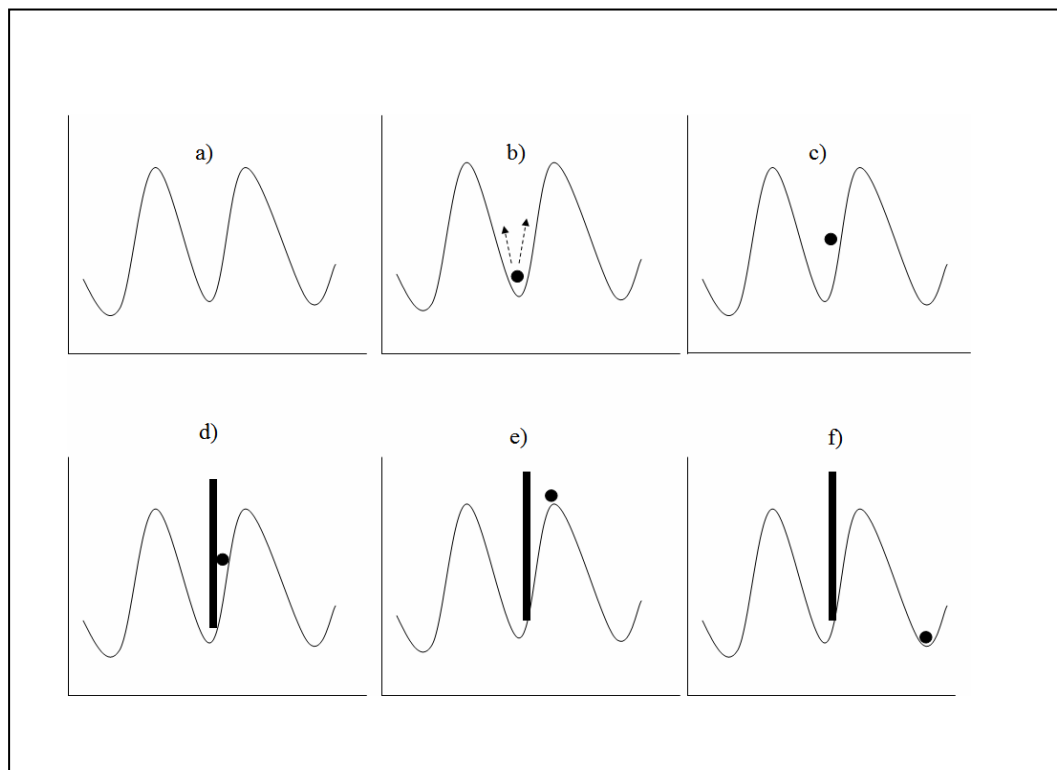


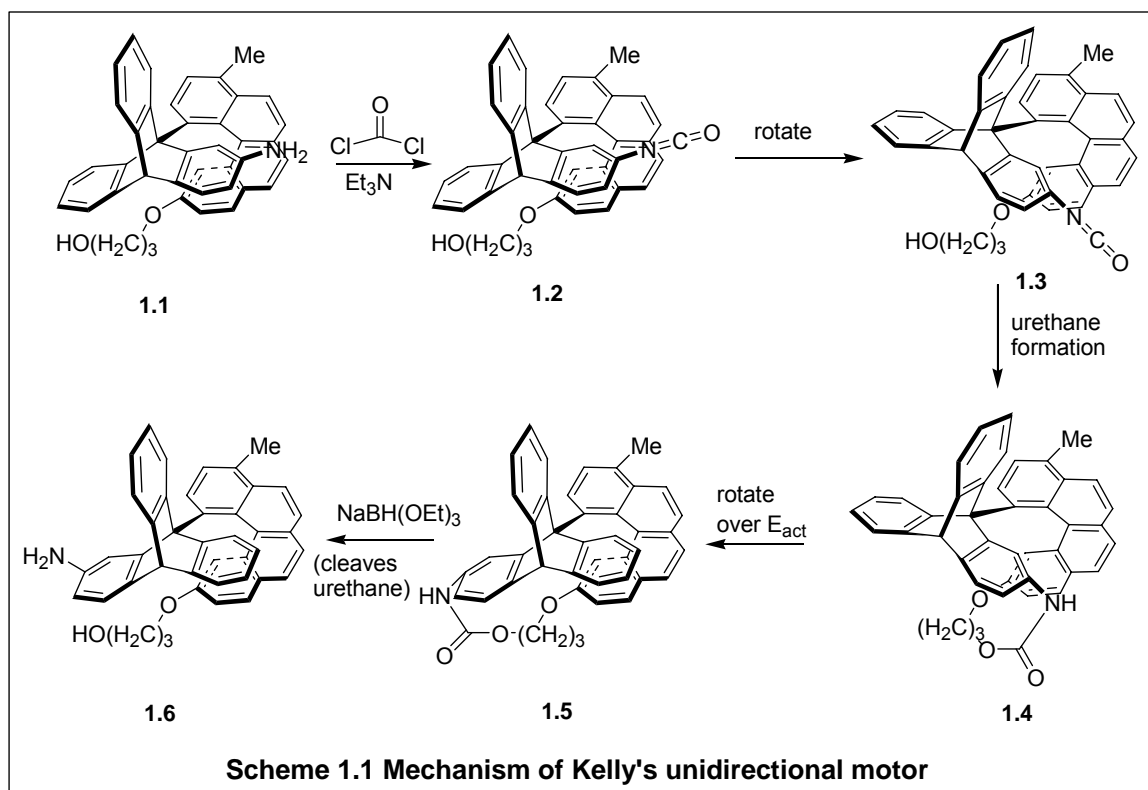
Figure 1.3 Energy transformation of Kelly's model

rotamer was trapped like in **d**), it could not rotate back to the original low-energy conformation. The random thermal energy drove the molecule to the top of the energy barrier in **e**). Eventually, in **f**), the excited rotamer could easily rotate to the next low-energy conformation.

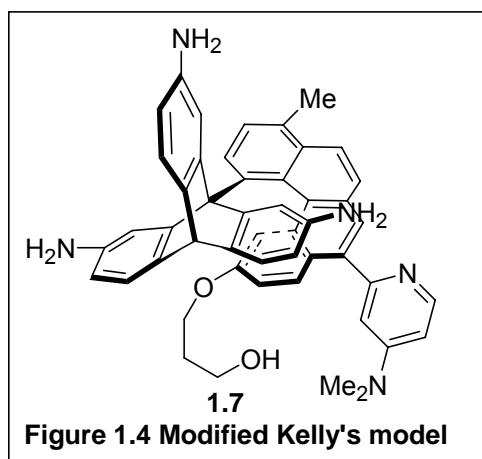
In terms of a molecular representation described in **Scheme 1.1**, the compound **1.1** was reacted with phosgene to form isocyanate derivative **1.2**. Triptycene rotated clockwise to form the conformation **1.3** whereupon the isocyanate group approached the hydroxyl group. It wouldn't rotate counterclockwise otherwise the isocyanate group goes further apart to interact with the hydroxyl group in the hydroxypropyl tether. The isocyanate group reacted with a hydroxyl group to form a relatively high-energy urethane conformation **1.4**. At room temperature, thermal energy could drive the unidirectional rotation from **1.4** to **1.5**, a relative low-energy and stable conformation. Compound **1.5** was cleaved by reduction to give **1.6**.

In this sequence involving 6 steps, a unidirectional 120° rotation around a single bond was achieved. Phosgene acted as chemical energy, like ATP in biological system, to “activate and bias a thermally induced isomerization reaction”. Unfortunately, this process fulfilled only one-third of a full 360° rotation and the rotation was not continuous and relatively slow.

A modified system (**Figure 1.4**) was synthesized recently by Kelly and



co-workers.¹¹ In this proposed repeatedly rotary motor, three amino groups were installed on the three blades of triptycene respectively. A 4-(dimethylamino)pyridine (DMAP) unit



was attached to the helicene. The DMAP unit made the proximal amino group so 'hot' that it could react with phosgene more easily than the other two amino groups.

The original operational process of this model could be similar to that in **Scheme 1.1**.

When phosgene was added to this system, it reacted with the DMAP unit first and could be selectively delivered to the proximal

tritylcylamino group. The intermediate could be further converted to an isocyanate derivative followed by rotation and formation of urethane. Eventually, the urethane could be cleaved to form the initial conformation.

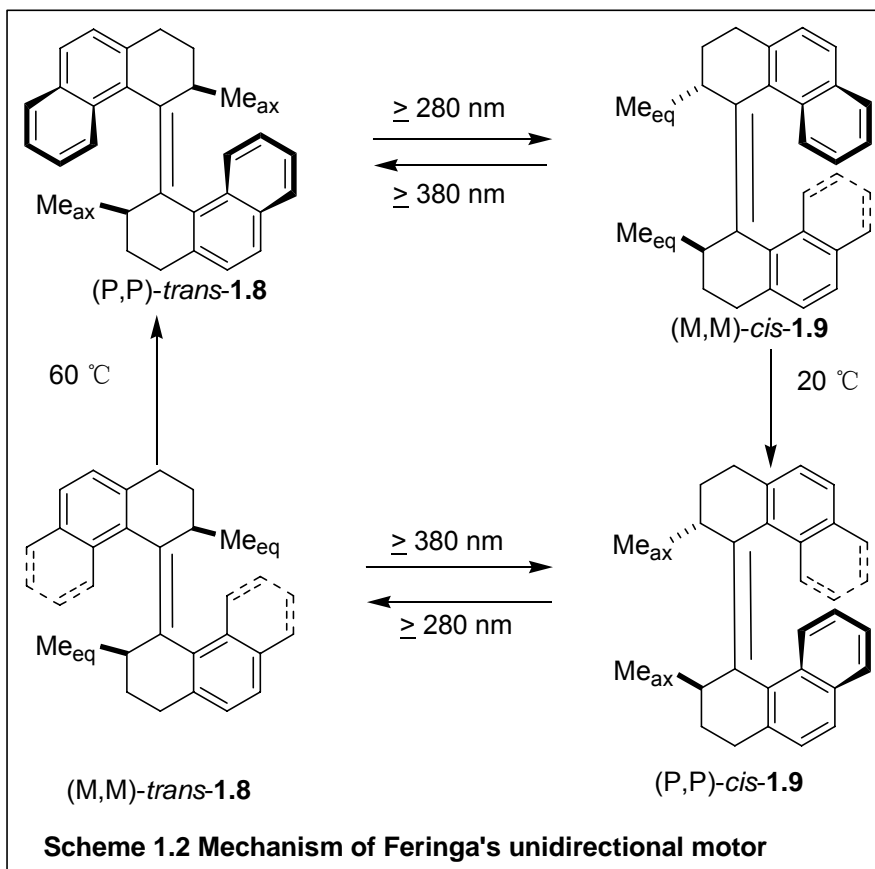
However, proposed models are not always realized. In reality, when phosgene was added, it was observed that the DMAP unit selectively delivered the phosgene or its substitute to the proximal amino group. Unfortunately, the isocyanate wasn't formed as expected. Even if the isocyanate intermediate was formed by manipulating the selective protection of three amino groups, the unidirectional rotation for this system was a failure. A reason could be the interaction between the isocyanate group and the DMAP unit preventing the rotation of triptycene.

1.1.3.2 Unidirectional Rotation around Double Bond

Feringa and co-workers¹² synthesized a light-driven unidirectional motor based on a central carbon-carbon double bond in a chiral, helical alkene. A full 360° unidirectional rotation was fulfilled in four discrete isomerizations activated by ultraviolet light and thermal energy. Two light-induced *cis-trans* isomerizations resulted in two 180° rotations around the carbon-carbon double bond and are respectively followed by thermally-driven helical inversions. The four steps came up with a full 360° unidirectional rotation.

Upon irradiation by UV light ($\lambda > 280$ nm) at - 55 °C, (P, P)-*trans*-**1.8** (**Scheme**

1.2) was converted to the conformation (M, M)-*cis*-**1.9** which is unstable because of two



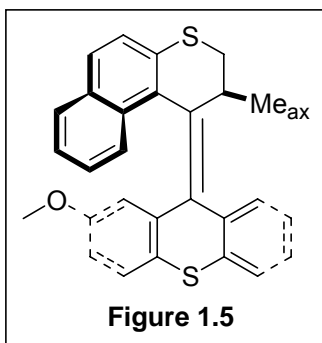
equatorial methyl substituents (P stands for the right-handed helicity, M stands for the left-handed helicity). At room temperature, (M, M)-*cis*-**1.9** rotated over low activation barrier to give (P, P)-*cis*-**1.9** by available thermal energy to form the more stable conformation (8.6 kcal/mol more stable). Irradiation of (P, P)-*cis*-**1.9** resulted in unstable (M, M)-*trans*-**1.8** in which two methyl groups are also equatorial. Raising the temperature to 60 °C allowed the formation of initial conformation (P, P)-*trans*-**1.8**. Through four steps induced by UV lights and thermal energy, a unidirectional 360° rotation had been accomplished. During those four steps, the UV irradiations were

reversible but the thermal activations were irreversible because the axial methyl groups made the (P, P)-*trans*-**1.8** and (P, P)-*cis*-**1.9** more stable than their counterparts, (M, M)-*trans*-**1.8** and (M, M)-*cis*-**1.9**, respectively.

If the system was irradiated at $\lambda > 280$ nm at 60 °C, a consecutive four-step isomerization would be observed since both two photoisomerization steps and thermal isomerization steps will happen under these conditions. Eventually, a continuous unidirectional rotation could be achieved.

This motor had two stereogenic centers and the chirality is necessary. The energy barrier for the thermal isomerization was still high and the rate of rotation was relatively slow.

A second generation light-induced molecular motor developed by Feringa *et al*¹³ was installed with only one stereogenic center (**Figure 1.5**). Meanwhile, the heteroatoms



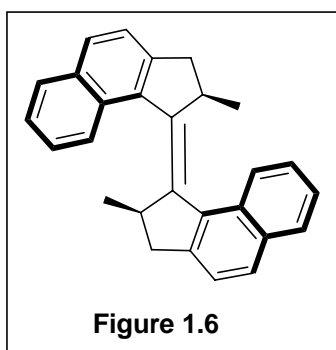
were introduced to further functionalize the systems in order that these systems could be connected to surfaces whereas the top half worked as a propeller and the bottom half was attached to a gold surface. Or the whole system became part of multicomponent molecular machinery by connecting with

other molecules via heteroatoms.

An extremely important feature for this second generation Feringa motor was that

the energy barrier for thermal isomerization was lowered and the rate of rotation had been enhanced by a factor of 3×10^3 . The time for thermal isomerization had been decreased from hours to minutes.

The rate determining step for the Feringa motors is the thermally driven helical inversion. Although there had been improvements in terms of the rotation speed in the second generation light-driven molecular motors, the fastest rotation still needed 2400 s. The energy barrier for thermal inversions was still relatively high and needed further decrease. Feringa and co-workers¹⁴ decided to replace six member rings with five member rings (**Figure 1.6**) between carbon-carbon double bond in the system. Compared

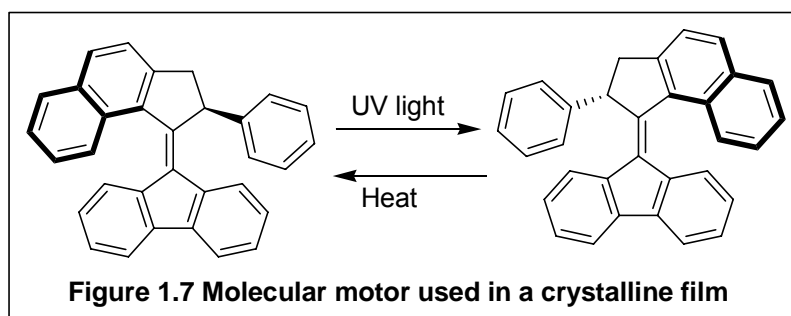


to the six member ring, the smaller five member ring also had 3 sp^2 hybridized carbon atoms making the ring planar. The key consideration was if conformation difference of the methyl substituents (axial and equatorial) still could be large enough to drive a unidirectional motion. As a matter of fact,

the newly designed molecular motors described in **Figure 1.6** were efficiently synthesized in a very high yield up to 76 %. The ^1H NMR and CD spectra data indicated that the newly designed motor rotated in a unidirectional fashion. More inspiringly, this motor had a lower energy barrier for the thermal inversions and was considerably faster than the previous light-driven molecular motors. The half-life of the fastest thermal

isomerization was only 18 s at room temperature.

The optimized molecular motors were designed to perform work to drive the motions of much larger objects. Feringa and co-worker prepared a liquid crystalline film embedded with the molecular motors they designed in **Figure 1.7**.¹⁵ A tiny glass rod was placed on the top of the film and the size of the rod was more than 10,000 times of the molecular motor itself.



As observed in **Figure 1.8**, when the liquid crystalline film was irradiated by the UV light (wavelength 365 nm), the glass rod rotated clockwise under an optical

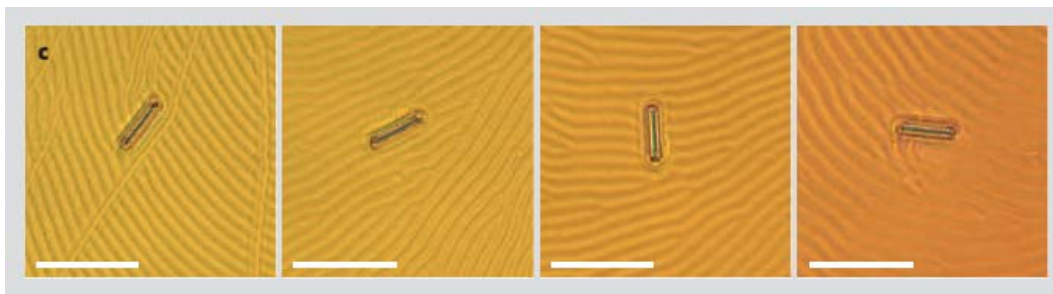


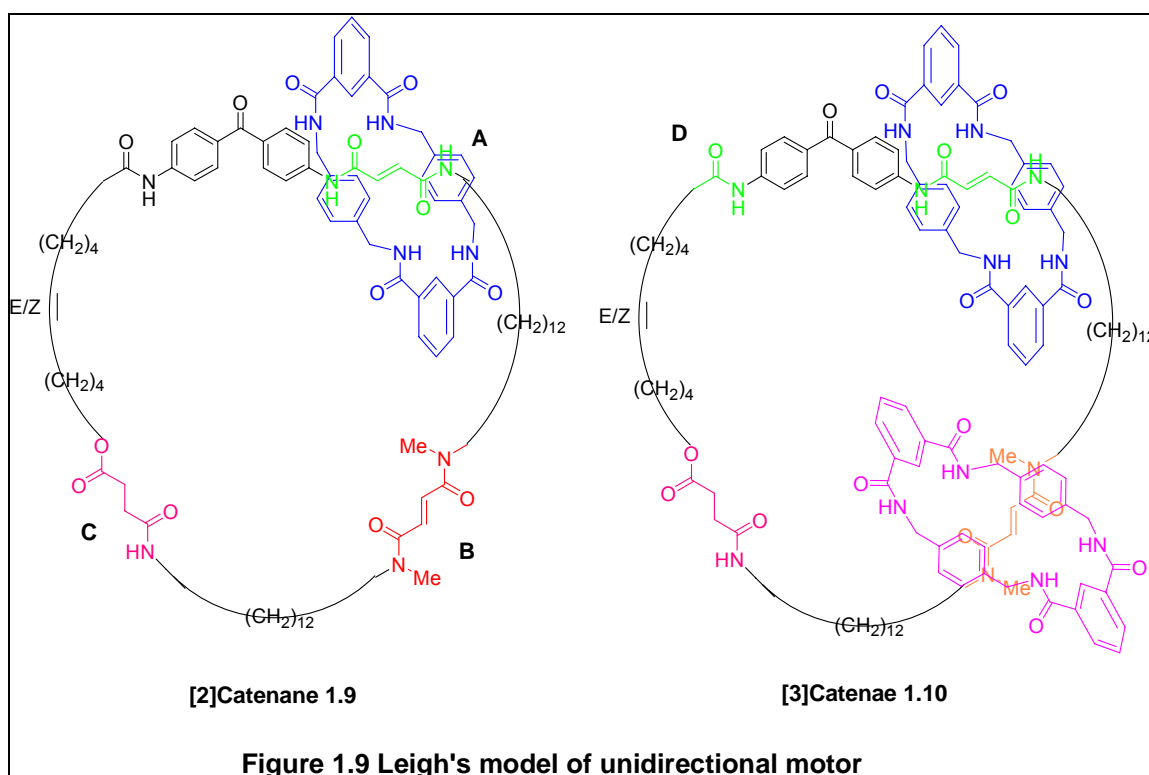
Figure 1.8 Movement of glass rod in film with molecular motor

microscope. This observation was attributed to the change in shape of the molecular motor during the rotation which induced the reorganization of the liquid crystalline film and its surface relief. As a result, the unidirectional rotation of glass rod on the film was

observed.

1.1.3.3 Unidirectional Rotation around Interlocked Mechanic Bond

A unidirectional molecular motor based on [3]catenanes were designed and synthesized by Leigh and co-workers (**Figure 1.9**).¹⁶ Initially, both [2]catenane and

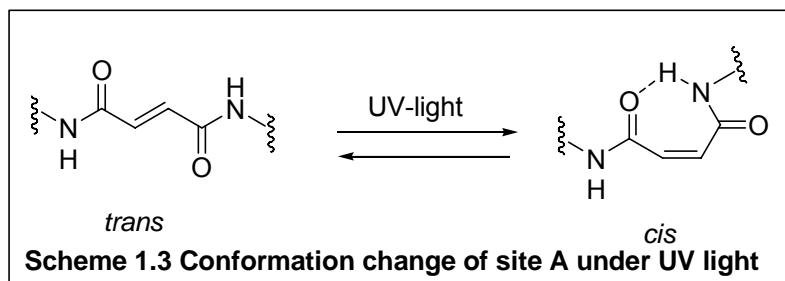


[3]catenane were obtained in which the larger macrocycle interacted with the smaller ring by hydrogen bonding.

In the [2]catenane **1.9**, there were three binding sites (**A**, **B** and **C**) to interact with the smaller benzyl amide ring by hydrogen bonding. At the ground state, the binding affinities of three sites to the smaller ring were ranked as $K_a(\mathbf{A}) > K_a(\mathbf{B}) > K_a(\mathbf{C})$. The

binding interaction between site **D** and benzyl amide ring only affects in [3]catenane.

The key feature in this system was that the binding affinities would decrease when the conformation of the carbon-carbon double bond in amide fumaramide group (for example, site **A**) changed from *trans* to *cis* (**Scheme 1.3**).



The decrease in the binding affinity would result in the transfer of the smaller ring from site **A** to site **B**. The same decrease of binding affinity would happen to site **B** if it was irradiated. Then the smaller ring could move to site **C**.

However, in [2]catenane **1.9**, even if site **A** was irradiated and converted to *cis* conformation, the circumrotation of benzyl amide could take place along the left or the right tethers. Consequently, [2]catenane **1.9** could not be confirmed as a unidirectional molecular motor because the smaller ring could circumrotate clockwise or counterclockwise randomly.

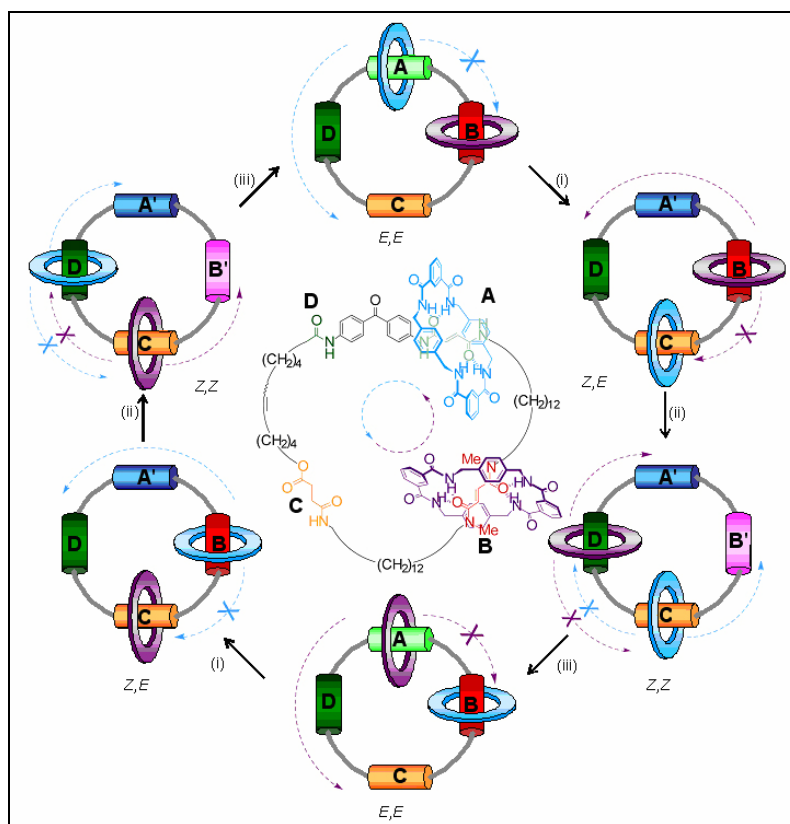
Better support for unidirectional motion was obtained as [3]catenane **1.10** (**Figure 1.9**). In [3]catenane **1.10**, two benzyl amide rings were interlocked mechanically with two binding sites in the larger macrocycle by hydrogen bonding. Initially, four binding sites (**A**, **B**, **C** and **D**) had different binding affinities, ranking as $K_a(\mathbf{A}) > K_a(\mathbf{B}) > K_a(\mathbf{C}) >$

$K_a(D)$. When some of the sites were photochemically, thermally, or chemically activated, the binding affinities would change and the ranking would be reorganized. The smaller rings would move away from the next highest affinity site to the relatively high-affinity site in the new stage.

A full 360° relatively unidirectional rotation was described in cartoon in **Scheme 1.4** (Blue and purple rings stood for benzyl amide macrocycles, **A** was secondary amide fumaramide group, **B** was tertiary amide fumaramide group, **C** is a succinic amide ester, **D** is an isolate amide as shown in **Figure 1.9**). The whole unidirectional rotation could be divided in the following processes:

- 1) Process (i): The *trans* double bond of site **A** was converted to a *cis* conformation under 350 nm UV light irradiation (**Scheme 1.3**). The hydrogen bonding between the blue ring and site **A** decreased. The binding affinities became $K_a(\mathbf{B}) > K_a(\mathbf{C}) > K_a(\mathbf{D}) > K_a(\mathbf{A})$. The blue ring rotated counterclockwise to site **C** because the clockwise direction was blocked by the purple ring.
- 2) Process (ii): the site **B** was irradiated by 254 nm UV light and the purple ring moved counterclockwise from **B** to **D** since the clockwise was blocked by the blue ring.
- 3) Process (iii): when both carbon-carbon double bonds in the site **A** and **B** were restored to *trans* conformations at 100°C , the purple and blue rings moved back to **A** and **B**, one clockwise and the other counterclockwise.

- 4) Repeated Process (i), the purple ring rotated counterclockwise from **A** to **C**.
- 5) Repeated Process (ii), the blue ring moved counterclockwise from **B** to **D**.
- 6) Repeated Process (iii), the blue ring and purple rings move back to the original status, one clockwise and the other counterclockwise.



Scheme 1.4 Cartoon mechanism of Leigh's unidirectional motor¹⁶

In a full 360° rotation, each smaller ring, no matter the blue or the purple, had undertaken three counterclockwise and one clockwise movements, which would equal to a net relative unidirectional counterclockwise motion. Unlike the Kelly's or Feringa's Models, this molecular rotary motor was not chiral, which demonstrated that chirality

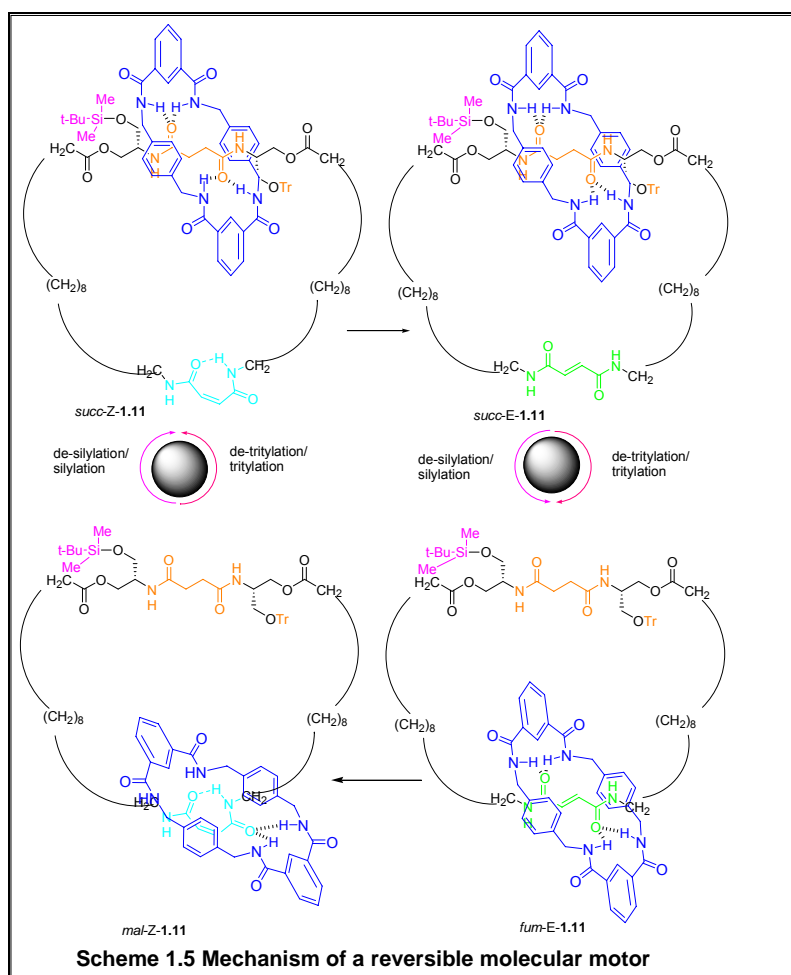
was not a prerequisite for a unidirectional motion.

1.1.3.4 Reversible Rotation around Interlocked Mechanic Bond

Unlike conventional motors, the behavior of molecular motors can be strongly affected by Brownian motion. However, in natural system, biological motors do not fight this effect but utilize these fluctuations as the forces to drive themselves clockwise or counterclockwise. For example, in the ATP synthase, the biological motor rotates counterclockwise when protons motivate the production of ATP from ADP. On the other hand, the molecular motor spins clockwise if ATP is consumed to release energy. So the ATP synthase is a reversible molecular motor which is driven by Brownian motion in both directions. As we discussed, artificial molecular motors mentioned above were able to rotate in one direction but not the other.

Recently, Leigh and co-workers¹⁷ developed an interlocked mechanically bonded molecular motor (**Scheme 1.5**), which is a [2]catenane containing two removable and constructible bulky groups to control reversible motions of benzyl amide macrocycle. In this system, there are two binding stations. Originally, one (the fumaramide station) is more energetically favorable than the other (the succinamide station). When the carbon-carbon double bond was activated by UV light, the isomerization of the double bond (from *fum* to *mal*) decreased the affinity of this binding station to such an

energetically disfavored level (*mal* < *succ*) that the small ring tended to move to the other binding station. Once the bulky groups were removed, the small ring would rotate clockwise or counterclockwise. An external energy source,



like UV light, changed the affinities of the binding sites for the small macrocycle. The thermal energy, Brownian motion, drove the small macrocycle to circumrotate to reach a new equilibrium. The external trigger and thermal fluctuation are both required for the reversible circumrotation of the small macrocycle.

The designed catenane was prepared as the isomer *fum*-E-**1.11** (**Scheme 1. 5**). When the system was operated to rotate in one direction, a series of processes were undertaken: 1) Photoisomerization to give *mal*-Z-**1.11**. 2) desilylation, followed by circumrotation of small macrocycle, and silylation to form *succ*-Z-**1.11**. 3) photoisomerization to give *succ*-E-**1.11**. 4) detritylation, followed by movement of the small ring, and tritylation to regenerate *fum*-E-**1.11**. The net result for those four operations was a clockwise rotation of the small benzyl amide ring around the large macrocycle. On the other hand, if the step 2) and step 4) above exchanged, the net rotation was a counterclockwise motion.

The behavior of the small ring around the large macrocycle could be demonstrated undoubtedly by isolation of the product of every synthetic step, like desilylation/silylation, detritylation/tritylation and comparison of the ¹H-NMR spectra of the products of each step.

To perform a full rotation, four sets of reactions must be processed: balance-breaking (photoisomerization), unlinking/linking, second balance-breaking and second unlinking/linking. Clockwise or counterclockwise rotation of the small ring depended on which balance-breaking and unlinking/linking steps are paired.

Although the time consumed and the reactions involved made this system less practical in some sense than unidirectional molecular motors, the design was

conceptually logical and the system behaved as expected.

From the above examples, it was concluded that a number of artificial unidirectional molecular motors have been achieved and simplicity of those models made them synthetically available and easily operate and control in terms of real applications. Moreover, a reversible molecular motor has been developed, which is conceptually similar to the natural molecular motor in the biological system. Molecular motors which can utilize random fluctuation without fighting it are ideal models and our ultimate goal as well.

Considering the characteristics of the molecular motor discussed above, we can conclude that a unidirectional molecular motor needs three features: 1) an element changing randomly, for instance, benzyl amide ring; 2) asymmetric in energy due to conformations or binding sites; 3) an directed energy input to avoid breaking the Second Law of Thermodynamics.¹⁷

However, artificial molecular motors have obvious shortcomings. Compared to biological systems, the artificial molecular motors developed so far are still primitive. We still need to figure out what work they can do and what they can drive. The examples in which microscopic circumrotation is transformed to mechanical work are still few. It is still a long way to achieve macroscopic movements from microscopic motion. On the other hand, the energy applied in those examples is usually a mixture of chemical,

photochemical, thermal energy, which makes the operations complicated and impractical. A simpler energy provided and operation conditions will be an appealing and challenging subject in the future development.

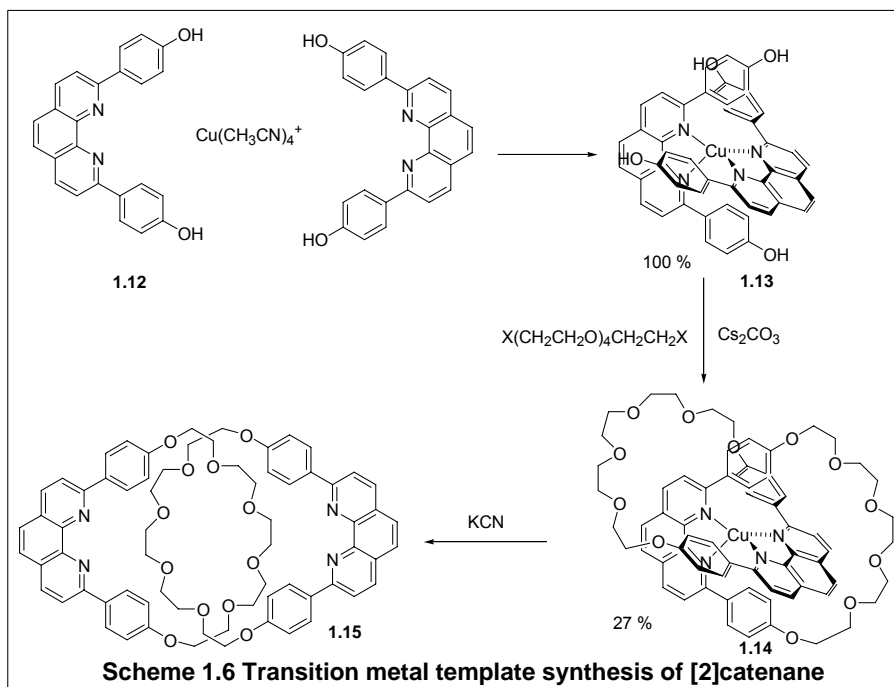
1.2 Catenanes and Template synthesis

Catenanes have attracted much attention in constructing the molecular machines in the past few decades due to their non-covalent mechanical bonds.^{18,19} The name of catenane was derived from the Latin word *catena* for the chain.^{2b} Catenanes consist of at least two interlocked macrocycles. Catenanes are appealing systems in that interlocked mechanical bonds can hold the components together in a particular conformation due to relatively weak nonbonding interactions. These nonbonding interactions are not as robust as covalent bonds which are difficult to break in order to perform a motion. The relative motion between the components in catenanes is easily described and imagined.

The synthesis of catenanes takes advantage of non-covalent interactions between components, like metal-ligand bonding²⁰, hydrogen bonding²¹, π - π stacking^{19,22}, donor-acceptor ability, hydrophobic-hydrophilic property etc. The discussion that follows focuses on metal-ligand bonding, hydrogen bonding, π - π stacking template syntheses of catenanes.

1.2.1 Transition Metal Template Synthesis of [2]catenanes

In 1983, Sauvage²³ reported the first metal-ligand template for the synthesis of catenanes. In this system, copper (I) was utilized as a template based on its tetrahedral coordination geometry. As shown in **Scheme 1.6**, two equivalents of phenanthroline ligands were coordinated with copper (I) to form the complex **1.13** followed by deprotonation and substitution to form **1.14**. The yield for the metal-ligand coordination complex was high-100 % but the substitution reactions were only in 27 % yield. The demetallation of copper with potassium cyanide gave a metal free [2]catenane in which the rings were no longer chemically bonded to one another. The



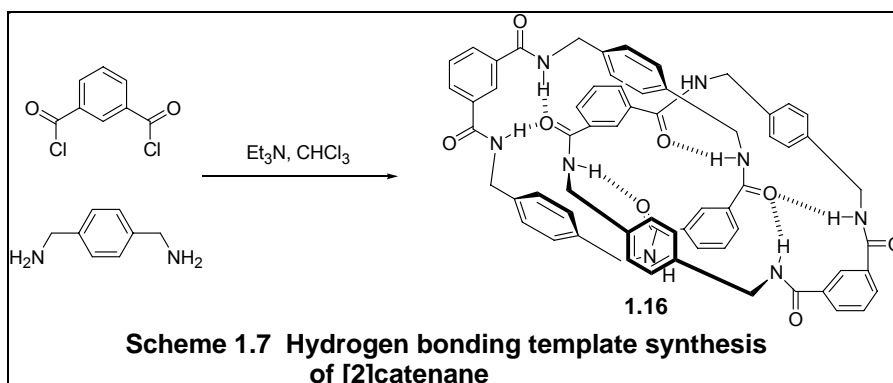
principle of this synthesis was very simple and the strategy was practical. This template has been applied in the preparation of various interlocked compounds including

catenanes, rotaxanes, knots.

1.2.2 Hydrogen Bonding Template Synthesis of [2]catenanes

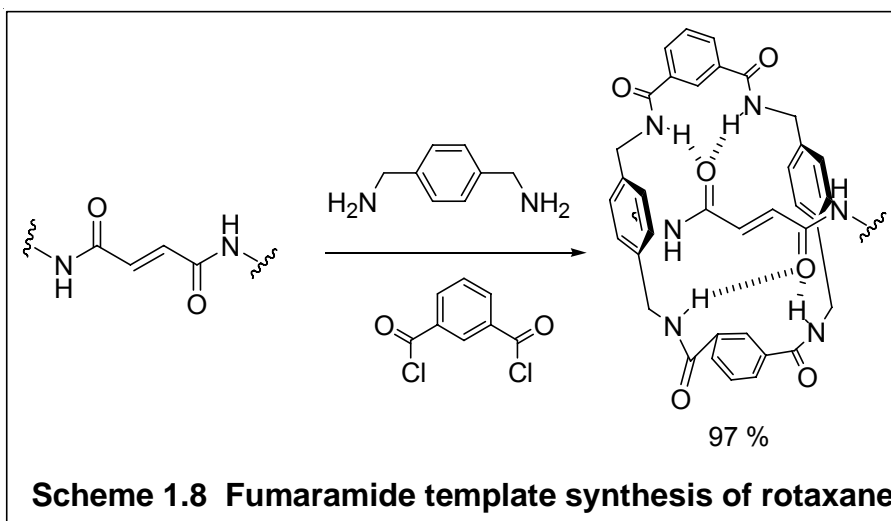
The first hydrogen bonding template synthesis of [2]catenanes was reported in 1992 by Hunter.²⁴ In 1995, Leigh developed a benzylic amide catenane **1.16** (Scheme 1.7).

The synthesis of the [2]catenane in **Scheme 1.7** was accomplished in one step with 20 % yield. The ¹H NMR spectrum had six different types of protons in d₆-DMSO which is the same as the parent macrocycle.²⁵ The structural data from these benzylic amide catenanes indicated that the formation of interlocked compounds



including catenanes or rotaxanes was based on the template assembly of macrocycle around the amide groups. It was found that the amide groups in simple peptides could template the cyclization of benzyl amide macrocycles to give peptide rotaxanes.²⁶ When the rigid fumaramide was used as a template (**Figure 1.8**), a rotaxane was obtained in 97

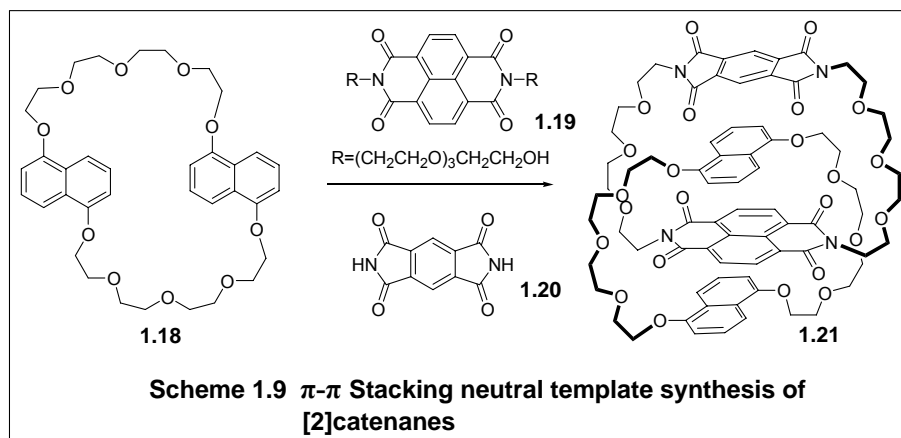
%, which further demonstrated that the mechanism of the hydrogen bonding template was reasonable.²⁷



As described in the early section in this chapter, this template synthesis was applied in the synthesis of catenanes as unidirectional or reversible molecular motors (**Figure 1.9** and **Scheme 1.5**).

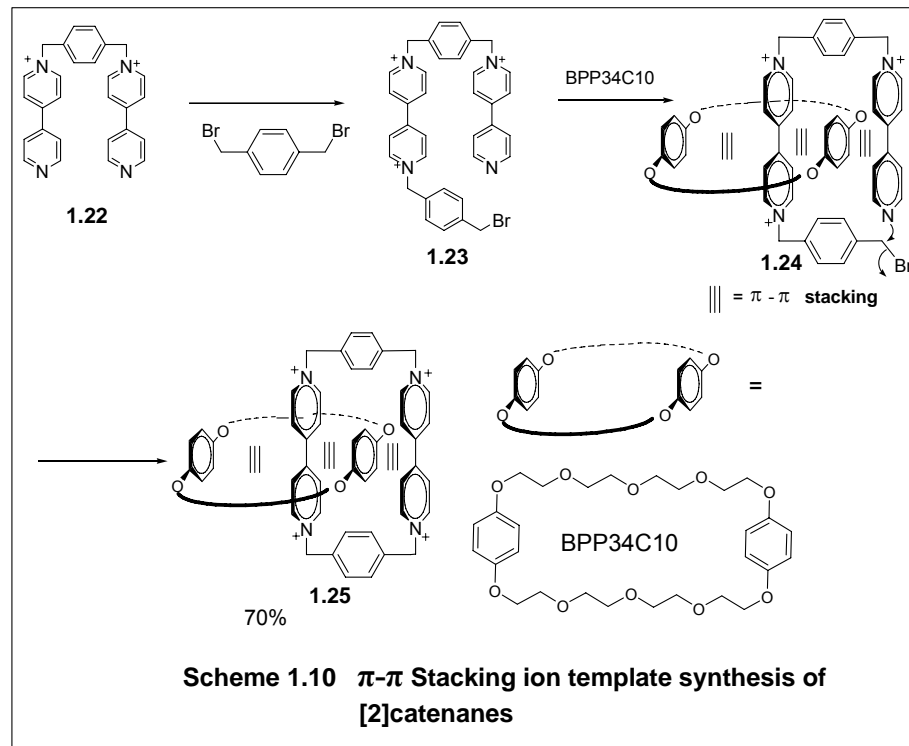
1.2.3 π - π -Stacking Template Synthesis of [2]Catenanes

π - π -Stacking template synthesis of [2]catenanes involves the electron-rich and electron-deficient components. Sanders²⁸ developed a method to template synthesis of catenanes by neutral templates. In this method described in **Scheme 1.9**, π -electron-rich crown ether **1.18** and π -electron-deficient diimides, pyromellitimide **1.20** and diol **1.19**, self-assembled by π - π stacking and undertook a ring closure via a Mitsunobu reaction to give catenane **1.21**.



Stoddart *et al* first reported an ion template synthesis of [2]catenane in 1988.²⁹ The ionic component, a tetracationic cyclophane, was used as π -electron-deficient acceptor and a crown ether, BPP34C10 (bis(p-phenylene)[34]crown-10) or DNP (1,5-dinaphtho[38]crown-10), was used as π -electron-rich donor,. In the synthesis described in **Scheme 1.10**, the precursor **1.22** first reacted with 1,4-xylylene dibromide to give a tricationic intermediate **1.23**. Intermediate **1.23** could exist for a short time and could be traced. Once the intermediate **1.23** was formed, the crown ether ring (like BPP34C10) treaded onto the dicationic dipyrindinium unit via π - π stacking. The electron-rich phenylene ring of the crown ether attracted the other monocationic dipyrindinium unit as in **1.24** to promote a template ring closure. Once the ring closure was completed, [2]catenane was obtained in 70 % yield.

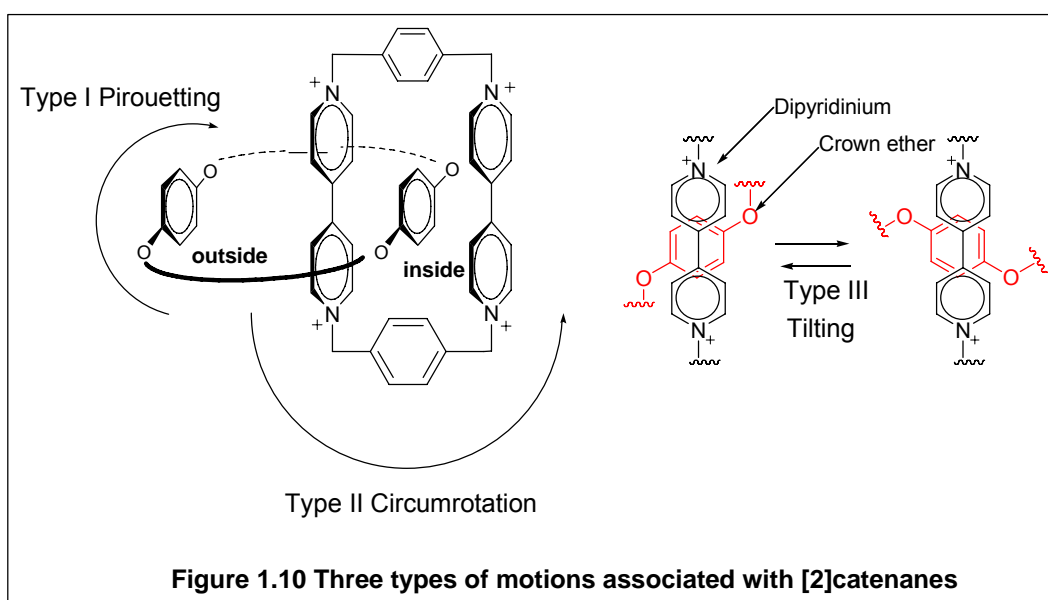
It was found that the electron-rich crown ether template was very efficient in the template synthesis of [2]catenanes. When the templates, bis(p-phenylene)[34]crown-10 (BPP34C10) and 1,5-dinaphtho[38]crown-10 (DNP38C10), were introduced in the



synthesis of [2]catenanes, the rate of ring-closure reaction increased up to 230 times (BPP34C10=0.1M) and 1900 times (DNP38C10=0.01 M) comparing to that without templates.³⁰

Stoddart and co-workers³¹ found that the ^1H NMR spectra of these catenanes became more and more complex when the temperature was lowered. They concluded that there were four types of conformational motions for these catenanes. Three of them could be observed via variable temperature ^1H NMR. As shown in **Figure 1.10**, Type I is a motion described as pirouetting, which means the crown ether ring rotating around one of the dipyridinium unit to interchange the “inside” and “outside” p-phenylene rings. Type II is the motion of the crown ether ring migrating from one dipyridinium unit to the other.

Type III involves one hydroquinone ring of the crown ether tilting or rocking inside the tetracationic cyclophane. Type IV is observed in the [2]catenane incorporating only resorcinol based crown ether, which involves displacement and reentry of bismetaphenylene-23-crown-10 (BMP32C10) into the electron-deficient cavity which is not observed in our study.³¹

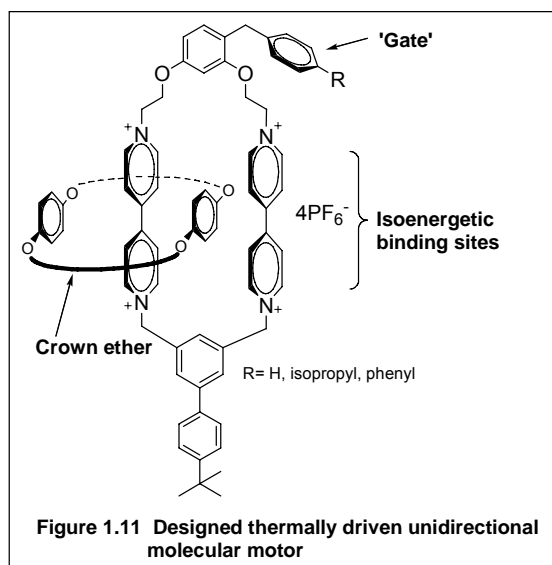


1.3 Exploration of Thermally Driven Molecular Motors

Kelly's model in section 1.1.3.1 used chemical energy to drive a unidirectional molecular motor through 120° rotation. In this model, the free energy of activation for a forward rotation was lowered by raising the free energy of the starting rotamer via addition of chemical reagent phosgene. At the same time, a reverse rotation was blocked by adding a larger energy barrier. Feringa's or Leigh's model utilized photochemical

isomerization to drive their unidirectional molecular motors. By changing a low-energy conformation to a high-energy conformation by photochemical energy, the system was highly unstable and could spontaneously release energy to form more stable conformation via forward motion. To the best of our knowledge, all the unidirectional molecular motors developed to date have to be driven by directed external energy input, no matter whether it was chemical or photochemical energy. No artificial thermally driven molecular motor has been demonstrated.

Our research group has been involved with the design and synthesis of molecular ratchet as a means to study potentially thermally driven unidirectional motors. The core



approach was to build systems with two isoenergetic binding sites and an adjustable biasing gate. Several [2]catenanes with biased gates were synthesized by Dr. David Martyn in our group (**Figure 1.11**).³² It was expected that random thermal fluctuations could drive the circumrotation preferentially

in one direction over another.

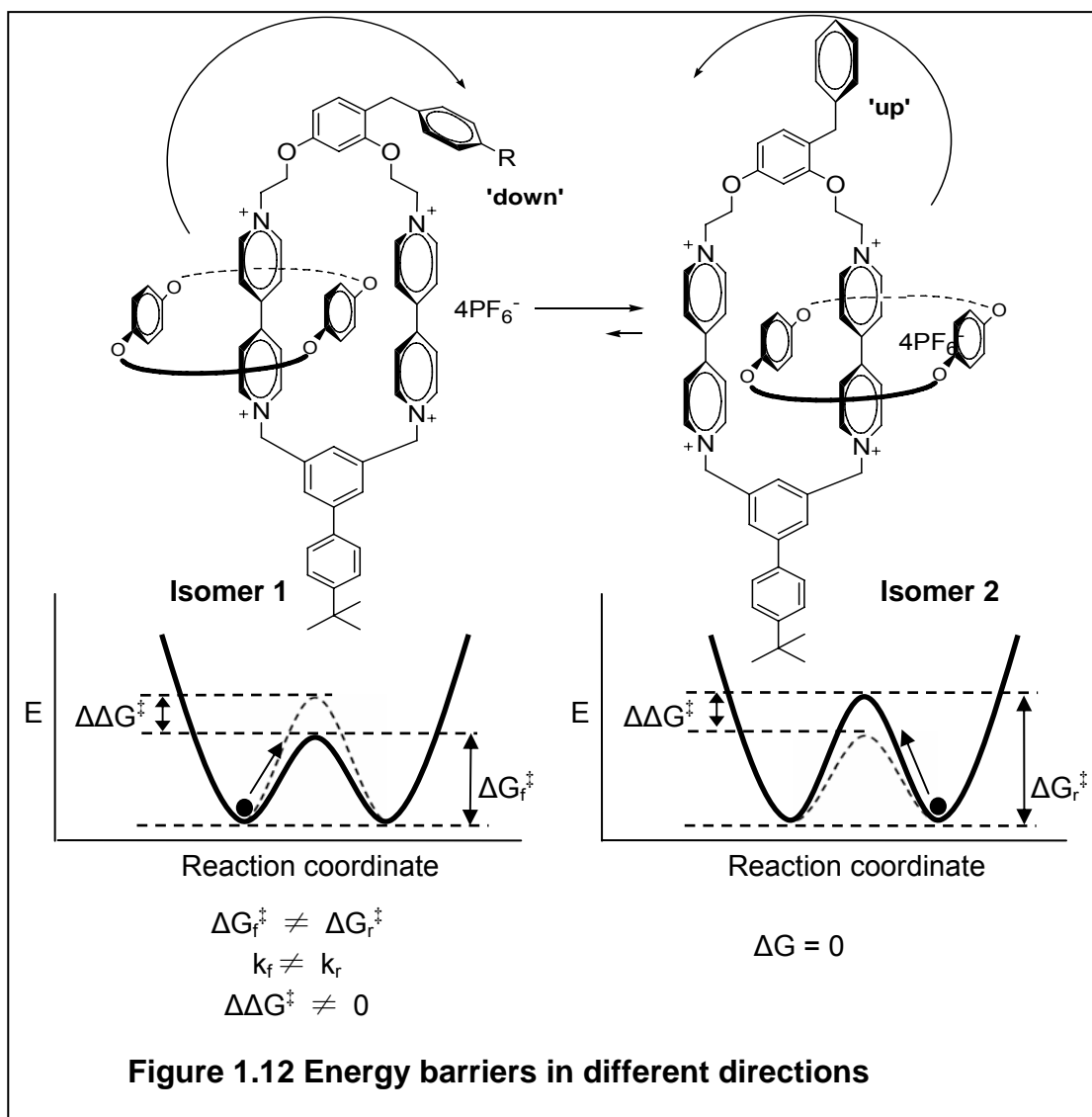
In these catenanes, the biasing gates were phenyl or substituted phenyl groups appended to a resorcinol spacer by a methylene carbon. Ethoxy groups were incorporated

to increase the space between gates and binding sites to reduce the possibility of direct interaction between the gate and the BPP34C10 ring when π - π stacked at the bistable dipyridinium units. If the gate didn't interact, the two binding sites would be isoenergetic.

The ratchet design envisioned that when the crown ether ring is on the left side, it could interact with the gate to push the gate down while translocating from left to right. On the other hand, when the crown ether ring is on the right side, it would have to overcome a wide 'up' gate to move to the other side since the motion of the crown ether ring was not expected to push the gate into a narrower conformation. These interactions could be interpreted as providing a modulation of the energy barrier as shown in **Figure 1.12**.

Possible energy barriers in different directions are described in **Figure 1.12**.³² If the two binding sites are isoenergetic ($\Delta G = 0$), the ground states energies would be the same. The forward movement could still require less energy due to the modulation of the energy surface but the reverse movement would require more energy. So the crown ether ring could potentially rotate preferentially.

To demonstrate the preference of formation of one conformation over another, the conformation population differences between two isoenergetic binding sites must be different when the crown ether passes over the biasing gate and when it passes over the bottom symmetric tether.



In the [2]catenanes with biasing gates synthesized by Dr. David Martyn, not only were the ground state conformations not 1:1 when the interconversion occurred along the bottom 1,3-xylyl tether, the same ratios were observed when the bottom path was blocked and interconversion occurred along the biased tether.

It was speculated that the ethoxy tethers enabled too much conformational

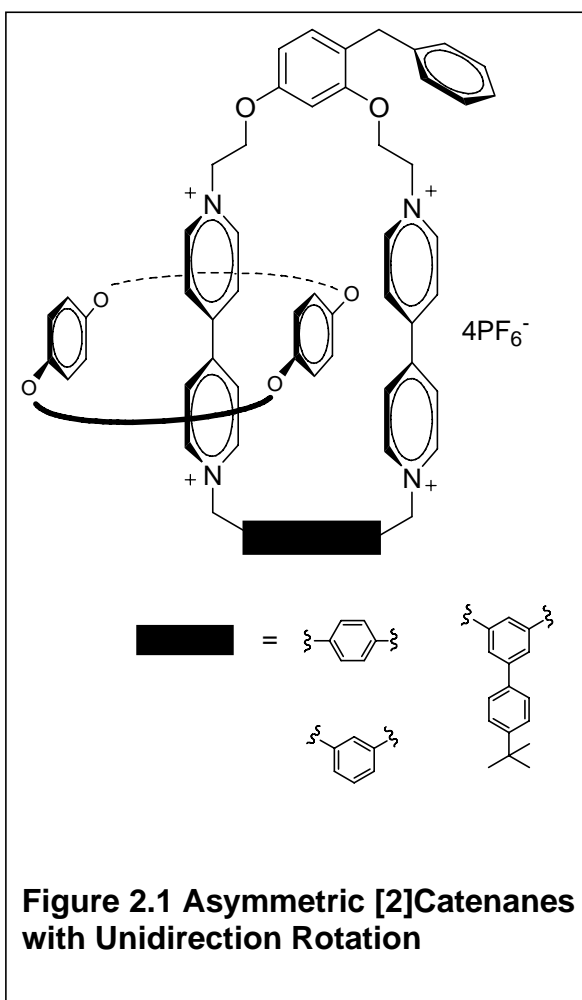
flexibilities in the catenanes and enabled direct interactions between the gate and the crown ether in a π - π stacked conformation. In spite of evidence for the conformational change of the gate during passage of the crown ether, no directional preference could be inferred.

Chapter 2

Synthesis of Symmetric [2]Catenanes and Path Selection Study

2.1 Design of Symmetric [2]Catenanes with Path Selection

As described in chapter 1, photochemically or chemically driven preferentially unidirectional motors have been developed. However, thermally driven molecular motors



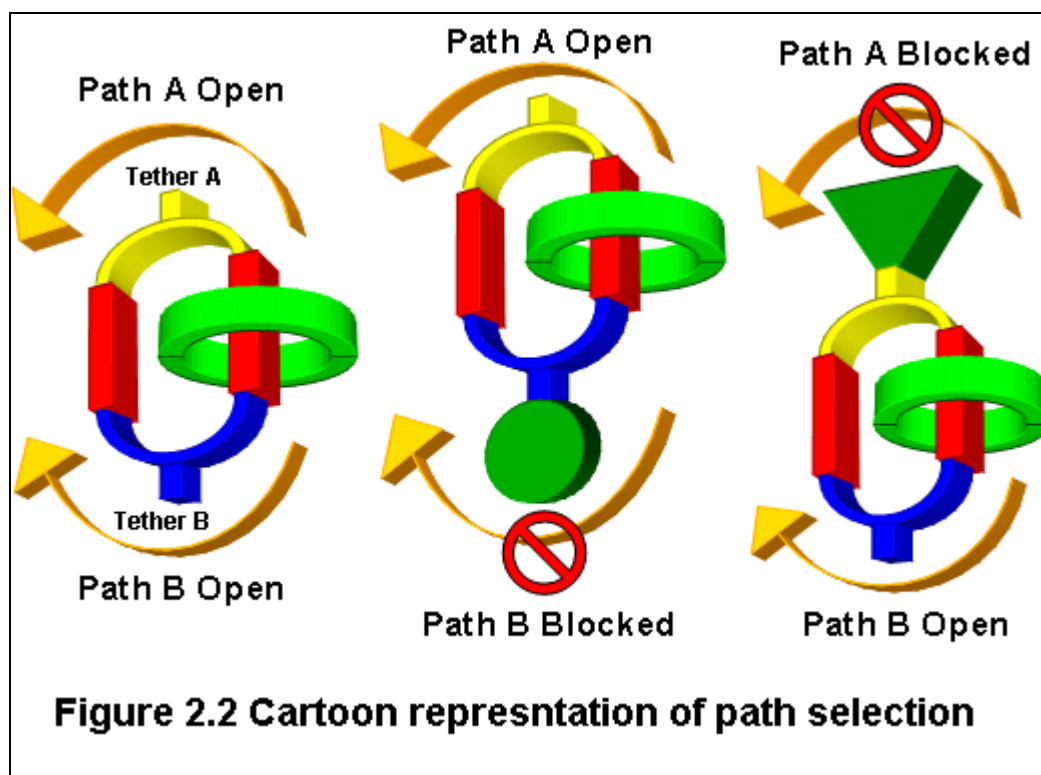
have not been demonstrated. In a designed model in our group (**Figure 2.1**),³² a benzyl group should act as a “gate” or a “pawl” for a ratchet. The conformational orientation of the benzyl group could change from a narrow but high energy one to an extended, low energy one. As described in the previous section, the energy needed for movement from the left to the right could be potentially lower than that needed from the right to the left if the movement of benzyl group modulates the energy

potential. In this case, the crown ether ring could prefer to circumrotate from the left to the right. A unidirectional movement of one ring round another ring could be thereby supported.

In details, the benzyl group functioned like as a “gate” which can exist in different conformations. The gate could be in a low-energy, extended conformation or high-energy but reactive, narrow conformation which is sterically disfavored. Thermodynamically, the narrow conformation would be at present at low concentration. When the crown ether ring (BPP34C10) circumrotates from the left to the right, the benzyl “gate” could be forced into the narrow conformation, which could help the crown ether ring pass over the gate. The correlated motion of the crown ether and the benzyl gate could lower the energy barrier. Once the crown ether ring settles down on the right side, the narrow, high-energy conformation would first need to be formed for the crown ether ring to move from the right to the left. Moreover, even if the narrow conformation was formed, the crown ether ring could push the gate away from itself, resulting in a wide conformation which could prevent the gate from moving back to the left side. In this case the correlated motion of the crown ether and the benzyl gate could raise the energy barrier.

However, in order to test this hypothesis and control molecular motion in [2]catenanes, we must demonstrate that the selective movement of one ring round another ring can be observed proceeding over tethers with different energy barriers. A cartoon

representation of this path selection was described in **Figure 2.2**.³³

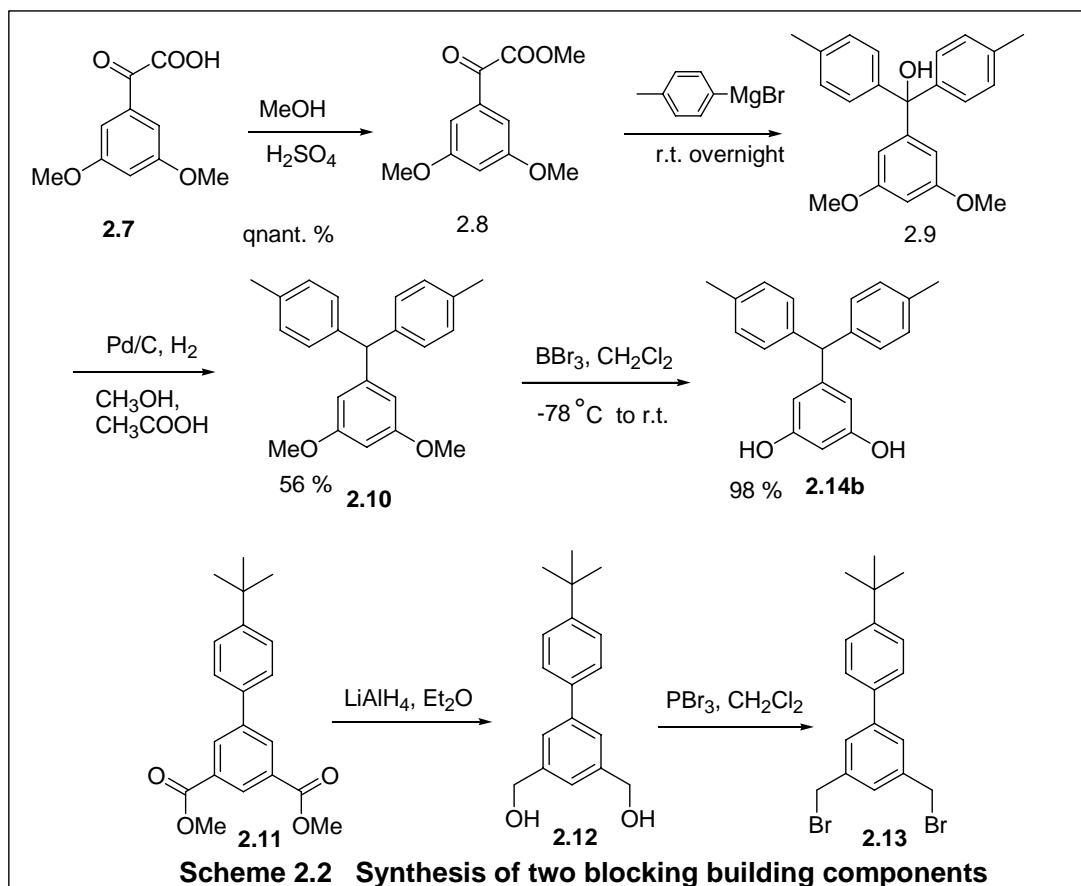


In the model based on [2]catenanes systems, sterically blocking groups were to be appended to either of two tethers which were connected by two 4,4'-dipyridium units. When there were no bulky blocking groups to impede circumrotation, the crown ether ring could move along pathway **A** or pathway **B**. When the bottom tether was appended with a blocking group, passage over the bottom pathway **B** would be prohibited and the crown ether ring could only circumrotate along pathway **A**. With a sterically bulky group incorporated onto the top tether, pathway **A** would be blocked and the crown ring could only move along pathway **B**. When both pathways **A** and **B** were blocked, the crown ether ring would stay on one side. The rate of interchange would give the needed

appended with the blocking group (5-bis(4-methylphenyl)methyl) to block the crown ether moving over the resorcinol tether. A 4-tert-butylphenyl group was appended on the 5'-position of bottom 1,3-xylyl spacer to block the crown ether ring from passing over this xylyl spacer. 1, 3-Xylyl and 1, 4-xylyl spacers were used as the bottom tethers to demonstrate the energy difference between wide and narrow spacers. As described below, path selection via addition or removal of an energy barrier in the form of sterically bulky groups was achieved.

2.2 Synthesis and Characterization of Building Components and Symmetric [2]Catenanes³³

As described in **Scheme 2.2**, the preparation of one blocking component started with the Fisher esterification of 3, 5-dimethoxybenzoic acid **2.7** to give ester **2.8**³⁴ in quantitative yield, followed by a Grignard addition of 2 equivalents of p-tolylmagnesium bromide solution (*in situ*) to form the tertiary alcohol **2.9**. In the ¹H NMR spectrum of **2.9**, the 3H singlet at 3.91 ppm for the methylester group in **2.8** disappeared, showing the success of addition of the Grignard reagent. In the ¹³C NMR spectrum, the peak at 55.16 ppm revealed the tertiary carbon connected to a hydroxyl group. The mass spectrum (ESI) showed a peak at m/z = 371.6 which could be M+Na⁺ (calculated m/z = 371.6). All those data supported the formation of the desired product.



Tertiary alcohol **2.9** was reduced by catalytic hydrogenation³⁵ to form triarylmethane **2.10** in a yield of 56 % by using catalytic Pd/C in methylene chloride with a trace amount of acetic acid and methanol. In the ¹H NMR spectrum of **2.10**, a singlet at 5.43 ppm was the tertiary proton close to three benzene rings. In ¹³C NMR, a peak at 55.26 ppm was assigned to this tertiary carbon. The mass spectrum (ESI) indicated a peak at m/z = 355.3 which was consistent to M+Na⁺ (calculated m/z = 355.18).

Product **2.14b** was obtained in a yield of 98 % via removal of the methyl groups with BBr₃.³⁶ In ¹H NMR spectrum, the 6H singlet which was 3.75 ppm for the methoxyl

groups in **2.10** no longer existed, showing the success of deprotection. The ^{13}C NMR spectrum showed that there were only two different peaks at the aliphatic region, one for the tertiary carbon and the other one for the methyl group on the tolyl groups. MS data (ESI) indicated a peak at $m/z = 327.5$ ($M+\text{Na}^+$, calculated $m/z = 327.15$).

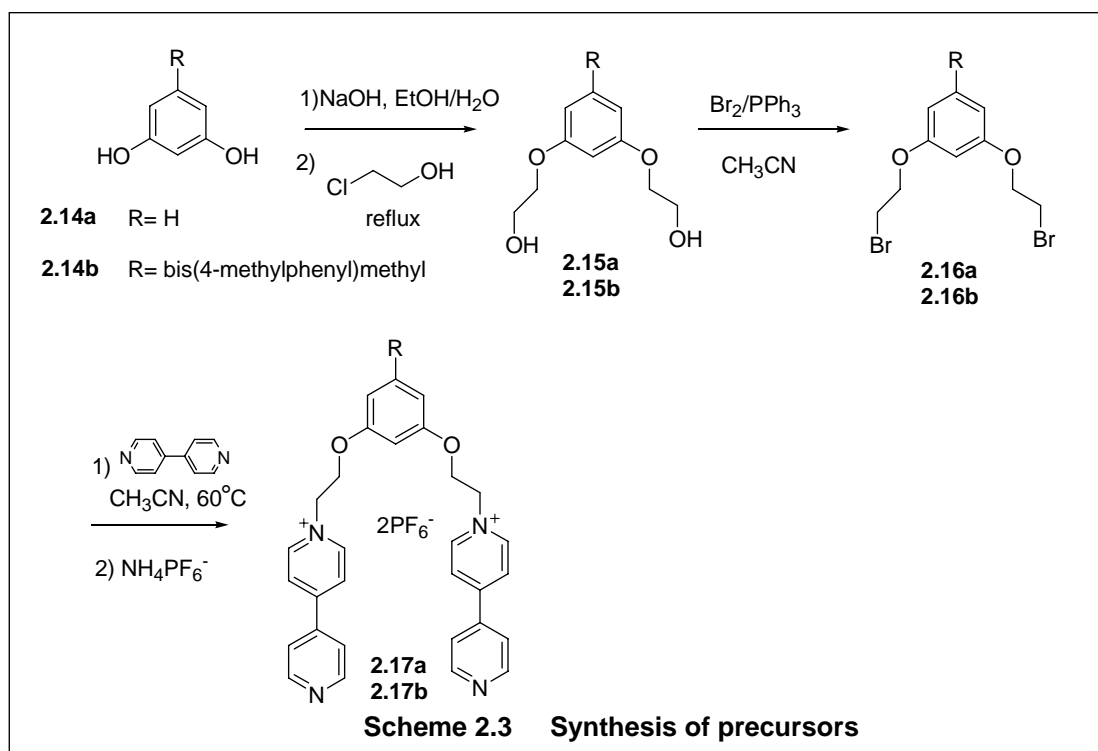
The xylyl-based blocking building component **2.13** was prepared according to literature methods³⁷ by Suzuki coupling to form **2.11** followed by reduction and bromination to give **2.13**.

The synthetic route for further functionalization of the resorcinol precursor was described in **Scheme 2.3**. The syntheses of unsubstituted resorcinol precursor and catenanes were established by Dr. David E. Martyn in our group.³² Following a similar route, substituted resorcinol **2.14b** was deprotonated by NaOH in ethanol to form the dianion as nucleophile, followed by its reaction with 2-chloroethanol under reflux to give 2-[3-(2-hydroxyethoxy)phenoxy]ethanol **2.15b** with a yield of 93 %.

In the ^1H NMR spectrum of the pure product **2.15b**, two new triplets were seen at 3.98 ppm ($J=4.7$ Hz), 3.88 ppm ($J=4.7$ Hz) which were assigned to the methylene protons in the ethyl tether. In the ^{13}C NMR, the two new peaks at 69.02 ppm and 61.31 ppm were assigned to be two methylene carbons in the ethyl tether. The mass spectrum indicated a peak at $m/z = 415.7$ which is the m/z of $M+\text{Na}^+$ (Calculate $M+\text{Na}^+$ $m/z = 415.20$).

Intermediates **2.15b** was brominated with Br_2/PPh_3 in acetonitrile to give 1,

3-bis-(2-bromoethoxy)benzene **2.16b**. In the ^1H NMR spectrum of **2.16b**, the bromine

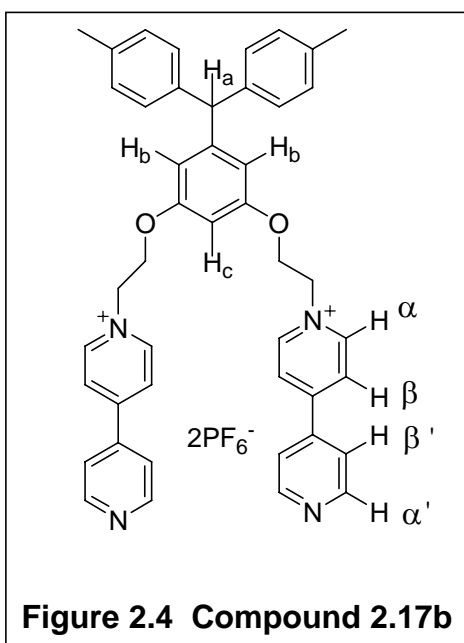


atom shifted the α protons downfield to 4.25 ppm ($J=6.2$ Hz) and β protons upfield to 3.63 ppm. Comparing the ^{13}C NMR spectra of **2.15b** and **2.16b**, a big shift from 61.31 ppm (alcohol **2.15b**) to 29.24 ppm (**2.16b**) was observed as a result of replacing hydroxyl group with a bromine atom. In the mass spectrum (ESI), three peaks ($m/z = 539.1$, 541.1 , 543.1) at a ratio of intensity 1:2:1 confirmed that there were two bromine atoms in the product. They corresponded to the isotopes $\text{M}+\text{Na}^+$, $\text{M}+2+\text{Na}^+$, $\text{M}+4+\text{Na}^+$ (calculated $m/z = 539.03$, 541.03 , 543.03).

The preparation of the precursor bis(dipyridinium) **2.17b** followed the procedure developed by Stoddart.³³ The product was mixed with a large excess of 4, 4'-dipyridyl

(5-8 eq.) and stirred at 65 °C for 2 days. The excess 4, 4'-dipyridyl was removed by recrystallization in chloroform. The obtained solid bromide salt was dissolved in water and ammonium hexafluorophosphate salt was added to perform anion exchange in a yield of 86 %.

In the ^1H NMR spectrum of **2.17b**, there were four multiplets in the downfield



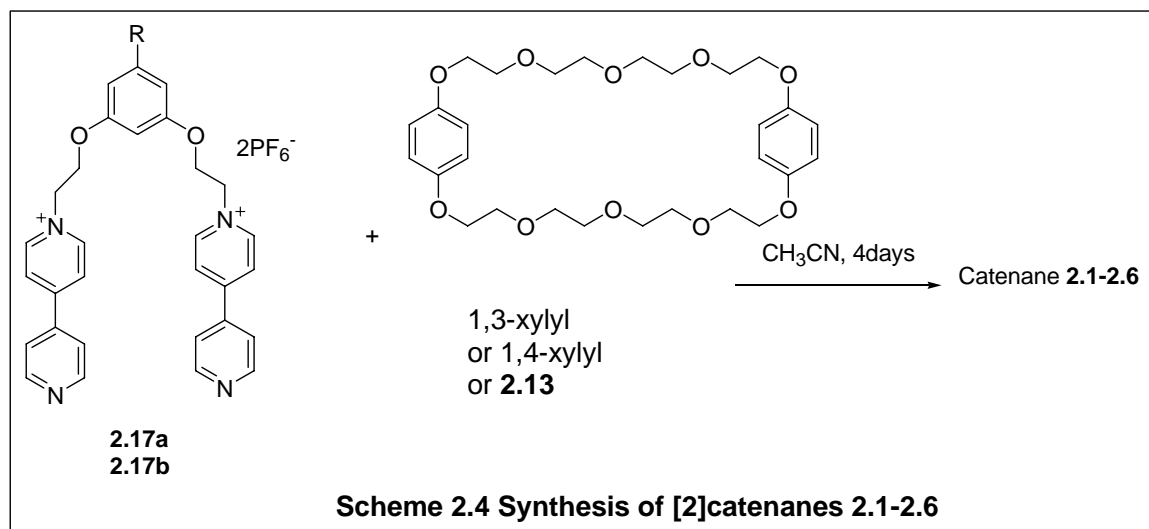
region, 9.34 ppm, 8.91 ppm, 8.67 ppm, 8.01 ppm which were assigned to the protons on the dipyridinium units. The most downfield signal at 9.34 ppm should be assigned to the α protons adjacent to the cationic nitrogen (**Figure 2.4**). The signal at 8.91 ppm was assigned to the α' protons adjacent to the neutral nitrogen. The signals at 8.67 ppm, 8.01 ppm indicated the protons on the β , β'

positions, respectively. Because of the effect of the cationic nitrogen, the signals of protons on the ethyl tether shifted downfield to 5.29 ppm and 4.63 ppm, which were both 1 ppm downfield relative to those in the dibromide derivative **2.16b**. The signal at 6.57 ppm (t, $J=2.1$ Hz, 1H) was assigned to Hc (**Figure 2.4**) and the signal at 6.40 ppm (d, $J=2.1$ Hz, 2H) was assigned to Hb. The chemical shift of Ha was located at 5.40 ppm (s, 1H).

In the ^{13}C NMR spectrum of **2.17b**, the α proton adjacent to cationic nitrogen in the ethyl moiety shifted from 29.24 ppm to 60.67 ppm compared to the dibromide derivative **2.16b**. This further supported the formation of the desired precursor **2.17b**.

In the mass spectrum (ESI), the peak at $m/z=335.2$ was assigned to the dication M^{2+} which had lost two PF_6^- from the salt (calculated $m/z = 335.18$). The peak at $m/z = 815.4$ was assigned to the monocation which was the loss of one PF_6^- from the neutral salt. This evidence further supported the authenticity of the desired product **2.17b**.

The synthesis of symmetric [2]catenanes was a three-component reaction (Scheme 2.4).³³ The precursor **2.17b**, 1.2 equivalents of 1,3-xylyl or 1,4-xylyl or **2.13**,



3 equivalents of BPP34C10 were mixed together in acetonitrile at room temperature. After a few hours, the solution turned orange and was allowed to stir for 4 days at room temperature. Over time, the solution became more and more red. Some yellow precipitate appeared which could be attributed to the insoluble catenanes or pseudo-rotaxane with

bromide anion instead of hexafluorophosphate anion.

2.3 Purification of Symmetric [2]Catenanes^{32,33}

In the resulting reaction mixture, there could be several possible species: desired [2]catenane, pseudo-rotaxane, excess BPP34C10 and unreacted dibromide. In terms of polarity, BPP34C10 and unreacted dibromide should be significantly less polar because they are neutral. The [2]catenanes and pseudo-rotaxane are more polar since they are charged. However, the difference of polarity between [2]catenanes and pseudo-rotaxane could be subtle and their separation by column could be difficult. So dethreading the pseudo-rotaxane seemed to be necessary. Considering those possibilities, a series of procedures have been developed to isolate the desired [2]catenanes. First of all, the solvent acetonitrile was removed via rotary evaporator to give a red residue. The residue was dissolved in minimum volume of methanol/acetone (1:1) and the solution was loaded on the preparative TLC plate. After drying, the preparative TLC plate was eluted twice with methanol/ethyl acetate (1:1) at 35 °C. The purpose of heating during eluting was to promote dethreading of the BPP34C10 ring from oligomeric pseudo-rotaxane. The R_f value of BPP34C10 was high in methanol/ethyl acetate (1:1) ($R_f = 0.9$). However, the R_f values for catenanes and oligomeric dipyridinium chain were low ($R_f = 0$). So the crown ether ring and unreacted starting materials were first eluted to the top of the plate.³²

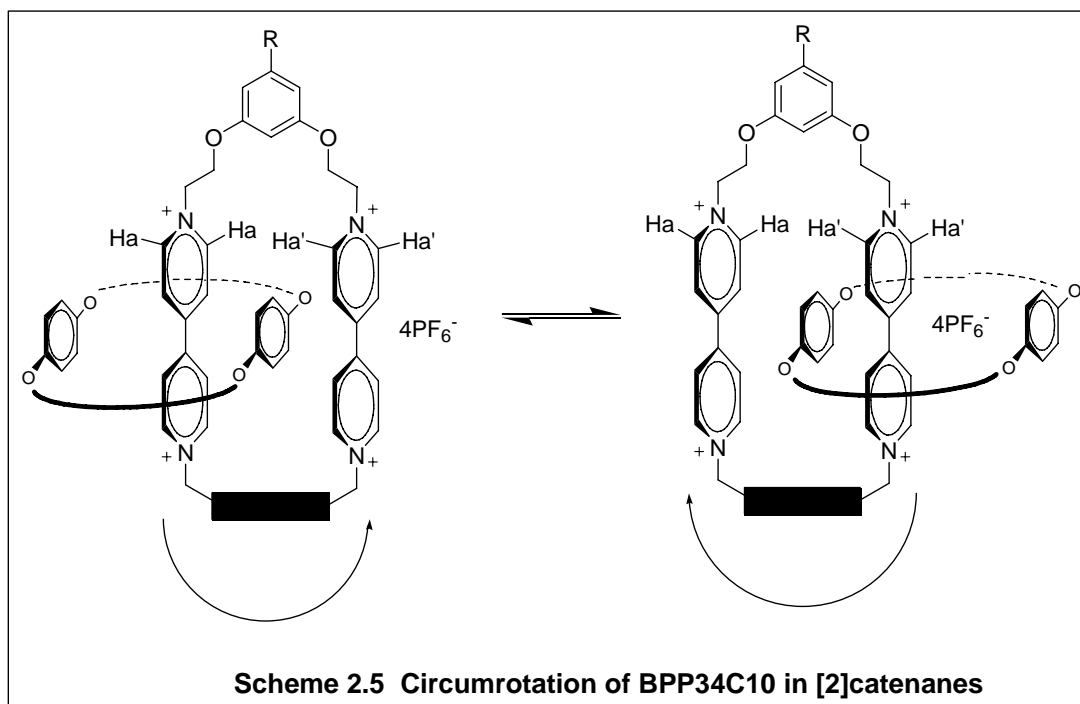
Then, the preparative TLC plate was eluted with methanol/2M ammonium chloride/nitromethane (7:2:1). The desired [2]catenanes moved up ($R_f = 0.3-0.5$) while the oligomeric dipyridinium chain did not move much ($R_f = 0.1$) because of the unshielded charge they have. The BPP34C10 ring shielded part of the charge in [2]catenanes, which promoted the [2]catenanes move higher compared to the oligomeric chain. The [2]catenanes on the preparative TLC plate appeared orange to red bands.

The orange/red band was removed from the plate. The silica gel containing the [2]catenanes was ground and washed with the final eluent-methanol/2M ammonium chloride/nitromethane (7:2:1). An excess of ammonium hexafluorophosphate was added to perform anion exchange. The methanol and nitromethane was removed via rotary evaporator and the red precipitate was suspended in the solution. The solution was filtered and the solid was washed with water several times and allowed to air dry for a while. The obtained solid was dissolved in d_6 -acetone for ^1H NMR, ^{13}C NMR and variable temperature NMR.

2.4 Characterization of [2]Catenanes

The [2]catenanes obtained were characterized via ^1H NMR. The relative movements of two rings of the interlocked molecules could be observed on the NMR timescale. As described by Stoddart, there are three types³¹ of movements for

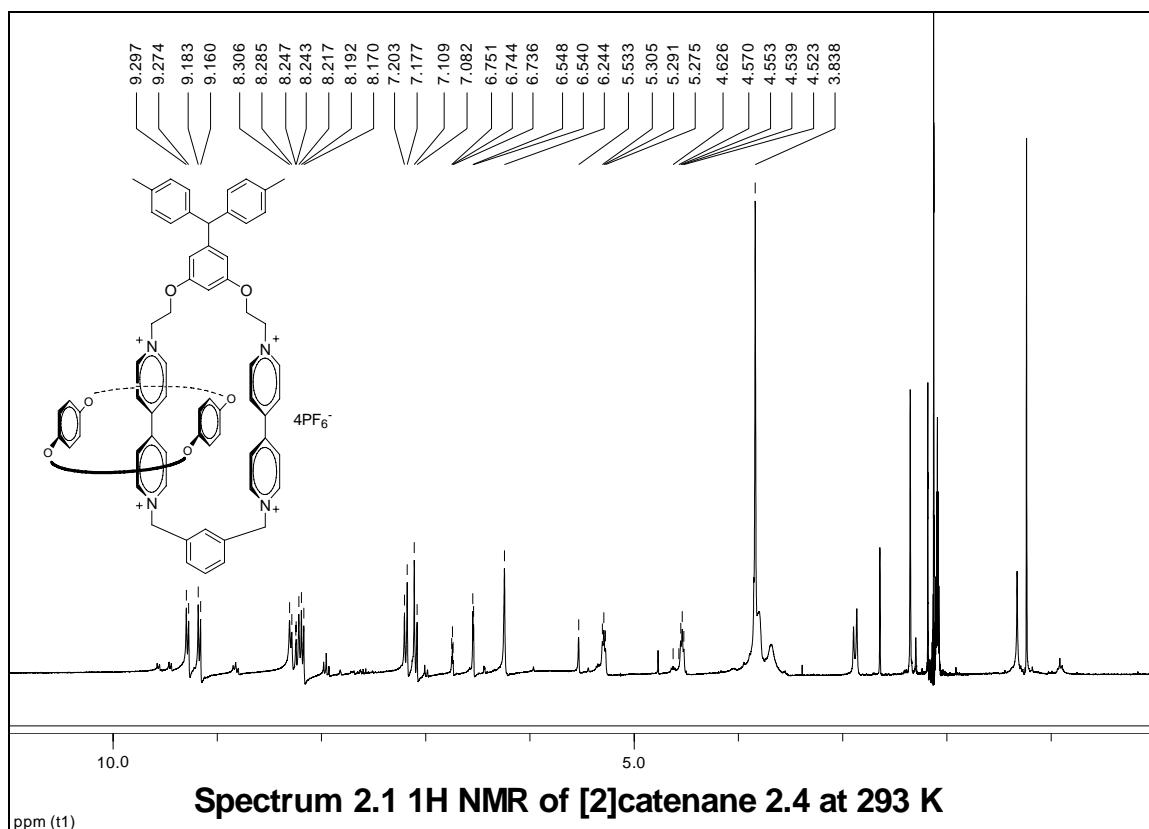
[2]catenanes: self-rotation of BPP34C10, circumrotation of BPP34C10 around the dipyridinium ring and BPP34C10 tilting. We want to focus on the circumrotation of BPP34C10 around the dipyridinium macrocycle as described in **Scheme 3.5**.



When the BPP34C10 ring theoretically stays π - π stacked to one dipyridinium, the Ha and Ha' should have different chemical shifts because Ha (left figure) was shielded by the BPP34C10 ring while Ha' was not. However, if the BPP34C10 ring circumrotated so rapidly, Ha and Ha' would be identical and only one set of averaged signals would be observed. When the temperature is lowered, the circumrotation becomes slower and slower. As sufficiently low temperature, it could be observed on the NMR time scale that the BPP34C10 would stay on one side and the two sets of signals could be observed. The details of such VT NMR spectra will be discussed in the section 2.5.

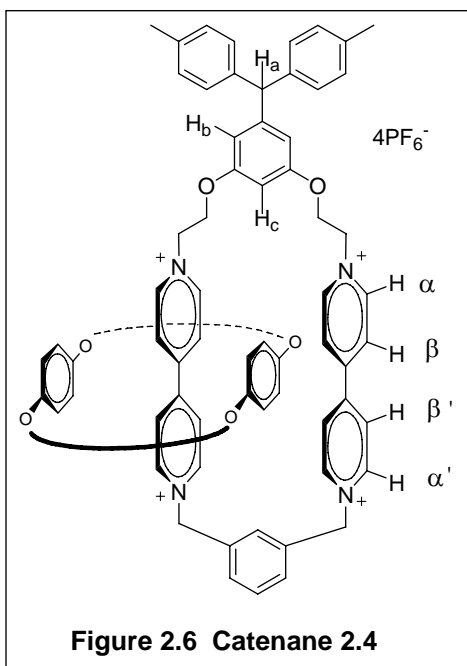
2.4.1 Characterization of [2]Catenane **2.4**

In the ^1H NMR spectrum 2.1 for [2]catenane **2.4** at room temperature was in the fast exchange region for dipyridinium units. The signal at 6.24 ppm (s, 4H) belonged to

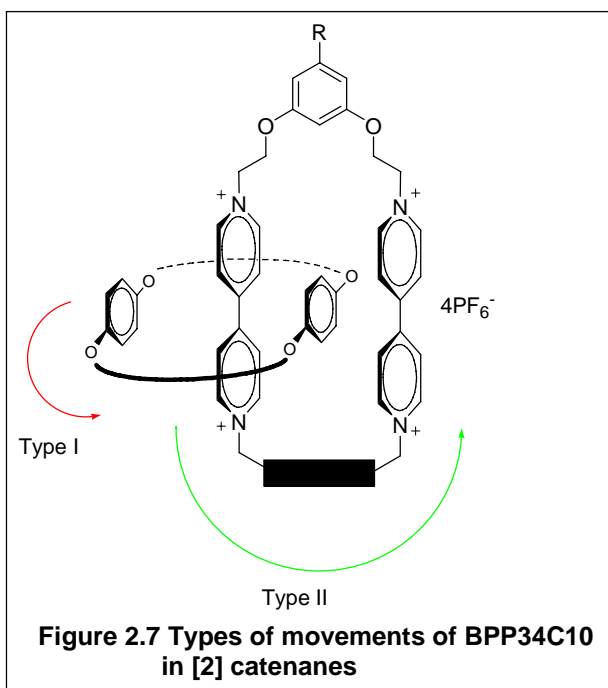


the methylene protons on the 1,3-xylyl tether because they were adjacent to the cationic nitrogen. Also the signals at 8.97 ppm for α' proton in **2.17b** shifted to 9.18 ppm because of this cationic nitrogen. The H_a was located 5.53 ppm (s, 1H). The signals at 6.74 ppm (t, $J=2.1$ Hz, 1H), 6.54 ppm (d, $J=2.1$ Hz, 2H) was assigned to H_c and H_b , respectively. There was little difference compared to the counterparts in the precursor. The signals of the protons of 1,3-xylyl tether ring were located between 8.24 ppm-8.18 ppm,

overlapping with the peaks for the β , β' protons on the dipyrindinium units.



For the dipyrindinium units (**Figure 2.6**), the signals of H_a shifted from 9.34 ppm (compound **2.17b**) to 9.29 ppm (catenane **2.4**) because they were partially shielded by the BPP34C10 ring. The signals of β , β' protons shifted from 8.01 ppm and 8.68 ppm (compound **2.17b**) to 8.31 ppm and 8.21 ppm because of the newly-produced cationic nitrogen connected to the 1,3-xylyl in the catenane **2.4**.



As we discussed before, there are three types of movements of the BPP34C10 crown ether ring in [2]catenanes.³¹ Type I (red arrow in **Figure 2.7**) is the rotation of BPP34C10 around one of the dipyrindinium unit as an axle. At room temperature, this movement was in a intermediate exchange region and the

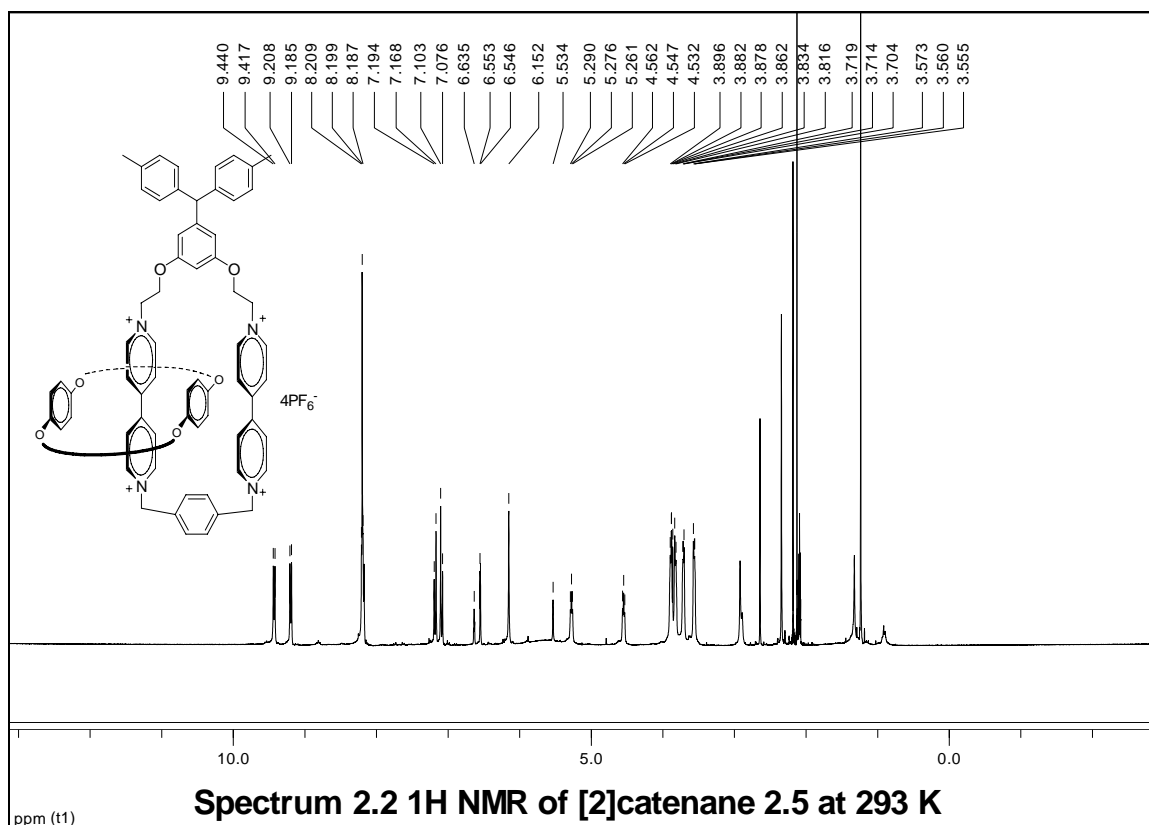
signals were near coalescence. At 3.83 ppm, a broad set of signals was attributed to the protons on the α , β , γ positions on the aliphatic chain of the BPP34C10. A slow rotation of BPP34C10 can explain the broadness. Since the internal p-phenylene ring of the BPP34C10 was shielded by both dipyridinium units and the external phenyl ring was interacted with only one dipyridinium unit, the internal p-phenylene ring should have a more downfield chemical shift than the external p-phenylene ring. However, internal and external phenyl rings of the BPP34C10 exchanged just fast enough to give an absence of these signals.

In the mass spectrum (ESI), the peak at $m/z = 801.0$ corresponded to the loss of two hexafluorophosphate anions ($[M+2PF_6]^{2+}$). We also observed the peaks at $m/z = 485.6$ ($[M+PF_6]^{3+}$), $m/z = 327.9$ (M^{4+}) which indicated loss of additional anions.

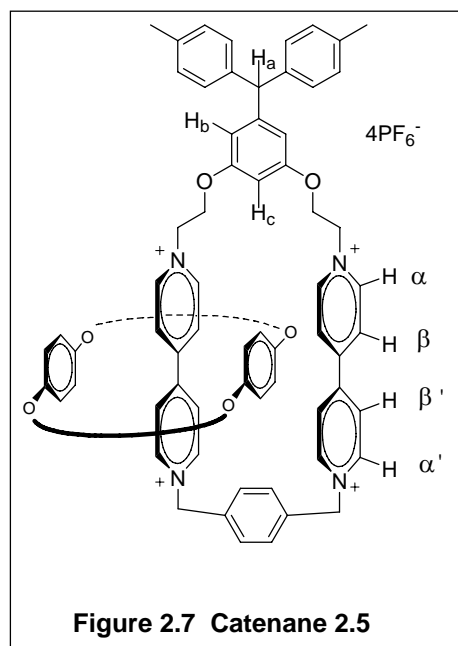
In the ^{13}C NMR spectrum of [2]catenane **2.4**, the number of carbons was consistent to the structure of the molecule. All the spectra and data supported the structure of the desired catenane.

2.4.2 Characterization of [2]Catenane 2.5

The 1H NMR of [2]catenane **2.5** was similar to that of [2]catenane **2.4** except some subtle differences. The signal for the H_α (**Figure 2.7**) shifted downfield from 9.34 ppm to 9.44 ppm (**Spectrum 3.2**). H_α' shifted from 8.97 ppm to 9.21 ppm because



of the effect of the cationic nitrogen. The chemical shifts of H_β , $\text{H}_{\beta'}$ and protons on the



1,4-xylyl ring were the same (at 8.18 ppm) and they were overlapped to form a broad, complicated signal. The chemical shifts for H_a (5.53 ppm (s, 1H)), H_b (6.55 ppm (d, $J=2.1$ Hz, 2H)), H_c (6.63 ppm (t, $J=2.1$ Hz, 1H)) were similar to those in [2]catenane 2.4. The signal at 6.15 ppm was assigned to the methyl protons in the 1,4-xylyl tether. The two triplets at 5.27 ppm and 4.54 ppm belonged to the

protons in the ethoxy spacer.

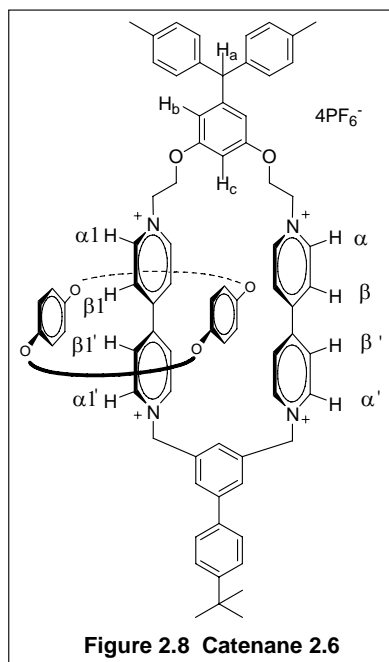
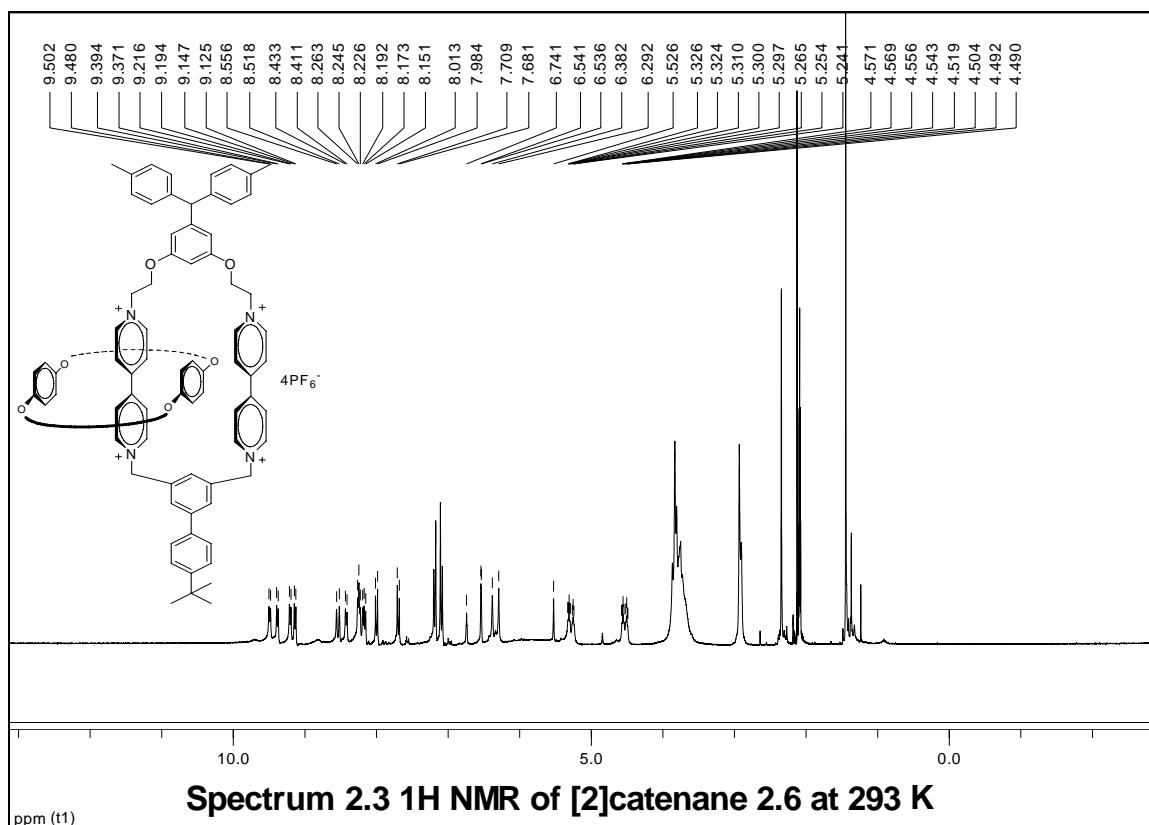
There were four broad peaks from 3.89 ppm to 3.56 ppm. They corresponded to the α , β , γ ether positions of the BPP34C10 group. As described above, the broadness could result from the intermediate exchange of BPP34C10 around the dipyridinium units.

In the ^{13}C NMR spectrum of [2]catenane **2.5**, the number of carbons was consistent with the structure of the molecule.

The mass spectrum (ESI) had the analogous species as [2]catenane **2.4** because they both had the same formula and similar structures. The peak at $m/z = 800.9$ corresponded to the dication ($[\text{M}+2\text{PF}_6^-]^{2+}$) with the loss of two hexafluorophosphate anions. The peaks at $m/z = 485.6$ was assigned to $[\text{M}+ \text{PF}_6^-]^{3+}$ (loss of three hexafluorophosphate anions) and $m/z = 327.9$ to M^{4+} (loss of all four hexafluorophosphate anions).

2.4.3 Characterization of [2]Catenane 2.6

The ^1H NMR of [2]catenane **2.6** at room temperature was quite different from those of [2]catenane **2.4**, **2.5** (**Spectrum 2.3**) in that it was in the slow exchange region. Two sets of signals were observed in the region for the protons of the dipyridinium units. As seen in **Figure 2.8**, the BPP34C10 ring was stuck on the one side of the dipyridinium unit because the blocking groups were both on the top and the bottom. The BPP34C10



ring was unable to circumrotate freely from one dipyrrolium to another. The protons on the left dipyrrolium unit ($\text{H}\alpha_1$, $\text{H}\alpha_1'$, $\text{H}\beta_1$, $\text{H}\beta_1'$) were shielded by the two p-phenylene ring of the BPP34C10 while the protons on the right side ($\text{H}\alpha$, $\text{H}\alpha'$, $\text{H}\beta$, $\text{H}\beta'$) interacted with only one p-phenylene ring of the crown ether ring. Those protons were not identical to their counterparts any more. The signals at 9.49 ppm and 9.38 ppm corresponded to $\text{H}\alpha$, $\text{H}\alpha_1$, respectively. More likely, $\text{H}\alpha$

was located at 9.49 ppm because it was more electron-deficient than H α 1 which interacted with the BPP34C10 more. The chemical shifts of H α ’, H α 1’ were 9.20 ppm and 9.13 ppm. The signal at 9.13 ppm more likely belonged to H α 1’ due to the shield by the BPP34C10.

Since there was ethyl spacers between the dipyridinium and the resorcinol moiety, the effect of BPP34C10 on resorcinol was so little that only one set of signals were observed (6.74 ppm (t, J=2.1 Hz, 1H) for H_c, 6.54 ppm (d, J=2.1 Hz, 2H) for H_b, 5.53 ppm (s, 1H) for H_a). However, the methylene groups adjacent to cationic nitrogen were influenced by the BPP34C10. There were two sets of signals observed. The singlets at 6.38 ppm (s, 2H) and 6.29 ppm (s, 2H) corresponded to the methylene protons on the substituted xylyl tether. The triplets at 5.32 ppm (t, J = 4.7 Hz, 2H), 5.25 ppm (t, J = 4.7 Hz, 2H), 4.56 ppm (t, J=4.7 Hz, 2H), 4.49 ppm (t, J=4.7 Hz, 2H) were assigned to the protons on the ethyl spacers.

The signals in the ¹³C NMR spectrum were complicated and hard to tell the numbers of carbons.

2.5 Variable Temperature ¹H NMR Study of [2]Catenanes

Once the structures of [2]catenanes were confirmed, the thermal properties of those catenanes were examined. Variable temperature ¹H NMR was performed on the

Varian 300 MHz or 400 MHz instruments.

As described before, in [2]catenanes **2.4** and **2.5**, the BPP34C10 circumrotated in the intermediate exchange region at room temperature so that the signals for the p-phenylene hydrogens could not be observed. The dipyridinium signals were rapidly exchanging at this temperature. When the samples (catenane **2.4** and **2.5**) were cooled down, the BPP34C10 rotated and translocated slowly enough on the NMR timescale to display the slow exchange spectra.

The free energy of activation³⁸ was calculated according to the following equation (2.1):

$$\Delta G^\ddagger_C = 4.58 T_C [9.972 + \log (T_C/\Delta\nu)] \text{ cal mol}^{-1} \quad (2.1)$$

Where T_C (K) is the coalescence temperature and $\Delta\nu$ (Hz) is the frequency difference of the separation between the two signals in the absence of exchange.

This equation is derived from the Eyring equation (2.2).

$$k = (k_B T/h) e^{-\Delta G^\ddagger/RT} \quad (2.2)$$

The equation changed to 3.3 if we take logarithms for this equation.

$$\Delta G^\ddagger_C = 4.58 T_C [10.32 + \log(T_C/k_C)] \text{ cal mol}^{-1} \quad (2.3)$$

$$k_C = 2.22 \Delta\nu \quad (2.4)$$

If we insert expression 2.4 into 2.3, we obtain equation 2.1.

However, determination of the coalescence temperature was subjective as pointed

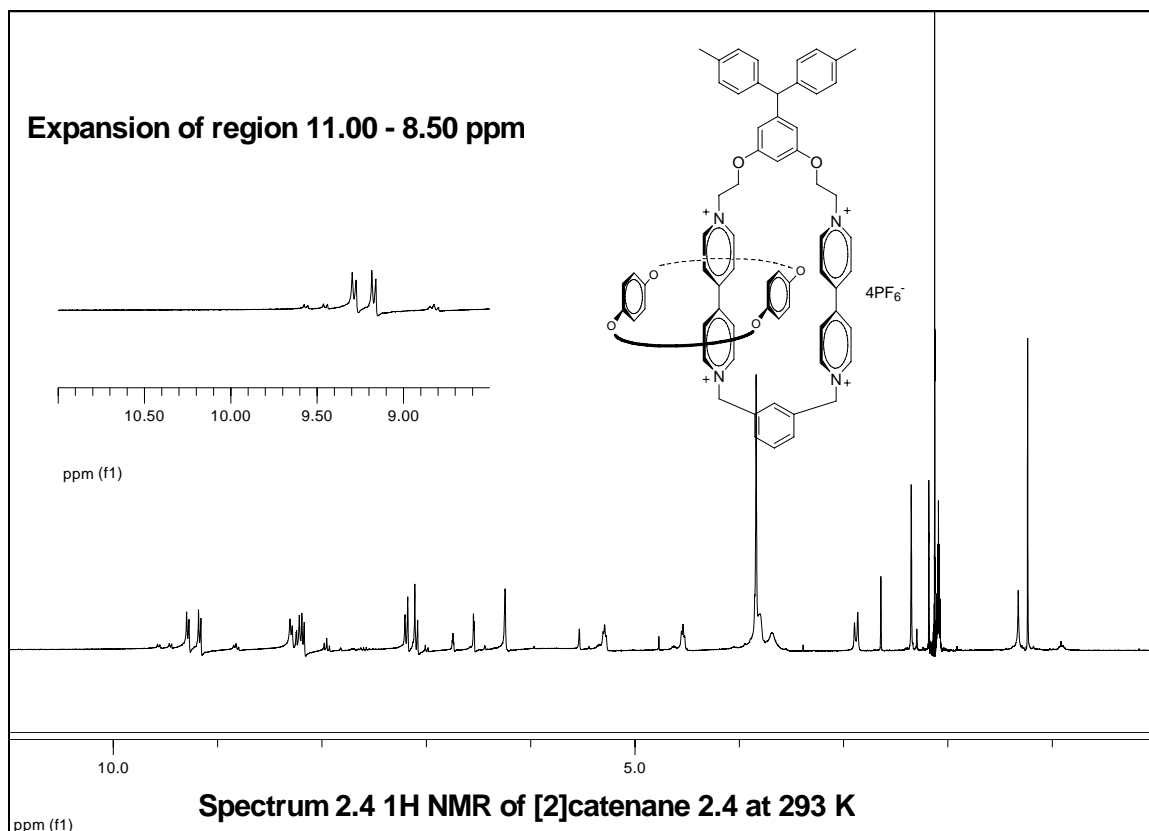
out by Friebolin: “Absolute values can seldom be measured with an accuracy better than $\pm 2\text{K}$.” The error of $\Delta G^\ddagger_{\text{C}}$ could be $\pm 0.2 \text{ kcal mol}^{-1}$ from this inaccuracy. When we determined coalescence temperature, we rounded it to the nearest five degrees which would not affect the calculation of free energy of activation very much. Also we rounded the free energy of activation to nearest $0.5 \text{ kcal mol}^{-1}$ to be consistent with the error in temperature measurements.³⁸

The stacked plots of different spectra at various temperatures clearly showed the coalescence process. All the samples were examined in d_6 -acetone and an internal standard was set at 2.05 ppm for d_6 -acetone. The coalescence temperature was determined at the intermediate exchange of an appropriate proton signal. It is worthwhile to note that it does not matter which proton signal was picked and the free energy of activation should be the same because they were affected by the same process of rotation of BPP34C10. Lower coalescence temperature of a certain proton (T_{C}) will be accompanied with higher frequency difference of the separation ($\Delta\nu$).

2.5.1 Variable Temperature ^1H NMR of [2]Catenane **2.4**

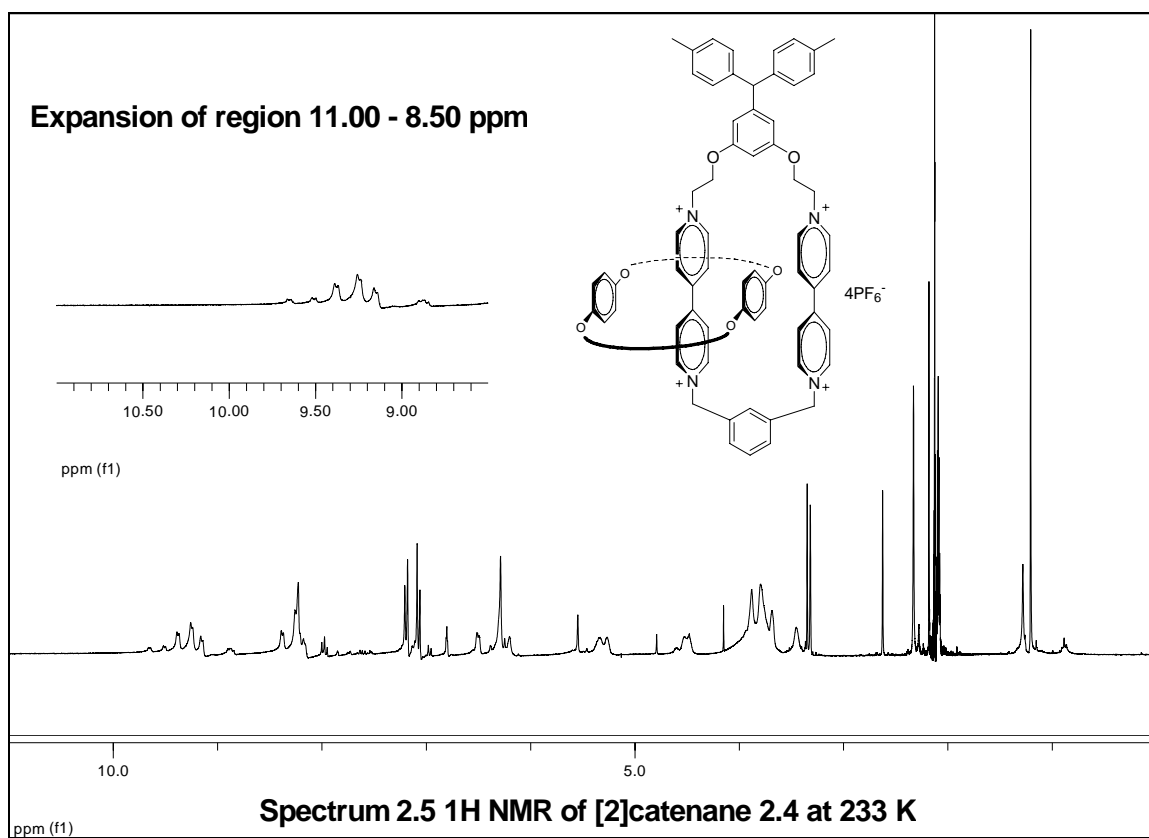
For [2]catenane **2.4**, the α , α' protons adjacent to cationic nitrogen were used to determine the free energy of activation. At higher temperature (20°C), two doublets of doublets were observed between 9.50 – 9.00 ppm (**Spectrum 2.4**) due to the fast change

of two conformations. At lower temperature (-40 °C, 233 K), three

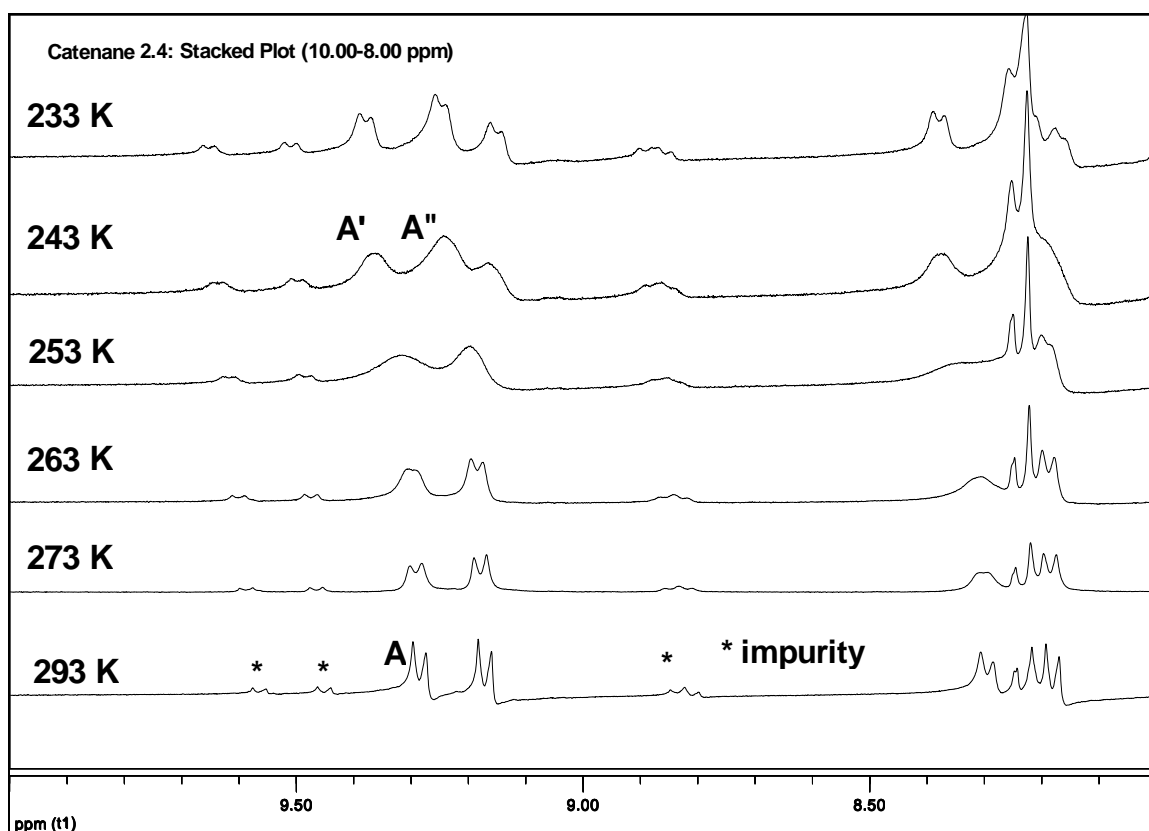


signals showed up in the region 9.50 -9.00 ppm (**Spectrum 2.5**) because of slow change of two isomers. Four signals should actually have been expected but two in the middle appeared to be overlapped. The frequency difference of the separation of the exchanging resonance ($\Delta\nu$) between A' and A'' (**Spectrum 2.6**) was 39.3 Hz. The coalescence temperature was determined to be 255 K. According to the calculation, the free energy of activation for circumrotation was 12.5 kcal mol⁻¹.

The stacked plots (**Spectrum 2.6**) display the changing progress of signals between 10.00-8.00 ppm from the higher temperature to lower temperature. At 293 K,



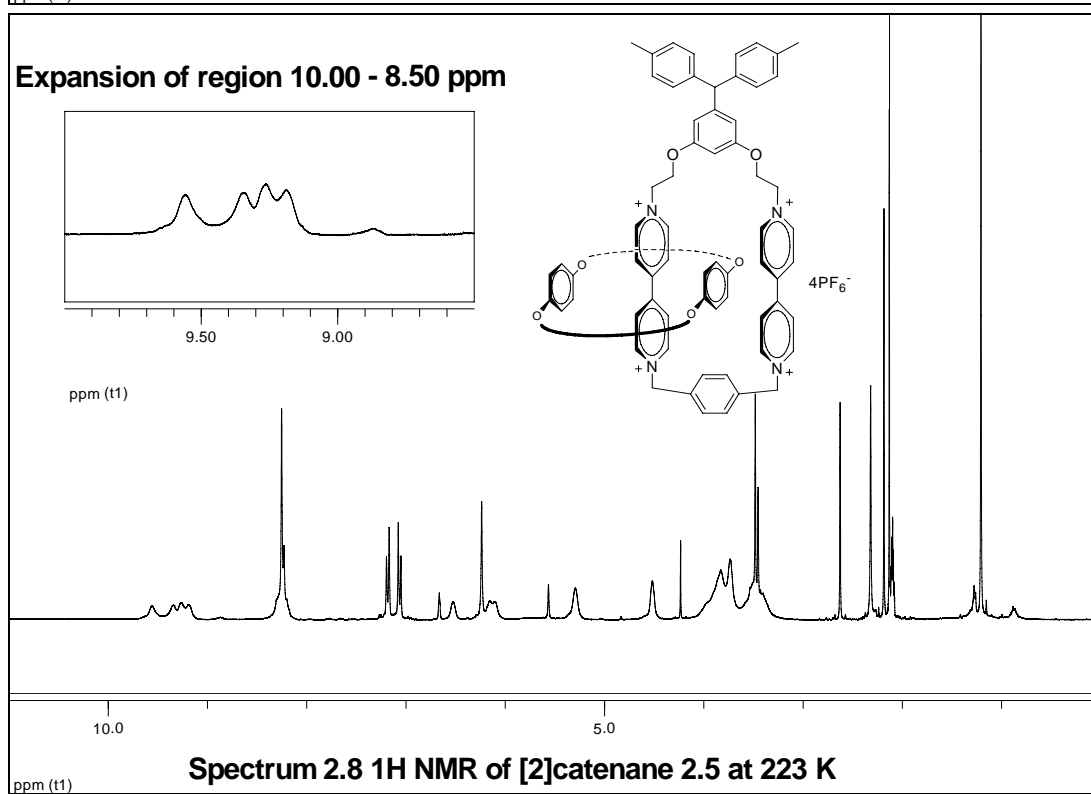
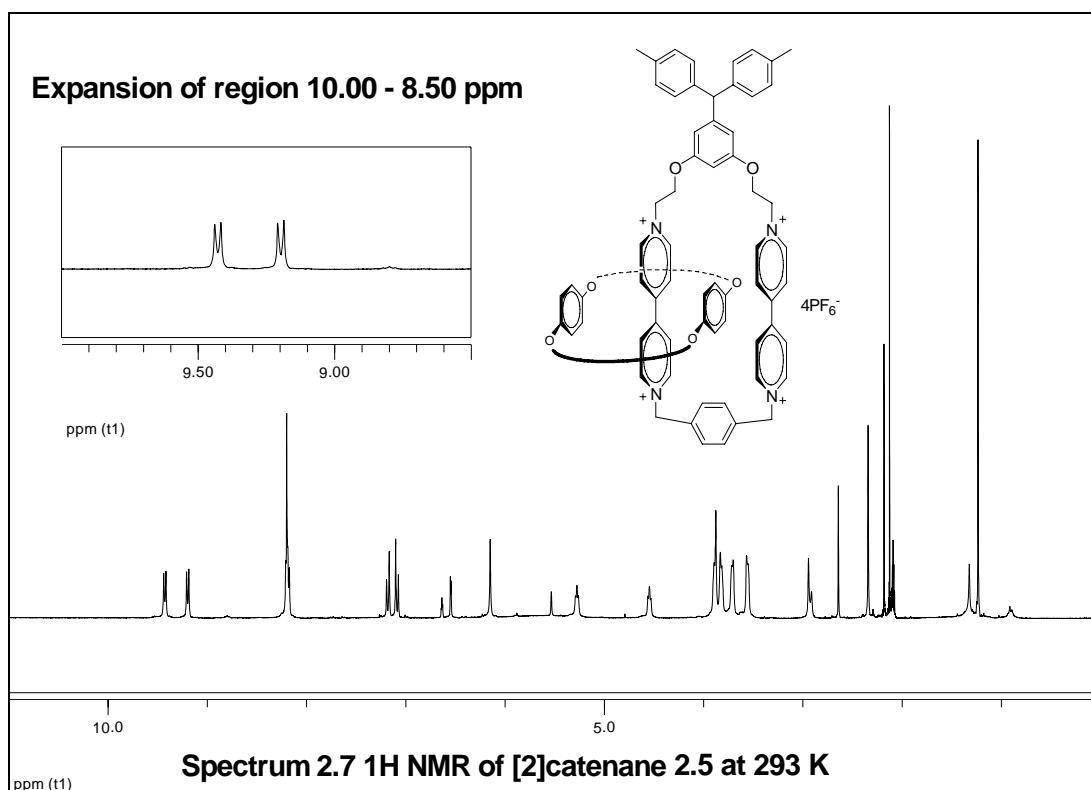
the signals were sharp doublets of doublets (9.50- 9.00 ppm) because of the fast exchange of conformations. With the decreasing of the temperature, the slow exchange of two conformations resulted in a broad signal. At low temperature, three distinct doublets showed up, which approached the slow exchange.



Spectrum 2.6 Stacked Plot of [2]Catenane 2.4

2.5.2 Variable Temperature ^1H NMR of [2]Catenane 2.5

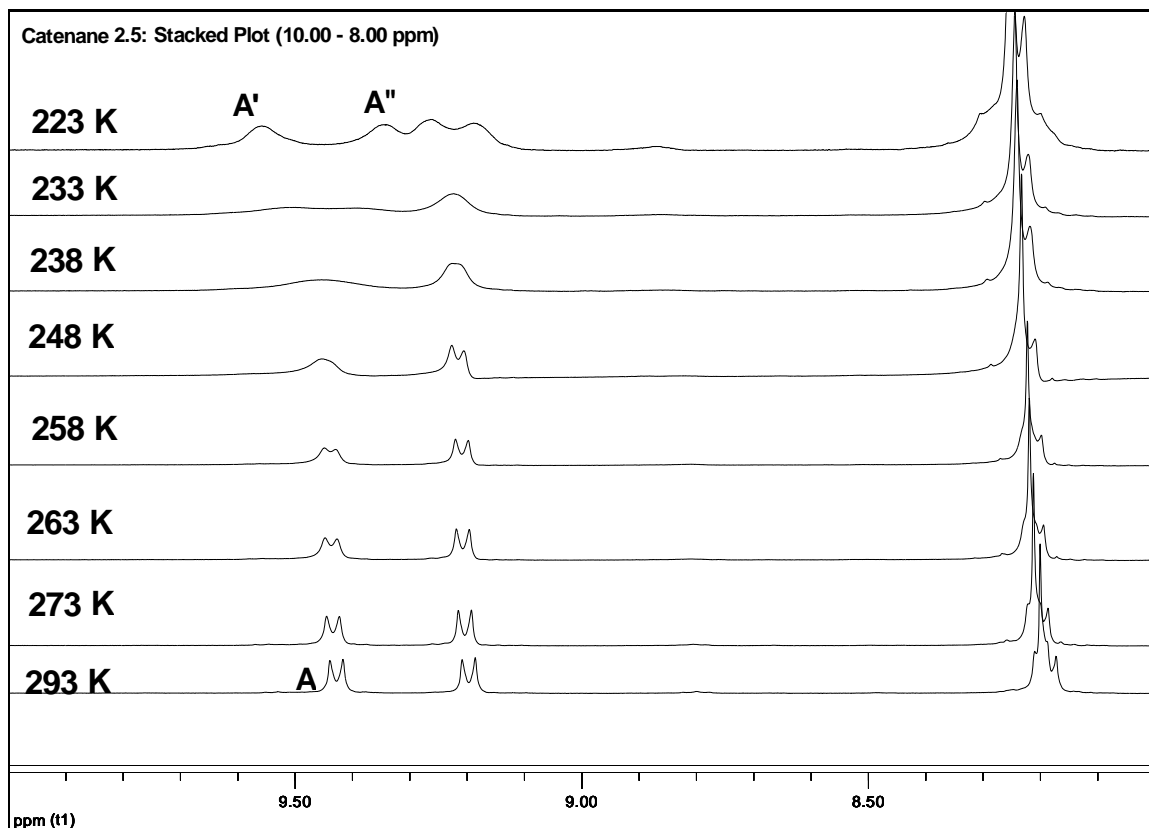
The protons which were selected to determine the free energy of activation for [2]catenane **2.5** containing 1,4-xylyl tether were also the α , α' protons adjacent to cationic nitrogen. At 293 K, the signals between 10.00 – 8.50 ppm were two multiplets (**Spectrum 2.7**). The fast exchange of two isomers of this catenane made the peaks sharp. At 223 K, four signals were observed between 10.00 – 8.50 ppm (**Spectrum 2.8**) as expected.



From the set of VT NMR spectra, the frequency difference of the separation of the exchanging resonance ($\Delta\nu$) between A' and A'' (**Spectrum 2.9**) was measured 64.8 Hz and the coalescence temperature for those protons was 241 K (-32 °C).

According those data, the free energy of activation was calculated to be 11.6 kcal mol⁻¹.

The stacked plot (**Spectrum 2.9**) indicated the change of the signals for proton A



Spectrum 2.9 **Stacked plot of [2]catenane 2.5**

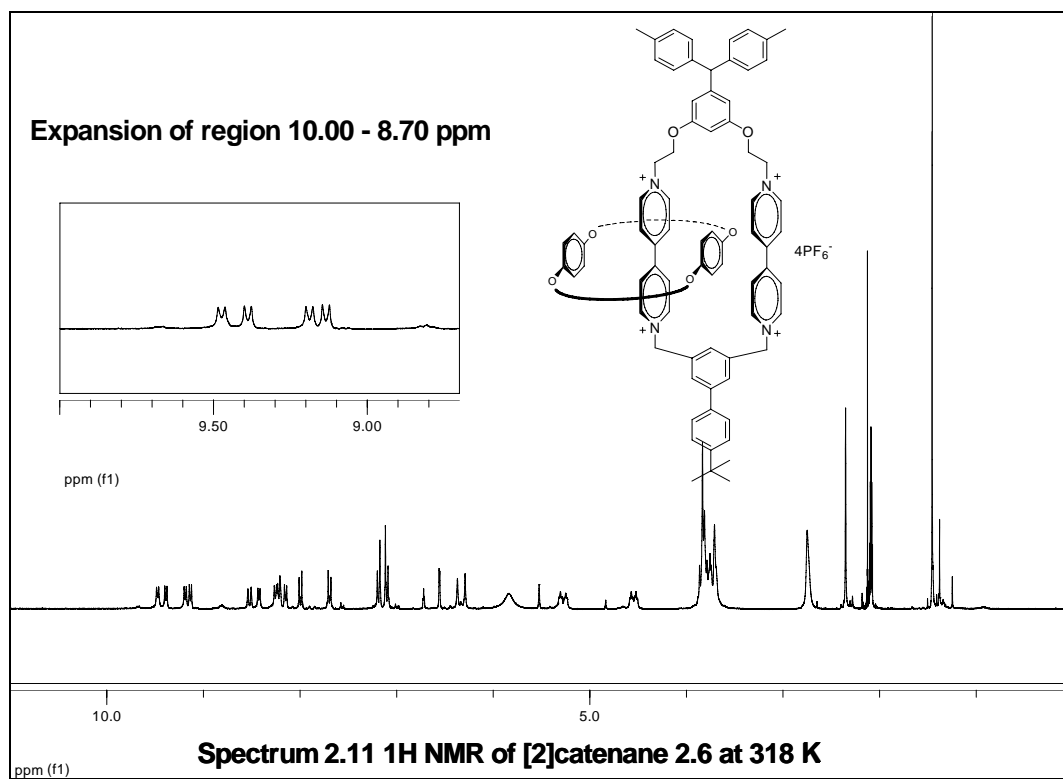
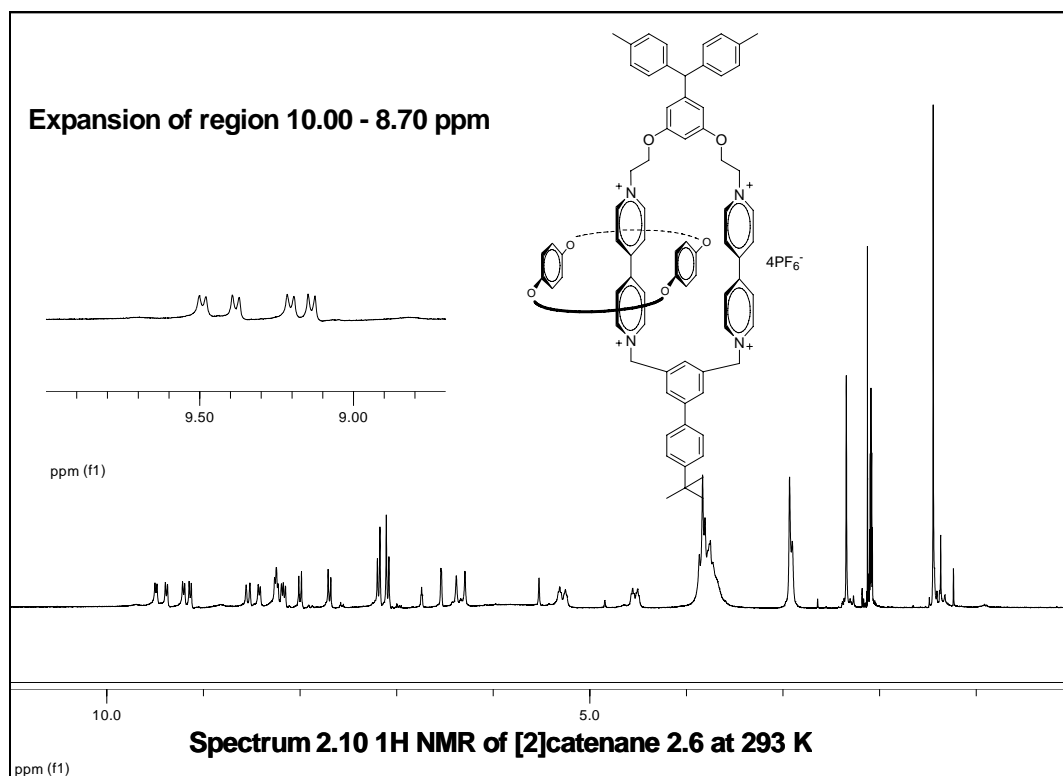
at different temperatures from 293 K to 223 K. At 293 K, a sharp doublet was observed for proton A. When the temperature approached 238 K, the signal became almost flat because this was close to the coalescence temperature. When the temperature continued

to decrease until 223 K, two signals A' and A'' demonstrated the slow exchange of two isomers of this catenane. As we mentioned previously, it does not matter which proton we picked to calculate the free energy of activation. To demonstrate this, if we picked the signal adjacent to the signal A to calculate the free energy of activation, it is also close to 11.6 kcal mol⁻¹ (calculated 11.7 kcal mol⁻¹) because the coalescence temperature is 233 K although the $\Delta\nu$ became 21.4 Hz.

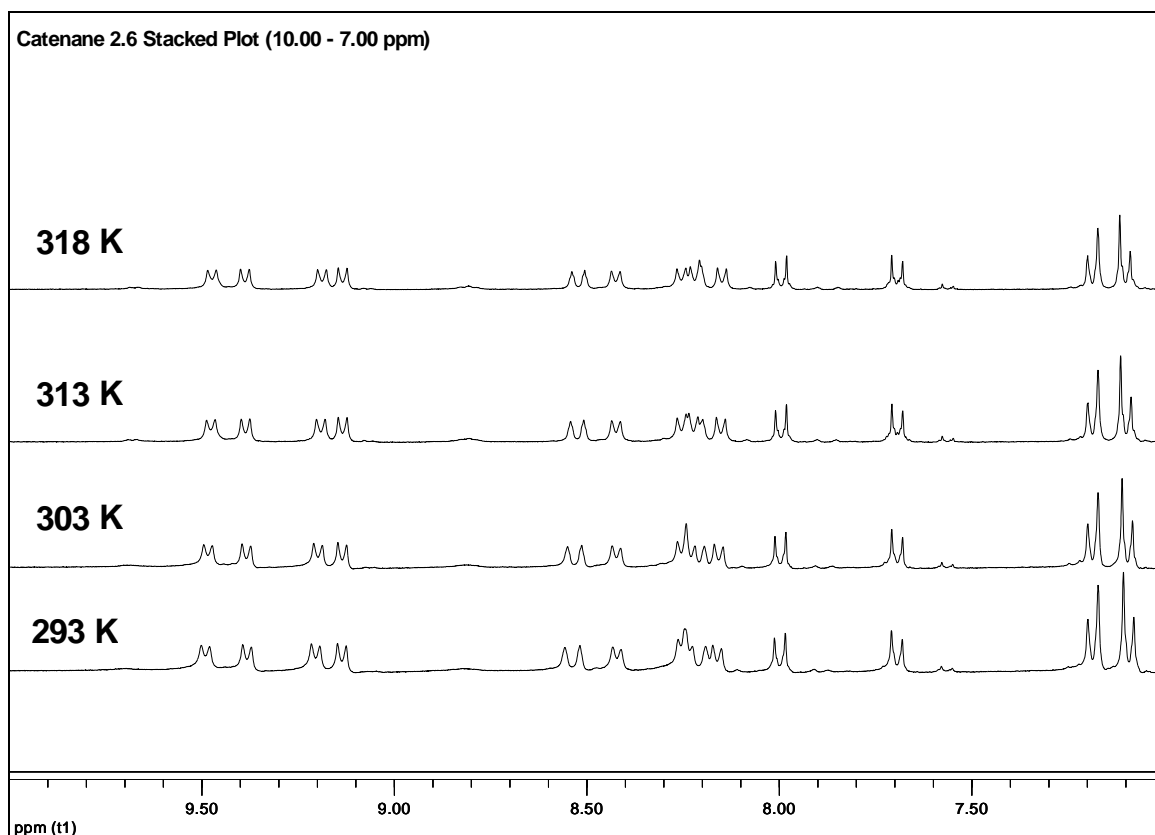
2.5.3 Variable Temperature ¹H NMR of [2]Catenane **2.6**

For [2]catenane **2.6**, the top and the bottom tethers were both blocked. The BPP34C10 ring couldn't circumrotate freely from one side to the other. At room temperature, two sharp sets of doublets of doublets were observed between 10.00 – 8.00 ppm (**Spectrum 2.10**).

Increasing the temperature didn't change dipyridyl portion of the spectrum (**Spectrum 2.11**) although the signals for the p-phenylene aromatic hydrogens on the BPP34C10 started to appear at 5.8 ppm. The boiling point of d₆-acetone limited the possibility of approaching higher temperature to observe the coalescence for this catenane. The coalescence temperature should be more than 55 °C and the frequency difference of the separation of the exchanging resonance ($\Delta\nu$) was 25.5 Hz. The free energy of activation should be significantly more than 18 kcal mol⁻¹.



The stacked plot of spectra (**Spectrum 2.12**) at different temperatures showed no change from 293 K to 318 K.



Spectrum 2.12 Stacked plot of [2]catenane 2.6

2.6 Summary and Conclusions

From the discussion above, three [2]catenanes were synthesized. Along with three other [2]catenanes prepared by Dr. David E. Martyn, the data of free energies of activation, frequency difference, coalescence temperatures of six [2]catenanes (see **Figure 2.7**) are summarized in Table 2.1. These data have been published in *Organic Letters*.

Table 2.1 Summary of Data of [2]Catenanes 2.1-2.6³³

[2]catenane	R		Coalescence temperature (K) ^a	Frequency difference (Hz)	Free energy of activation (kcal mol ⁻¹) ^b
2.1	H	1,3-xylyl	240	15.8	12
2.2	H	1,4-xylyl	220	19.5	11
2.3	H	t-butylphenyl-1,3-xylyl	255	22.3	13
2.4	ditolylmethyl	1,3-xylyl	255	39.3	12.5
2.5	ditolylmethyl	1,4-xylyl	240	64.8	11.6
2.6	ditolylmethyl	t-butylphenyl-1,3-xylyl	>335	25.5	>18 ^c

a) approximated to the nearest 5 K

b) an error of 5K in the coalescence temperature corresponds to ± 0.2 kcal mol⁻¹ error of free energy of activation

c) No exchange observed by 2D ¹H NMR EXSY

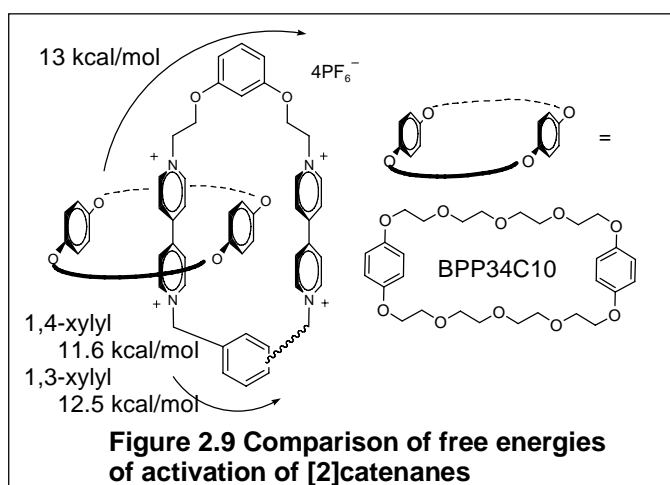
From this table, it indicated that the energy barrier required for BPP34C10 to pass over either the unblocked resorcinol and 1,3-xylyl tethers is 11.6 kcal mol⁻¹ (in [2]catenane **2.1**). However, for [2]catenane **2.3**, the energy barrier required for circumrotation of BPP34C10 was 13 kcal mol⁻¹, which is 1 kcal mol⁻¹ higher than that in [2]catenane **2.1** even BPP34C10 could pass over the same top unblocked resorcinol tether. If the equation: $\Delta G = \Delta H - T\Delta S$ is referred, the explanation could be the increasing entropy due to more pathways in [2]catenane **2.1**.

Interestingly, the energy barrier required to pass over 1,3-xylyl tether in [2]catenane **2.1** is 12 kcal mol⁻¹ while the energy barrier required for 1,4-xylyl in [2]catenane **2.2** is 11 kcal mol⁻¹. Similarly, the energy barrier required to pass over 1,3-xylyl tether in [2]catenane **2.4** is 12.5 kcal mol⁻¹ while the energy barrier required for

1,4-xylyl in [2]catenane **2.5** is $11.6 \text{ kcal mol}^{-1}$. It could be concluded that passage over 1, 3-xylyl tether required higher energy than passage over 1, 4-xylyl tether. Energetically, passage over the narrower, more tightly turning 1, 3-xylyl tether demands more energy than the longer, wider 1, 4-xylyl tether.

Passage over 1,3-bis(ethoxy) tether in resorcinol moiety requires 13 kcal mol^{-1} , similar to 1, 3-xylyl tether in [2]catenane **2.4**.

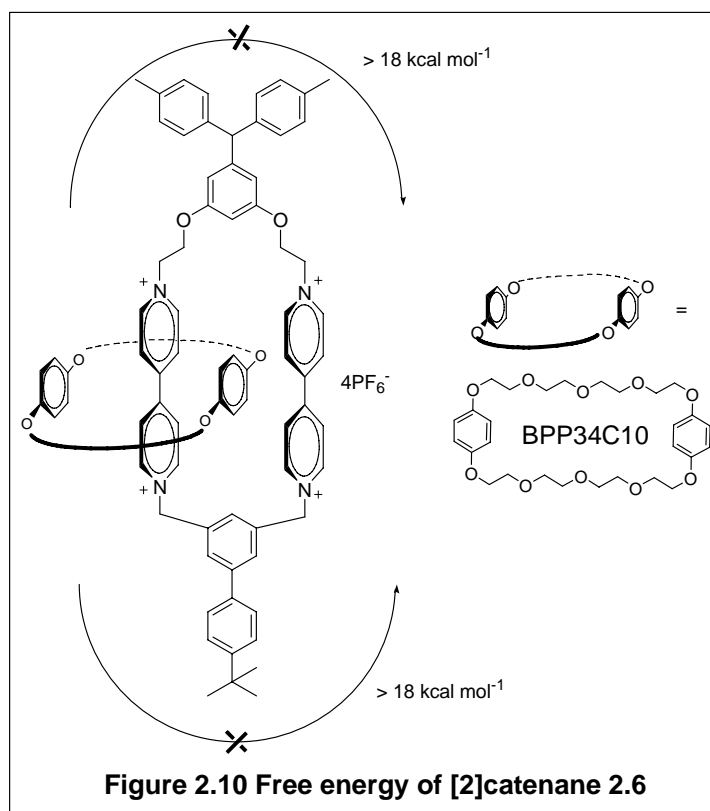
A graphic summary of the energy barriers required for different pathways is



described in **Figure 2.9**. The energy barriers data are based on either top blocked or bottom blocked. When both tethers are blocked (**Figure 2.10**), the energy barrier required for circumrotation of BPP34C10 is more than 18

kcal mol^{-1} . We do not know what the actual free energy of activation would be because of the limit of the boiling point of solvent.

In conclusion, when blocking groups were appended on the tethers of [2]catenanes, it was possible to control the path selection of circumrotation of BPP34C10 around the dipyrrolium macrocycle. If the top was blocked, the BPP34C10 could



translocate along the bottom tether. If the bottom was blocked, the BPP34C10 would pass over the top tether. If both the top and the bottom were blocked, no circumrotation of BPP34C10 was observed. If both were open, the BPP34C10 ring could move freely along either the top or the bottom. The energy barriers required for different pathways were: 13 kcal mol⁻¹ for 1, 3-bis(ethoxy) tether, 12.5 kcal mol⁻¹ for 1,3-xylyl and 11 kcal mol⁻¹ for 1,4-xylyl tether. We demonstrated that the ability of the selective movement of one ring round another ring can be achieved along different pathways.

Chapter 3

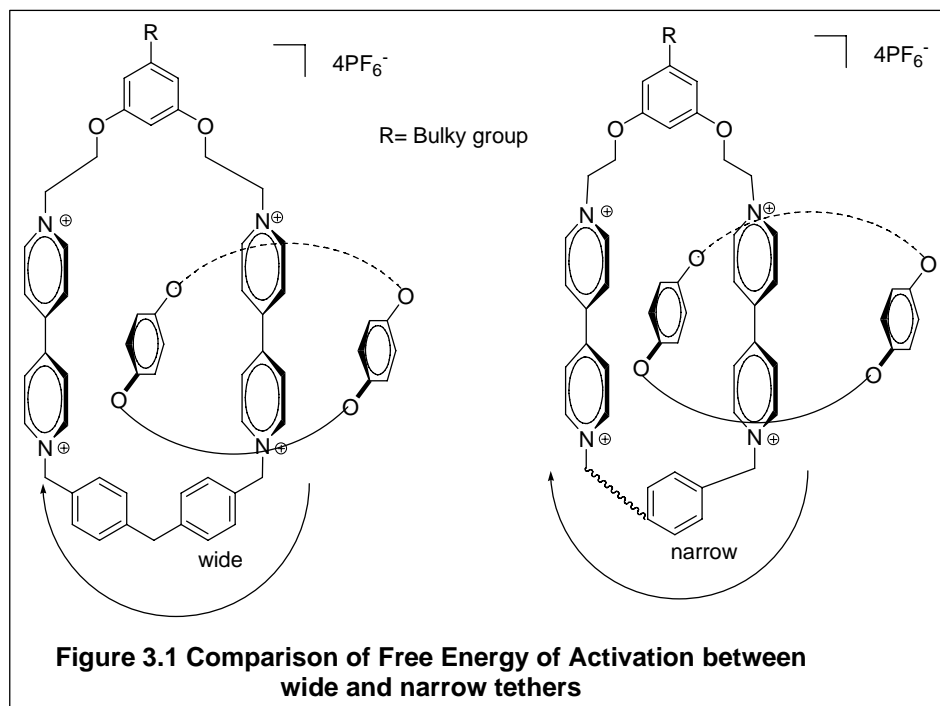
Synthesis and Study of Symmetric [2]Catenanes with Wider Rigid Tethers

3.1 Design of [2]Catenanes with Wider Rigid Tethers

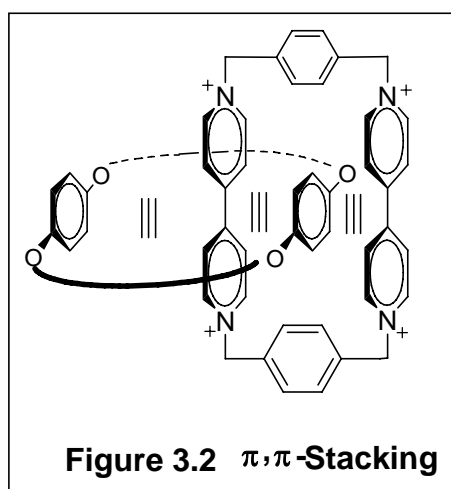
As described in chapter 2, in the resorcinol-based bistable [2]catenanes we developed, it is possible to control the molecular motion of the BPP34C10 by blocking or unblocking two different pathways for translocation. For further study, we planned to determine the effect of changing the size or length of tethers on the energy barrier required for circumrotation of BPP34C10.

To determine the size effect, we introduced wider, unblocked or blocked bottom tethers, based on bis(4-methylphenyl)methane, while we kept the top resorcinol-based tethers. We anticipated that wider tethers would require lower energy for BPP34C10 to pass over than the narrow 1, 3-xylyl or 1,4-xylyl tethers (**Figure 3.1**) in terms of geometry. In the new system, the wider bis(4-methylphenyl)methane and its blocked counterpart were used instead of narrow 1,3-xylyl, or 1,4-xylyl tethers. If the top pathways derived from resorcinol were both blocked in two different systems, comparing the free energy of activation for BPP34C10 to pass over the bottom different pathways in two different systems would tell us in which system BPP34C10 ring could circumrotate more easily and require less energy. On the other hand, a blocked counterpart of

bis(4-methylphenyl)methane was incorporated to figure out if circumrotation of BPP34C10 would still be blocked in the system with wider tethers.



As reviewed in chapter 1, Stoddart *et al.*^{31,39,40,41} pointed out that the internal



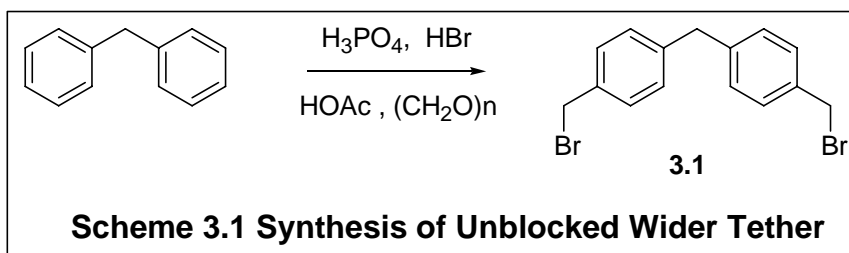
hydroquinone ring of BPP34C10 π - π -stacked with both dipyridinium moieties in their tetracationic cyclophane in [2]catenanes while the external hydroquinone ring interacted with only one dipyridinium unit (**Figure 3.2**). This conclusion was based on the ^1H NMR observations. This phenomenon was also observed by us in the

resorcinol-derived [2]catenanes we developed in chapter 2. In the ^1H NMR spectrum of the BPP34C10 in [2]catenanes at low temperature, the chemical shift of the hydroquinone rings of BPP34C10 was around 6.1 and 3.8 ppm. These peaks were averaged at 5.0 ppm at room temperature in the resorcinol-based [2]catenanes in chapter 2 due to intermediate exchange between these widely spaced signals. The explanation could be that the electron rich BPP34C10 was shielded by both electron deficient dipyridinium moieties. However, this interaction could best occur at a certain distance between the hydroquinone ring of BPP34C10 and both dipyridinium moieties in the tetracationic cyclophane. If the distance were too large, this interaction would just occur between the hydroquinone ring of BPP34C10 and one dipyridinium unit with a corresponding decrease in the chemical shift difference between these two hydroquinone rings. To address this point, the ^1H NMR spectra for those catenanes should be carefully analyzed.

Furthermore, we also speculated that the energy required to pass over the same tether with different blocked groups (wide or narrow) on the bottom would be different. Since the same top tethers as in chapter 2 were used, it is readily possible to compare the difference of the energy barrier passing over the same top tether but different bottom tethers.

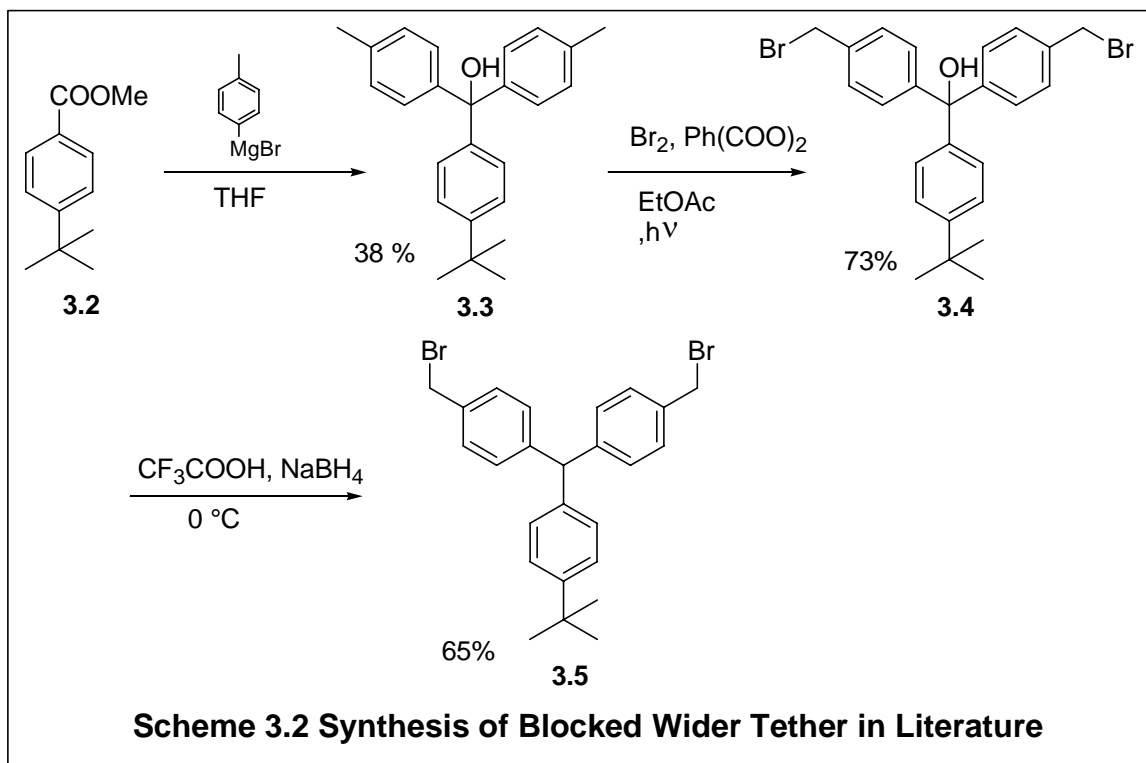
3.2 Synthesis and Characterization of the Wider Rigid Tethers

The synthesis of unblocked wider tether (**3.1**), bis(4-bromomethylphenyl)methane, was accomplished according to modification of the literature procedure (**Scheme 3.1**).⁴² Instead of gaseous HBr, aqueous conc. HBr was used in this reaction. In one pot, the diphenylmethane, paraformaldehyde, acetic acid, phosphoric acid and aqueous hydrobromic acid were mixed and refluxed 24 h. In addition to the desired product, the reaction produced the side product, 1-benzyl-4-bromomethylbenzene, with only one methylene bromide added. However, the purification of product was easily achieved via trituration.



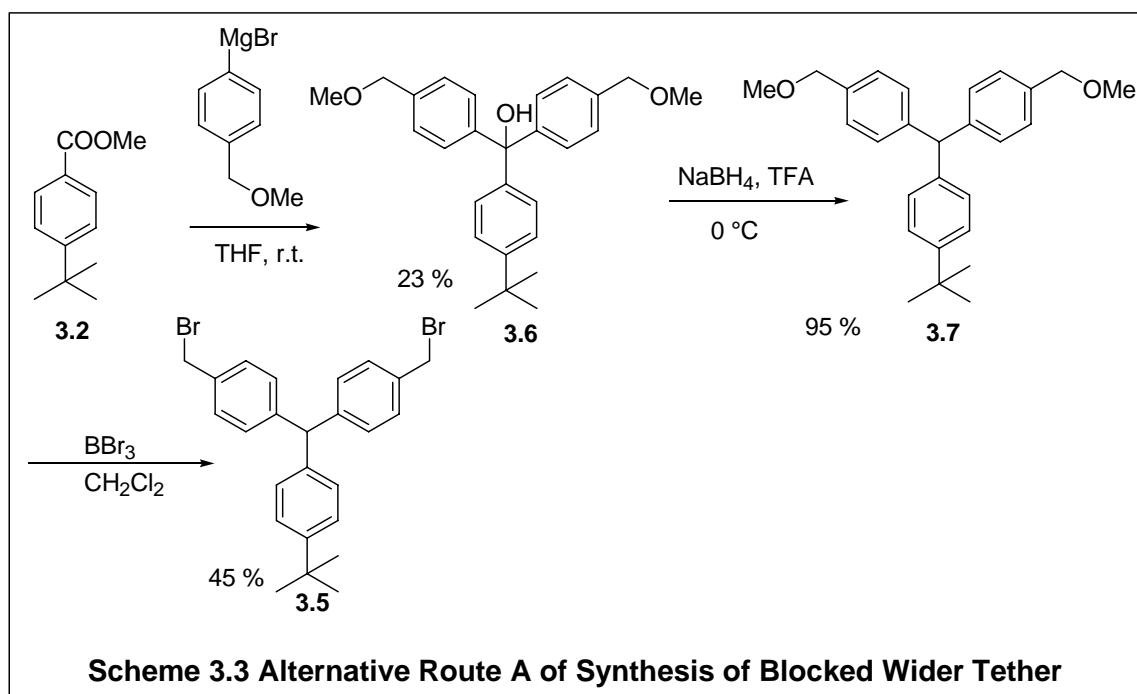
The preparation of blocked wider tether (**3.6**) was also accomplished as reported in the literature (**Scheme 3.2**).⁴³

As described in **Scheme 3.2**, methyl 4-tert-butylbenzoate reacted with excess Grignard reagent, p-methylphenyl magnesium bromide, to give triarylmethanol **3.3** in a yield of 38 %. Bis(bromomethyl) adduct **3.4** was obtained with a yield 73 % (crude) after radical bromination of the benzylic methyl groups in ethyl acetate.⁴³ The tertiary hydroxyl group in **3.4** was reduced by sodium borohydride in trifluoroacetic acid³⁵ to



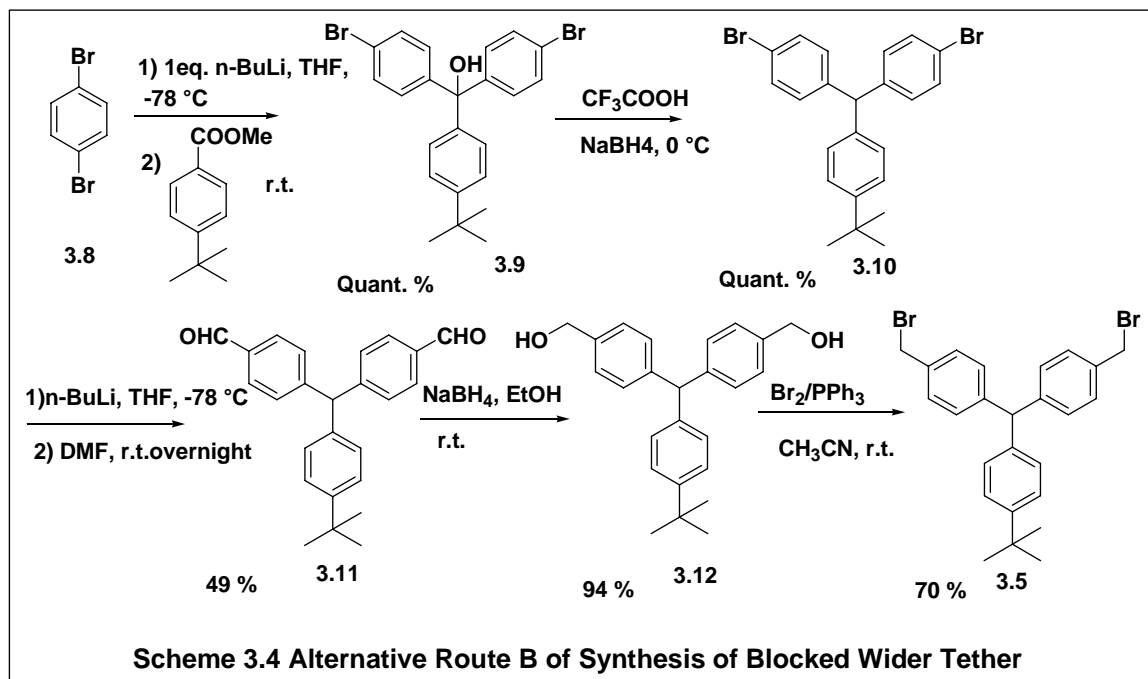
give the blocked wider tether (**3.5**) in a yield of 65 %. The total yield was 18 % for the three steps. However, the wider tether **3.5** was not pure because some over-brominated side products were unavoidably produced in the radical bromination step and affected the purity of the final product. It was later found that this impurity in the blocked wider tether would cause the later catenation to fail.

An alternative route is described in **Scheme 3.3**. p-Methoxyphenyl magnesium bromide was made from methyl-4-bromo-benzoate via 4 steps⁴⁴ and was added to the solution of 4-tert-butylbenzoate. The triarylmethanol **3.6** was obtained in only a yield of 23 %, followed by reduction with sodium borohydride in trifluoroacetic acid³⁵ to get dimethoxy intermediate **3.7**. Bromination with BBr₃ gave the tether **3.5** in a yield of 45



%.³⁶ The advantage of this route was that it avoided over-bromination and enabled better purification. The yield for the whole route was 9 %.

A second alternative route is presented in **Scheme 3.4**. 1, 4-Dibromobenzene was metal-halogen exchanged with 1 equivalent of n-BuLi solution at -78 °C, followed by addition of 4-tert-butylbenzoate to give triarylmethanol **3.9** in quantitative yield. A Gribble reduction of triarylmethanol **3.9** with sodium borohydride in trifluoroacetic acid³⁵ gave **3.10** in quantitative yield. The signal at 5.45 (s, 1H), which was attributed to the proton next to three aryl groups, indicated completion of the reduction. The aldehyde **3.11** was prepared through metal-halogen exchange with n-BuLi followed by addition of DMF and hydrolysis.⁴⁵ The yield of this transformation was moderate (49 %). Reduction followed by bromination with Br₂/PPh₃ give the blocked wider tether **3.5** in sufficient



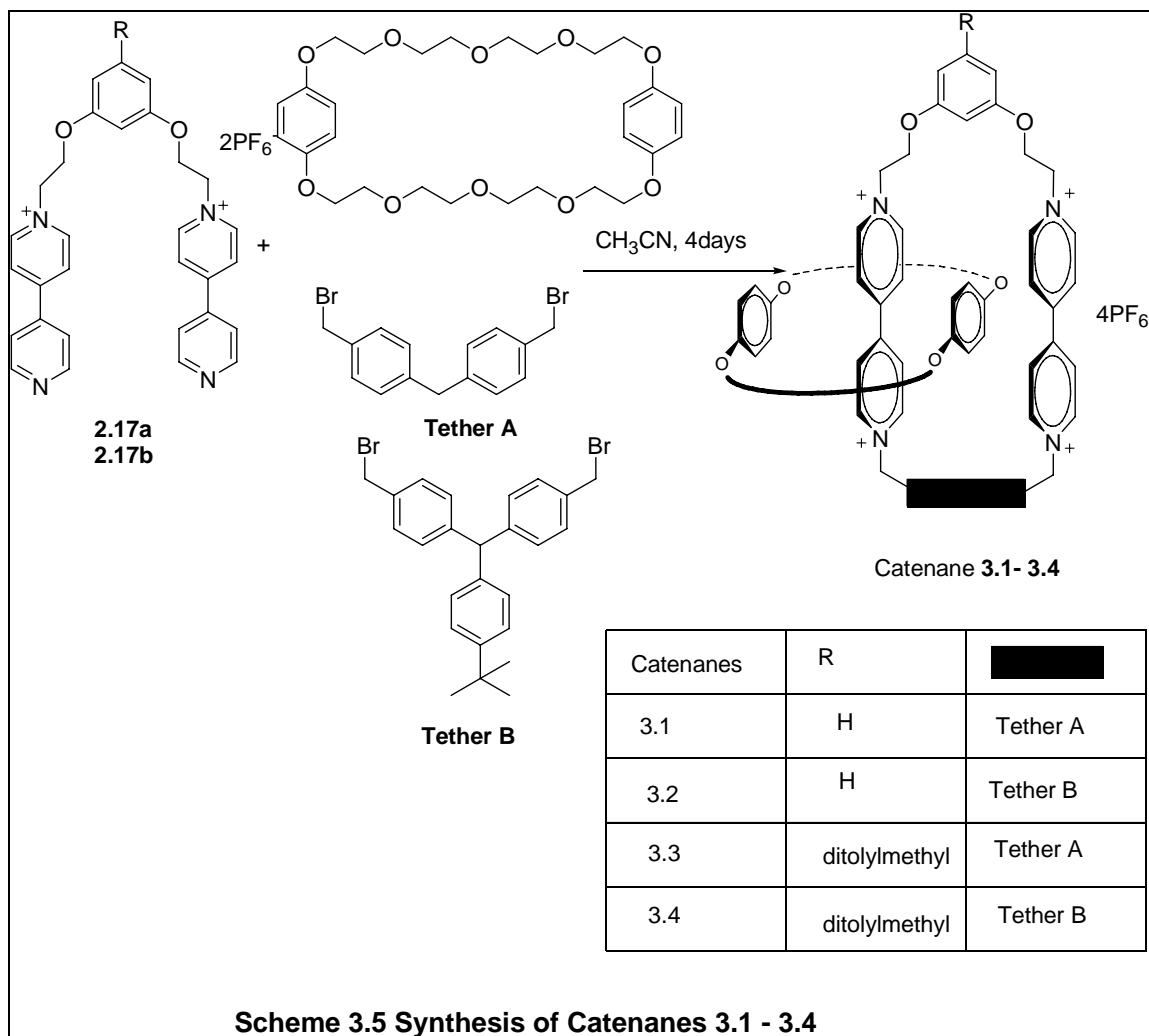
quantities. In the mass spectrum (EI+DIP), the peak at $m/z = 484$ was attributed to M (calculated $m/z = 484.04$). The peaks at 486 and 488 belonged to M+2 and M+4. The ratio of three peaks was 1:2:1, indicating the presence of two bromine atoms.

The yields for the last two steps were 94 % and 70 %, respectively. The total yield for this route was 32 %. Although there were more steps in this route compared to other routes, the yields were acceptable and the isolations for each step were fairly easy. In conclusion, the second alternative route B was the best way to prepare the blocked wider tether **3.5**.

3.3 Synthesis and Characterization of [2]Catenanes with Wider Rigid Tethers

3.3.1 Synthesis and Purification of [2]Catenanes

The synthesis of [2]catenanes **3.1-3.4** followed the procedures in Chapter 2 with some minor modification (**Scheme 3.5**).⁴⁷ The [2]catenanes were prepared through three



component reactions between one equivalent of precursor (**2.17a** or **2.17b**), 1.3 equivalents of bis(4-bromomethylphenyl)methane (**tether A** or **3.1**) or triaryl dibromide (**tether B** or **3.5**) and 1.6 equivalents of BPP34C10 in acetonitrile at room temperature for 4 days. After one day, the initial yellow solution became orange. After three days, some yellow precipitate appeared which could be attributed to the insoluble catenanes

with bromide anions or pseudo-rotaxane with bromide anions instead of hexafluorophosphate anion.

The purification of [2]catenanes also followed the procedures in chapter 2. After 4 days, in the final reaction mixture, several possible species could be present: desired [2]catenane, pseudo-rotaxane, excess BPP34C10 and unreacted dibromide. The solvent acetonitrile was first removed via rotary evaporator to give a red residue. The residue was dissolved in methanol/acetone (1:1) and the solution was loaded on the preparative TLC plate. The preparative TLC plate was eluted twice with methanol/ethyl acetate (1:1) at ca. 50 °C. The BPP34C10 moved to the top of the plate ($R_f = 0.9$). Then, the preparative TLC plate was eluted with methanol/2M ammonium chloride/nitromethane (7:2:1). The [2]catenanes moved up ($R_f = 0.3-0.5$) as an orange band while the nearly colorless oligomeric dipyridinium chain didn't move at all ($R_f = 0-0.1$).

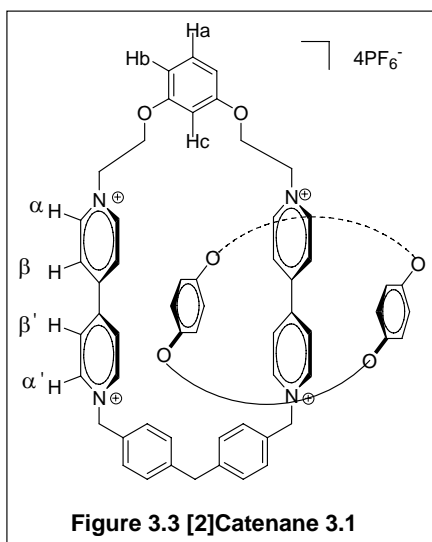
The orange/red band was removed from the plate. The silica gel containing the [2]catenanes was ground and washed with the final eluent-methanol/2M ammonium chloride/nitromethane (7:2:1). An excess of ammonium hexafluorophosphate was added to perform an anion exchange. The methanol and nitromethane were removed via rotary evaporator and the red precipitate was suspended in the remaining solution. The solution was filtered and the solid was washed with water several times and allowed to air dry for a while. The yield varied from 18 – 24 % for [2]catenanes **3.1-3.4**. The obtained solid

was dissolved in d_3 -acetone to take ^1H NMR, ^{13}C NMR and variable temperature NMR spectra.

3.3.2 Characterization of [2]Catenane **3.1**

[2]Catenane **3.1** with both unblocked tethers was prepared and isolated to give a yield of 22 %.

The ^1H -NMR spectrum at 293K (**Spectrum 3.1**) for [2]catenane **3.1** was at fast exchange region for dipyrindinium signals. The signal at 9.31 (t, $J=5.9$ Hz, 8H) corresponded to the α , α' protons (**Figure 3.3**). The signal looked to be partial overlap of

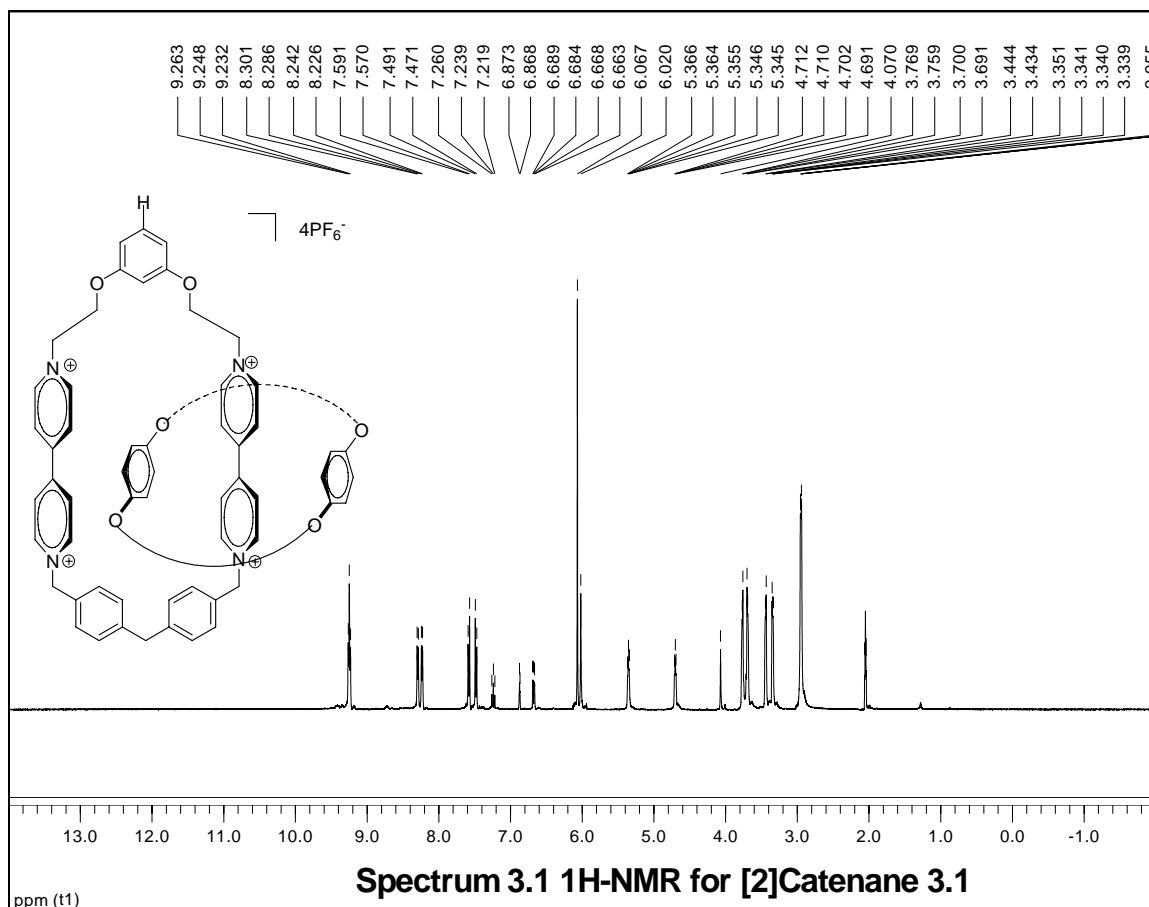


doublets the α and α' protons. The signals at 8.29 (d, $J=6.4$ Hz, 4H), 8.23 (d, $J=6.3$ Hz, 4H) were attributed to β , β' protons in the dipyrindinium units. The two doublets at 7.58 (d, $J=7.8$ Hz, 4H), 7.48 (d, $J=8.0$ Hz, 4H) corresponded to the protons in the phenyl rings of the unblocked wider tether. The triplet at 7.24 (t, $J=8.4$, 1H) was assigned to Ha of the resorcinol

moiety (**Figure 3.3**).

The triplet at 6.87 (t, $J=2.1$ Hz, 1H) could be Hc and a doublet of doublet at 6.67 (dd, $J=8.4$, 2.1 Hz, 2H) could be Hb. The singlet at 6.07 (s, 8H) belonged to the

phenylene rings of BPP34C10. This is a very interesting observation and we will discuss it in a following section.



The singlet at 6.02 (s, 4H) should correspond to the methylene protons adjacent to cationic nitrogen in the wider tether. Two triplets at 5.36 (t, $J=4.1$ Hz, 4H), 4.76 (t, $J=4.1$ Hz, 4H) were assigned to the protons of the ethoxy spacer. The singlet at 4.07 (s, 2H) was for the methylene protons between two aryl groups of the wider tether. The broad signal at 3.76~3.35 (m, 32H) corresponded to the protons of the aliphatic chain of BPP34C10.

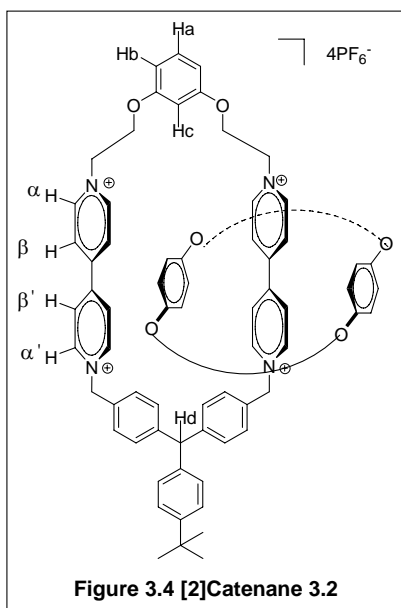
The ¹³C NMR data were derived from the HSQC spectrum since there was such a

small amount of product. In the mass spectrum (ESI), the peak at $m/z = 450.5$ was attributed to $[M^{4+}PF_6^-]^{3+}$ which was the result of loss of three PF_6^- anions. The peak at $m/z = 748.3$ corresponded to $[M^{4+} 2PF_6^-]^{2+}$ which could result from loss of two PF_6^- anions. All the spectroscopic data supported the formation of [2]catenane **3.1**.

3.3.3 Characterization of [2]Catenane **3.2**

Following an analogous three component reaction and purification, [2]catenane **3.2** with the blocking triaryl tether was obtained in a yield of 24 %.

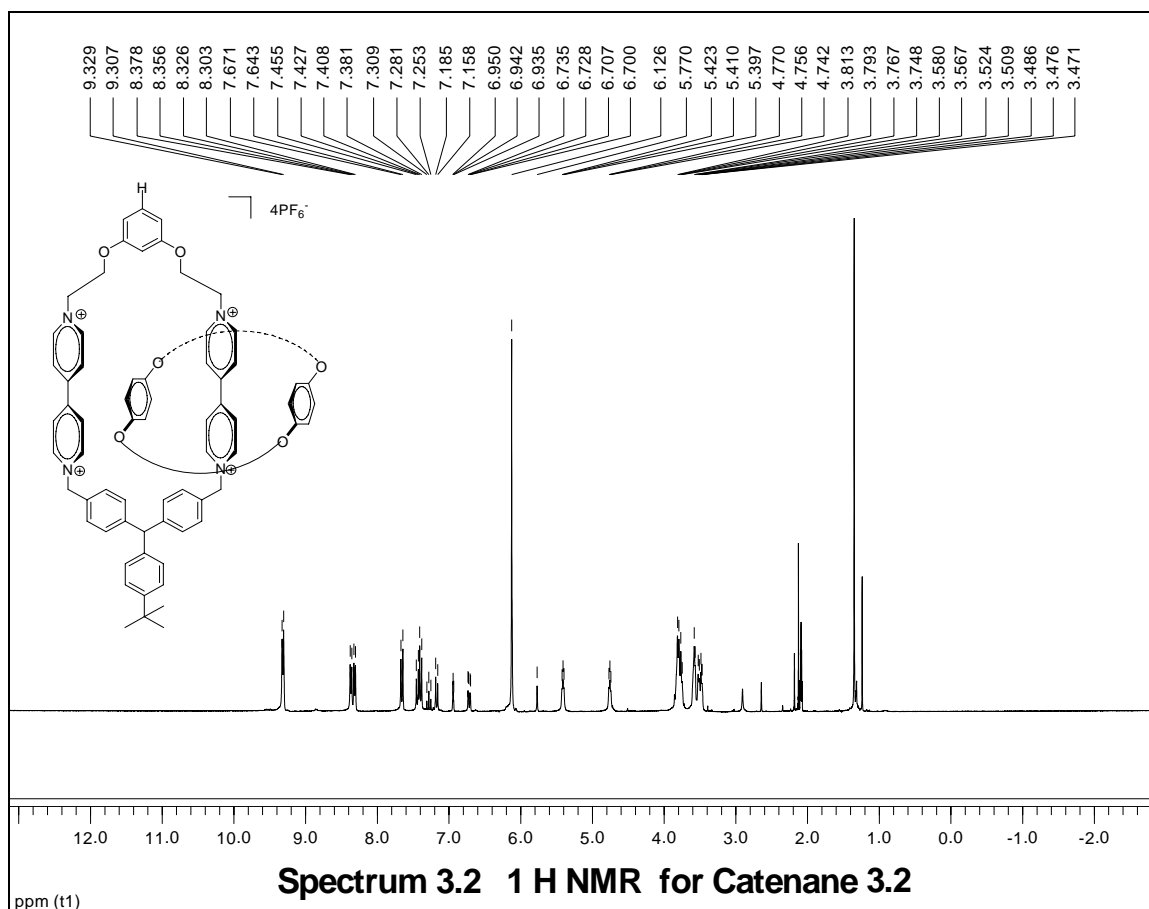
In the 1H -NMR spectrum (**Spectrum 3.2**), the signal at 9.31 (d, $J=5.9$ Hz, 8H)



corresponded to the α, α' protons (**Figure 3.4**). The signals at 8.37 (d, $J=6.7$ Hz, 4H), 8.31 (d, $J=6.7$ Hz, 4H) belonged to β, β' protons. The triplet at 7.28 (t, $J=8.5$ Hz, 1H) was assigned to Ha and the triplet at 6.94 (t, $J=2.3$ Hz, 1H) corresponded to Hc (**Figure 3.4**). The doublet of doublets at 6.72 (dd, $J=8.5, 2.3$ Hz, 2H) was for Hb. The singlet at 6.13 (s, 12H) should be a overlap of the protons of the BPP34C10 phenyl ring and the methylene

protons close to cationic nitrogen in the blocked wider tether. The singlet at 5.77 (s, 1H) was the tertiary hydrogen near three aryl groups in the blocked wider tether. The triplets

at 5.44 (t, $J=3.8$ Hz, 4H), and 4.76 (t, $J=4.1$ Hz, 4H) were assigned to the methylene protons in the ethoxy spacer. The broad peaks between 3.85~3.47 (m, 32H) belonged to the protons of the BPP34C10 aliphatic chain.

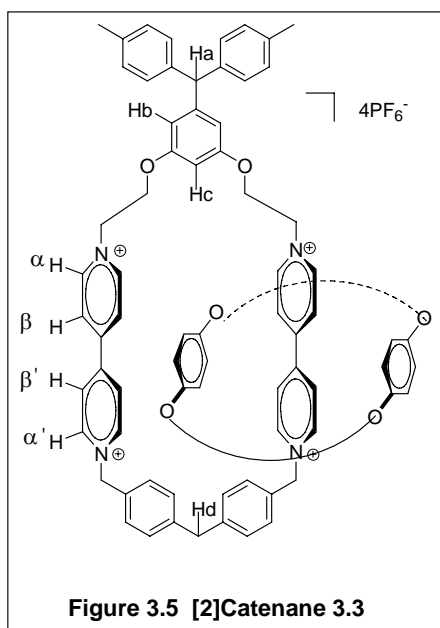


The ^{13}C NMR data were derived from the HSQC spectrum. In the mass spectrum (ESI), the peak at $m/z = 494.9$ was attributed to $[\text{M}^{4+}\text{PF}_6^-]^{3+}$ which was the result of loss of three PF_6^- anions. The peak at $m/z = 814.3$ was assigned to $[\text{M}^{4+}2\text{PF}_6^-]^{2+}$ which could result from loss of two PF_6^- anions. All the spectroscopic data supported the structure of [2]catenane **3.2**.

3.3.4 Characterization of [2]Catenane 3.3

[2]Catenane **3.3** with a blocking 5-(bis(4-methylphenyl)methyl)-1,3-resorcinol was obtained in a yield of 18 %.

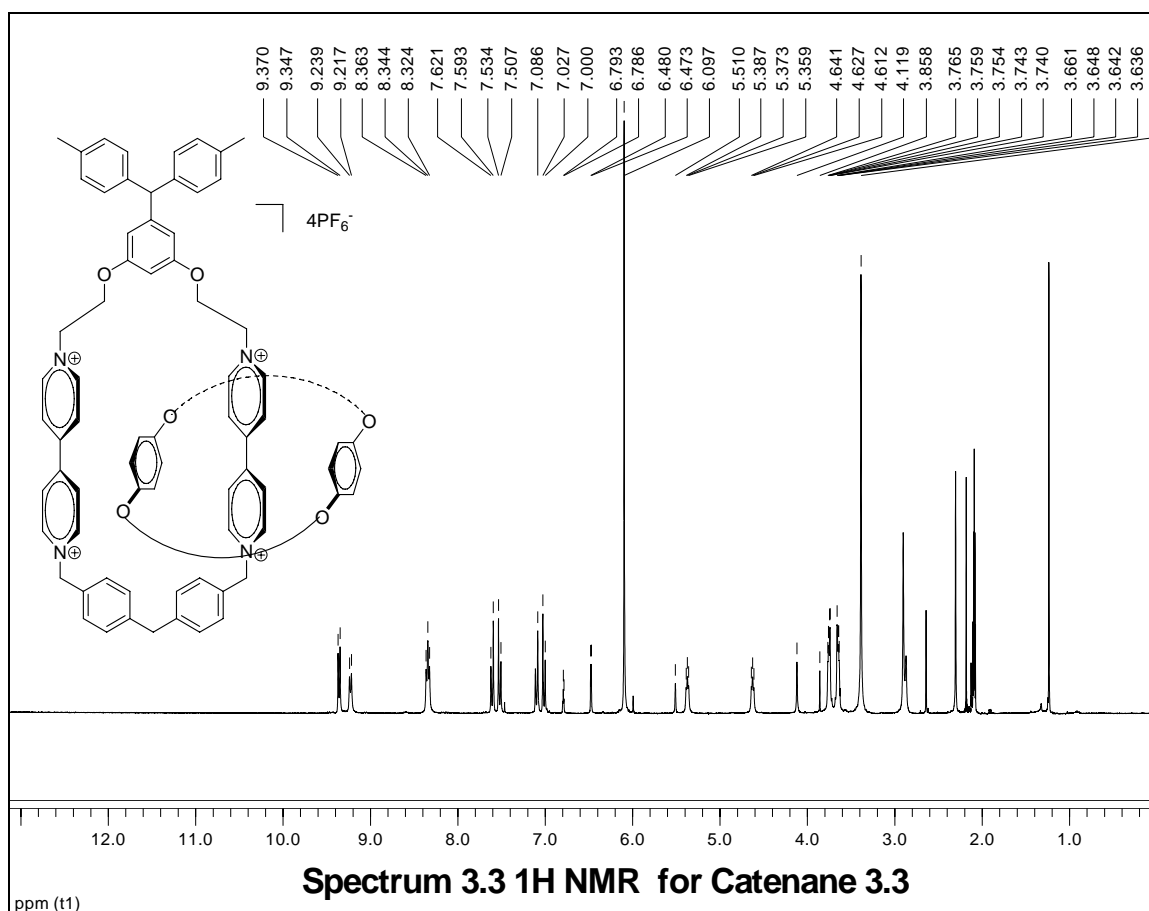
In the ^1H -NMR spectrum (**Spectrum 3.3**), the α , α' protons in the dipyridinium



unit was located at 9.36 (d, $J=7.0$ Hz, 4H), 9.23 (d, $J=6.7$ Hz, 4H) (**Figure 3.5**). The signal at 8.34 (m, $J=6.5$, 5.3 Hz, 8H) indicated an overlap of the chemical shifts of β , β' protons in the dipyridinium units. Two doublets of doublets at 7.61, 7.52, 7.10, 7.01 ppm were assigned to the protons of phenyl rings on the tolyl and unblocked wider tether. The triplet at 6.80 (t, $J=2.1$ Hz, 1H) belonged to Hc and the doublet at 6.47 (d, $J=2.1$ Hz, 2H) were assigned

to Hb. The proton Ha was located at 5.51 (s, 1H). Compared to Hd's chemical shift at 4.12 (s, 2H), Ha shifted downfield because there were three aryl groups around it while Hds were around two aryl groups. The triplets at 5.37 (t, $J=4.1$ Hz, 4H), 4.61 (t, $J=4.1$ Hz, 4H) corresponded to the protons on the ethoxy tether. The broad peaks between 3.76~3.39 (m, 32H) should be the protons on the aliphatic chain of the BPP34C10.

The mass spectrum also supported the formation of [2]catenane. In the mass

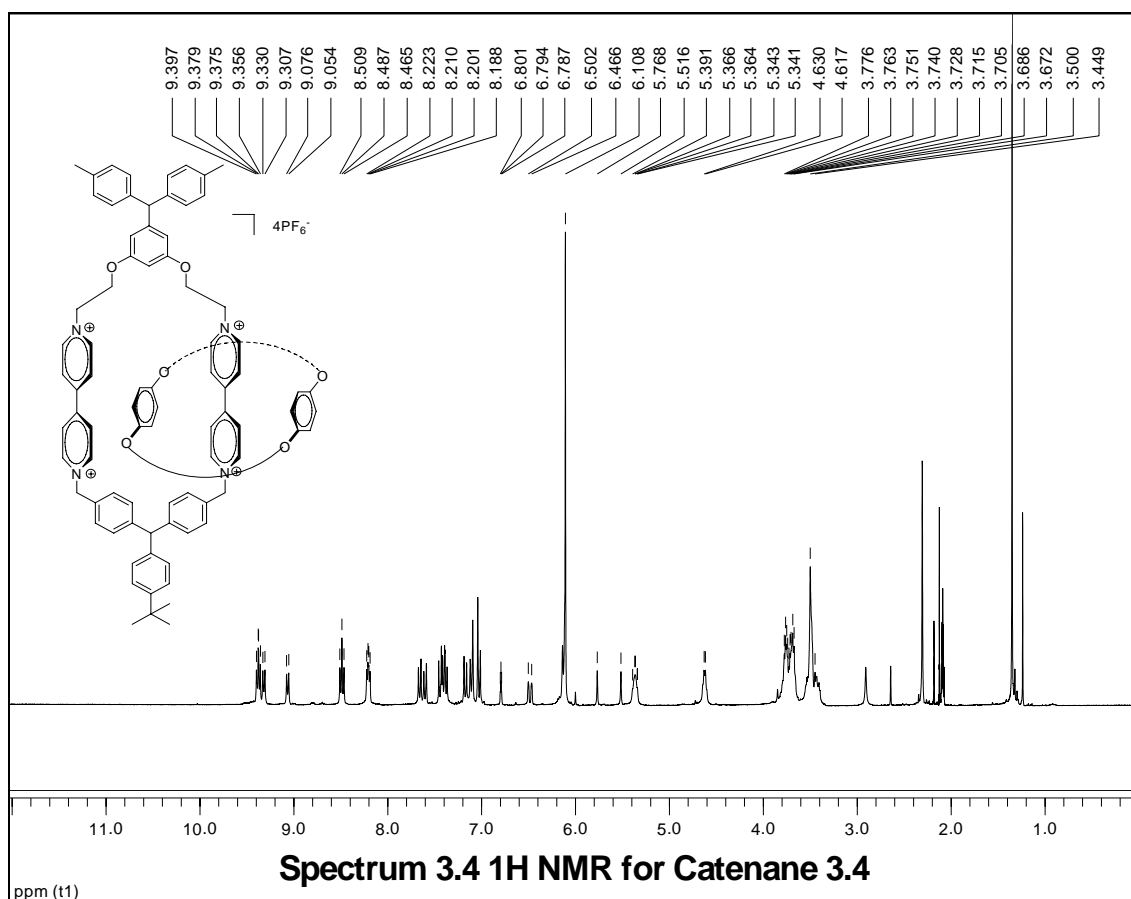


spectrum (ESI), the peak at $m/z = 515.2$ corresponded to $[M^{4+}PF_6^-]^{3+}$ which was the result of loss of three PF_6^- anions. The peak at $m/z = 845.8$ was attributed to $[M^{4+}2PF_6^-]^{2+}$ which could result from loss of two PF_6^- anions. All the spectroscopic data supported the successful formation of [2]catenane **3.3**.

3.3.5 Characterization of [2]Catenane **3.4**

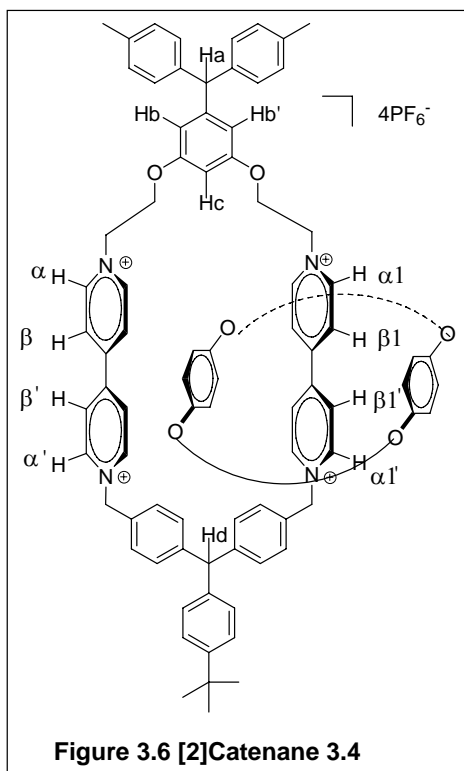
[2]Catenane **3.4** containing two blocking groups was prepared in a yield 19 %. The 1H -NMR spectrum (**Spectrum 3.4**) is much more complicated than the previous

[2]catenanes since it is now in the slow exchange region for the dipyridinium. As discussed in chapter 2, this slow exchange is reasonable due to two blocking groups limiting free circumrotation of BPP34C10.



It appeared that the dipyridinium units were strongly affected by the BPP34C10 while the top and bottom spacers were barely affected because only one set of signals were observed for the protons on them. In details, eight signals for the protons in the dipyridinium units were observed at 9.38 (m, $J=6.7, 5.6$ Hz, 4H), 9.32 (d, $J=7.0$ Hz, 2H), 9.07 (d, $J=6.7$ Hz, 2H), 8.49 (m, $J=6.8, 6.5$ Hz, 4H), 8.21 (dd, $J=6.7, 2.1$ Hz, 4H). Some

of them overlapped to form triplet-like signals. The α , $\alpha 1$ or β , $\beta 1$ protons were not identical any more. The triplet at 6.79 (t, $J=2.1$ Hz, 1H) was attributed to Hc (**Figure 3.6**). The two doublets at about 6.48 ppm might correspond to Hb and Hb' which were not identical due to the desymmetrizing effect of the BPP34C10 π - π -stacking on one



dipyridinium unit. The singlets at 5.77 (s, 1H), 5.52 (s, 1H) should be attributed to Ha and Hd. The triplets at 5.36 (m, 4H), 4.62 (m, 4H) were assigned to the ethoxy group. The broad peak at 3.79~3.41 (m, 32H) belonged to the protons of the aliphatic chain of BPP34C10.

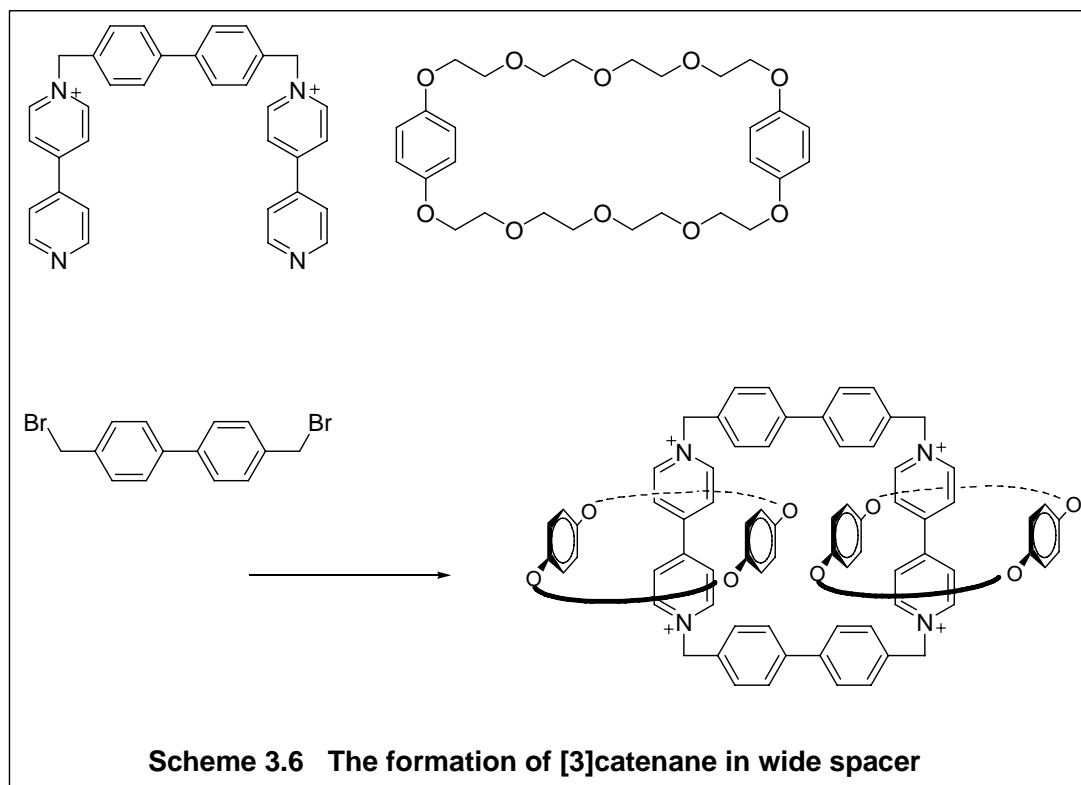
The ^{13}C NMR data were derived from HSQC. Only protonated carbons were characterized. In the mass spectrum (ESI), the peak at $m/z = 911.9$ corresponded to $[\text{M}^{4+} 2\text{PF}_6^-]^{2+}$ could

result from loss of two PF_6^- anions. All the spectroscopic data supported the formation of [2]catenane **3.4**.

3.3.6 Unique findings in [2]catenanes 3.1 - 3.4⁴⁷

Some interesting, unique findings were observed for the [2]catenanes **3.1-3.4**.

Stoddart *et al*⁴⁶ had reported that [3]catenanes were formed when wider spacers were used (**Scheme 3.6**). The distance between two dipyridinium units was large enough to accommodate two BPP34C10 rings in one dipyridinium tetracationic cyclophane. During the formation of [2]catenanes with our wider bis(4-methylphenyl)methyl tethers, only [2]catenanes were observed and no [3]catenanes were isolated. Apparently, although the length of the wider tethers for [2]catenanes **3.1-3.4** made it possible to form [3]catenanes, 1,3-ethyloxy spacer was narrow enough to prevent the formation of [3]catenanes.

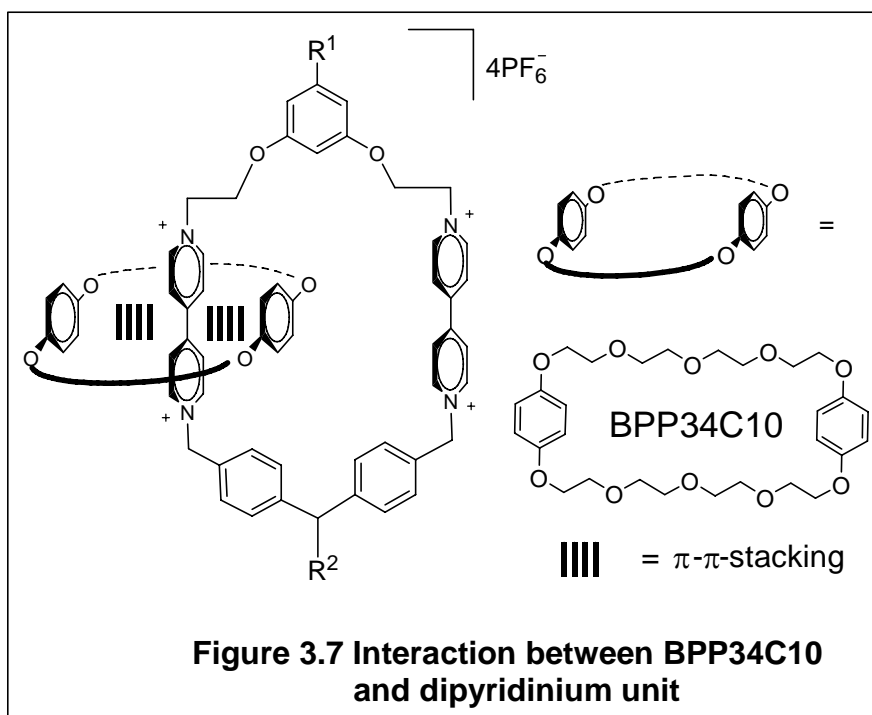


Another interesting finding⁴⁷ was concluded from the ¹H NMR spectra of the [2]catenanes **3.1-3.4**. As we reviewed in chapter 2, according to the ¹H NMR spectra for [2]catenanes **2.1-2.6**, the protons of the internal hydroquinone ring of BPP34C10 had a

very high upfield chemical shift located near 3.8 ppm due to π - π -stacking with both dipyridinium moieties while the external hydroquinone ring was found near 6.1 ppm since it only interacted with one dipyridinium unit. Above room temperature, both sets of signals coalesced to give a single averaged signal near 5.0 ppm.

Interestingly, [2]catenanes **3.1-3.4** exhibited quite unique ^1H NMR spectra because even at room temperature only one set of signals for the protons on the two hydroquinone rings were found at about 6.1 ppm.

An explanation is described in **Figure 3.7**. The internal and external



hydroquinone rings both interacted with only one dipyridinium group through only a single π - π -stacking. The internal and external hydroquinone rings therefore had similar

¹H NMR resonance environments. They both shared an averaged signal at 6.1 ppm.

It can be concluded that the internal hydroquinone ring can only interact with one dipyridinium unit due to the distance between the rings. Because of the similarity of the chemical shift environment for the internal and external hydroquinone rings, there was no difference between them. This finding has not been previously reported in dipyridinium-based [2]catenanes system.

3.4 Variable Temperature ¹H NMR Study of [2]Catenanes

The thermodynamic properties of [2]catenane **3.1-3.4** was determined by variable temperature ¹H NMR study as described in chapter 2. The free energy of activation was calculated according to the following equation:

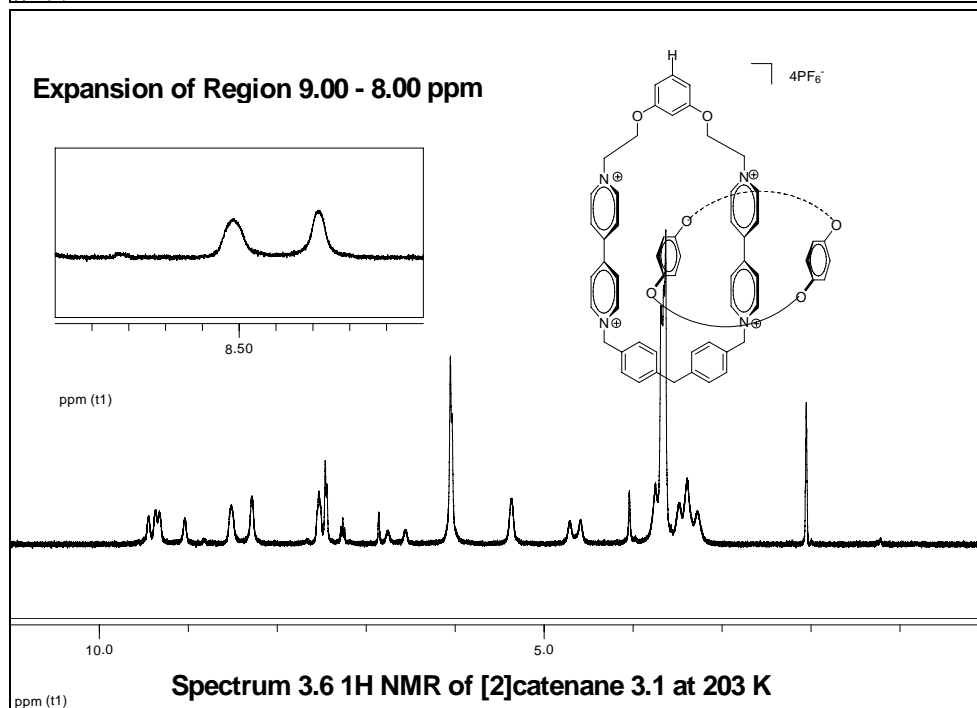
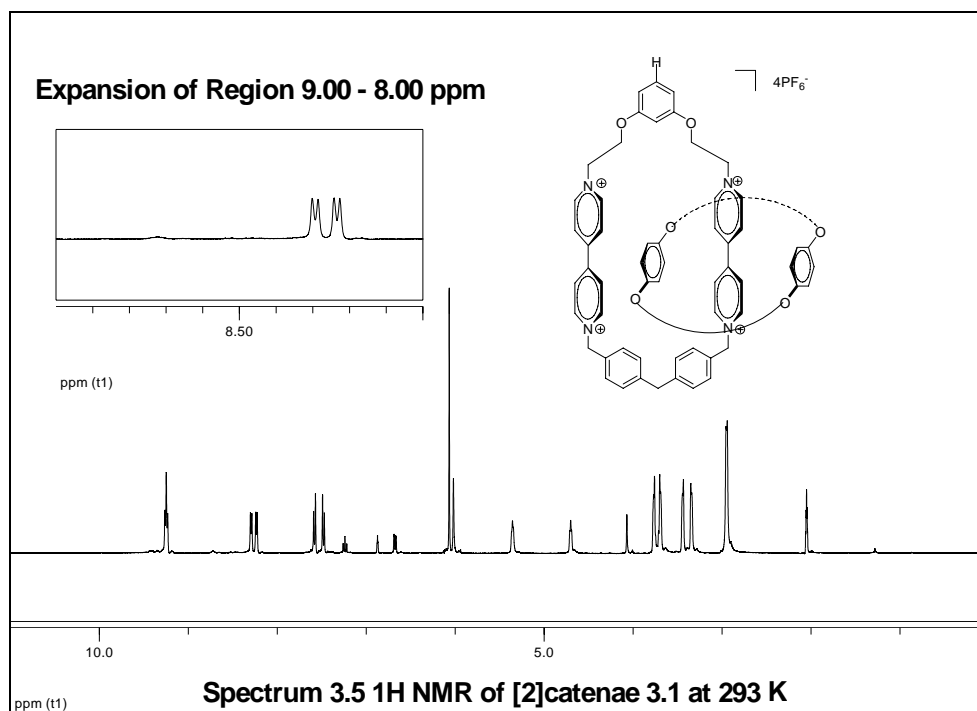
$$\Delta G^\ddagger_C = 4.58 T_C [9.972 + \log (T_C/\Delta\nu)] \text{ cal mol}^{-1}$$

Where T_C (K) is the coalescence temperature and $\Delta\nu$ (Hz) is the frequency difference of the separation between the two signals in the absence of exchange.

3.4.1 Variable Temperature ¹H NMR of [2]Catenane 3.1

In [2]catenane **3.1**, the β , β' protons on the dipyridinium units were used to determine the free energy of activation (ΔG^\ddagger). At 20 °C, two sharp doublets were shown at 8.20 – 8.30 ppm (**Spectrum 3.5**). At lower temperature 203 K, two broad peaks were

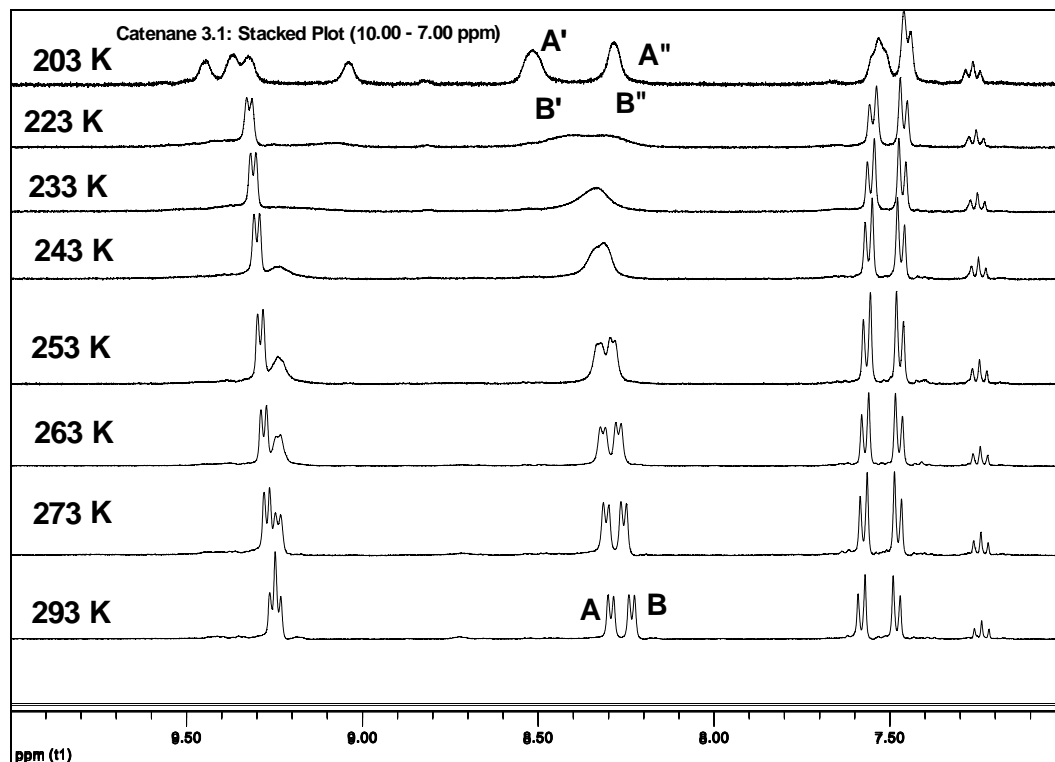
observed at 9.00 -8.00 ppm (**Spectrum 3.6**).



From the above two spectra for [2]catenane **3.1**, frequency difference of the

separation of the exchanging resonance ($\Delta\nu$) (between A' /A'' and B'/B'' in **Spectrum 3.7**) was 79 Hz. The coalescence temperature was approximately 228 K (-45 °C). According to these data, the free energy of activation for circumrotation was calculated to be 10.8 kcal mol⁻¹.

The stacked plot (**Spectrum 3.7**) indicated the gradual change of the signals between 10.00 – 7.00 ppm with the change of temperature from 293 K to 203 K. At 293 K, the β , β' protons on the dipyridinium units were doublets of doublets in sharp shape. At 203 K, the β , β' protons became the broad signals because of the slow exchange of two conformations.

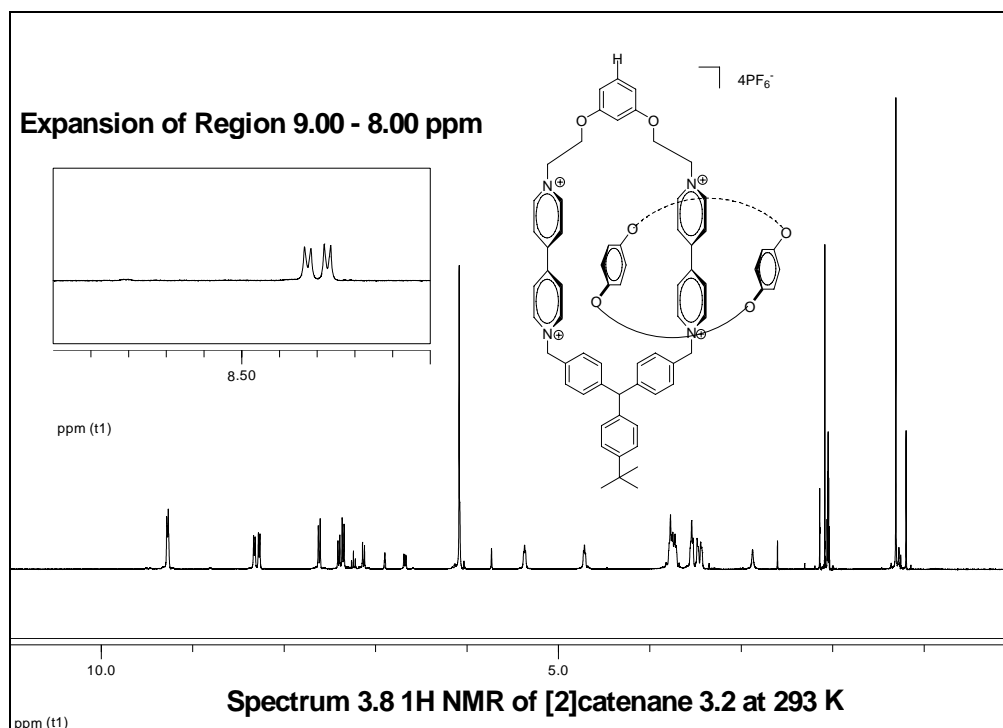


Spectrum 3.7 Stacked Plot of [2]Catenane 3.1

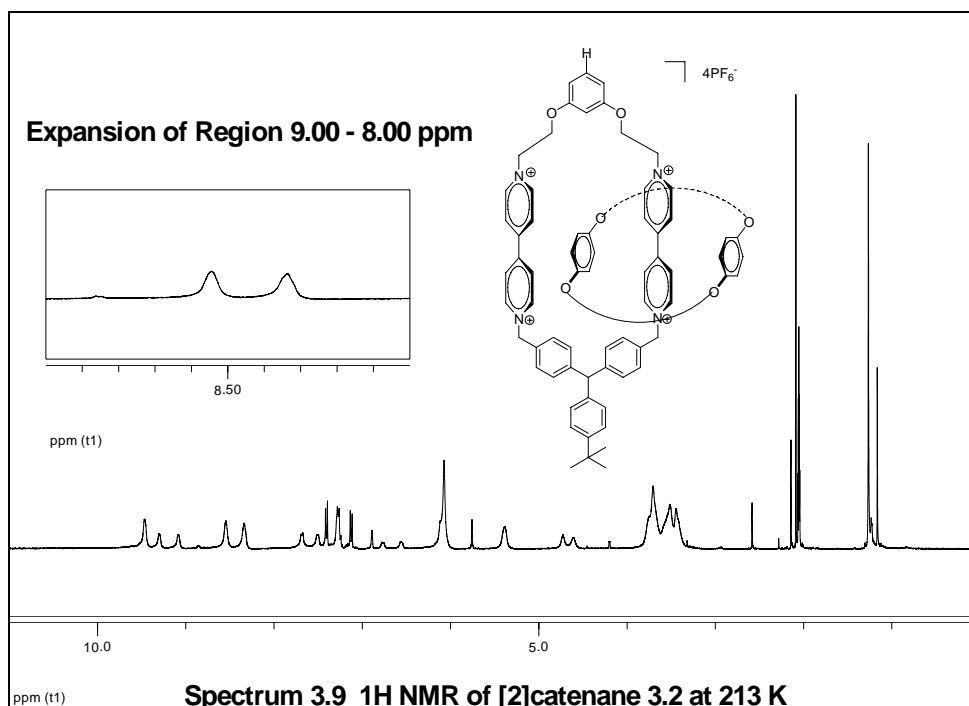
3.4.2 Variable Temperature ^1H NMR of [2]Catenane 3.2

For [2]catenane **3.2**, the β , β' protons on the dipyridinium units were also used to determine the free energy of activation (ΔG^\ddagger). At 293 K, two sharp doublets were shown at 9.00 – 8.00 ppm (**Spectrum 3.8**). At lower temperature (213 K), two broad peaks were observed at 9.00 -8.00 ppm (**Spectrum 3.9**).

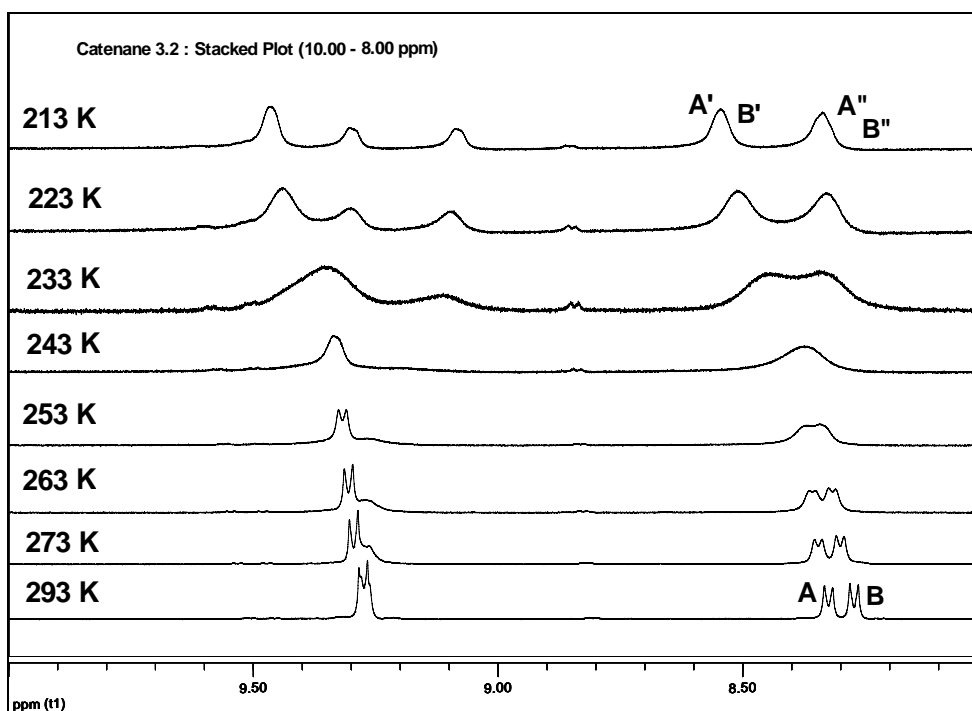
According to measurement, the frequency difference of the separation of the exchanging resonance ($\Delta\nu$) was 79 Hz (between A'/A'' and B'/B'' in **Spectrum 3.10**). The



coalescence temperature was approximately 238 K (-35 °C). According to these data, the free energy of activation for circumrotation was calculated to be 11.4 kcal mol⁻¹.



The stacked plot (**Spectrum 3.10**) showed the gradual change of the signals



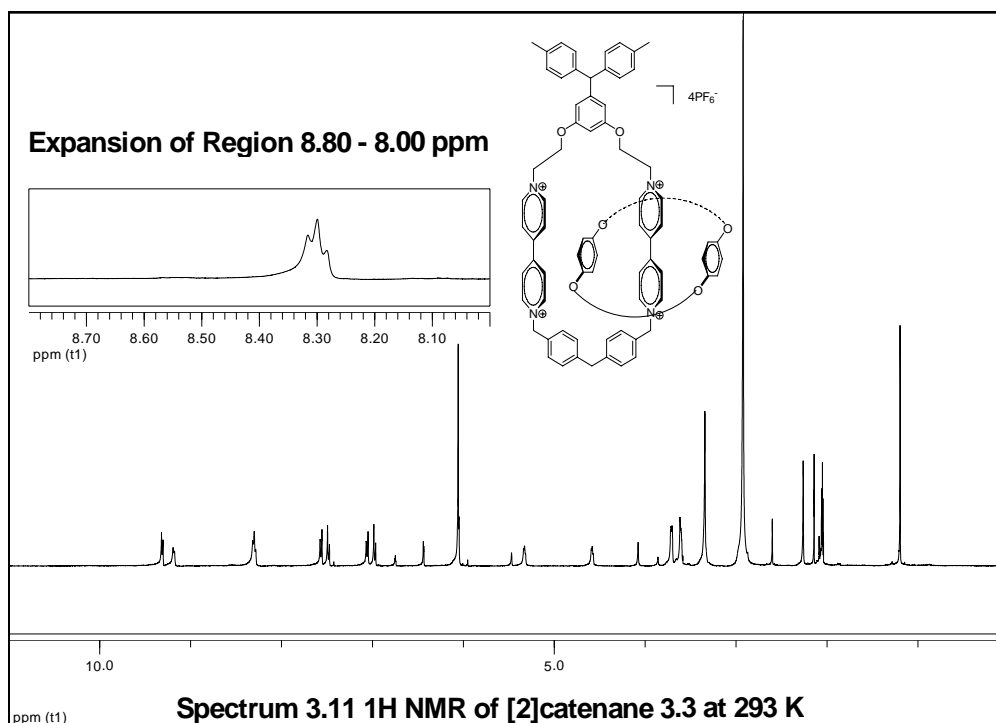
Spectrum 3.10 Stacked Plot of [2]Catenane 3.2

between 10.00 – 8.00 ppm. At 293 K, the fast exchange of two conformations made the

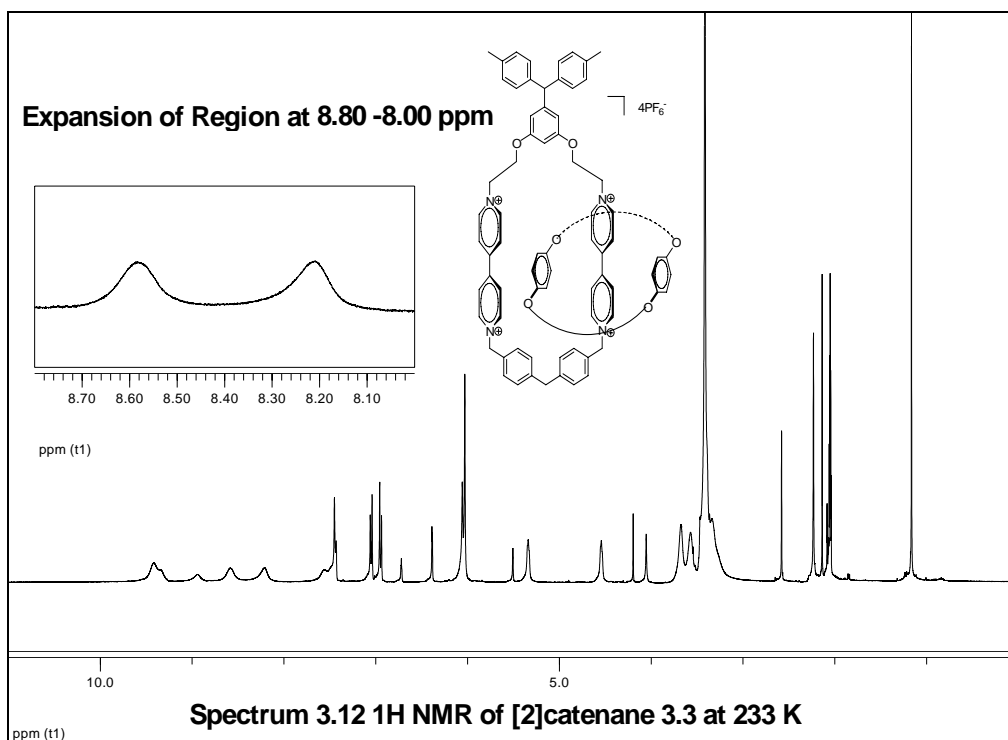
signals sharp. At low temperature (213 K), the β , β' protons turned into two sets of peaks again after a coalescence occurred (-35 °C). At 293 K, the α , α' protons corresponded to two overlapped doublets. With the decreasing of temperature, the peaks coalesced and further turned into three peaks.

3.4.3 Variable Temperature ^1H NMR of [2]Catenane 3.3

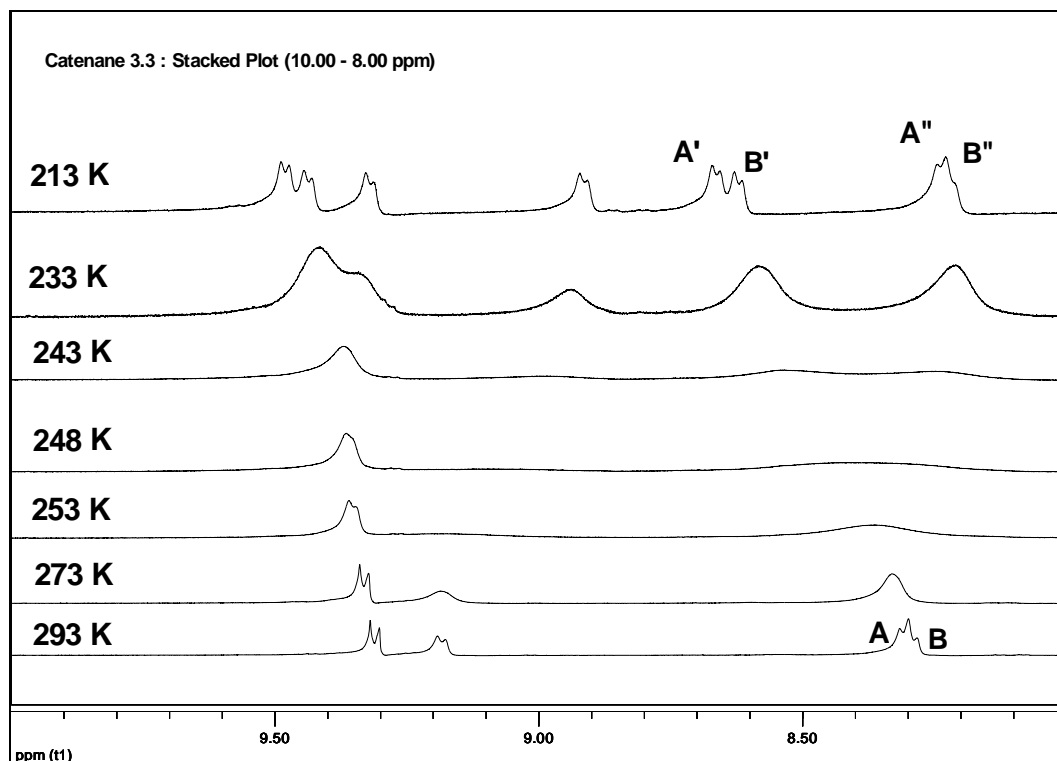
In [2]catenane **3.3**, the β , β' protons on the dipyrindinium units were used to determine the free energy of activation (ΔG^\ddagger). At 293 K, two overlapped doublets of doublets were shown at 8.80 – 8.00 ppm (**Spectrum 3.11**). At lower temperature (233 K), three broad peaks were observed at 9.00 -8.00 ppm (**Scheme 3.12**).



From those two spectra, it was measured that the frequency difference of the separation of the exchanging resonance ($\Delta\nu$) was 166 Hz (between A'/A'' and B'/B'' in **Spectrum 3.10**). The coalescence temperature was approximately 248 K (-35°C). So the free energy of activation for circumrotation was calculated to be 11.5 kcal mol⁻¹.



The stacked plot (**Spectrum 3.13**) indicated the change of signals between 10.00 – 8.00 ppm from 293 K to 213 K. At 293 K, four doublets were shown on the spectrum while eight doublets were observed (two overlapped) at 213 K (-60 °C). The slow exchange of two conformations made each α , α' , β , β' proton different.



Spectrum 3.13 Stacked Plot of [2]Catenane 3.3

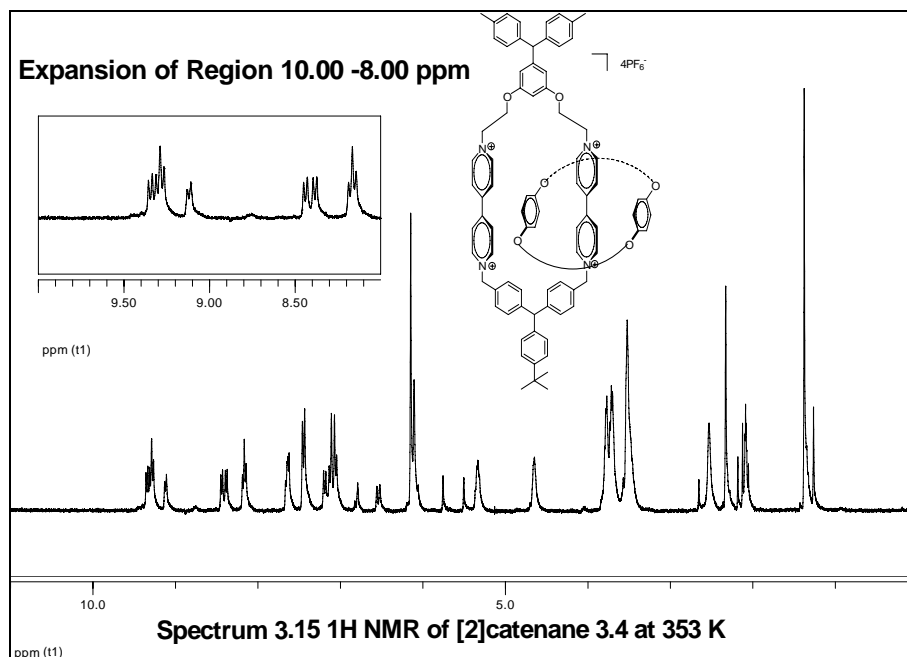
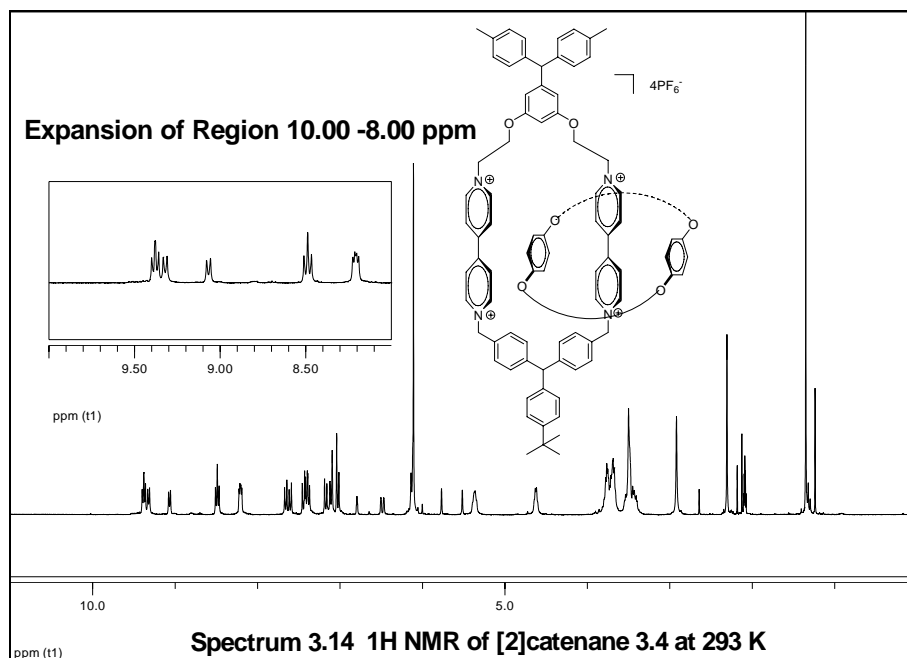
3.4.4 Variable Temperature ^1H NMR of [2]Catenane 3.4

Catenane **3.4** was with both tethers blocked dissolved in d_3 -acetonitrile to enable higher temperature in variable temperature ^1H NMR. However, no coalescence was observed even up to 353 K (80 °C).

At 293 K, there were eight signals as expected for the dipyridinium protons. Some signals were overlapped. For instance, the signal at 8.49 (m, $J=6.8, 6.5$ Hz, 4H) was two overlapped doublets (**Spectrum 3.14**).

Apparently, the BPP34C10 ring could not circumrotate over the bulky groups at

room temperature. Even at the higher temperature 353 K (80 °C), no obvious changes were observed for the signals of dipyrindinium units (**Spectrum 3.15**).

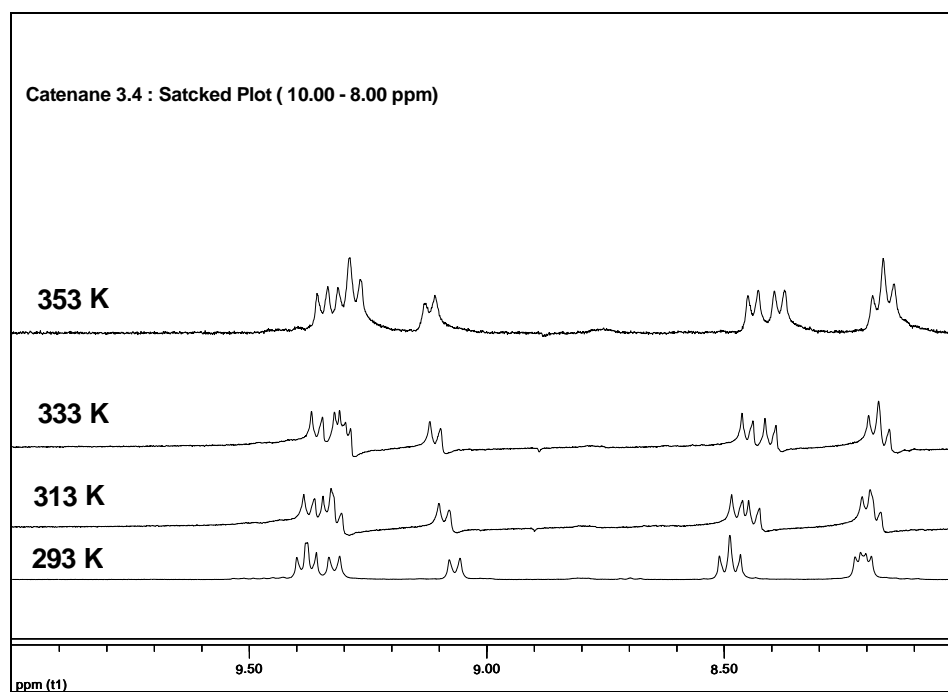


The coalescence temperature for [2]catenane **3.4** exceeds what we can reach within the

limit of our NMR instrument and the boiling point of the solvent (d_3 -acetonitrile).

We can assume that the frequency difference of the separation of the exchanging resonance ($\Delta\nu$) is the difference of two α , α_1 was 84 Hz. Since the coalescence temperature must be more than 353 K, the free energy of activation must be more than $17.1 \text{ kcal mol}^{-1}$.

The stacked plot (**Spectrum 3.16**) of spectra at different temperatures showed no move toward coalescence from 293 K to 353 K.



Spectrum 3.16 Stacked Plot of [2]Catenane 3.4


3.5 Summary and Conclusions

According to the above discussion, four catenanes with wider tethers were

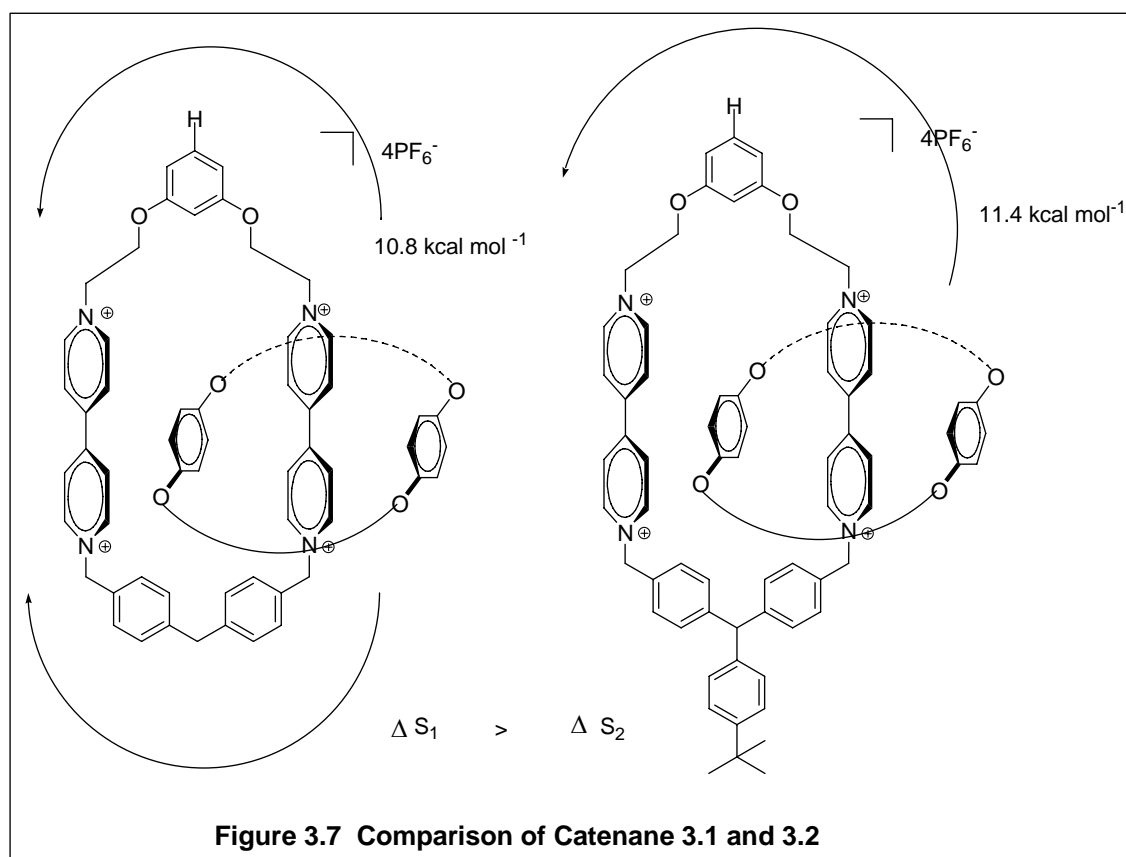
synthesized. Variable temperature ^1H NMR spectra were taken to measure the low temperature frequency difference and coalescence temperature of the catenanes. The free energies of activation of four catenanes were calculated. All the data are summarized in Table 3.1.⁴⁷ The structure of [2]catenanes **3.1-3.4** referred to **Scheme 3.5**. These data have been accepted by *Journal of the Organic Chemistry* and will be published soon.

According to Table 3.1, the free energies of activation of catenanes **3.2** and **3.3** are almost identical (11.4 and 11.5 kcal mol⁻¹). In other words, passage over either the rigid bis(p-benzyl)methane and the flexible 1,3-bis(ethyloxy)phenyl tethers requires the same energy barrier.

Table 3.1 Summary of Data of [2]catenanes 3.1 - 3.4⁴⁷

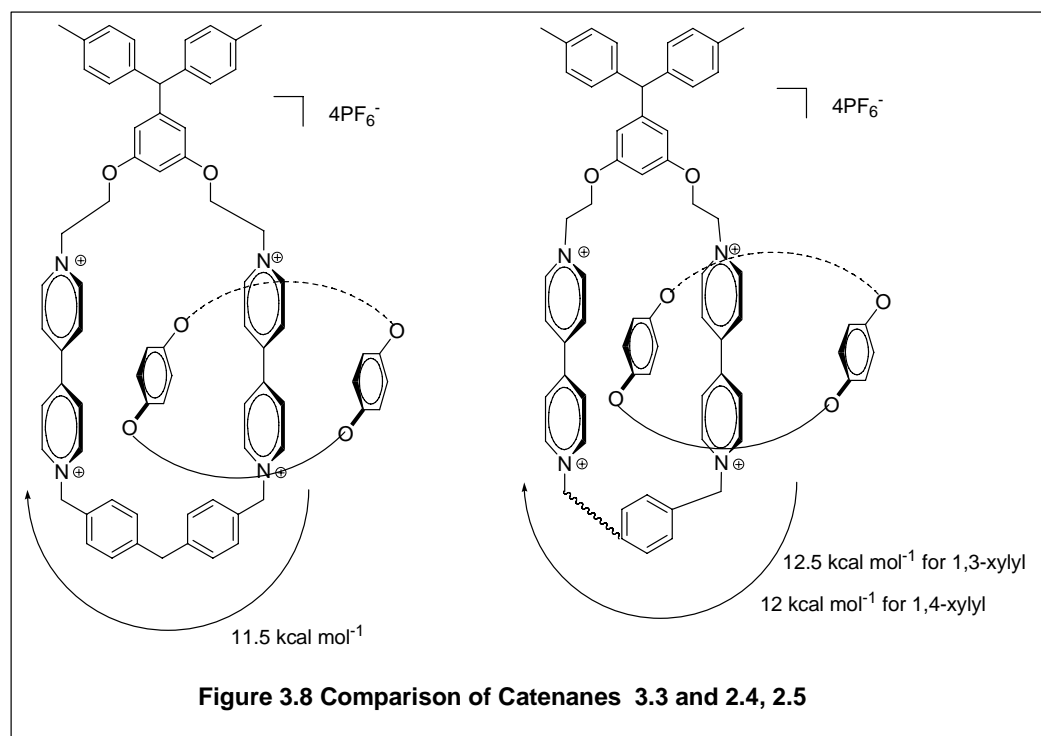
[2]catenane	R		Coalescence temperature (K)	Frequency difference (Hz)	Free energy of activation (kcal mol ⁻¹)
3.1	H	Tether A	228	79	10.8
3.2	H	Tether B	238	79	11.4
3.3	Ditoylmethyl	Tether A	248	166	11.5
3.4	Ditoylmethyl	Tether B	>353	84	>17.1

Interestingly, it is noted that the energy barrier for catenane **3.1** is 0.6 kcal mol⁻¹ lower than the energy barrier for catenane **3.2** (**Figure 3.7**) even if the BPP34C10 ring passed over the same resorcinol tether in both catenanes. Comparing the two catenanes, the only difference is that movement of the crown ether in catenane **3.1** is open along both tethers while the catenane **3.2** has one path blocked.



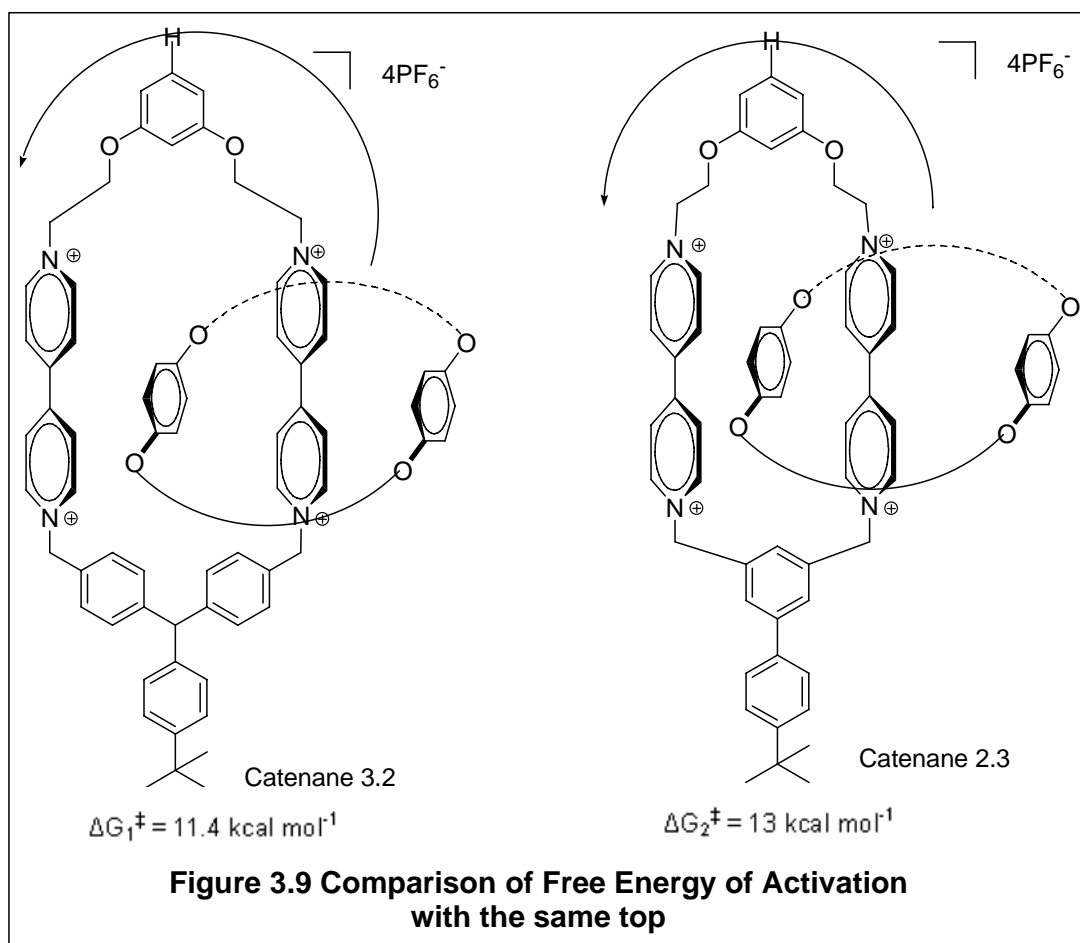
The explanation could be: according to the thermodynamic equation: $\Delta G = \Delta H - T\Delta S$, [2]catenane **3.1** has more ΔS since the BPP34C10 can circumrotate over the resorcinol or bis(p-phenyl)methane tether while the BPP34C10 can only pass along the resorcinol tether. Assuming that the ΔH s are the same, the more the ΔS , the lower the ΔG .

Comparing the results between in Table 3.1 and in Table 2.1 in chapter 2, it is noted that the [2]catenane **3.3** with wider tether and blocked top required 0.5 -1.0 kcal mol⁻¹ lower energy barrier than the top-blocked [2]catenane **2.4** and **2.5** with relatively narrow 1,3-xylyl, 1,4-xylyl tethers (**Figure 3.8**).



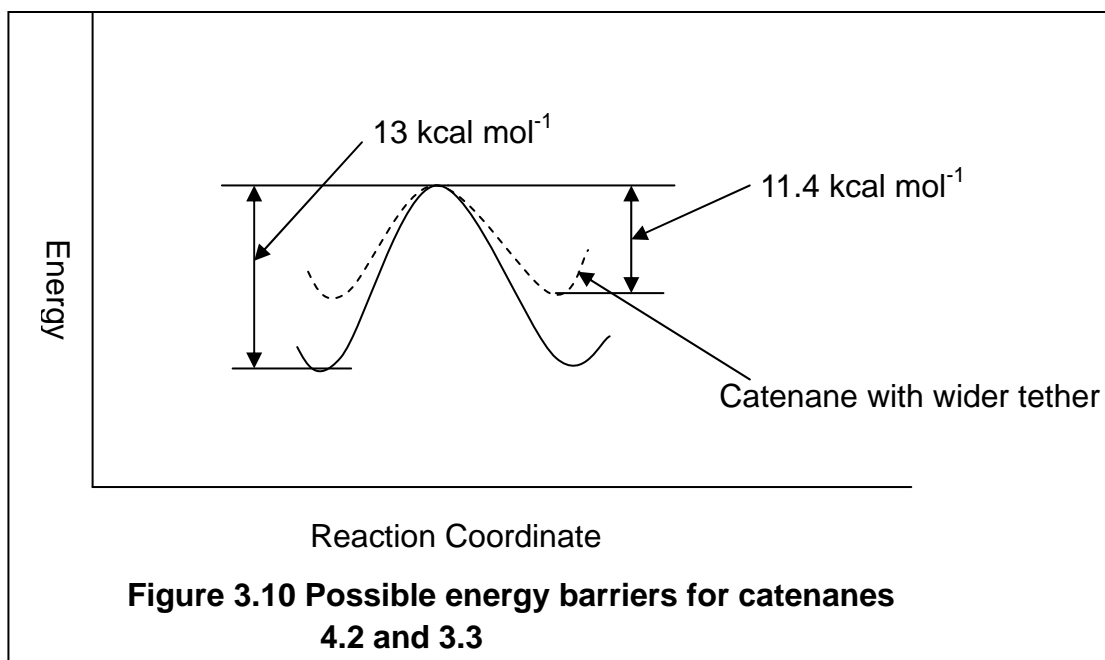
In other words, the 1,3-xylyl, 1,4-xylyl are too narrow, too restricted for BPP34C10 to do the conformation exchange while the bis(p-phenyl)methyl tether seems more smooth for BPP34C10 to circumrotate.

If we compared the free energies of activation between catenanes **3.2** and **2.3** (**Figure 3.9**), it turned out that they were different even if the BPP34C10 circumrotated over the same tether. The energy barrier required for passage over the resorcinol tether in [2]catenane **2.3** was $1.6 \text{ kcal mol}^{-1}$ higher than that required for passage over the resorcinol tether in [2]catenane **3.2**. The interesting result could be explained by a lowering of the unfavorable energetic interactions in the transition state structures or a raising of the ground state energies.



According to the discussion in the early section in this chapter, there is only a single π - π -stacking interaction in catenane **3.2** while the BPP34C10 was π - π -stacked with both dipyridinium units in catenane **2.3**. It seems more reasonable that the activation barrier differences are due to ground state destabilization in catenane **3.2** (**Figure 3.10**). This interpretation would give a value to the second π - π stacking interaction of about 1.5 kcal/mol.

In summary, similar to catenanes **2.1** -**2.6** in chapter 2, it was possible to block one or both of pathways if some bulky groups were incorporated to the top or bottom



tethers. Compared to catenanes **2.1 - 2.6**, the catenanes (**3.1 -3.4**) with the wider tethers demanded lower energy barrier for the BPP34C10 to circumrotate round the tetracationic cyclophane than those with the narrow, rigid tethers.

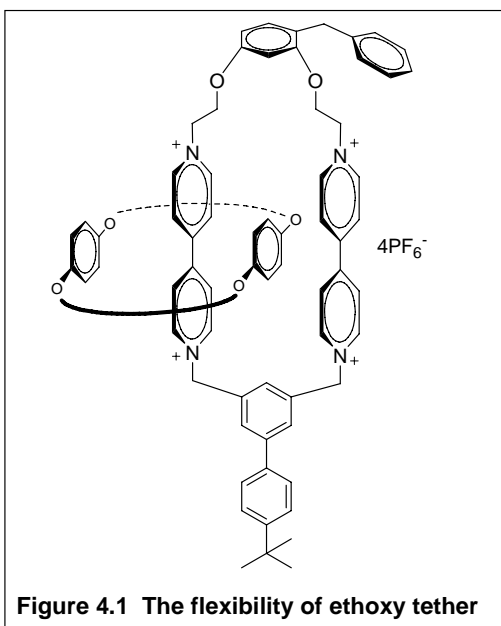
The wider bis(p-benzyl)methyl tether allowed the hydroquinone ring of BPP34C10 to have one single π - π -stacking interaction with only one dipyridinium unit. The energy barrier difference for circumrotation in catenanes might result from the ground states difference. This also demonstrated that it was possible to alter energy barrier in bistable [2]catenanes and illustrated an ability to use movement in [2]catenanes to probe the energetics of non-covalent interactions.

Chapter 4

Synthesis and Study of [2]Catenanes with Photoisomerizable Gates

4.1 Design of Model of [2]Catenane with Photoisomerizable Gates

In the model of asymmetric [2]catenanes we previously designed, there were two design shortcomings establishing a molecular ratchet.³² One was the flexibility of the



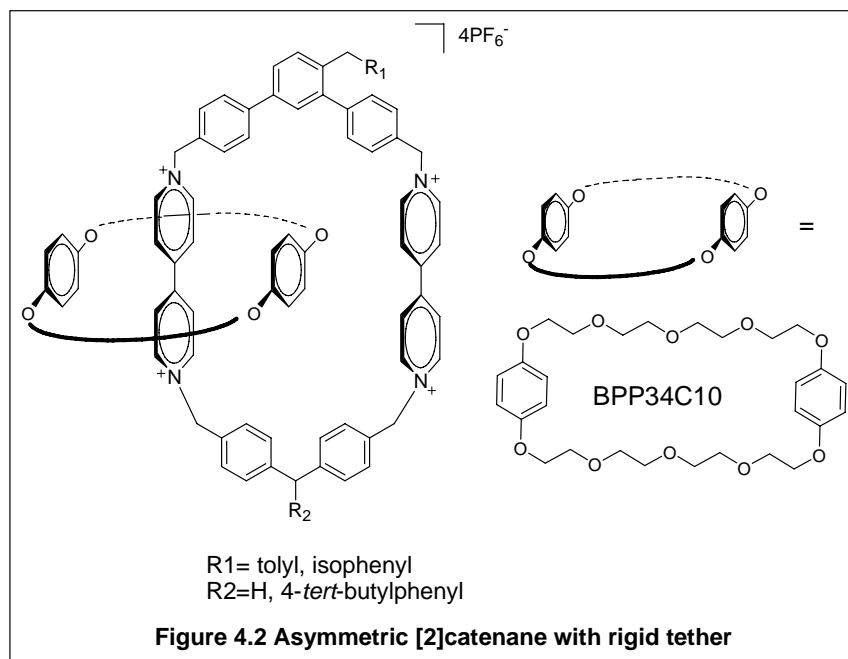
ethoxy tethers. Originally, the design of incorporation of ethoxy group was to isolate the two ground state dipyrrolium binding sites from the top resorcinol tether with gates. However, the flexibility of ethoxy spacer apparently led to unexpected consequences. Considering the number of freely rotating bonds in the ethoxy spacer, we could imagine that the

resorcinol moiety including the unsymmetrically gate could easily fold down perpendicular to the dipyrrolium units. The perpendicular orientation could lower the energy of activation for circumrotation in reverse direction and eliminate the gate effect.

Another drawback was that the ground states might not be identical. As we

discussed before, if the ground states are different and the ratio comes from $\Delta G \neq 0$, the system would be harder to establish.

To address these concerns, we needed to decrease the flexibility of this tether. A



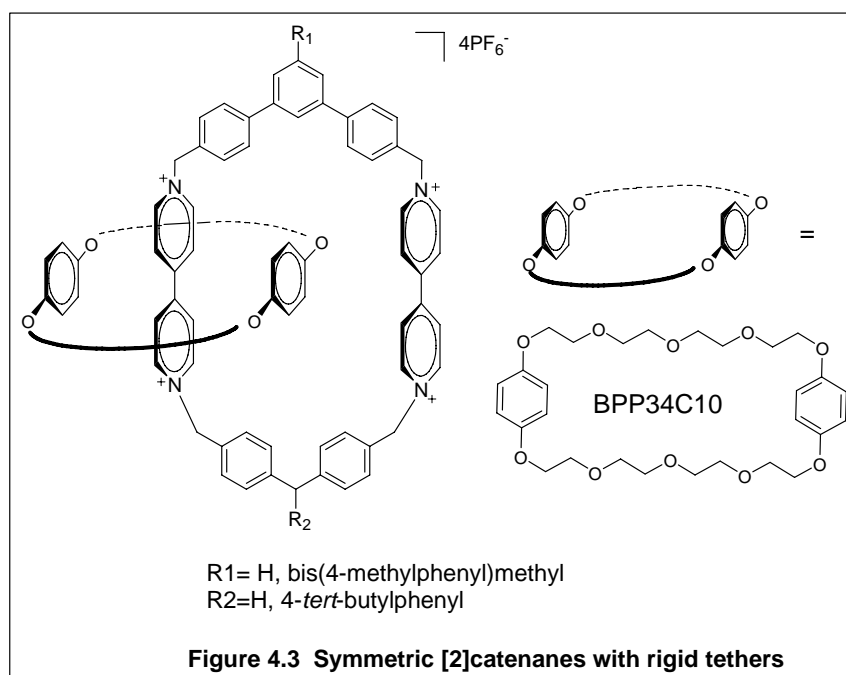
catenane with rigid phenyl spacer instead of ethoxy spacer was designed (Figure 4.2). In this system, the resorcinol tether was replaced by phenyl rings. Because of its

rigidity, the phenyl ring with the gate in the middle would less likely be able to fold. In this scenario, the ‘up’ or ‘down’ of the gate might lead to different interactions with the crown ether as it passed over in either direction and could result in different ratios of conformations.

Before preparing such asymmetric [2]catenanes, we first needed to demonstrate that the symmetric [2]catenane could be prepared. Two concerns were considered about this system. Since the phenyl spacers are so wide, [3]catenanes might be formed instead

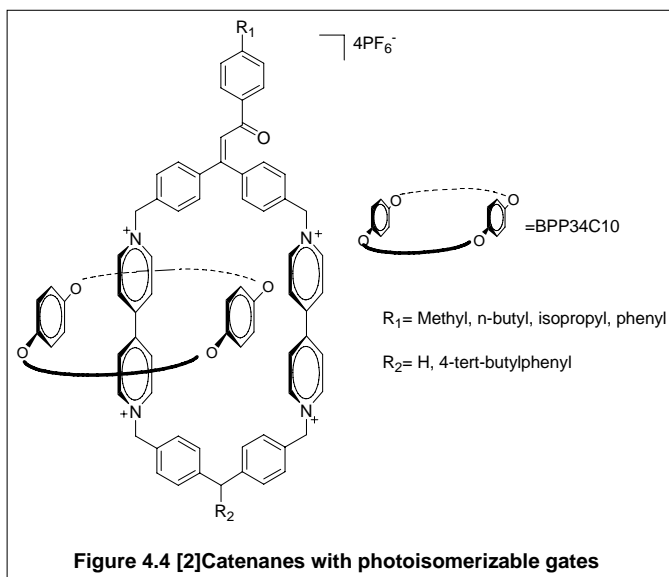
of [2]catenanes. [3]Catenanes couldn't indicate the preference of circumrotation of BPP34C10 and they are meaningless for studying unidirectional rotation. On the other hand, catenation might not happen due to the distance of two dipyridinium units and the length of the tether B could reduce the desired template effect.

Targeted symmetric [2]catenanes with rigid tethers are shown in **Figure 4.3**. In this system, the bulky groups would be incorporated on the top or the bottom tethers. The bottom tether B could be narrow 1,3-xylyl, 1,4-xylyl or wide bis(p-benzyl)methyl tethers.



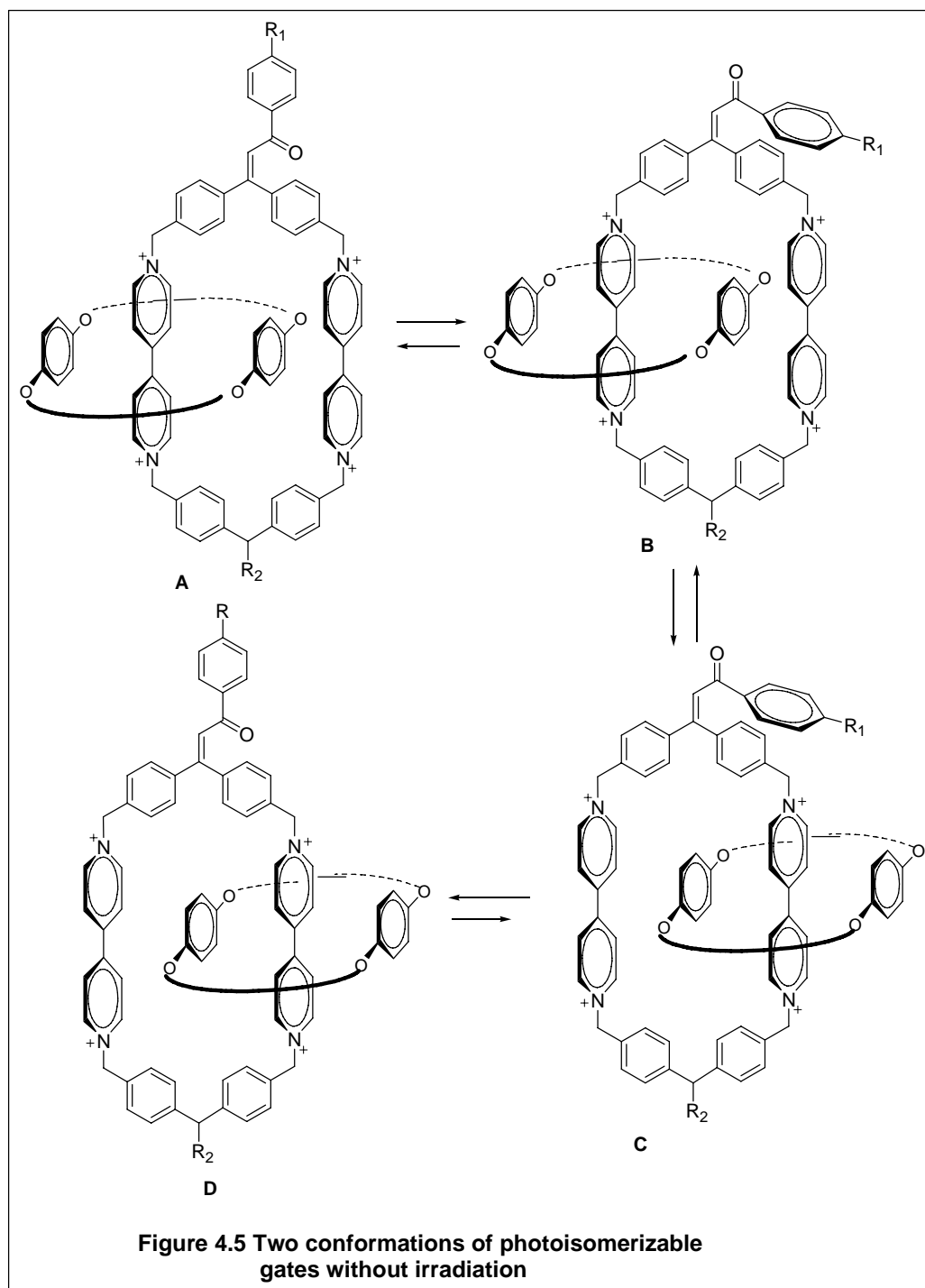
A related design we considered was a series of [2]catenanes with photoisomerizable carbon carbon double bonds (**Figure 4.4**). In this system, on the top tether, an enone conjugated with two phenyl rings would keep them in the same plane and favor the rigidity of the top tether. The gate could still have 'up' or 'down' positions

since the single bond between carbonyl group and carbon carbon double bond could rotate freely.



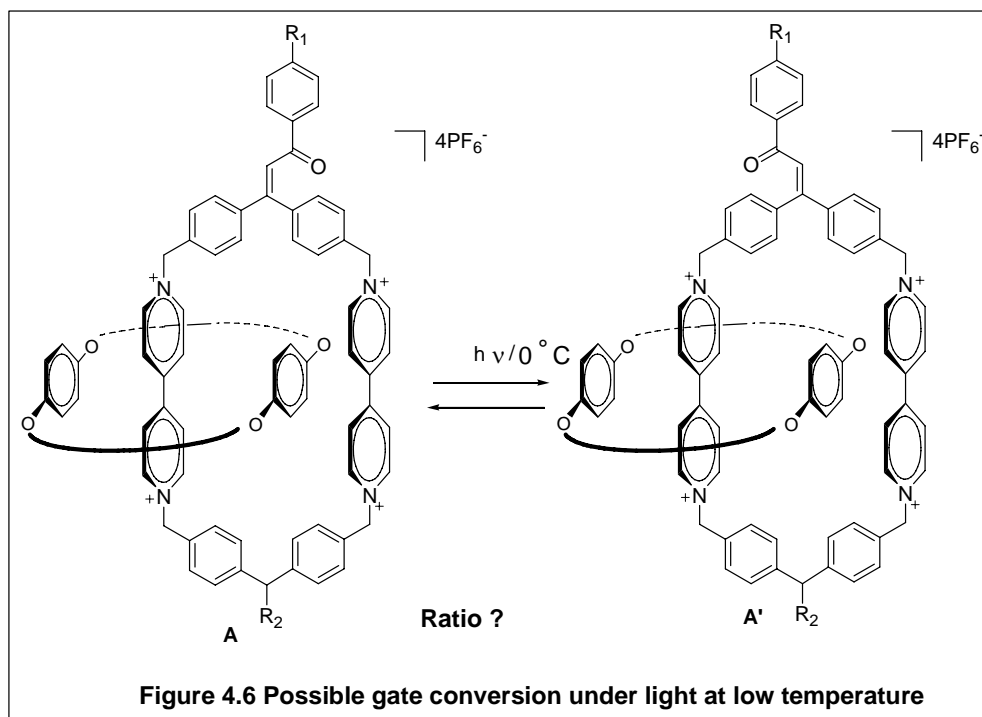
As described in **Figure 4.5**, in conformation A, the wide, ‘up’ gate is more stable but would present a higher energy barrier for BPP34C10 to pass over the extended gate. The gate could rotate ‘down’ to a higher energy but more reactive conformation. When conformation A transforms to conformation B via a free rotation of a single bond in which the gate is narrow or ‘down’, the energy barrier would become lower and BPP34C10 could move to the right side by translocation to form a conformation C. Then the gate would then be expected to go back to the ‘up’ status because this conformation is more thermodynamically stable.

On the other hand, if conformation D goes back to conformation A, a wide, ‘up’ gate might prohibit this movement. So the preference for circumrotation in one direction



could be observed. This motion of the gate could provide the needed modulation of the potential surface. A unidirectional ratchet might be therefore obtained.

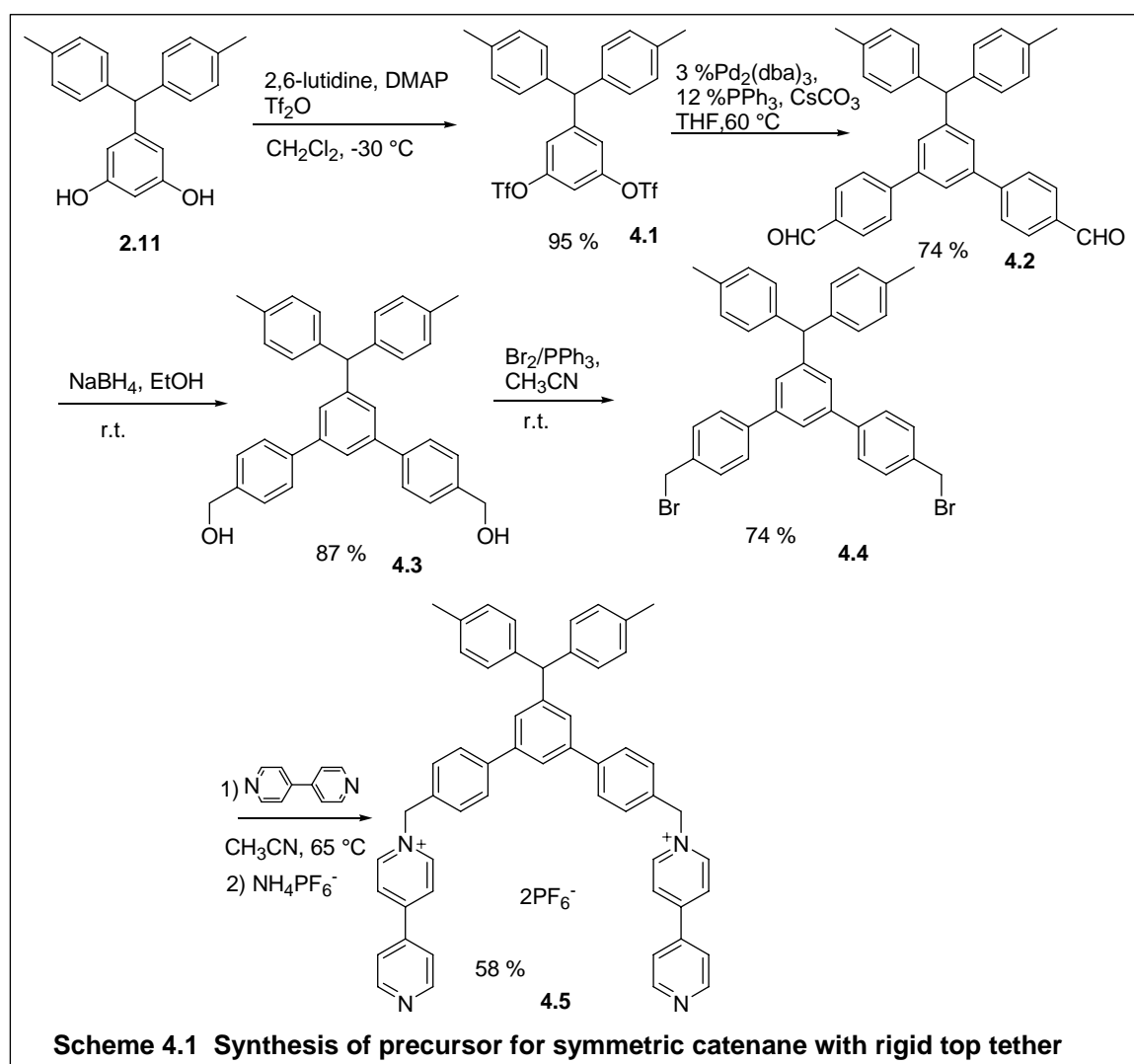
As for the consideration of possible difference of ground states, an experiment was designed as described in **Figure 4.6**. The conformations could be photoisomerized under UV light at low temperature. Since the temperature is low enough, the circumrotation of BPP34C10 over the biased gate would be slow. Since the isomerization does not involve an interaction of the BPP34C10 with the gate, we could control the actual ΔG° difference in the bistable states. Given the rigid phenyl-spacers isolating the biasing gate, we expected this energy difference to be 0. If the thermal isomerization gave a non 1:1 ratio of conformational isomers, we could have stories supporting for thermal ratcheting.



4.2 Synthesis of Symmetric [2]Catenanes with Rigid Top Tether

4.2.1 Synthesis and Characterization of the Precursor for Symmetric [2]Catenanes with Rigid Top Tether

The preparation of the precursor **4.5** (Scheme 4.1) started with triflation of compound **2.11**⁴⁸ to make a good leaving group for a Suzuki coupling. The yield of



triflation was 95 %. The reaction was performed with 2,6-lutidine as a base and DMAP as

a catalyst to give compound **4.1**.⁴⁸ In the ¹H NMR spectrum for **4.1**, the tertiary hydrogen near the triaryl shifted downfield a little (5.15 ppm) when compared to compound **2.11** (5.33 ppm). The protons on the resorcinol ring shifted downfield from 6.19 (t, J=2.3 Hz, 1H), 6.14(d, J=2.3 Hz, 2H) to 7.12-7.05 (m, 1H). In the ¹³C NMR spectrum for **4.1**, an obvious signal was the quartet of carbon coupled with fluorine which had a coupling constant 321 Hz. In the mass spectrum (ESI), the peak at m/z = 591.8 corresponded to the species [M+Na⁺] (calculated 591.04).

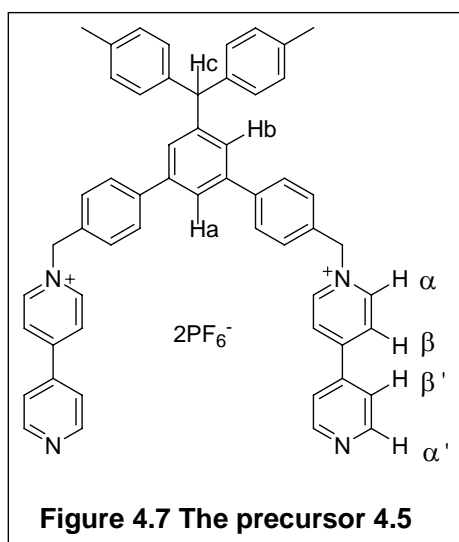
Dialdehyde **4.2** was obtained in 74 % yield via Suzuki coupling⁴⁹ by treatment of bis(triflate) **4.1** with 4-formylphenylboronic acid⁵⁰ catalyzed by Pd₂(dba)₃ and PPh₃. In the ¹H NMR spectrum of dialdehyde **4.2**, the singlet at 10.09 (s, 2H) indicated the presence of the dialdehyde group. In the ¹³C NMR spectrum, the peak at 191.8 ppm corresponded to the carbonyl carbon. In the mass spectrum (ESI), the peak at m/z = 503.3 was attributed to [M+Na⁺] (calculated 503.02).

Dialdehyde **4.2** was reduced by sodium borohydride to give diol **4.3** in 87 % yield. In the ¹H NMR spectrum of diol **4.3**, the singlet at 10.09 ppm disappeared and a singlet at 4.75 ppm (s, 4H) was assigned to the benzylic methylene group. In the ¹³C NMR spectrum, the number of carbons was consistent with the structure of **4.3**.

Diol **4.3** was treated with Br₂/PPh₃ reagent to give dibromide **4.4** in 74 % yield. In the ¹H NMR spectrum of **4.4**, the chemical shift for the benzyl protons shifted upfield to

4.64 ppm compared to the diol (4.75 ppm). The number of carbons in the ^{13}C NMR spectrum was consistent with the structure of **4.4**.

To prepare the dipyridinium precursor **4.5**, dibromide **4.4** was treated by excess 4, 4'-dipyridyl at 65 °C for 4 days. After the reaction was complete and the solvent was removed, the excess 4, 4'-dipyridyl was washed out with chloroform. The residue was dissolved in water and ammonium hexafluorophosphate was added to the aqueous solution to perform an ion exchange. The yield of **4.5** was 58 %. In the ^1H NMR



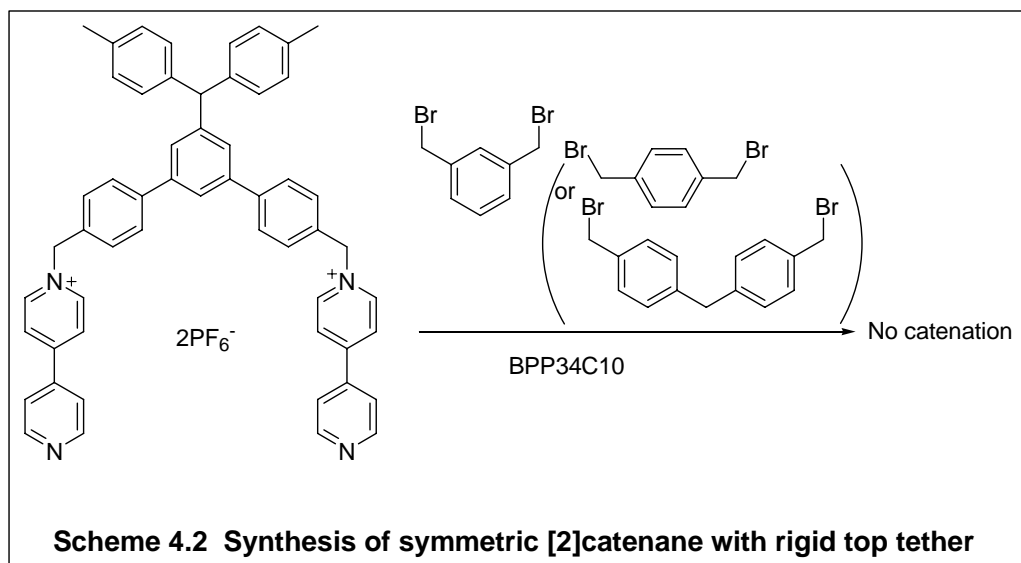
spectrum of for **4.5**, the multiplet at 9.39 ppm (m, 4H) corresponded to the α protons of the dipyridinium units which were adjacent to the cationic nitrogen atoms (**Figure 4.7**). The peak at 8.90 (m, 4H) was attributed to the α' protons close to the neutral nitrogens. The two signals at 8.90 (m, 4H) and 8.05 (m, 4H) were assigned to β , β' protons in the dipyridinium units. The doublet at

7.54 (d, $J = 1.54$ Hz, 2H) corresponded to proton Hb. The signal for proton Hc was a triplet which was overlapped with other signals. The singlet at 6.17 (s, 4H) was assigned to the protons of the benzyl groups adjacent to the cationic nitrogen. The singlet at 5.76 (s, 1H) was assigned to the tertiary hydrogen Hc. The number of carbons in the ^{13}C NMR

spectrum was consistent with the structure of **4.5**. In the mass spectrum of **4.5**, the peak at $m/z = 381.3$ corresponded to M^{2+} which was loss of two PF_6^- anions. All these spectroscopic data supported the structure of the precursor **4.5**.

4.3.2 Synthesis of [2]Catenanes with a Rigid Top Tether

Initially, the synthesis of [2]catenane with a rigid top tether followed the procedure we developed previously (**Scheme 4.2**).³³



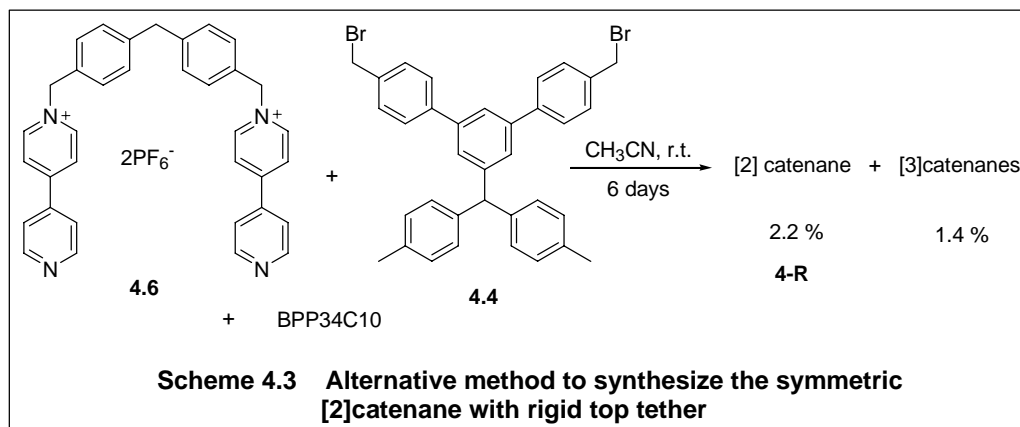
The precursor **4.5** (1 eq.), BPP34C10 (1.6 eq.) and tethers (m-xylylene dibromide, p-xylylene dibromide or bis(4-bromomethylphenyl)methane, 1.3 eq.) were dissolved in acetonitrile and stirred for 4 or 5 days. At the second or third day, yellow precipitate had appeared. Removing the solvent via vacuum, the residue was loaded on the preparative TLC plate. Unfortunately, development of this plate in eluents (EtOAc:Methanol = 1:1

and Methanol:2M NH₄Cl: CH₃NO₃=7:2:1) did not display the formation of catenanes according to R_f values of a orange/red band. Only the band with R_f= 0-0.1 was observed, indicating that oligomers were the main products. The reason for the failure of the catenation could be that the tethers were not long enough to form catenanes.

An alternative method to synthesize symmetric [2]catenane with rigid top tether is described in **Scheme 4.3**. The labels ‘top’ or ‘bottom’ is relative. We used compound **4.6** as a precursor and the compound **4.4** as a tether. Precursor **4.6**, derived from treatment of bis(4-bromomethylphenyl)methane with excess 4,4'-dipyridyl, was mixed with BPP34C10 (1.6 eq.) and tether **4.4** (1.3 eq.) in acetonitrile. The mixture was stirred at room temperature for 5 days. The solvent was removed by evaporation and the residue was loaded on the preparative TLC plate. The plate was developed in eluents: EtOAc:Methanol = 1:1 at 40 °C twice and Methanol:2M NH₄Cl: CH₃NO₃ = 7:2:1 once. The orange/red band with R_f = 0.6 was characterized by ¹H NMR spectroscopy and mass spectrometry. It appeared that this fraction was [3]catenane according to the mass spectrum.

In the mass spectrum for Fraction 1, the peaks at m/z=1156.57, 724.72, 507.54 corresponded to [M⁴⁺2PF₆]²⁺(calculated 1159.46), [M⁴⁺PF₆]³⁺(calculated 724.66) and M⁴⁺(calculated 507.25). The yield for this fraction was 1.5 %. Fraction 2 with R_f = 0.3 was likely [2]catenane according to the mass spectrum in a yield of 2.3 %. Insufficient

material was obtained to enable meaningful ^1H NMR spectra to be acquired and these compounds assignments are quite tentative.



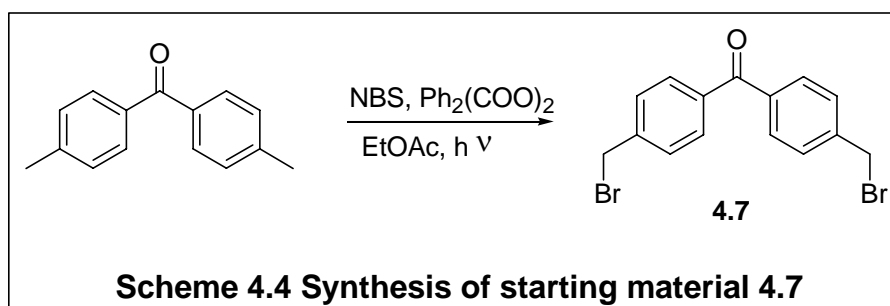
Although a symmetric [2]catenane with a rigid “top” tether was likely synthesized, a precursor was not derived from the “top” tether but the “bottom” tether in our synthetic route. In other words, if we want to prepare asymmetric [2]catenanes with biased gates, we would have to use the spacers with biased gates as bottom tethers. On the other hand, the yield was low due to the formation of [3]catenane and the overall size and width of the tether may also contribute to low yield. Because of those disadvantages, this asymmetric catenane was not promising for further study.

4.3 Synthesis and Characterization of [2]Catenanes with Photoisomerizable Gates

4.3.1 Synthesis of the Precursors of [2]Catenanes with Photoisomerizable Gates

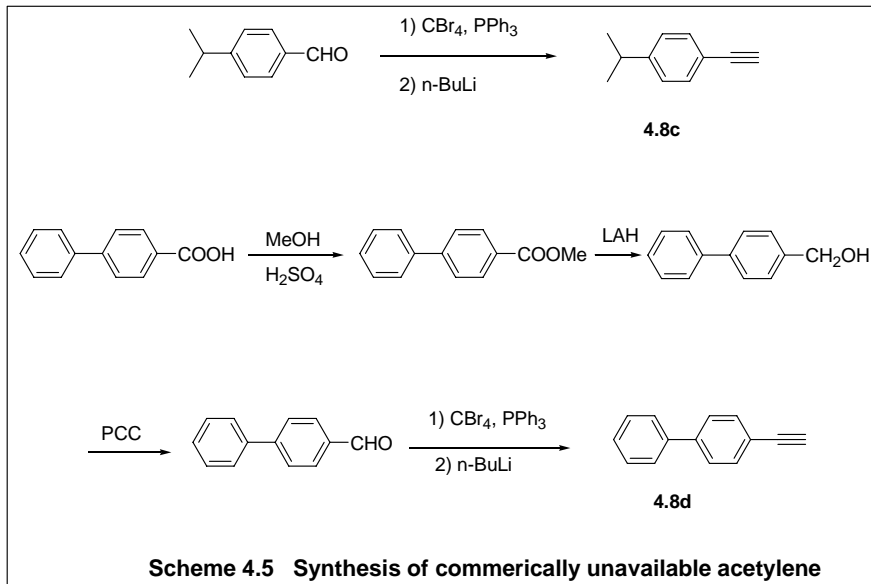
The synthesis of [2]catenanes with photoisomerizable gates began with the preparation of the starting material **4.7** (bis[4-(bromomethyl)phenyl]methanone) by

treatment of 4,4'-dimethylbenzophenone with NBS in a radical bromination (**Scheme 4.4**).⁵¹

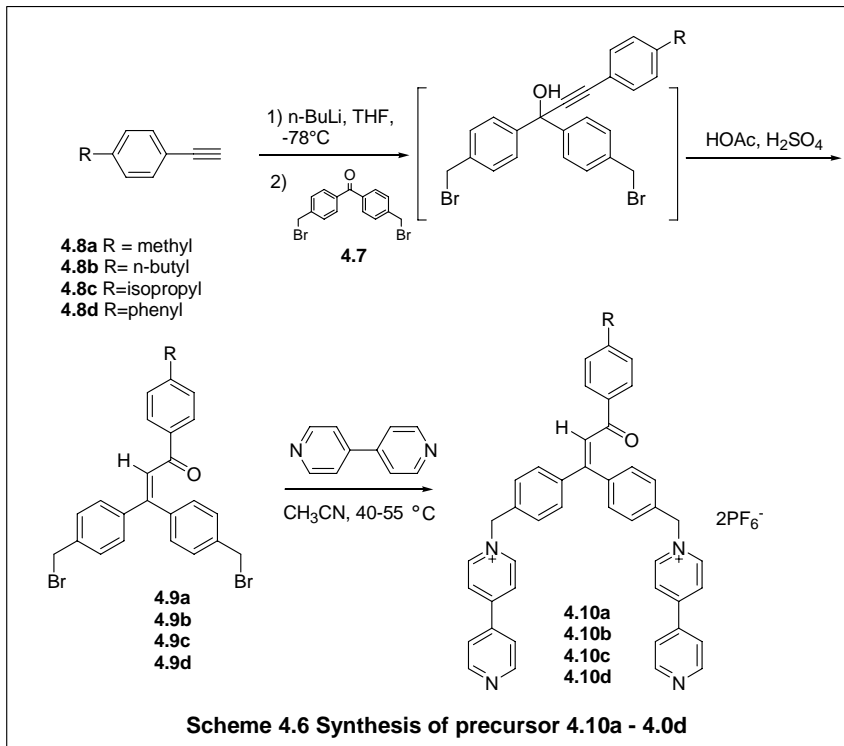


A modification of this radical bromination was to use ethyl acetate instead of hazardous CCl_4 as a solvent. The ^1H NMR and ^{13}C NMR spectra supported the structure of dibromide **4.7**.

The starting materials 4-methylphenylacetylene (**4.8a**), 1-butyl-4-ethynylbenzene (**4.8b**) were commercially available. 1-Ethynyl-4-isopropylbenzene (**4.8c**) was prepared from 4-isopropylbenzaldehyde according to a Corey-Fuchs protocol (**Scheme 4.5**).⁵² 4-Ethynyl-1,1'-biphenyl (**4.8d**) was obtained from p-phenylbenzoic acid via four steps: Fisher esterification, LAH reduction, PCC oxidation and Corey-Fuchs reaction (**Scheme 4.5**).⁵⁴

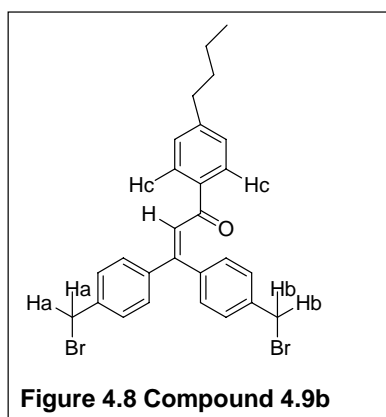


The synthesis of the precursors **4.10a** – **4.10d**⁵³ (**Scheme 4.6**) started with the deprotonation of aromatic alkyne with n-BuLi at -78 °C. Dibromide **4.7** was added to the



deprotonated alkyne solution and the mixture kept at -78 °C. The low temperature prevented the nucleophile from attacking the reactive benzyl bromide. The intermediate propargylic alcohol was transformed to α , β -unsaturated ketone (**4.9a-4.9d**) via Meyers-Schuster rearrangement⁵³ under acid condition: acetic acid and catalytic sulfuric acid in 31-39 % yield after chromatography. Enones **4.9a-4.9d** were treated with excess 4, 4'-dipyridyl followed by anion exchange with ammonium hexafluorophosphate to give the dipyridyls **4.10a – 4.10d**.

Compound **4.9a** and **4.10a** were synthesized in our laboratory by Jessica



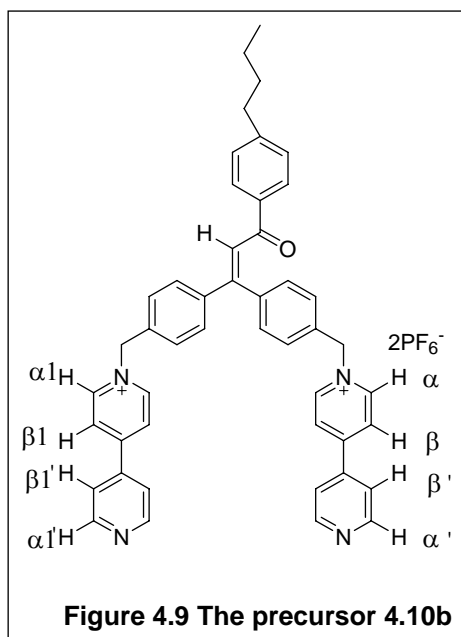
Evans. Dibromide **4.9b** was obtained in a yield of 39 %.

In compound **4.9b**, the benzyl protons Ha and Hb (**Figure 4.8**) were not identical because Hb was close to the carbonyl group and would be affected by this group while Ha was far away from the carbonyl group. In the

¹H NMR spectrum of **4.9b**, the singlets at 4.47 (s, 2H), 4.42 (s, 2H) corresponded to the different benzyl protons Ha and Hb. The Hc in the compound **4.9b** was so close to the carbonyl group that the chemical shift of these compound move downfield to 7.81 (d, J=8.1 Hz, 2H). The triplet at 2.61(t, J=7.8 Hz, 2H) was attributed to the benzyl methylene group in the butyl group. Another triplet at 0.91 (t, J=7.2 Hz, 3H) was assigned to the protons of terminal carbon of the butyl group. The

signals at 1.56 (m, 2H) and 1.31 (m, 2H) corresponded to the middle methylene protons in the butyl group. In the ^{13}C NMR spectrum, the benzyl carbons attached to bromine atoms did not show difference. The number of carbons in the ^{13}C NMR spectrum was consistent with the structure of the compound **4.9b**. In the mass spectrum (ESI), the peaks at $m/z = 547.0$, 549.1 , 551.0 corresponded to $[\text{M}+\text{Na}^+]$, $[\text{M}+2+\text{Na}^+]$, $[\text{M}+4+\text{Na}^+]$. The ratio 1:2:1 of the peaks supported the presence of two bromine atoms.

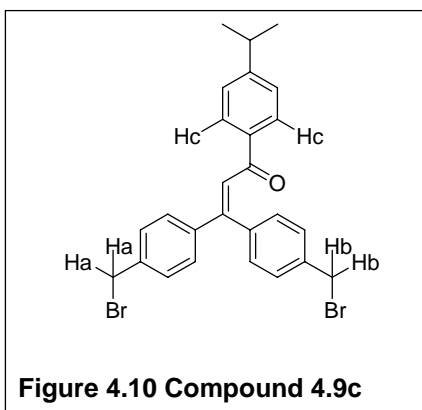
Dipyridyl **4.10b** was prepared in 54 % yield by treatment of dibromide **4.9b** with excess 4, 4'-dipyridyl followed by an anion change to give hexafluorophosphate salt. The protons of the different dipyrindinium units could appear at different chemical shifts, like $\text{H}\alpha$ and $\text{H}\alpha 1$ due to the effect of carbonyl group or could be the same, like $\text{H}\alpha'$ and $\text{H}\alpha 1'$



which are far away from the carbonyl group (**Figure 4.9**). The multiplets at 8.90 (m, 8H), 8.39 (d, $J=6.9$ Hz, 4H), 7.87 (m, 6H) corresponded to the protons of the dipyrindinium units. The benzyl protons were located at 5.84 (s, 2H), 5.80 (s, 2H). The signals at 2.70 (t, $J=7.6$ Hz, 2H), 1.63 (m, 2H), 1.38 (m, 2H), 0.97 (t, $J=7.2$ Hz) belonged to the butyl protons. In the mass spectrum (ESI) for **4.10b**, the peak at $m/z = 339.16$ was assigned to

M^{2+} which was loss of two PF_6^- anion. Loss of one PF_6^- anion produced a monocation $[M^{2+}PF_6^-]^+$ which display a peak at $m/z=823.42$. All the data demonstrated the formation of the precursor **4.10b**.

Dibromide **4.9c** was prepared in 38 % yield following the same protocol in

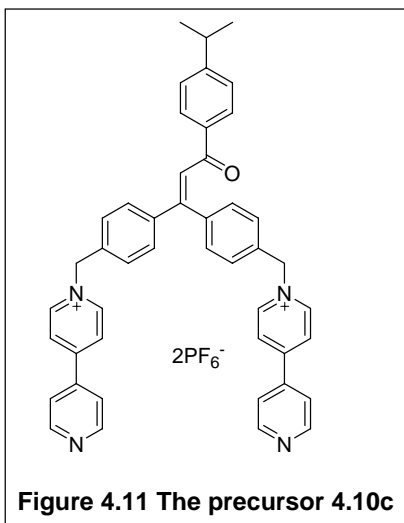


Scheme 4.6. The benzyl protons were different because of their relative orientation to the carbonyl group (**Figure 4.10**). The signals for those benzyl protons appeared as two singlets at 4.56 (s, 2H), 4.51 (s, 2H). The doublet at 7.91 (d, $J=8.7$ Hz, 2H) was assigned to the protons close to carbonyl group – Hc

(**Figure 4.10**). The signals at 2.99 (m, $J=6.6$ Hz, 1H), 1.31 (d, $J=6.6$ Hz, 6H) demonstrated the presence of isopropyl group. In the ESI spectrum, the 1:2:1 ratio of intensity of three peaks at $m/z = 533.04$ ($M+Na^+$), 535.02 ($M+2+Na^+$), 537.01 ($M+4+Na^+$) supported the presence of two bromine atoms in compound **4.9c**. All those spectroscopic data confirmed the structure of dibromide **4.9c**.

Dipyridyl **4.10c** was obtained in a yield of 61 % by reaction between dibromide **4.9c** and excess 4,4'-dipyridyl. The signals at 8.91 (m, 8H), 8.40 (d, $J=6$ Hz, 4H), 7.92 (d, $J=8.1$ Hz, 2H), 7.87 (d, 5.1 Hz, 4H) corresponded to the protons in the dipyridinium units (**Figure 4.11**). Compared to the benzyl protons in dibromide **4.9c**, the benzyl protons in

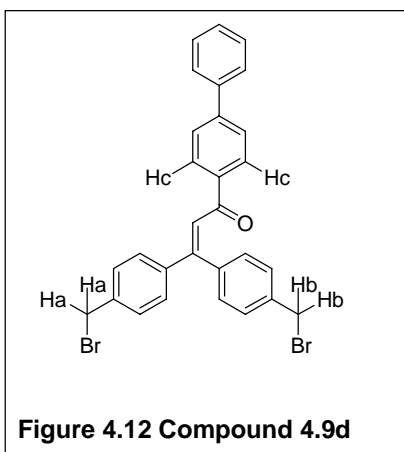
4.10c shifted downfield 1.3 ppm to 5.85 (s, 2H), 5.81 (s, 2H) because they were adjacent



to the cationic nitrogen atoms. In the mass spectrum, the peak at $m/z = 332.16$ indicated the species M^{2+} , resulting from loss of two PF_6^- of the precursor **4.10c**. The data from 1H NMR, ^{13}C NMR and ESI supported the successful synthesis of the precursor **4.10c**.

The compound **4.9d** was prepared with 31 % yield. In the compound 4.9d, the benzyl protons Ha and

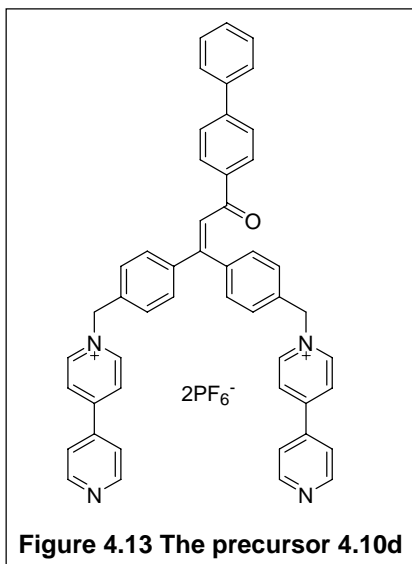
Hb were not identical either because Ha is close to the carbonyl group while Hb is far away from the carbonyl group (**Figure 4.12**). In the 1H NMR spectrum, two different benzyl protons appeared as two singlets at 4.57 (s, 2H), 4.50 (s, 2H). The doublet at 8.08



(d, $J=8.4$ Hz, 2H) corresponded to Hc close to the carbonyl group. Biphenyl rings made the 1H NMR complicated, especially the aromatic region.

Dipyridyl **4.10d** (**Figure 4.13**) was prepared in 71 % yield by treatment of dibromide **4.9d** with excess 4, 4'-dipyridyl following the same procedure for the precursors **4.10b** and **4.10d**. The signals at 8.90 (m, 6H), 8.75 (d, $J = 6.9$ Hz, 2H), 8.38 (d, $J = 6.9$ Hz, 2H), 8.23 (d, $J = 6.9$ Hz, 2H), 7.99 (d, $J = 8.4$ Hz, 2H), 7.85 (m, 2H) were

attributed to the protons on the dipyridinium units. Two singlets at 5.84 (s, 2H), 5.75 (s,



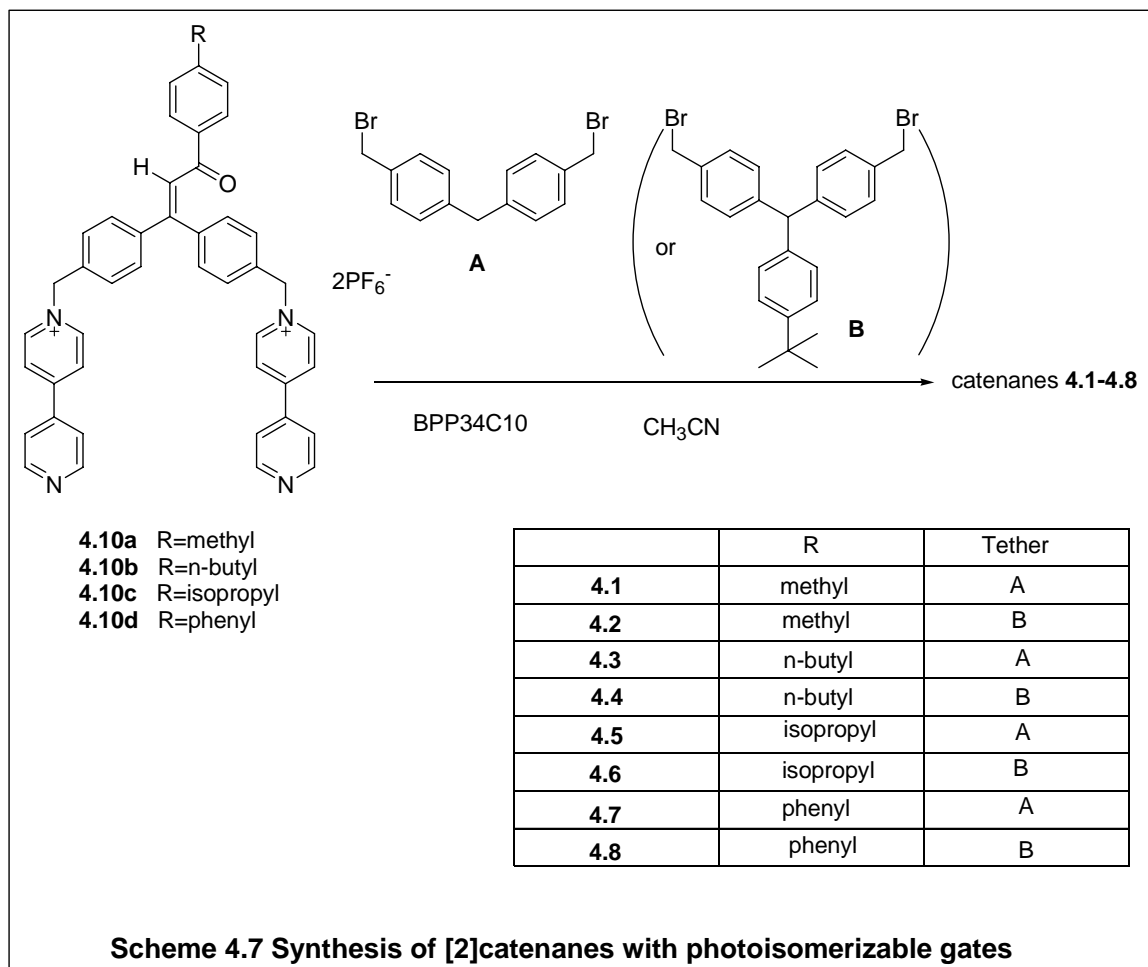
2H) are benzylic proton signals close to the cationic nitrogen. The ¹³C NMR was consistent with the structure of the precursor **4.10d**. In the ESI spectrum, the peak at $m/z = 349.18$ was consistent with the species M^{2+} which was loss of two PF₆⁻ anion. Loss of one PF₆⁻ produced the monocationic species which appeared at $m/z = 843.31$ ($M^{2+}PF_6^-$). All these data

supported the structure of the desired compound **4.10d**.

4.3.2 Synthesis of [2]Catenanes with Photoisomerizable Gates

The synthesis of [2]catenanes with photoisomerizable gates followed the procedures we developed in chapter 2 as described in **Scheme 4.7**. The precursors **4.10a** - **4.10d** (1 eq.), BPP34C10 (1.6 eq.), tether A or B (1.3 eq.) were dissolved in acetonitrile and the mixture was stirred at room temperature for 4 or 5 days. Usually, some yellow precipitate appeared at the second or third day.

The purification of catenanes followed the procedure described in section **2.3**. After 4 or 5 days, the solvent acetonitrile was removed under reduced pressure to give a red residue. The residue was dissolved in methanol/acetone (1:1) and the solution was



loaded evenly on the preparative TLC plate. After drying, the preparative TLC plate was eluted twice with methanol/ethyl acetate (1:1) at 35 °C. The R_f value of BPP34C10 was high in methanol/ethyl acetate (1:1) (R_f = 0.9). Then the preparative TLC plate was eluted with methanol/2M ammonium chloride/nitromethane (7:2:1). The desired [2]catenanes moved up (R_f = 0.4 - 0.5) while the oligomeric dipyrrolic chain didn't move.

The red band was removed from the plate. The silica gel containing the [2]catenanes was grounded and washed with the final eluent-methanol/2M ammonium

chloride/nitromethane (7:2:1). An excess of ammonium hexafluorophosphate was added to perform anion exchange. The methanol and nitromethane were removed via rotary evaporator and a red precipitate was suspended in the remaining solution. The solution was filtered and the solid was washed with water several times and allowed to air dry.

If needed to improve the purity of the [2]catenanes, another isolation with a preparative TLC plate was performed. The isolated solid was dissolved in acetone and loaded on the preparative TLC. Repeating the previous procedure, the TLC plate was developed with methanol/acetone (1:1) and methanol/2M ammonium chloride/nitromethane (7:2:1).

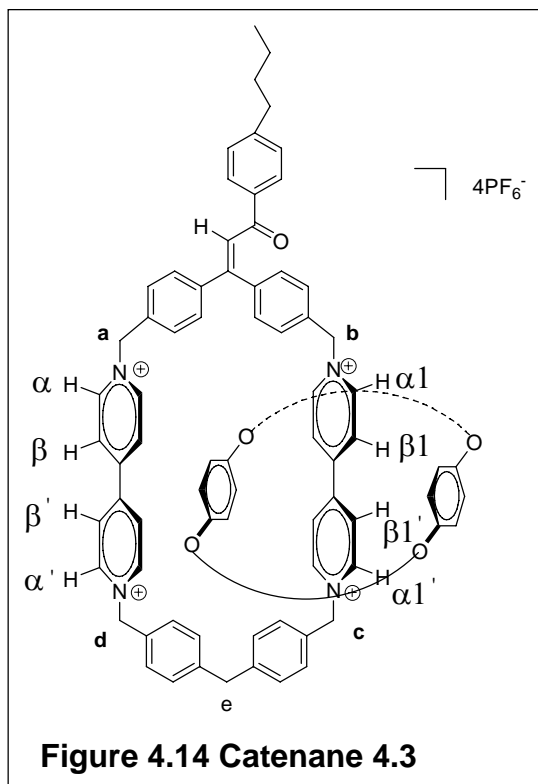
Catenane **4.1** and **4.2** were prepared in our laboratory by Jessica Evans-Fessler. They were discussed in her undergraduate thesis. The synthesis of the six catenanes **4.3-4.8** was original to this thesis and they will be discussed in the following sections.

4.3.3 Characterization of [2]Catenanes with Photoisomerizable Gates

4.3.3.1 Characterization of [2]Catenane 4.3

[2]Catenane **4.3** was obtained in 1.3 % with two preparative TLC plates. In terms of the structure of [2]catenane **4.3** (**Figure 4.14**), the protons on the dipyrindinium units are different. Since BPP34C10 moves fast at room temperature, there should be eight signals for those α , α' , $\alpha 1$, $\alpha 1'$, β , β' , $\beta 1$, $\beta 1'$ protons in the ^1H NMR spectrum. On the

other hand, the benzylic protons at positions a, b, c, d should be different too. In the ^1H

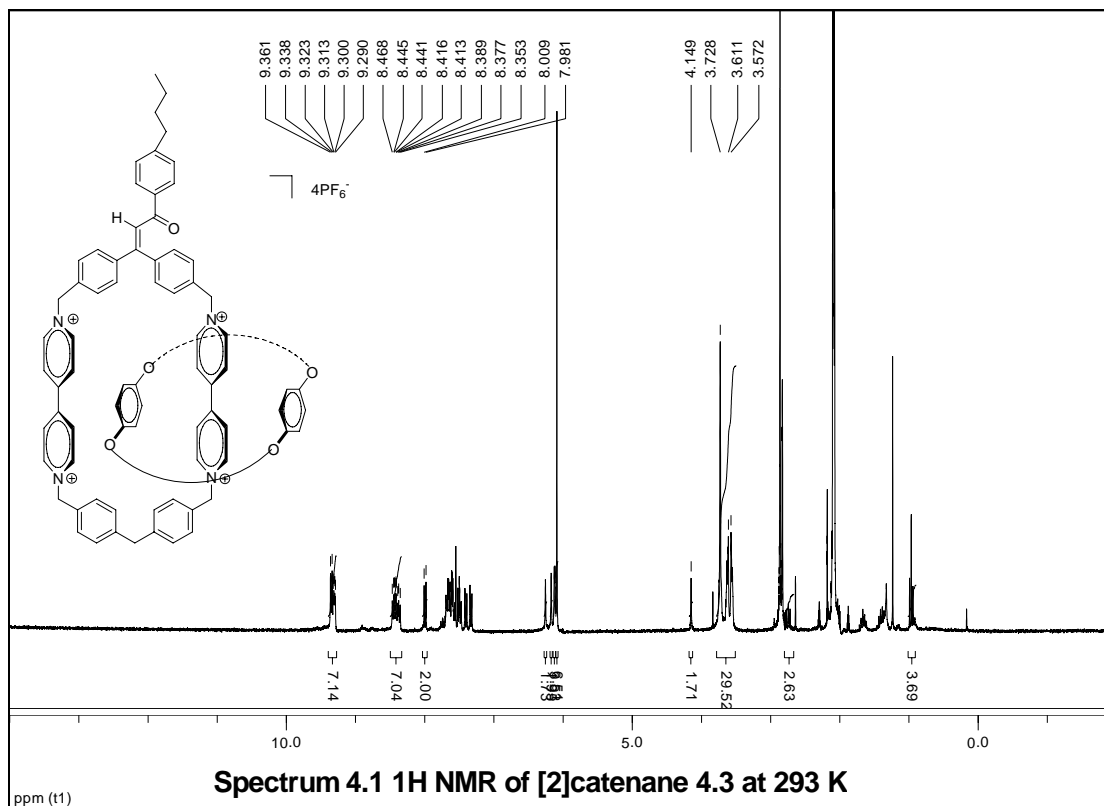


NMR spectrum of catenane **4.3** (**Spectrum 4.1**), the multiplets at 9.39-9.27 (m, 8H) corresponded to the α , α' , $\alpha 1$, $\alpha 1'$ protons of the dipyrindinium units which are adjacent to the cationic nitrogen. The multiplets at 8.43 (m, 8H) were attributed to β , β' , $\beta 1$, $\beta 1'$ protons. The doublet at 7.99 (d, $J = 8.39$ Hz, 1H) was assigned to the protons adjacent to the carbonyl group of the gate. The singlets at 6.25 (s, 2H), 6.17 (s, 2H), 6.12 (two

singlets) were assigned to the benzylic protons Ha, Hb, Hc, Hd. The benzylic protons He between two aryl ring was located at 4.15 (s, 2H). The integration at 3.78-3.51 ppm was 32H.

In the mass spectrum (ESI), the peak at $m/z = 518.26$ was assigned to the tricationic species $[\text{M}^{4+}\text{PF}_6^-]^{3+}$ which was loss of three PF_6^- anions (calculated 517.89). The dicationic species $[\text{M}^{4+}2\text{PF}_6^-]^{2+}$ was found at $m/z = 849.36$ (calculated 849.32). No [3]catenane was detected.

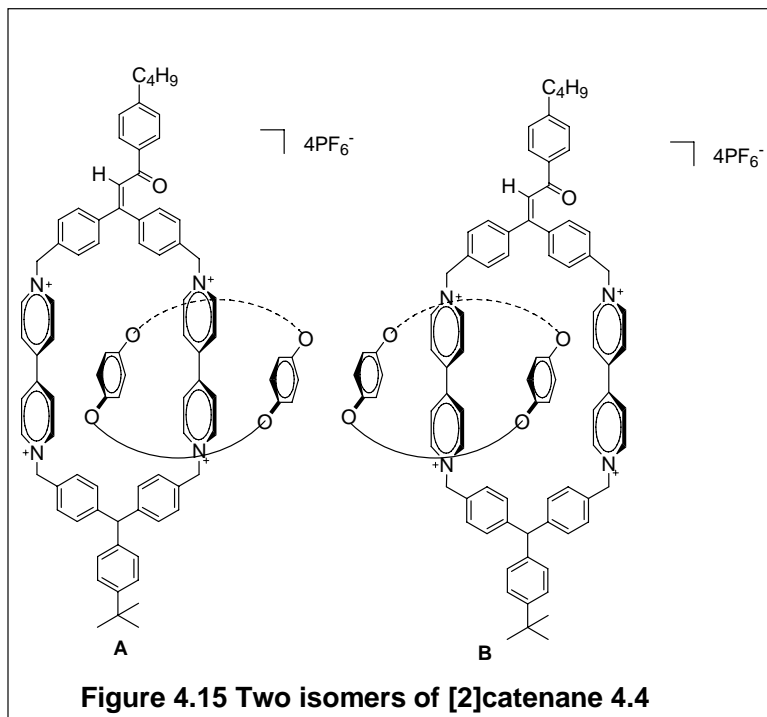
All the data supported the formation of [2]catenane **4.3**.



4.3.3.2 Characterization of [2]Catenane 4.4

[2]catenane **4.4** was obtained in a slightly impure form in 5.6 % yield. As shown in **Figure 4.15**, when the catenane **4.4** was formed, two isomers A and B could be both obtained since movement of the BPP34C10 ring over the hindered tethers was slow at room temperature. Since they are not identical, the ¹H NMR spectrum of catenane **4.4** was very complicated. Theoretically, sixteen different protons could appear in the ¹H NMR spectrum for the dipyridinium units. In the ¹H NMR spectrum of catenane **4.4** (**Spectrum 4.2**), the multiplets between 9.42-9.32 ppm were attributed to the α protons of

the dipyridinium units. The multiplets at 8.58-8.40 ppm and 8.34-8.22 ppm corresponded

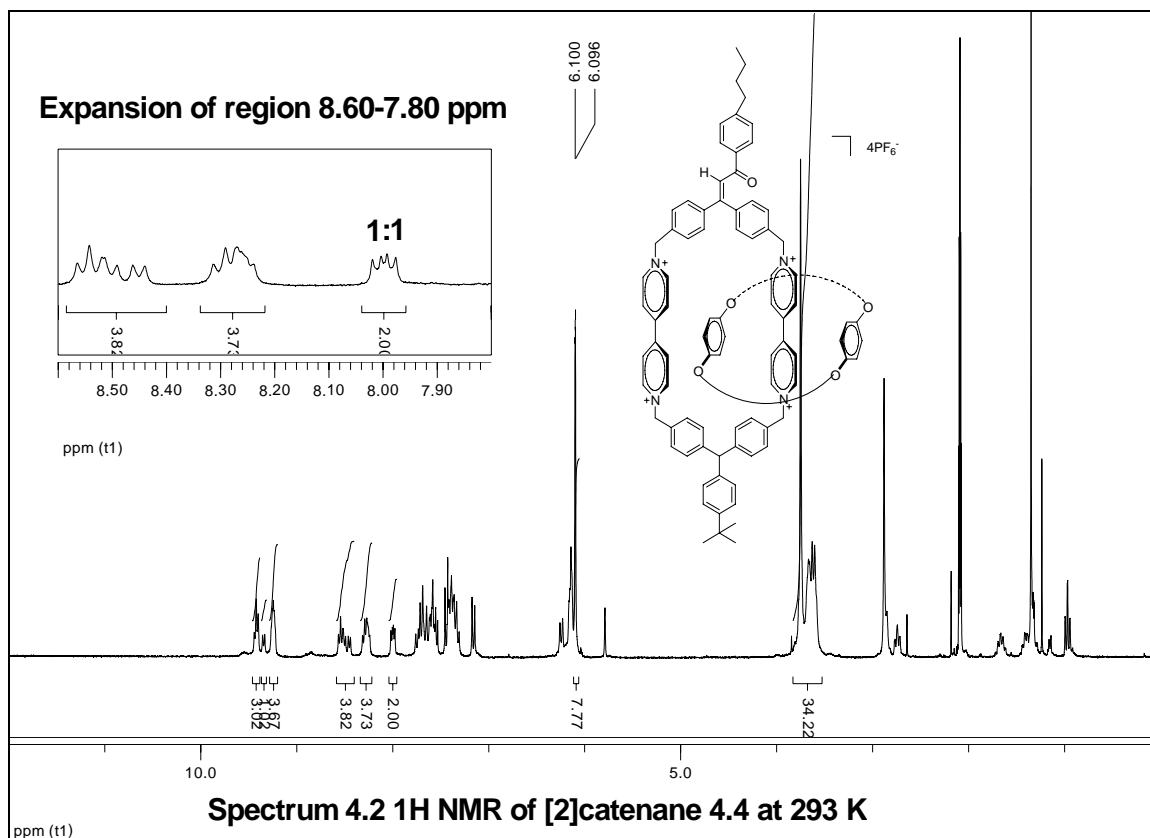


to the β protons. The two doublets at 8.04-7.96 ppm were assigned to the protons adjacent to the carbonyl group of the gate. The integration for the BPP34C10 aliphatic hydrogens at 3.83-3.53 ppm was the expected

32H.

The 8H singlet at 6.1 ppm (s, 8H) was assigned to the internal and external hydroquinone protons of the BPP34C10. Similar to the catenanes described in chapter 3, the internal hydroquinone ring of the BPP34C10 in catenane **4.4** only π - π stacked with one dipyridinium unit due to the distance between the rings. The internal and external hydroquinone rings therefore had similar ^1H NMR resonance environments. They both shared an averaged signal at 6.1 ppm.

In the ^1H NMR spectrum of catenane **4.4** at room temperature (**Spectrum 4.2**), the ratio of two doublets near 8.00 ppm was 1:1, which demonstrated that the



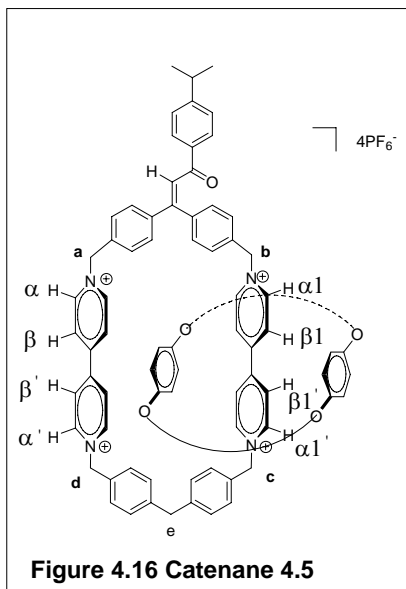
unsymmetric gate did not twist the rigid tether and interact with the BPP34C10 ring.

In the mass spectrum (ESI), the tricationic species $[\text{M}^{4+}\text{PF}_6^-]^{3+}$ was found at $m/z = 561.90$ (calculated 561.92). The peak at $m/z = 915.45$ was assigned to the dicationic species $[\text{M}^{4+}2\text{PF}_6^-]^{2+}$ which was loss of two PF_6^- anions (calculated 915.37). However, some species might be assigned to [3]catenane. The peak at $m/z = 519.97$ corresponded to species which was loss of four PF_6^- anions in the [3]catenane.

4.3.3.3 Characterization of [2]Catenane 4.5

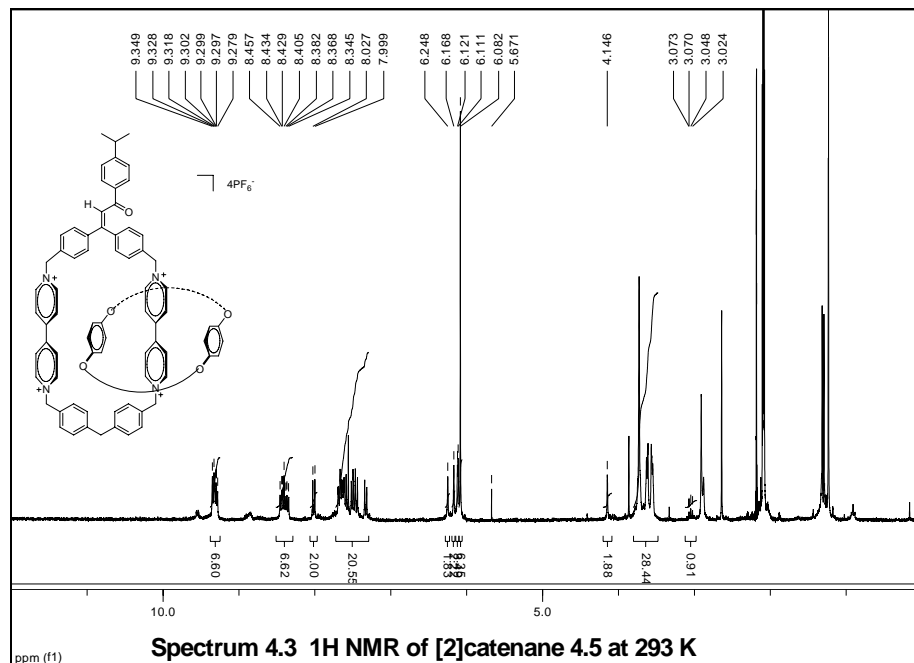
[2]Catenane was obtained in 1.3 % yield after two preparative TLC plates. Similar

to [2]catenane **4.3**, the protons on the dipyrindinium units in catenane **4.5** were



differentiated (**Figure 4.16**). Eight signals could be found in the ^1H NMR spectrum for the dipyrindinium units. The benzylic protons adjacent to the cationic nitrogen were also different. As expected (**Spectrum 4.3**), eight protons at α positions appeared as multiplets at 9.38-9.25(m, 8H) and eight protons at β positions was found around 8.41 (m, 8H). The doublet at 8.01 (d, $J = 8.35$ Hz, 1H) corresponded to the protons adjacent to

the carbonyl group of the gate. The singlets at 6.25 (s, 1H), 6.17 (s, 2H), 6.12(s, 2H),



6.11 (s, 2H) were attributed to the benzylic protons Ha, Hb, Hc, Hd adjacent to the

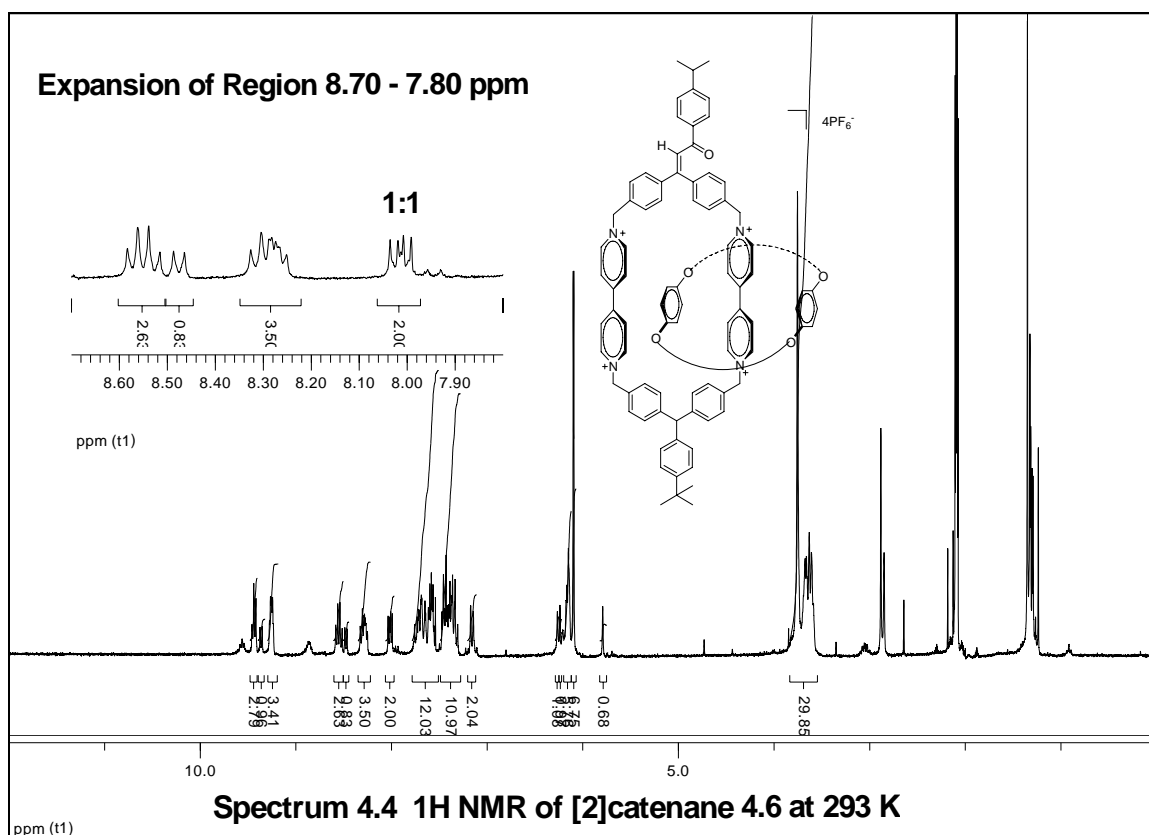
cationic nitrogen. The benzylic protons He of the bottom tether was found at 4.15 (s, 1H). Integration at 3.12-2.98 ppm for the BPP34C10 aliphatic hydrogens was 32H, indicating the formation of [2]catenane not [3]catenane.

In the mass spectrum (ESI), the peak at $m/z = 842.13$ was assigned to the dicationic species $[M^{4+}2PF_6^-]^{2+}$ which was loss of two PF_6^- anions (calculated 842.31). The monocationic species $[M^{4+}3PF_6^-]^+$ was found at $m/z = 1830.27$ (calculated 1829.58). Interestingly, a peak at $m/z = 1110.47$ should be resulted from the formation of [3]catenane ($[M^{4+}2PF_6^-]^{2+}$, calculated 1110.44). This [3]catenane could be detected from some impurity in the 1H NMR spectrum.

4.3.3.4 Characterization of [2]Catenane 4.6

Similar to [2]catenane 4.4, [2]catenane 4.6 also formed two isomers (**Figure 4.15**). Sixteen different signals for the protons of dipyridinium units could be observed, some of which could be overlapped.

In the 1H NMR spectrum of [2]catenane 4.6 (**Spectrum 4.4**), the signals between 9.43- 9.19 ppm were assigned to the α protons of the dipyridinium moieties. The multiplets between 8.55 - 8.30 ppm corresponded to the β protons. The signals for the benzylic protons are too complicated to distinguish. The integration between 3.83-3.55



ppm was 32H which corresponded to the aliphatic protons of the BPP34C10. This integration supported the formation of [2]catenane instead of [3]catenane. The ratio of two doublets near 8.00 ppm, which corresponded to the hydrogens protons adjacent to the carbonyl group of the gate, was 1:1, demonstrating that the unsymmetric gate did not twist the rigid tether and interact with the BPP34C10 ring.

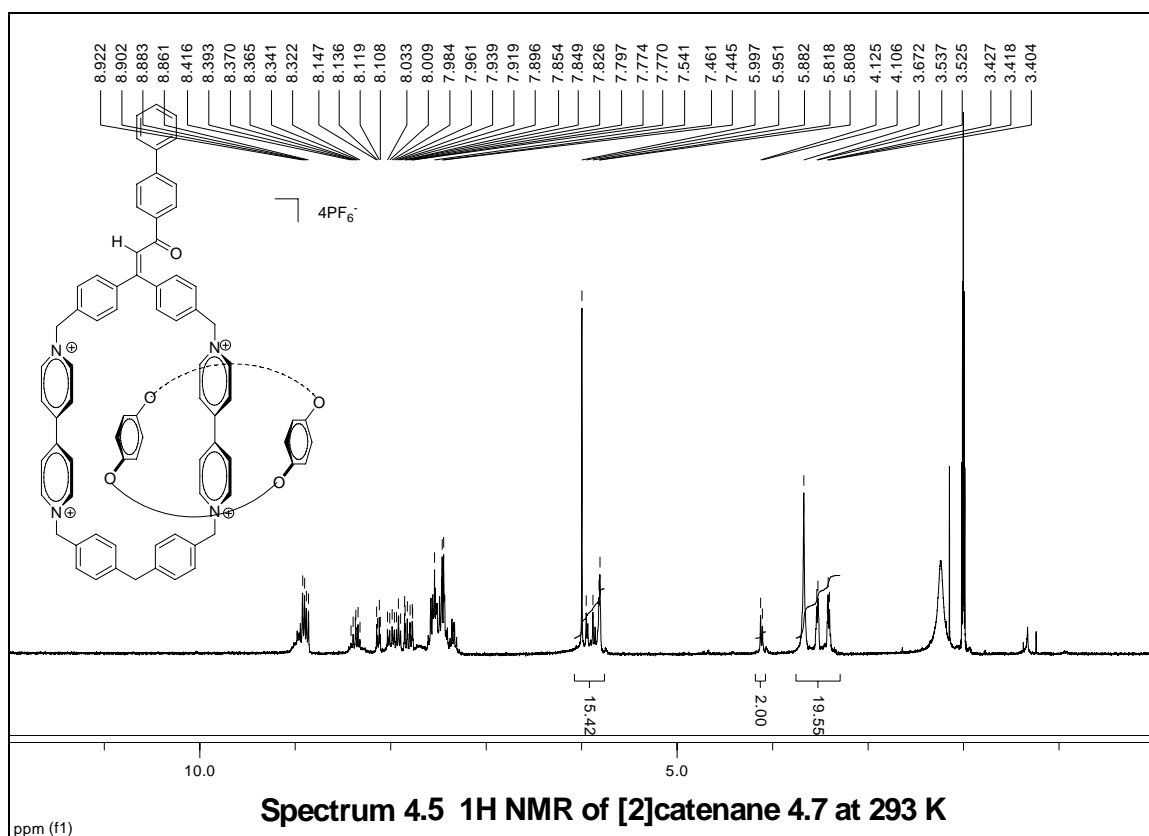
In the mass spectrum (ESI), the tetracationic species $[\text{M}^{4+}]$ was found at $m/z = 381.80$ (calculated 381.85). The peak at $m/z = 557.40$ was assigned to the tricationic species $[\text{M}^{4+}\text{PF}_6^-]^{3+}$ which was loss of three PF_6^- anions (calculated 557.25). The peak at $m/z = 908.27$ was attributed to the dicationic species $[\text{M}^{4+}2\text{PF}_6^-]^{2+}$ (calculated 908.36).

Some species might indicate the formation of [3]catenane. The peak at $m/z = 515.40$ corresponded to tetracationic species $[M^{4+}]$ which was loss of four PF_6^- anions in the [3]catenane. The peak at $m/z = 1176.60$ was assigned to the species $[M^{4+}2PF_6^-]^{2+}$ (calculated 1176.49). The impurity in the 1H NMR spectrum could explain this result.

Unfortunately, it is hard to separate [2] and [3]catenanes completely on the preparative TLC plates since they had similar R_f values.

4.3.3.5 Characterization of [2]Catenane 4.7

The 1H NMR spectrum of [2]catenane **4.7** was more complicated than those of



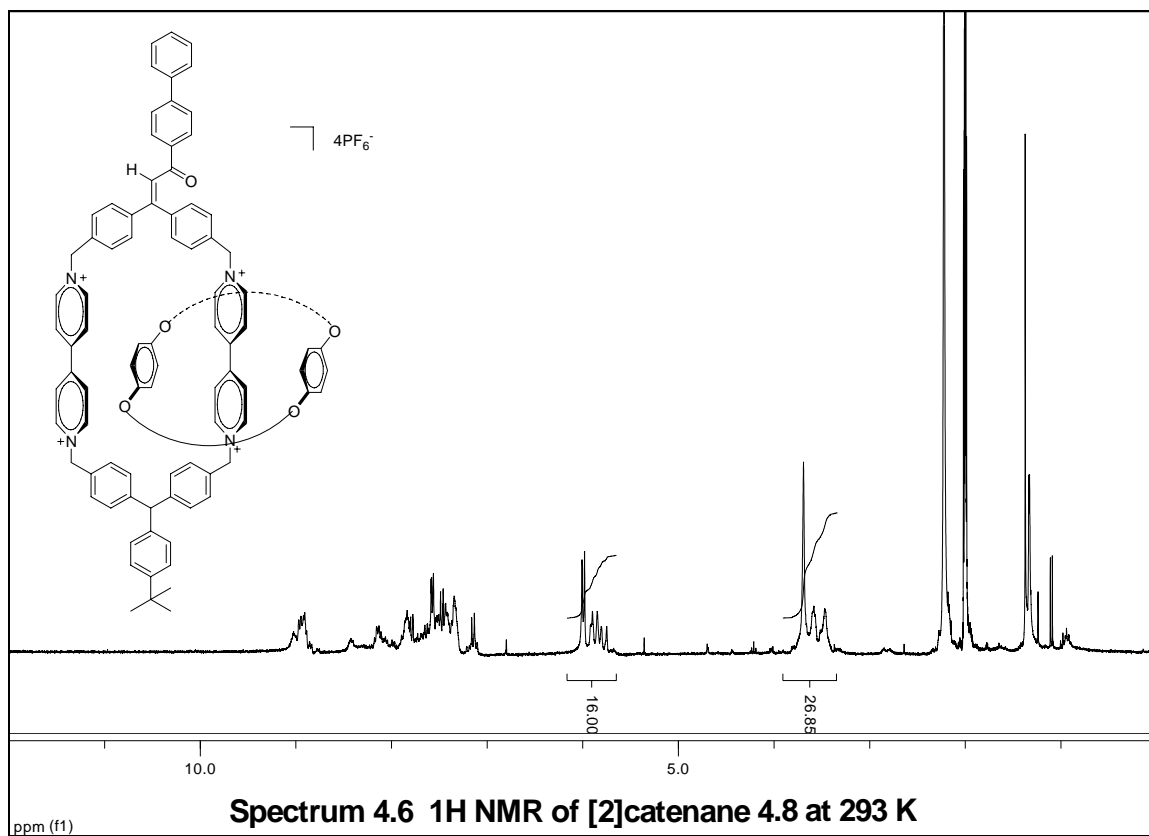
catenanes **4.3** and **4.5** due to the phenyl group. The integration ratio of the signals at 5.99-5.88 ppm (benzylic protons plus hydroquinone protons) and the signals at 3.67-3.40 (the aliphatic protons in BPP34C10) indicated formation of [2]catenane instead of [3]catenane. The signals at 4.12 ppm corresponded to the methylene protons between two aryl at the bottom tether.

In the mass spectrum (ESI), the peak at $m/z = 859.20$ was assigned to the dicationic species $[M^{4+}2PF_6^-]^{2+}$ which was loss of two PF_6^- anions (calculated 859.30). The peak at $m/z=1127.33$ showed the formation of [3]catenane ($[M^{4+}2PF_6^-]^{2+}$, calculated 1127.43).

4.3.3.6 Characterization of [2]Catenane 4.8

The 1H NMR spectrum of [2]catenane **4.8** (**Spectrum 4.6**) was even more complicated than any other of our catenanes since there were two isomers and the biphenyl group made it hard to assign the signals for the spectrum. The ratio of benzylic protons and BPP34C10 aliphatic protons was reasonable for indicating the formation of [2]catenanes instead of [3]catenanes.

In the mass spectrum (ESI), The peak at $m/z = 925.20$ was attributed to the dicationic species $[M^{4+}2PF_6^-]^{2+}$ (calculated 925.35). There are evidence of the formation of [3]catenane. The peak at $m/z = 1193.00$ was attributed to dicationic species of

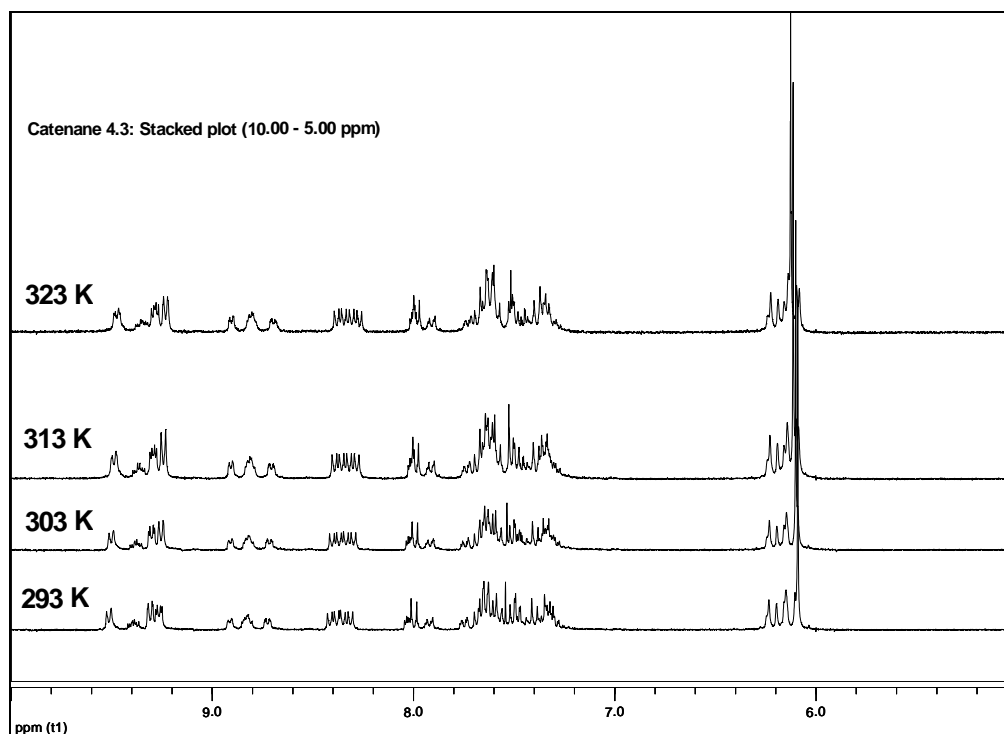


[3]catenane $[\text{M}'^{4+}2\text{PF}_6^-]^{2+}$ (calculated 1193.48). The peak at $m/z=747.87$ corresponded to the tricationic species $[\text{M}'^{4+}\text{PF}_6^-]^{3+}$ (calculated 747.33).

4.3.4 Variable Temperature ^1H NMR of [2]Catenane

4.3.4.1 Variable Temperature ^1H NMR of [2]Catenane 4.3

As for [2]catenane **4.3** with the unblocked bottom tether, the BPP34C10 can easily move back and forth along the bottom tether. It is not surprising that there was no obvious change at variable temperature (from 293 K to 323 K) as shown in the stacked plot ^1H NMR **Spectrum 4.7**.

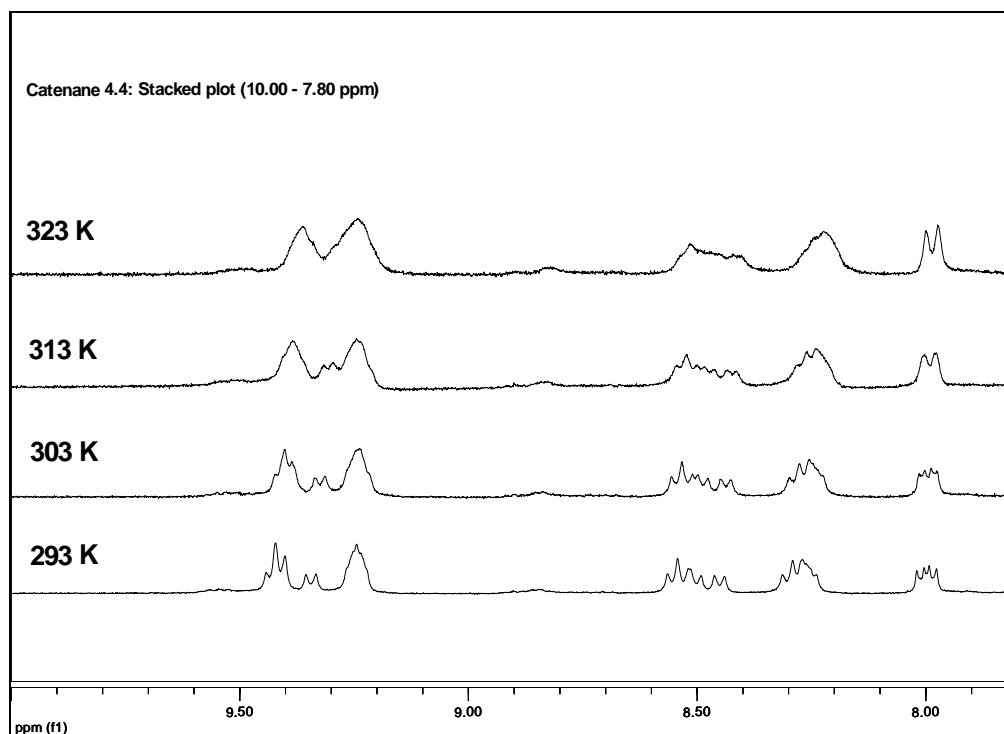


Spectrum 4.7 Stacked Plot of [2]Catenane 4.3

The bottom tether requires less energy to pass over than the top tether which had an asymmetric gate. The BPP34C10 ring would always circumrotate along the bottom tether as a 'shortcut'. The exchange of two conformers was fast above room temperature and coalescence temperature must be under 0 °C.

4.3.4.2 Variable Temperature ^1H NMR of [2]Catenane 4.4

As for [2]catenane **4.4** with the bottom tether blocked by the 4-tert-butylphenyl group, the crown ether ring could possibly circumrotate along the top tether of n-butylphenyl gate under higher temperature.



Spectrum 4.8 Stacked Plot of [2]Catenane 4.4

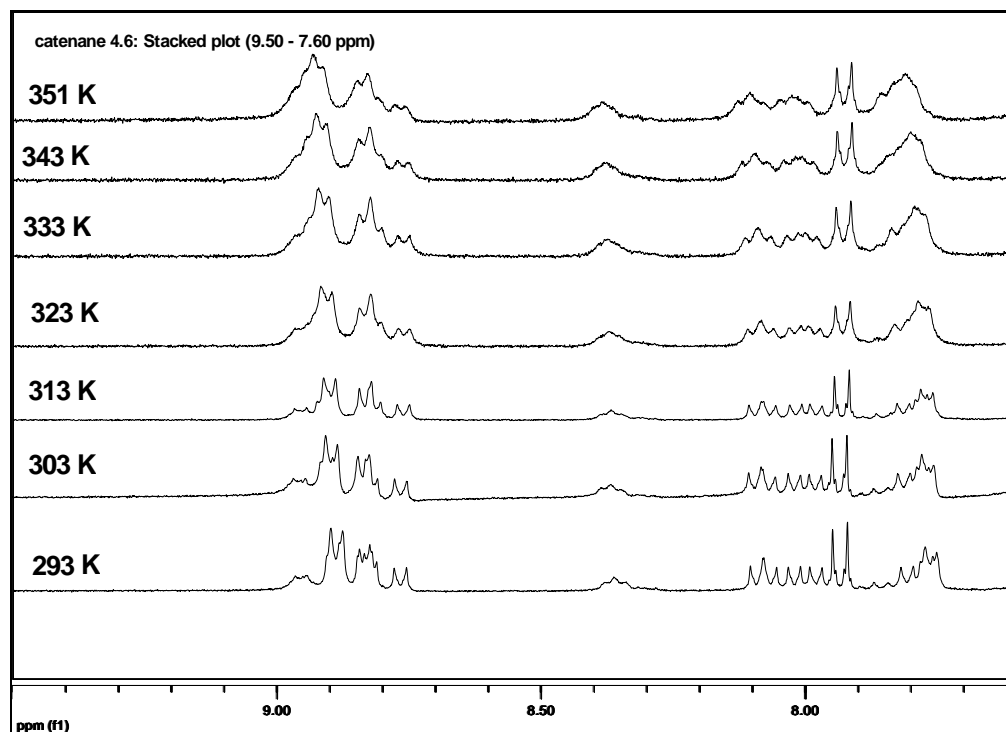
In **Spectrum 4.8**, at room temperature, the signals at 8.00 ppm were two doublets which could be assigned to the protons adjacent to the carbonyl group. The ratio of two doublets at 8.00 ppm was 1:1. When the temperature was increased from 293 K to 323 K, the two doublets became one doublet. At 323 K, thermal energy drove the BPP34C10 to pass over the asymmetric gate quickly and the two doublets were averaged into one. However, coalescence temperature was not reached. Since the limit of the temperature which our NMR instrument can tolerate and the boiling point of the solvent we used, we were not able to calculate the free energy of activation according to the previous method.

4.3.4.3 Variable Temperature ^1H NMR of [2]Catenane 4.6

Catenane **4.5** had the same bottom tether and similar top tether as catenane **4.3** and the variable temperature (high temperature range) ^1H NMR spectrum for catenane **4.5** was not collected.

As for catenane **4.6**, the bottom tether was blocked by 4-tert-butylphenyl and the BPP34C10 would not be able to pass over the bottom tether even at 80 °C according to the previous observation in chapter 3. At higher temperature, the crown ether ring could move over the top gate.

According to the stacked plot ^1H NMR **Spectrum 4.9**, no obvious coalescence

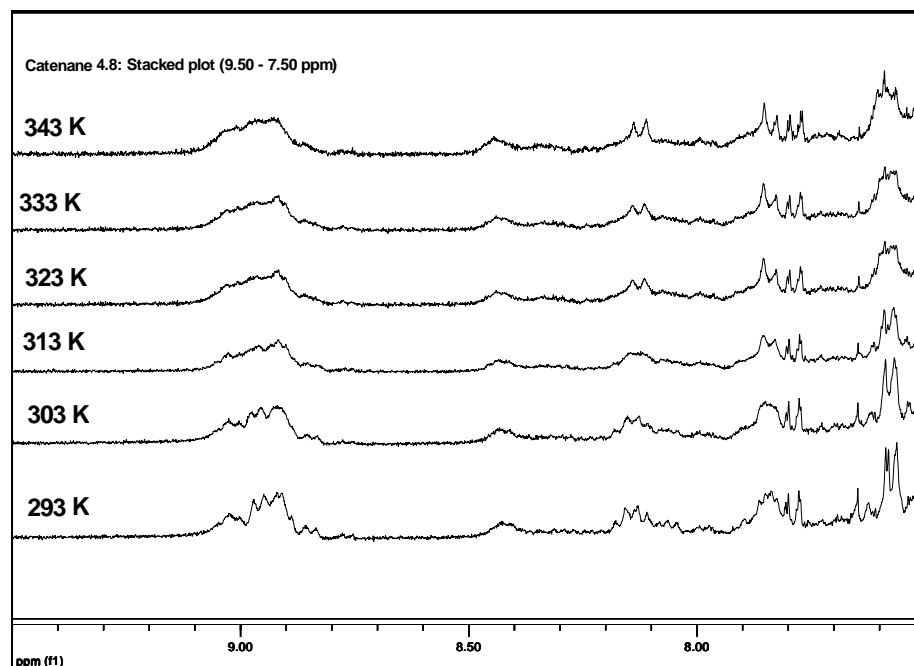


Spectrum 4.9 Stacked Plot of [2]Catenane 4.6

was observed even at 352 K. The coalescence was not been achieved by 78 °C. Due to the same reason of the limit of our NMR instrument, we have to seek other method to calculate the free energy of activation.

4.3.4.4 Variable Temperature ^1H NMR of [2]Catenane 4.8

Catenane **4.8** had a very complicated spectrum and had some impurities which could be attributed to the complexity resulting from the biphenyl gate. According to the stacked plot ^1H NMR **spectrum 4.10**, the coalescence was not achieved at 60 °C. Based on the same reason of the limit of our NMR instrument, we have to seek other method to calculate the free energy of activation.

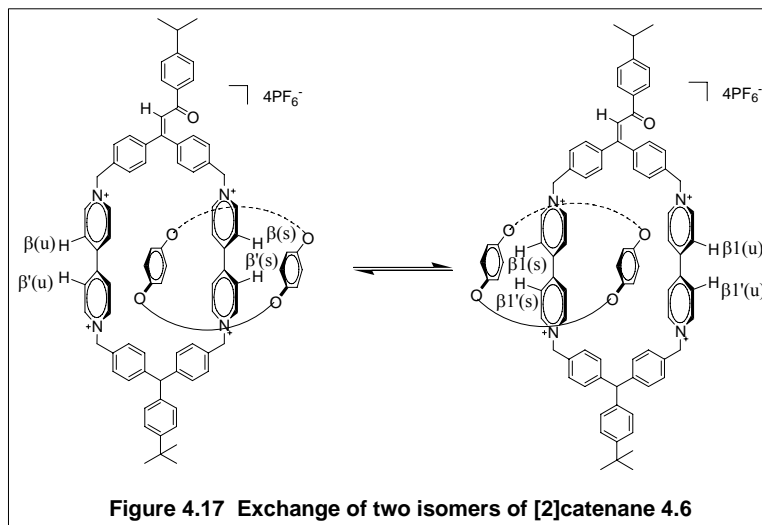


Spectrum 4.10 Stacked Plot of [2]Catenane 4.8

4.3.5 2D-EXSY Spectra of Catenanes 4.2, 4.4, 4.6, 4.8 at 313 K

4.3.5.1 2D-EXSY Spectrum of Catenanes 4.6

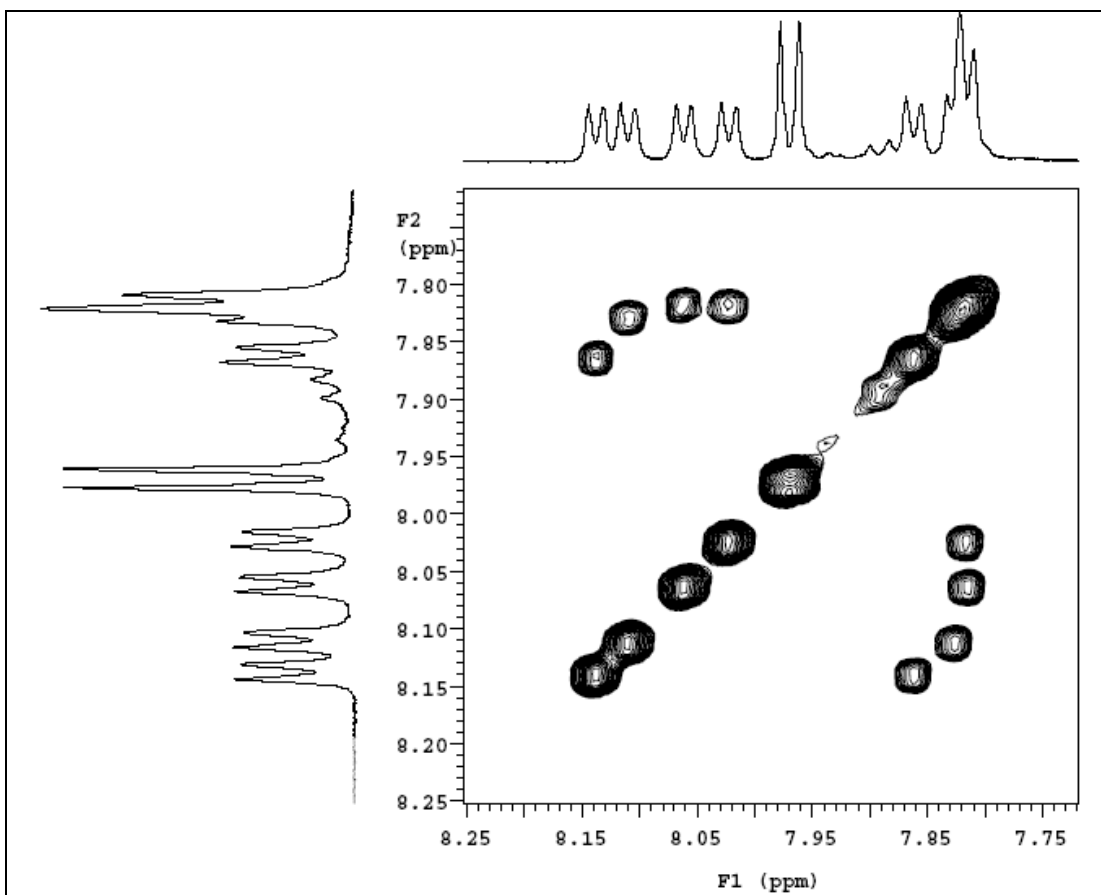
As described in **Figure 4.17**, two isomers are exchanging as the BPP34C10 passes over the gate in catenane **4.6**. Because of the orientation of the protons in two dipyrindinium moieties to the carbonyl group, the gate caused the different chemical shift environment for those protons in two dipyrindinium sides. The shield effect of the BPP34C10 also made those dipyrindinium protons different in terms of chemical shift environment. Base on those factors, there were sixteen signals for the dipyrindinium



protons. For instance, there were four different signals for the unshielded β protons and four, maybe overlapped, for the shielded β protons in the 2D-EXSY spectrum. The unshielded protons at the $\beta(u)$, $\beta'(u)$, $\beta1(u)$, $\beta1'(u)$ positions were located at 8.15- 8.00 ppm and the four shielded protons at the $\beta(s)$, $\beta'(s)$, $\beta1(s)$, $\beta1'(s)$ positions were found at 7.87-7.80 ppm.

The 2D-EXSY NMR technique is well suited to measuring the rate of exchange between isomers below their coalescence temperature.³⁸

In the 2D-EXSY spectrum of [2]catenane **4.6** (**Spectrum 4.11**), the doublet near



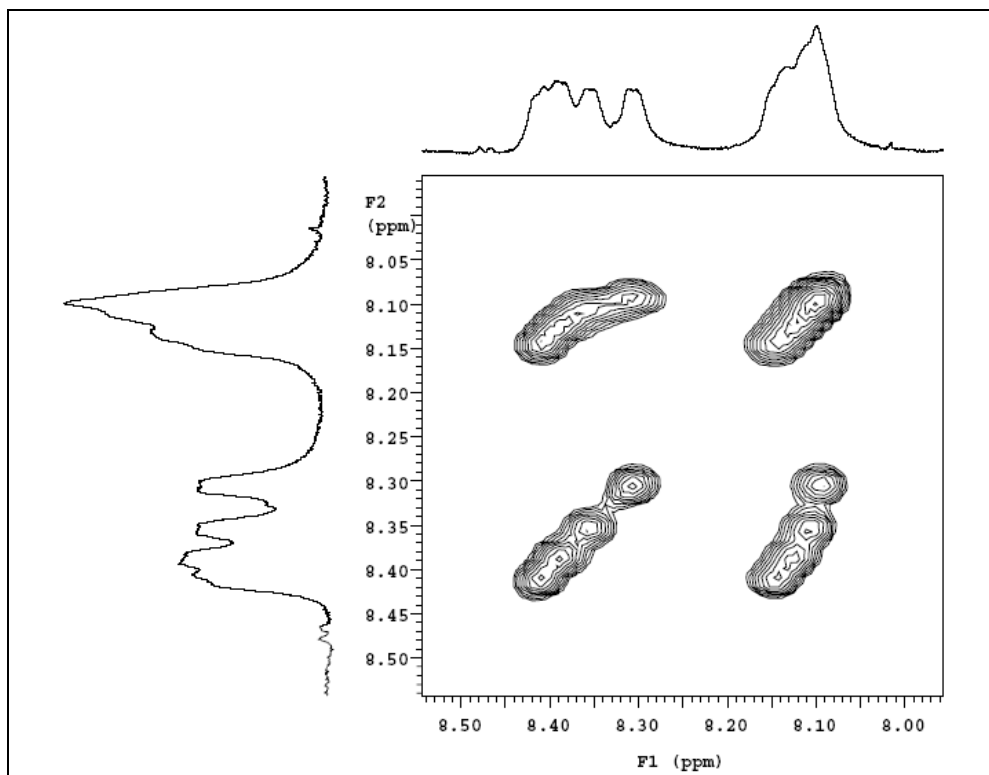
Spectrum 4.11 2D-EXSY of [2]catenane 4.6 at 313 K

8.15 ppm (unshielded) was correlated to the doublet near 7.87 ppm (shielded), indicating that those assigned protons were exchanging at 313 K although it was not clear which β protons they were. The ratio of the two signals was 1:1 which means there was no ground state difference for the forward or reverse circumrotation of the BPP34C10 even an

unsymmetric gate was incorporated in the system. Three other β proton pairs were also correlated as shown in the spectrum.

4.3.5.2 2D-EXSY Spectrum of Catenanes 4.2

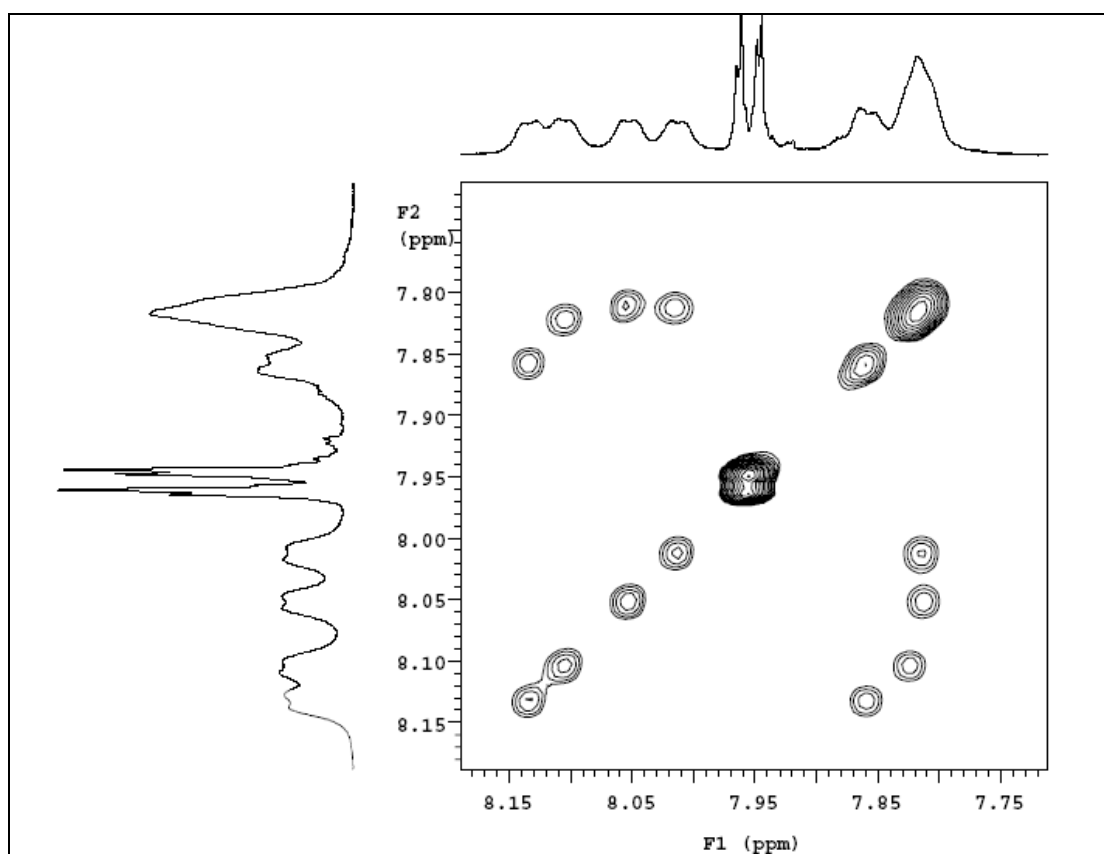
In the 2D-EXSY spectrum of catenane **4.2** (**Spectrum 4.12**), the signals near 8.45 - 8.28 ppm were assigned to the unshielded β protons in the dipyrindinium units and the signals near 8.20 - 8.15 ppm corresponded to the shielded β protons. The correlation of those protons demonstrated the exchange of two conformers of catenane **4.2**. The ratio of two isomers seemed to be 1:1.



Spectrum 4.12 2D-EXSY of [2]catenane 4.2 at 313 K

4.3.5.3 2D-EXSY Spectrum of Catenanes 4.4

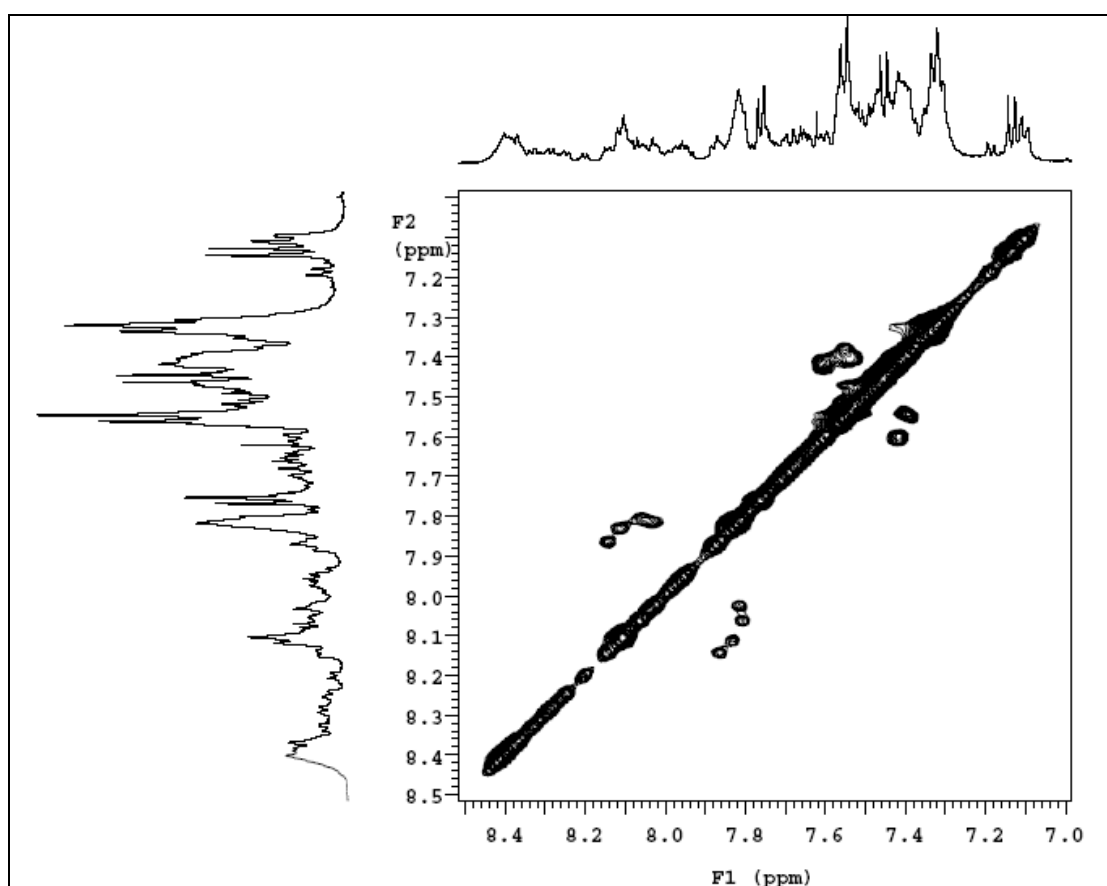
In the 2D-EXSY spectrum of catenane **4.4** (**Spectrum 4.13**), four signals near 8.15-8.00 ppm were assigned to the unshielded β protons in the dipyridinium units and the signals near 7.86 -7.80 ppm corresponded to the shielded β protons. The correlation of those protons demonstrated the exchange of two conformers of catenane **4.2**. Almost 1:1 ratio of two isomers was observed which indicated no evidence for preferential circumrotation.



Spectrum 4.13 2D-EXSY of [2]catenane 4.4 at 313 K

4.3.5.4 2D-EXSY Spectrum of catenanes 4.8

The 2D-EXSY spectrum of catenane **4.8** was complicated due to the biphenyl gate and the difficulty of purification. The exchange of dipyridinium β protons was observed as in **Spectrum 4.14**. However, it was difficult to determine the ratio of two isomers from this spectrum.



Spectrum 4.14 2D-EXSY of [2]catenane **4.8** at 313 K

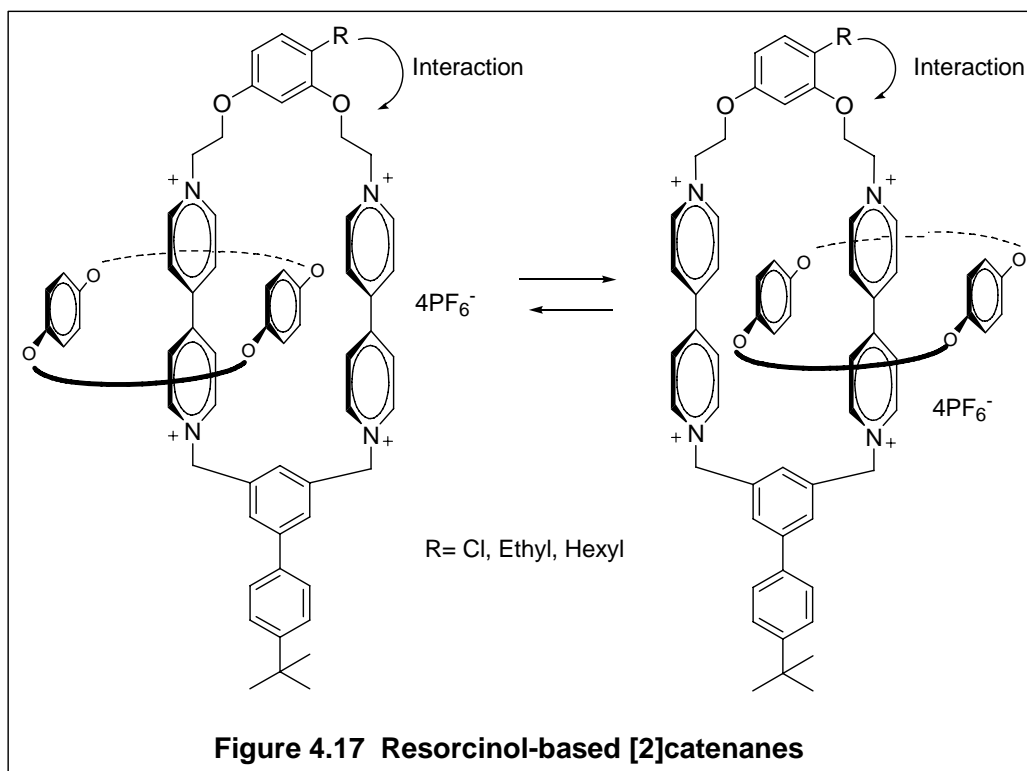
4.4 Summary and Conclusions

The enone double bonds in catenanes **4.4**, **4.6** were irradiated with UV light at 0

$^{\circ}\text{C}$ and the ^1H NMR study indicated 1:1 ratio of two conformers. The ground states energies of two binding sites are the same.

In the resorcinol-based catenanes previously developed in our group, there were clearly two isomers as described in **Figure 4.17**³² for each catenane according to the low temperature ^1H NMR spectra. It was found that the ratios of two isomers were not 1:1 but 1.5:1 and 3.5:1.

The remote 4-substituent was incorporated to cause the different activation energy barriers but not the ground states differences. However, the interaction between



4-substituent and 3-ethoxy spacer still existed. Perhaps due to twisting induced to minimize this interaction, the ground state conformational energy differences ranged

from 1.5:1 to 3.5:1.

In catenanes **4.4**, **4.6**, **4.8**, we expected to see different ratios of two isomers determined by NMR technology to support potential ratcheting. However, at variable temperature NMR spectra of these catenanes, we did not observe different ratios to demonstrate the preferential circumrotation in either direction. No biasing gate effect was observed as designed. On the other hand, at room temperature, 1:1 ratio indicated that the unsymmetric gate did not twist the rigid tether and interact with the BPP34C10 ring. It did not affect the ground states for two conformers.

In the 2D EXSY spectra of these catenanes **4.2**, **4.4**, **4.6**, **4.8**, the exchange of two isomers were observed, indicating that the BPP34C10 passed over the gates with no preference.

Since variable temperature ^1H NMR spectra could not tell the coalescence temperature for each blocked catenanes because of the limits of our NMR instrument, we sought to use 2D-EXSY spectra to determine the exchanging signals for each catenane. The rate constant data and the free energies of activation will be obtained through analysis of 2D-EXSY data by our collaborator, Dr. Nimmo in our department.

Chapter 5

Towards a Unidirectional Molecular Motor:

Synthesis of Tristable [2]Catenanes

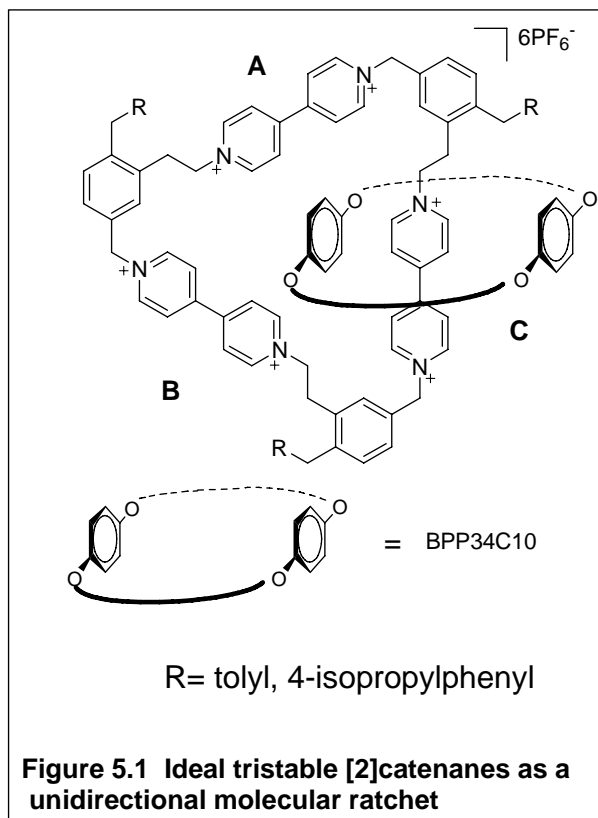
5.1 Design of Tristable [2]Catenane as a Unidirectional Molecular Motor

In the symmetric [2]catenanes in chapter 2 and chapter 3, the ratio of two conformers at low temperatures was 1:1 indicating that the two isomers are isoenergetic. Although we could select the path for the BPP34C10 migration, the ring circumrotated around the tetracationic cyclophane equally without any directional preference.

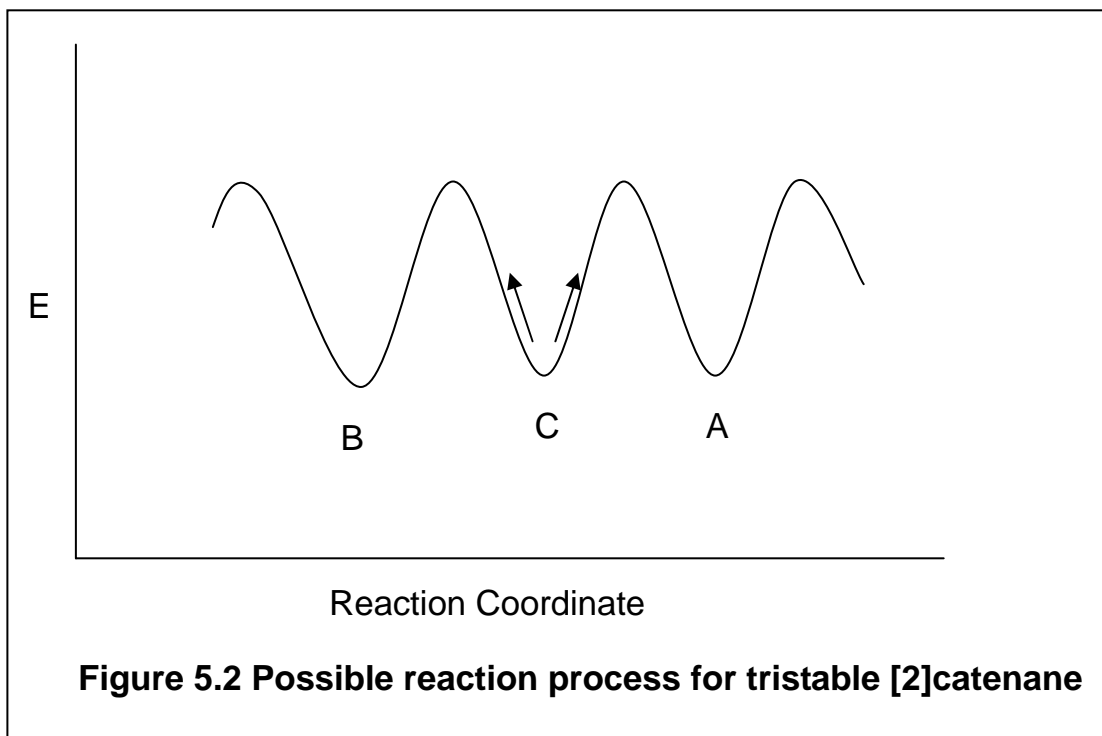
In our prior study work and in chapter 4, we sought to test the use of an asymmetric gate in bistable [2]catenane as a molecular ratchet. In our study, we need to establish the rate of the forward and reverse circumrotation from the ratio of isomers determined by NMR spectroscopy. We had to rely on model comparison to determine the ΔG° of the isomers (passage over an unbiased gate or by photoisomerization of the gate). When that pathway for interconversion was blocked by placing a bulky group on the pathway or by turning off the light, we could potentially reestablish a different equilibrium constant by isomerizing over the gate. If the blocking did not affect binding and the ratios of conformers changed, we could have evidence for preferential

unidirectional motion. The problem with those designs, however, is that we would be comparing two different compounds or conditions and that would hinder forming a strong conclusion regarding thermal ratcheting.

In order to allow a direct comparison of microscopic rates of forward and reverse processes, we designed a tristable [2]catenanes as a unidirectional molecular ratchet (**Figure 5.1**). The molecule was composed of a C_3 -symmetric cationic cyclophane interlocked with the crown ether ring. In this system, there are now three identical electron-deficient dipyridinium binding sites for the electron-rich crown ether ring. Three asymmetric gates will be incorporated on every phenyl spacer in this system.

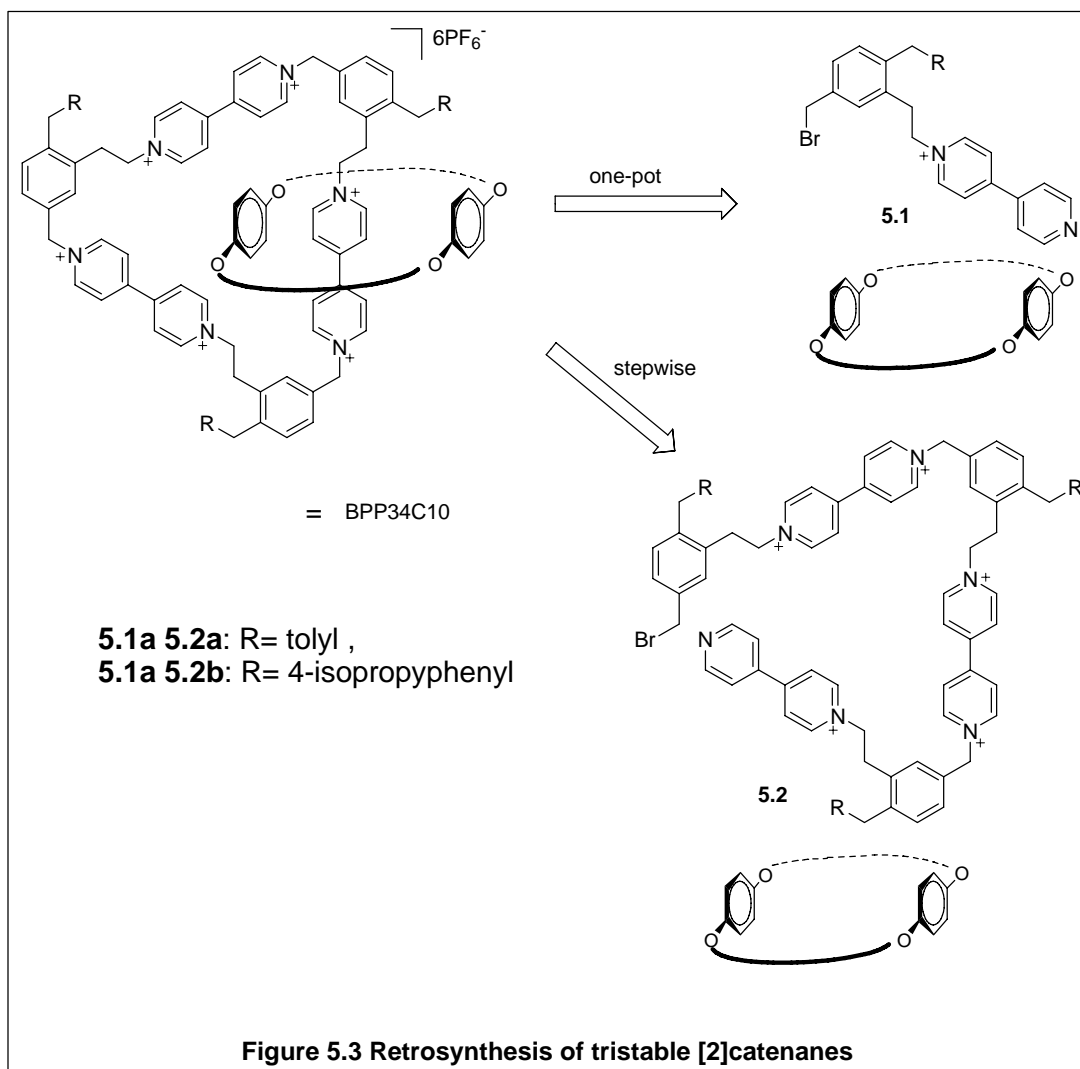


In this system, three binding sites are identical in terms of the structure and every site should have the same ground state. As described in **Figure 5.2**, for the forward movement of the BPP34C10 ring from C→A we would have the microscopic reverse process of A→C. By the symmetry of this system the reverse process A→C would be identical to the process starting from C but moving back to B. Thus we have a design in which we could get the rates of C giving A or B by appropriate NMR measurements. Should these rates be different we would have strong evidence for a unidirectional ratchet.



5.2 Retrosynthesis of the target molecules

Since the cationic cyclophane of the target molecule is C_3 -symmetric, we could first synthesize a monomer **5.1** described in **Figure 5.3**. Then in one pot, three monomers and BPP34C10 could undergo a self-assembly to form a “trimer”. The driving force to form the trimer instead of some oligomers could be the π - π -stacking between the BPP34C10 and dipyridinium units.



However, if this strategy does not work, we would need to prepare the precursor **5.2** first via a stepwise route as described in **Figure 5.3**. Once the precursor is obtained, a psuedorotaxane could be formed after the BPP34C10 treads on the precursor. Performing a ring closure could lead to the desired catenane. Since there are two binding sites in the precursor for the BPP34C10, [3]catenanes could also be formed. Even [3]catenanes could exhibit a unidirectional motion.

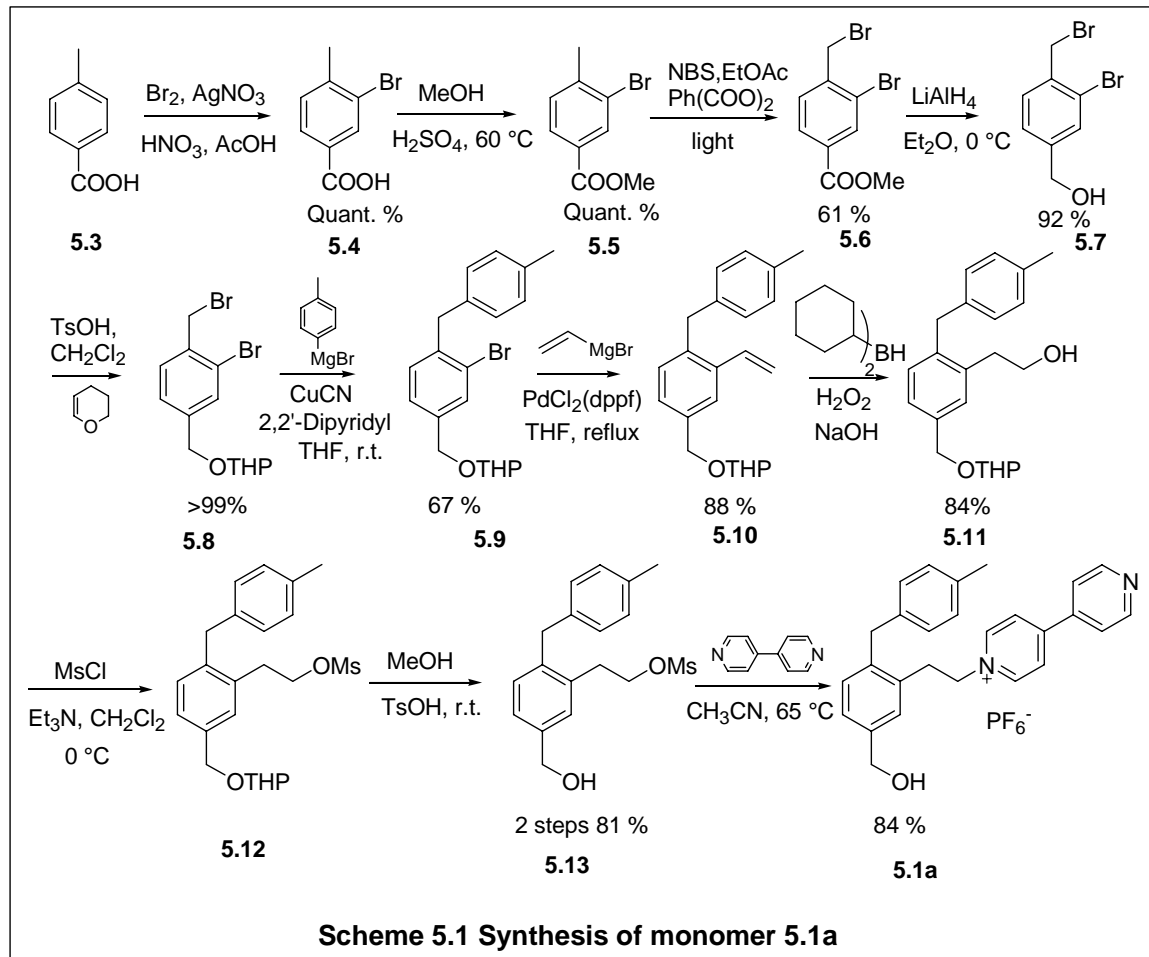
5.3 Synthesis and Characterization of Intermediates and Precursors

5.3.1 Synthesis and Characterization of Intermediates and Monomer 5.1a

The preparation of monomer **5.1a** began with bromination of p-toluic acid **5.3** according to literature⁵⁵ to give **5.4** in quantitative yield. The ¹H NMR data were consistent with the literature.⁵⁵

Bromotoluic acid **5.4** was converted to ester **5.5** in a quantitative yield via Fisher esterification in methanol with catalytic sulfuric acid at 60 °C for 3 days. The ¹H NMR spectrum was consistent with the literature.⁵⁶

The transformation from ester **5.5** to benzyl bromide **5.8** was reported in the literature⁵⁶ and the procedure was followed with some minor modifications. To prepare benzyl bromide **5.6**, a radical bromination was performed on compound **5.5** with NBS in ethyl acetate instead of carbon tetrachloride. A yield of only 61 % was obtained because

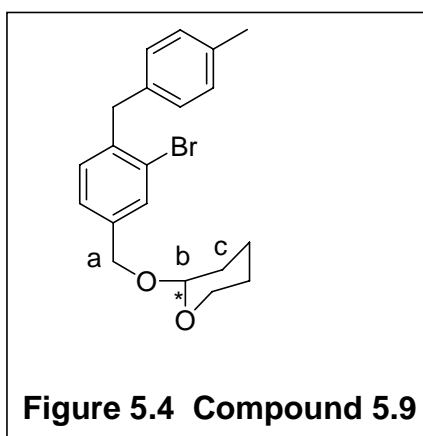


an inseparable over-brominated side product was produced. The ^1H NMR data were consistent with the literature.⁵⁶

Reduction of benzyl bromide **5.6** by LiAlH_4 gave benzyl alcohol **5.7** at 0 °C in THF. The control of temperature and time was very important since the benzyl bromide can not tolerate the LiAlH_4 reduction above 0 °C. Even so, a trace amount of side product resulting from the reduction of benzyl bromide was still observed. Recrystallization from isopropanol gave the pure compound **5.7** in 92 % yield.^{56b} The ^1H NMR data were

consistent with the literature.⁵⁶

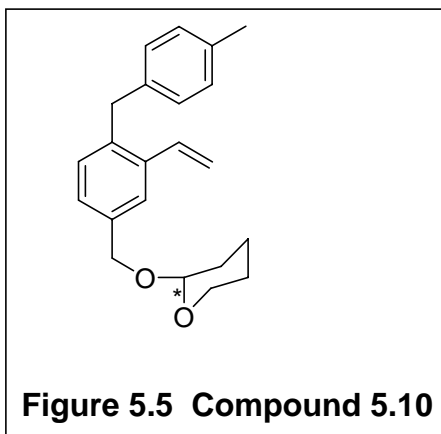
The hydroxyl group in compound **5.7** was protected by a THP group to give **5.8**. Since there was a chiral center on the THP group, the methylene groups on the benzyl position and adjacent to this chiral proton showed on the AB system in the ¹H NMR spectrum. The ¹H NMR data is consistent with the literature.⁵⁶



Compound **5.9** was prepared in a yield of 67 % from a coupling reaction between **5.8** and p-methylphenyl magnesium bromide with a catalytic amount of copper(I) cyanide and 2,2'-dipyridyl. In the ¹H NMR spectrum, the signal at 4.75 (m, 2H) corresponded to an overlap of Hb and one of Ha (Figure 5.4). The doublet at 4.47 (d, *J* = 12.2 Hz, 1H) was attributed to the other Ha. The multiplets at 4.00-3.87 (m, 1H) and 3.65-3.49 (m, 1H) corresponded to Hc adjacent to the Hb. The singlet at 4.10 (s, 1H) corresponded to the methylene protons between the two phenyl ring. The number of carbons in the ¹³C NMR spectrum was consistent with the structure.

Styrene derivative **5.10** was prepared via Kumada coupling⁵⁷ between compound **5.9** and a vinyl Grignard reagent under catalytic PdCl₂(dppf) conditions in 88 % yield. The reaction in THF was refluxed overnight and behaved very well. A Stille coupling

was also tried to make this compound **5.10**, but the isolation of product from the tin residue was difficult. In the ^1H NMR spectrum, the methylene groups close to the chiral center still established doublets of doublets in an AB system (**Figure 5.5**). The signals at 5.65 (td, $J = 17.37, 1.19, 1.19$ Hz, 1H), 5.25 (td, $J = 10.98, 1.18, 1.18$ Hz, 1H)



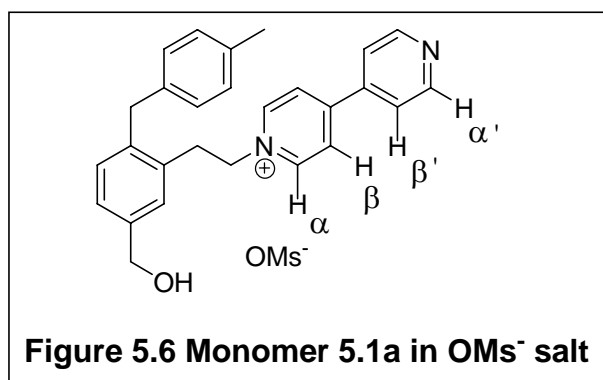
corresponded to the terminal protons on the alkene group. The number of carbons in the ^{13}C NMR spectrum was consistent with the structure. In the mass spectrum (ESI), the peak at $m/z = 345.1933$ was attributed to $[\text{M}+\text{Na}^+]$ (M Calculated 322.1933).

Alcohol **5.11** was obtained via hydroboration of styrene derivative **5.10**. Cyclohexene was initially reacted with borane⁵⁸ to make a bulky reagent to improve the regioselectivity of the hydroboration. Fortunately, no side product was observed in the crude products. In the ^1H NMR spectrum, the triplets at 3.76 (t, $J = 6.90$ Hz, 2H) 2.91 (t, $J = 6.87$ Hz, 2H) were assigned to the methylene protons on the ethyl alcohol. The rest of spectrum was similar to that in compound **5.10**. The number of carbons in the ^{13}C NMR spectrum was consistent with the structure. In the mass spectrum (ESI), the peak at $m/z = 363.22$ was attributed to $\text{M}+\text{Na}^+$ (M calculated 340.20). The structure of compound **5.11** was supported by those data.

The hydroxyl group in alcohol **5.11** was mesylated⁵⁹ to give a good leaving group

in mesylate **5.12**. Without purification, mesylate **5.12** was deprotected with methanol/TsOH⁶⁰ to remove the THP to give benzyl alcohol **5.13** in 81 % yield for the two steps from **5.11** to **5.13**. In the ¹H NMR spectrum, the triplet for the methylene next to the mesyl group shifted downfield about 0.9 ppm compared to alcohol **5.11**. The number of carbons in the ¹³C NMR spectrum was consistent with the structure. In the mass spectrum (ESI), the peak at m/z = 357.1 was attributed to M+Na⁺ (M calculated 334.12). The structure of compound **5.13** was supported by these data.

Compound **5.13** reacted with excess 4,4'-dipyridyl at 65 °C to give a salt with a mesylate counterion, MsO⁻. This salt precipitated out from the reaction solution. The solid was dissolved in water and excess ammonium hexafluorophosphate was added to perform an anion exchange. The monomer **5.1a** was obtained in a yield of 84 %. In the ¹H NMR spectrum for **5.1a** as an OMs⁻ salt (soluble in water), the signal at 8.62 (m, 2H) was attributed to the α proton adjacent to cationic nitrogen (**Figure 5.6**). The peak at 8.21 (m, 2H) was attributed to an α' proton since they are close to a neutral nitrogen. The

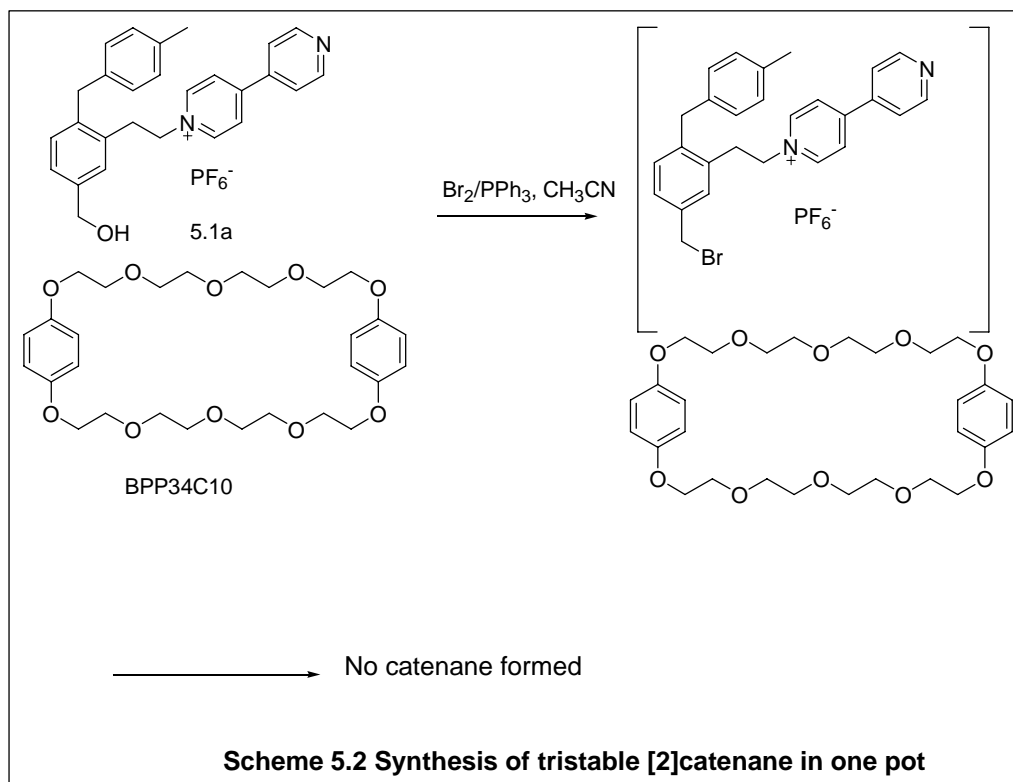


multiplets at 7.75-7.55 (m, 2H) and 7.80 (m, 2H) corresponded to β, β' protons of the dipyrrolium moiety. The number of carbons in the ¹³C NMR spectrum was consistent with the

structure. In the mass spectrum (ESI), the peak at $m/z = 395.1$ corresponded to M^+ without anion (M calculated 395.21). The structure of **5.1a** was supported by those data.

5.3.2 Synthesis of Tristable [2]Catenane in One Pot

Once the monomer **5.1a** was obtained, several efforts to synthesize tristable [2]catenane in one pot were made. As described in **Scheme 5.2**, monomer **5.1a** and the



BPP34C10 were dissolved in acetonitrile and pre-made Br_2/PPh_3 reagent was added. Unfortunately, a yellow precipitate appeared immediately. The reason could be that there were plenty of bromide anions in Br_2/PPh_3 reagent and they replaced the PF_6^- in **5.1a** to form an insoluble salt. The BPP34C10 was still dissolved in acetonitrile. Threading might

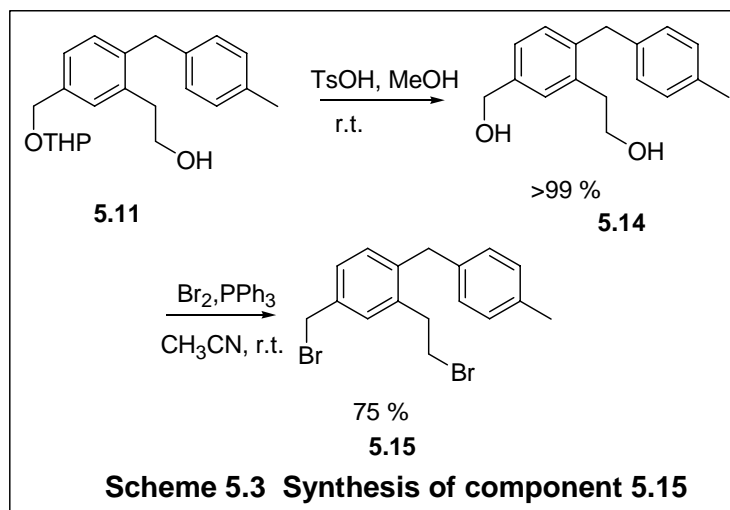
never happen for subsequent catenation. On the other hand, bromination could be still going and a “head to tail ” SN_2 reaction could happen. But only oligomers and psuedorotaxane were apparently formed. In short, the one pot strategy didn't work and further stepwise synthesis of the precursor was required.

5.3.3 Extended Route for Tristable [2]Catenane: Synthesis and Characterization of Intermediates and Precursor 5.2a

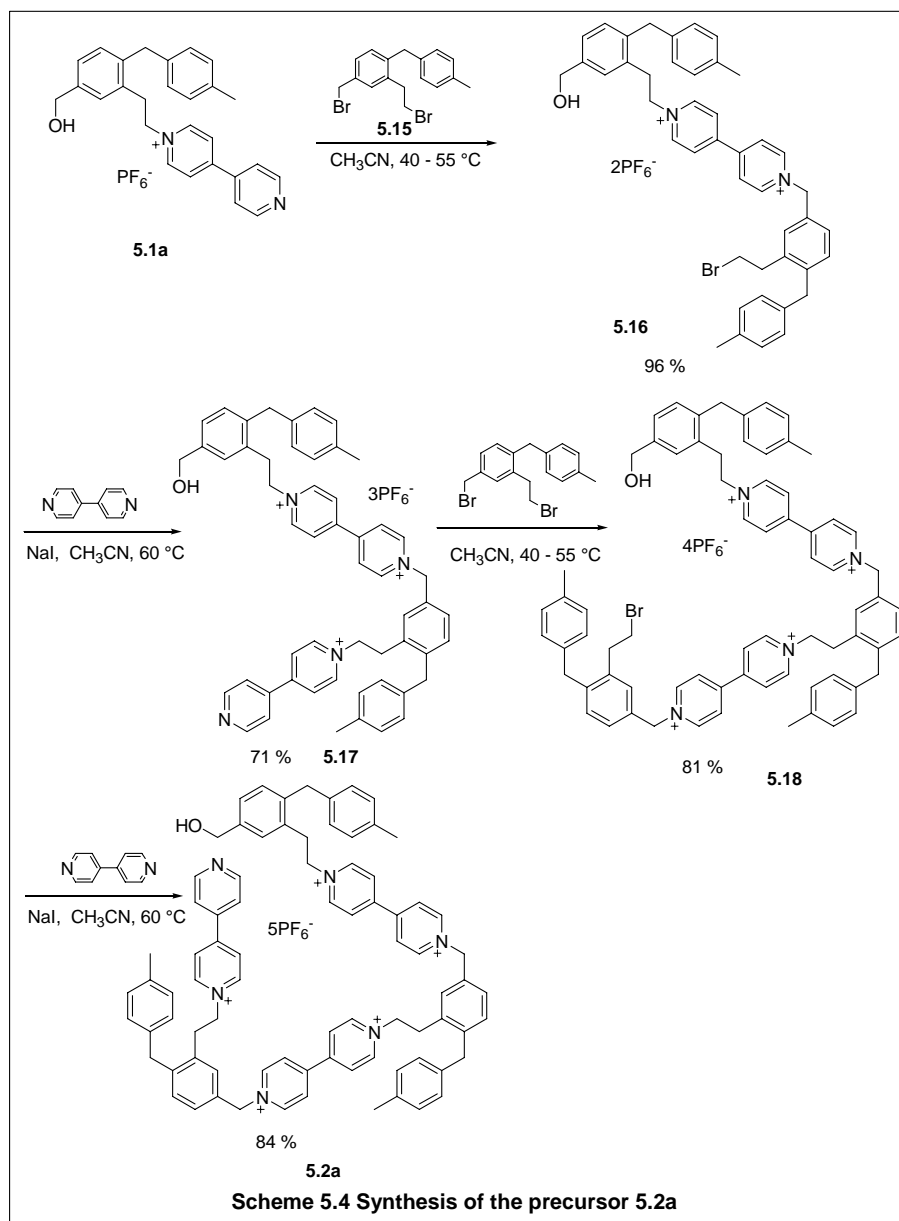
The extended route required preparation of the key component **5.2a**. Protected benzyl ether **5.11** was deprotected to give diol **5.14** in a yield of 99 %.⁶⁰ In the ^1H NMR spectrum, the broad peak at 4.75 (b, 2H) was attributed to the benzyl methylene protons due to the effect of the adjacent hydroxy group. The singlet at 4.09 (s, 2H) corresponded to the methylene group between two aryl rings. The broad peak at 3.82 (b, 2H) was assigned to the methylene protons closest to the hydroxyl group in the ethyl side chain. The triplet at 2.96 (t, $J = 6.80$, Hz, 1H) was assigned to the other methylene protons in the ethyl alcohol.

Diol **5.14** was brominated with Br_2/PPh_3 reagent in CH_3CN to give **5.15** (Scheme 5.3). In the ^1H NMR spectrum of **5.15**, the triplets at 3.45 (t, $J = 7.73$, 2H) and 3.19 (t, $J = 7.73$ Hz, 2H) corresponded to the ethyl methylene protons. Those two peaks had shifted closer compared to those in **5.14**. The number of carbons in the ^{13}C NMR

spectrum was consistent with the structure.



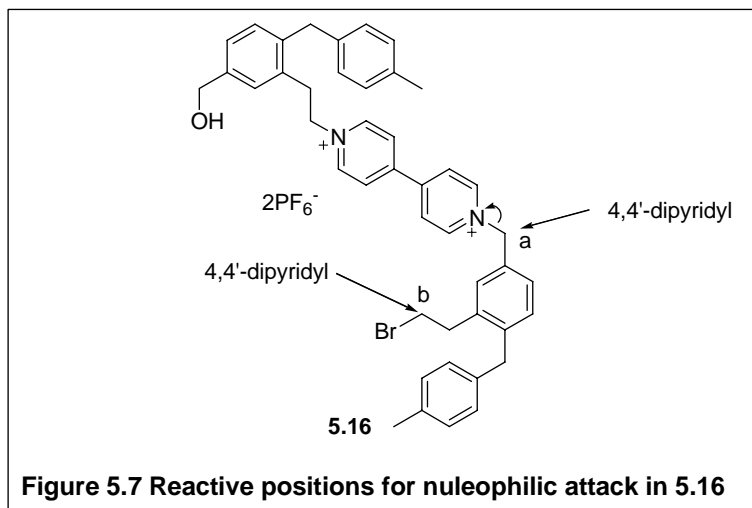
As described in **Scheme 5.4**, the synthesis of the key precursor **5.2a** continued with the reaction between **5.1a** and **5.15** in acetonitrile at 40 -55 °C. Two equivalents of **5.15** were used since it was easy to remove from the reaction mixture and the excess favored substitution at the more reactive benzylic bromide site. Dipyrindyl **5.16** was obtained in a yield of 96 %. In the ^1H NMR spectrum, the signals at 9.04 (d, $J = 6.92$ Hz, 2H) and 8.59 (d, $J = 6.89$ Hz, 2H) were attributed to the α , α' protons of the dipyrindinium unit. The doublets at 8.42 (d, $J = 6.90$ Hz, 2H), 8.30 (d, $J = 6.82$ Hz, 2H) corresponded to the β , β' protons of the dipyrindinium moiety. The singlet at 5.84 (s, 2H) was attributed to benzyl methylene close to the cationic nitrogen. The triplet at 4.69 (t, $J = 7.17$ Hz, 2H) was assigned to the methylene protons adjacent to cationic nitrogen on the ethyl group. The singlet at 4.51 (s, 2H) corresponded to methylene protons of the benzyl alcohol. The singlets at 4.09 (s, 1H), 4.03 (s, 1H) were attributed to the methylene groups between two



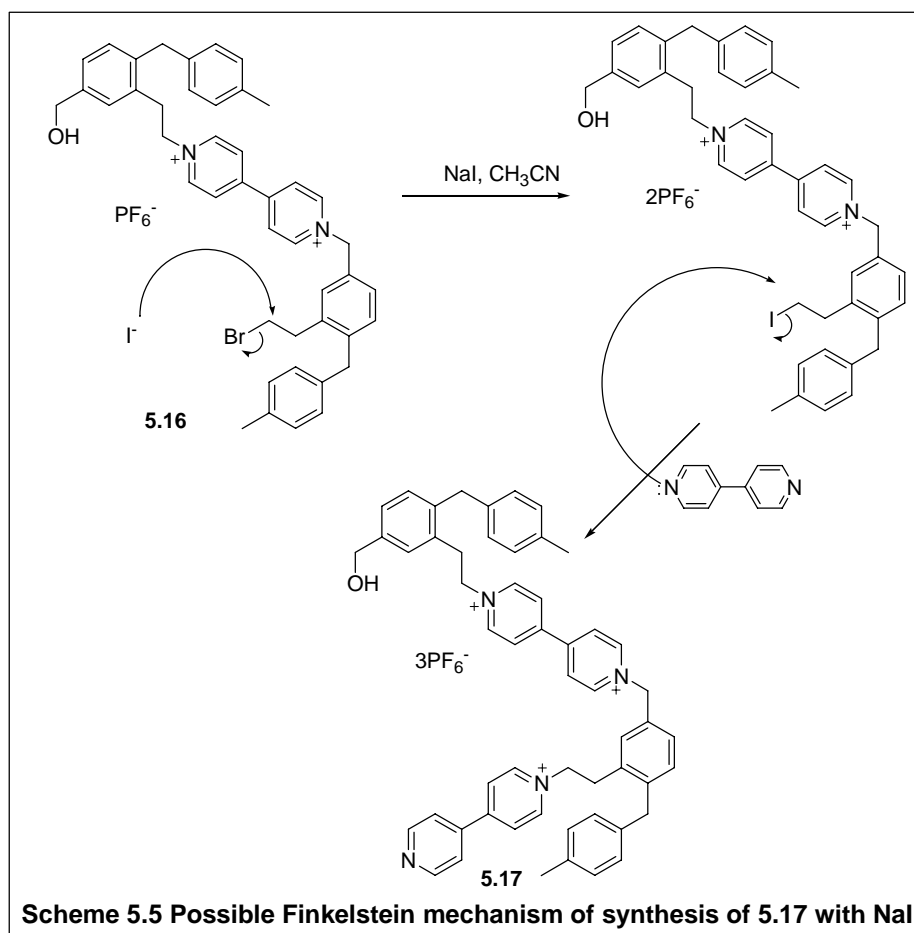
phenyl rings. Triplets at 3.55, 3.36 and 3.24 ppm corresponded to the protons of the ethyl groups. Two singlets at 2.33(s, 3H), 2.30 (s, 3H) were attributed to the methyl group on the tolyl 'gate'. The ^{13}C NMR spectrum was consistent with the structure. In the mass spectrum (ESI), a peak at $m/z=841.2$ was assigned to $\text{M}^{2+}\text{PF}_6^-$ (calculated 841.24). The

structure of **5.16** was supported by these data.

Compound **5.16** reacted with excess 4,4'-dipyridyl to give compound **5.17** in a yield of 71 % (**Scheme 5.4**). Excess 4, 4'-dipyridyl was used to minimize the side reaction in which both sides of 4,4'-dipyridyl reacted with the alkyl bromide. It was noted that catalytic sodium iodide was necessary to accelerate the reaction. If there was no NaI, the bromide would not be a good enough leaving group in this case. The temperature required to substitute the bromide must be over 75 °C and reaction rate was too slow. On the other hand, the high temperature might result in increased undesired side products. There are two reactive sites **a** and **b** (**Figure 5.7**) for nucleophilic attack in compound **5.16**. It seemed that the benzyl position **a** was more reactive than the position **b**. When the temperature was over 75 °C, some side products were produced that were perhaps indicative of reactions at site **a**. It was difficult to separate these side products from the desired compound **5.17**.



When NaI was added to the reaction, a Finkelstein reaction was expected to form an iodide leaving group followed by a S_N2 substitution with 4,4'-dipyridyl as detailed in **Scheme 5.5**. The temperature could be lowered to 40 - 55 °C for this reaction.



In the ¹H NMR spectrum of **5.17**, eight signals were observed between 9.10- 7.80 ppm which were assigned to the protons of the dipyrrolium units. The multiplet at 7.82 (m, 2H) corresponded to the α protons adjacent to the neutral nitrogen of the dipyrrolium moiety. The apparent triplet at 8.26 (t, *J* = 6.17 Hz, 4H) was actually an overlap of two doublets of β protons. The methylene protons of the two ethyl groups

were almost identical and overlapped at 4.68 (t, $J = 7.06$ Hz, 4H) and 3.39 (m, 4H). The chemical shift of the methylene group of the benzyl alcohol group was located at 4.52 (s, 2H). The benzyl methylene group closest to the cationic nitrogen had a chemical shift of 5.79 ppm (s, 2H). The methylene protons between the two aryl rings and the methyl protons on the tolyl gate had very close chemical shifts.

In the mass spectrum (ESI) for **5.17**, the peak at $m/z = 459.27$ corresponded to the piece $[M^{3+}PF_6^-]^{2+}$ (calculated 459.20). The peak at $m/z = 257.85$ was assigned to the piece M^{3+} (calculated 257.81). From these data and the ^{13}C NMR data, the structure of **5.17** was supported.

Compound **5.18** was produced in 81 % yield when compound **5.17** reacted with component **5.15**, following the procedure we used in the early step from **5.1a** to **5.16**.

The 1H NMR spectrum of **5.18** was complex. The signal which was at 7.82 ppm in the intermediate **5.17** disappeared, indicating that the neutral nitrogen in dipyrдинium became the cationic nitrogen and the conversion did happen. It seemed that three sets of signals for the ethyl groups were observed. The ^{13}C NMR spectrum was consistent with the structure of **5.18**.

In the mass spectrum (ESI) of **5.18**, the peak at $m/z = 407.21$ corresponded to the species $[M^{4+}PF_6^-]^{3+}$ which is loss of three PF_6^- anions (calculated 406.48). The peak at $m/z = 682.31$ was assigned to the species $[M^{4+}2PF_6^-]^{2+}$ which was loss of two PF_6^- anions.

The structure of compound **5.18** was supported by these data.

The key precursor **5.2a** was prepared in a yield of 84 % by incorporating another 4,4'-dipyridyl to **5.18**.

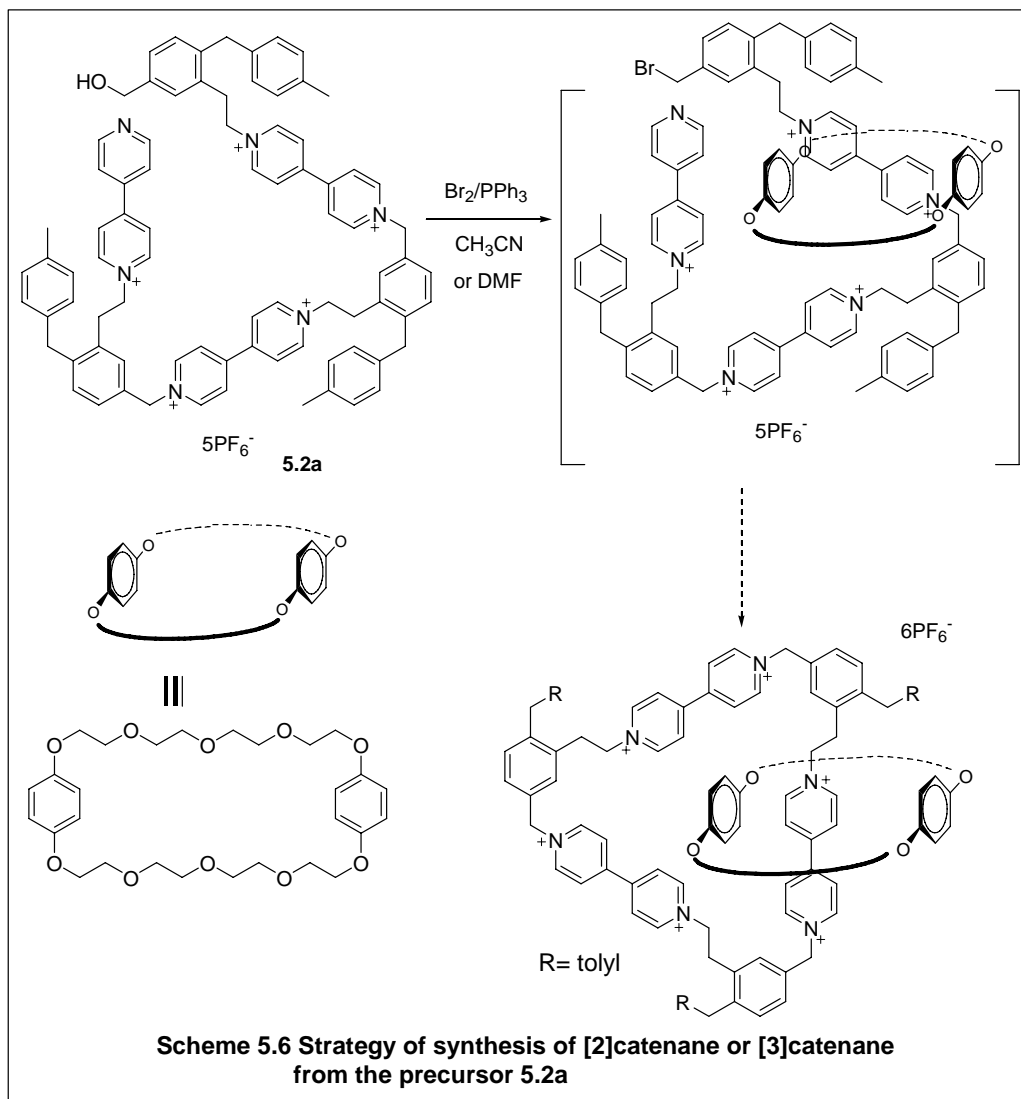
In the ^1H NMR spectrum of **5.2a**, 12 signals between 9.10 – 7.8 ppm indicated the 12 different types of protons of the three dipyridinium units. The two singlets at around 5.80 ppm corresponded to the benzyl methylene protons adjacent to cationic nitrogens. The chemical shift for methylene of benzyl alcohol was 4.54 ppm which was a broad doublet due to the hydroxyl group.

In the mass spectrum (ESI) for **5.2a**, the peak at $m/z = 324.2$ corresponded to the tetracationic species $[\text{M}^{5+}\text{PF}_6^-]^{4+}$ (calculated 324.1) which was loss of four PF_6^- anions. The peak at $m/z = 480.6$ was assigned to $[\text{M}^{5+}2\text{PF}_6^-]^{3+}$ which was a tricationic species. The peak at $m/z = 793.4$ was attributed to $[\text{M}^{5+}3\text{PF}_6^-]^{2+}$ which was loss of two PF_6^- anions. All these data supported the structure of the precursor **5.2b**.

5.3.4 Attempts in Synthesis of [2]Catenane or [3]Catenanes from the Key Precursor

5.2a

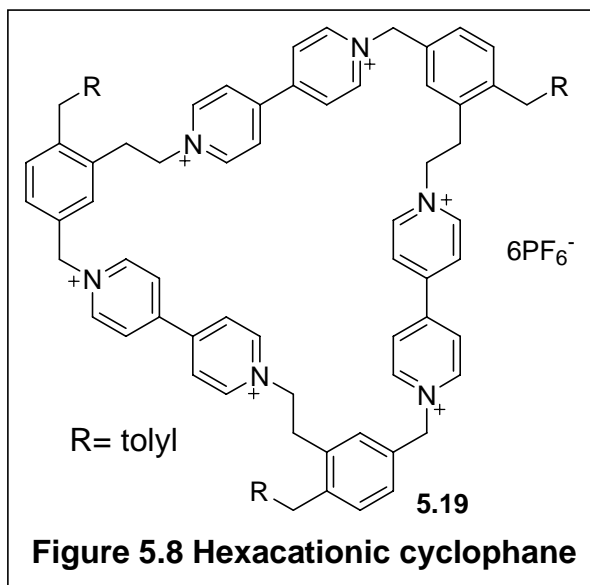
Once this key precursor **5.2a** was obtained, several efforts were made to synthesize the [2] or [3]catenanes as in **Scheme 5.6**. There were three dipyridinium units in this precursor, two of which could π - π -stack with the BPP34C10 ring because they



were dicationic. Initially, the BPP34C10 could thread on this precursor before the benzyl alcohol was activated. Once the BPP34C10 was threaded on and the benzyl hydroxyl group was converted to a good leaving group, the ring closure could happen and the desired catenane could be formed.

The first try was performed in acetonitrile. The precursor **5.2a** and BPP34C10 were dissolved in acetonitrile. The Br_2/PPh_3 reagent was made *in situ* and added to the

reaction mixture. Unfortunately, the yellow precipitate showed up immediately. The reaction was stirred at room temperature for 5 days. The formation of catenane was not evident in the ^1H NMR spectrum. However, when this mixture was heated at $50\text{ }^\circ\text{C}$ overnight, evidence for the formation of the hexacationic cyclophane was observed (**Figure 5.8**). In the mass spectrum of **5.19**, the peak at $m/z = 857.3$ corresponded to the species $[\text{M}^{6+}4\text{PF}_6^-]^{2+}$ (calculated 857.24). The peak at $m/z = 523.2$ was assigned to the



species $[\text{M}^{6+}3\text{PF}_6^-]^{3+}$ (calculated 523.17).

The peak at $m/z = 579.2$ could be assigned to the species $[\text{M}^{6+}4\text{PF}_6^-\text{Na}^+]^{3+}$ (calculated 579.16). We had not previously seen the m/z for the dipyridinium ring without the BPP34C10 in the fragment. The absence of BPP34C10 in this mass spectrum led us

to conclude that the cyclophane was formed without catenation. In crude ^1H NMR spectrum for **5.19**, the simple peaks also might indicate the formation of hexacationic cyclophane because it is C_3 symmetric.

Another attempt was performed in DMF. The precursor **5.2a** and BPP34C10 was dissolved in acetonitrile. The Br_2/PPh_3 reagent was made *in situ* and added to the reaction

mixture. The reaction mixture was stirred at room temperature for 5 h and DMF was added to dissolve the precipitate. The solubility was improved and little amount of precipitate persisted. The mixture was stirred for 5 days. Unfortunately, no evidence for the formation of catenanes was obtained by TLC or NMR spectroscopy.

It was also a concern that the leaving group might not be good enough to perform the ring closure. So the hydroxyl group was transformed to a mesylate. Basically, the precursor **5.2a** and BPP34C10 was dissolved in acetonitrile. Triethylamine was added at room temperature and the mixture was cooled down to 0 °C and methanesulfonyl chloride (MsCl) was added. The reaction remained at 0 °C for a few hours and was allowed to warm to room temperature. The mixture was stirred overnight and some precipitate appeared. The reaction mixture was stirred for 4 or 5 more days. The ^1H NMR spectrum did not indicate the formation of any catenane. However, the mesylate did form according to the chemical shift on the ^1H NMR spectrum.

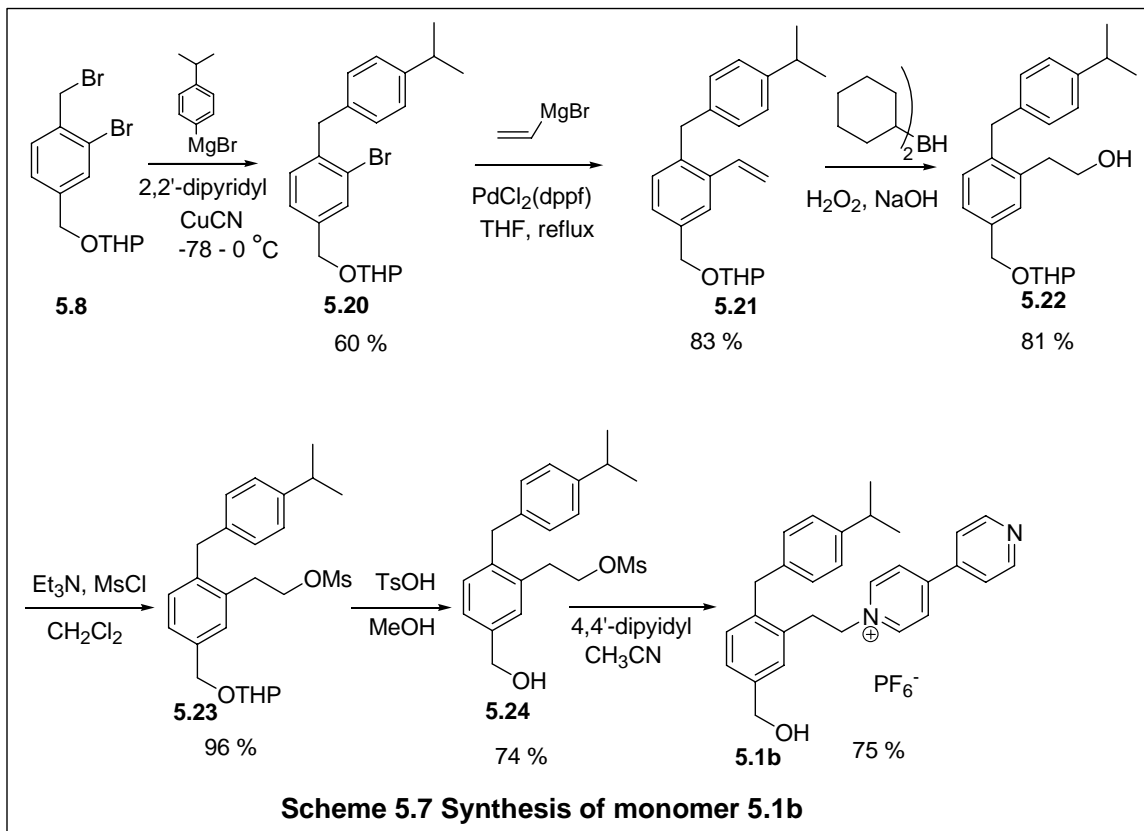
The desired [2] or [3]catenane could not be obtained from these traditional method. The reason could be that the “head” and “tail” in the precursor were too far to make the ring and the template effect seen for bistable [2]catenanes was not strong enough here. On the other hand, the two BPP34C10 might have repelled each other to prevent the formation of catenane in the initially formed pseudo-rotaxane. In this case, a high-pressure apparatus might be needed to promote the ring closure.

5.3.5 Synthesis of the Monomer **5.1b**

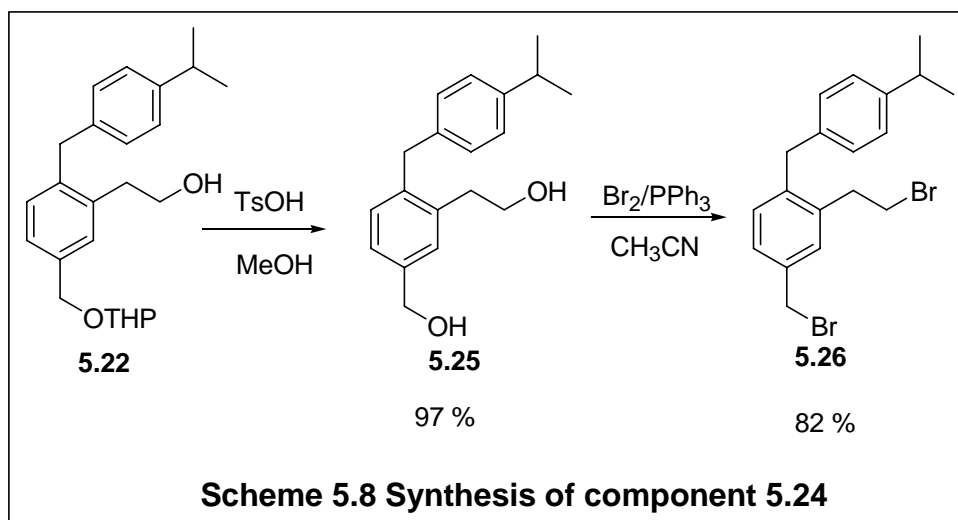
During the preparation of precursor **5.1a**, the precursor **5.1b** was also prepared in which an isopropylphenyl group was installed as a 'gate'. The consideration was that the tolyl group might not be bulky enough to make the trimer function as a ratchet. According to the previous observation, the isopropylphenyl gate was the one which resulted in the biggest ratio of two isomers in bistable [2]catenanes.

The preparation of the monomer **5.1b** followed the route in **Scheme 5.1**. As described in **Scheme 5.7**, compound **5.8** was coupled with isopropyl Grignard reagent with catalytic CuCN and 2, 2'-dipyridyl to give **5.20** in 60 % yield. A Kumada coupling⁵⁷ was performed to convert **5.20** to styrene derivative **5.21** in a yield of 83 %. Hydroboration⁵⁸ of **5.21** with dicyclohexyl borane regioselectively gave alcohol **5.22** in 81 % yield. Mesylation⁵⁹ followed by deprotection⁶⁰ led to intermediate **5.24** with a good leaving group and an unprotected alcohol. The yield for two steps was 71 %. Intermediate **5.24** reacted with excess 4, 4'-dipyridyl to give the monomer **5.1b**.

Dibromide **5.24** was synthesized to make the precursor **5.2b** as described in **Scheme 5.8**. Without mesylation, the intermediate **5.22** was deprotected to give diol **5.23** in 97 % yield. Bromination of diol **5.23** with Br₂/PPh₃ reagent gave the component **5.24** in a yield of 82 %. In all cases, the ¹H NMR and ¹³C NMR and MS data supported the formation of these intermediate components.



Since the catenation of precursor **5.1a** was disappointing, we decided to wait until we have access to a suitable high-pressure apparatus to attempt the ring closure.



Since the compounds in **Scheme 5.7** and **5.8** are similar to those in **Scheme 5.1** and **5.3** and we already discussed them in details in the early section in this chapter, characterization of these compounds will be left for the experimental part.

5.4 Summary and Conclusions

Originally, an attempt to synthesize a tristable catenane via a four-component reaction in one pot was not successful. It was more likely that oligomers and pseudo-rotaxanes were formed. Then the precursors for the tristable catenanes were successfully synthesized through more than 16 steps. However, the formation of tristable catenanes was not successful under traditional methods. As we can figure out so far, the ring closure without BPP34C10 threading was achieved and only C_3 -symmetric cationic cyclophane was formed. The repelling of BPP34C10 in psuedorotaxane and weak templating could prevent the ring closure.

Chapter 6

Conclusions and Future Perspectives

To achieve a unidirectional molecular motor driven by thermal energy, we designed bistable [2]catenanes with asymmetric gates. We sought to establish evidence for preferential circumrotation in one direction. The preference could be determined by the ratio of two isomers under low temperature ^1H NMR spectra. Before approaching this goal, we need to demonstrate the ability to control the movements in the interlocked system.

In our system with symmetric bistable [2]catenanes, bulky groups were incorporated on one or two of the tethers to block one or two pathways. When the top path was blocked, the crown ether ring (BPP34C10) circumrotated along the bottom unblocked pathway. When the bottom path was blocked, the crown ether ring moved along the top path. When both paths were blocked, the crown ether resided in the one side of the binding sites without circumrotation. The energy barriers required for passage over the unblocked tethers ranged from 11 to 13 kcal/mol. It was found that 1,3-xylyl tether was narrower than 1,4-xylyl tether, requiring high energy barrier for the crown ether ring to pass over. When both pathways were open, the BPP34C10 ring could move freely along either pathway. The energy barrier required for this catenane was lower than that of

any blocked catenanes, which could be attributed to the increasing entropy. At low temperature, the ratio of two isomers was 1:1 for unblocked catenanes. This indicated that two binding sites were isoenergetic. There was no preference for circumrotation in either direction.

To demonstrate the ability to modulate the energy barriers for circumrotation, we introduced wider tethers in symmetric bistable catenanes. In the catenanes with wider tethers, the energy barriers required for circumrotation ranged from 10.8 to 11.5 kcal/mol, about 1 kcal/mol lower than that for catenanes with 1,3-xylyl, 1,4-xylyl tethers. It seems that it was easier for crown ether rings to pass over the longer, wider tethers. On the other hand, no [3]catenanes was ever observed during the formation of these catenanes according to the integration in the ^1H NMR spectra and species in the MS spectra. The wider tethers might be spacious enough for two crown ether rings interacting with two binding sites but the 1,3-ethoxy resorcinol top tether preventing the formation of [3]catenanes. Interestingly, according to the ^1H NMR spectra, the internal hydroquinone ring of BPP34C10 π - π stacked with only one dipyrindinium unit. The distance of two dipyrindinium units was too far and the internal hydroquinone ring only interacted with one dipyrindinium unit at a time.

We designed the rigid tethers with Photoisomerizable gates to avoid the twist induced by the interaction between the gates and the ethoxy tethers. The 1:1 ratio of two

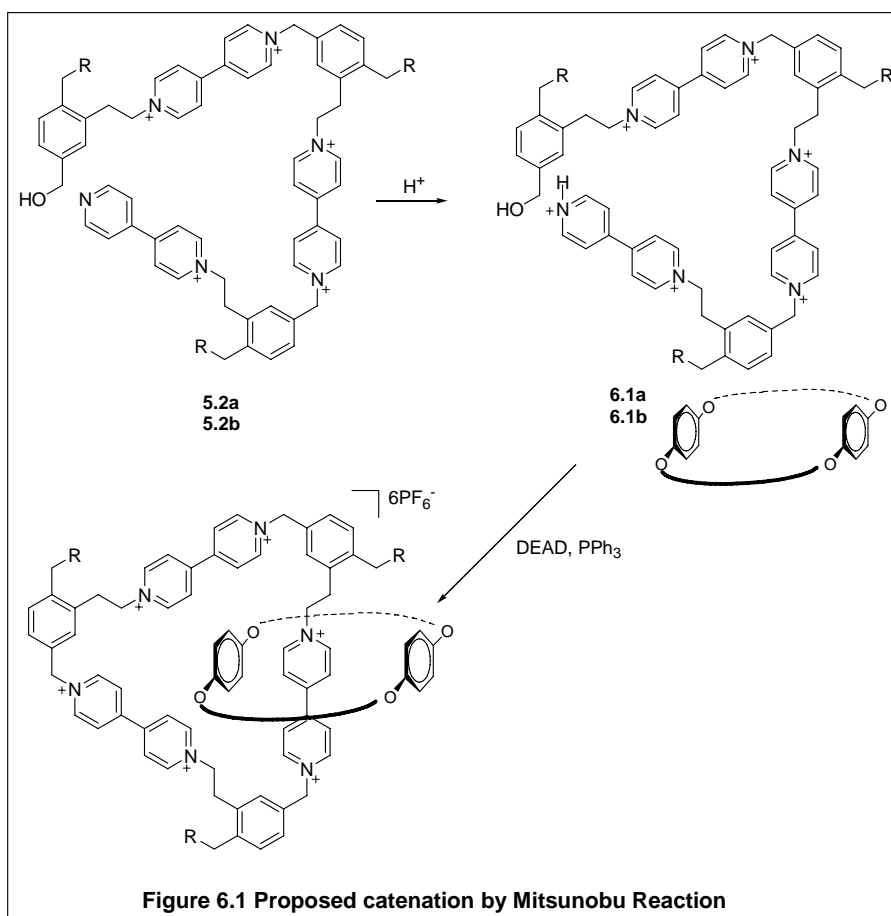
isomers displayed that the ground states of two binding sites were identical and were not affected by the gates. However, at low temperature (0 °C), the catenanes were irradiated by UV light and no preference of isomers was observed. Expand with rate data for correlated motion, evidence for ratcheting was not achieved.

The tristable [2]catenanes would be a perfect model for a unidirectional motor because it would be C_3 symmetric and the ground states of three binding sites should be identical. If there was preference for circumrotation of the crown ether ring, strong evidence for a unidirectional molecular motor would have been achieved. However, most of the synthesis has been accomplished except the last step. Without the BPP34C10 threaded on, ring closure reaction could happen easily. However, when the BPP34C10 were in the system, the two electron-deficient binding sites might coordinate with two electron-rich BPP34C10 rings which would repel each other to fail the ring closure. The catenation did not happen.

Another reason for failure of catenation could be resulted from the solubility decrease due to the anion exchange. When bromination reagents (Br_2/PPh_3 or PBr_3) were used, excess bromide anions could exchange with PF_6^- anion to precipitate the precursor as a bromide salt to fail the catenation. The reagents Br_2/PPh_3 might not a good choice.

For the future work, we need to accomplish the ring closure for tristable [2]catenane. We might resort to some new methods to develop this step. A Mitsunobu

reaction could be an option. As described in **Figure 6.1**, the neutral nitrogen of the precursor **5.2a** or **5.2b** could be protonated by mild acid to give acidic salt **6.1a** or **6.1b** since some acid is necessary in a typical Mitsunobu reaction. In the precursor **6.1a** or **6.1b**, a hydroxyl group and an acid exists in one molecule. Providing protons required for the Mitsunobu reaction, the acidic dipyridinium itself would be restored to the neutral dipyridyl which could be the desired nucleophile for the Mitsunobu reaction. The condition for a Mitsunobu reaction is mild, usually at room temperature which is the common condition for catenation.



Another suggestion is to use very high pressure, like 12 kbar to enforce the ring closure. In details, we would activate the benzyl alcohol in the precursor **5.2a** followed by adding the BPP34C10 in the system. The system would be kept under 12 kbar for a few days. We are seeking a collaborator with the special high pressure apparatus.

Once the tristable catenane was made, we would use 2D-EXSY spectrum to determine possible unidirectional circumrotation.

Experimental

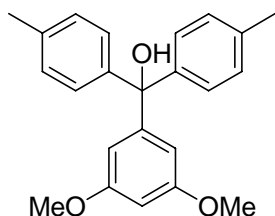
General Experimental Data:

Chemicals and solvents were purchased from Fisher/Acros or Aldrich and used without further purification unless noted. Preparative thin-layer chromatography (TLC) was performed using either 2 mm, 1 mm or 0.5 mm glass-backed sheets pre-coated with silica gel 60 F254 purchased from Fisher Scientific. Column chromatography was carried out using silica gel 60 F (0.040 to 0.063 mm particle size). ^1H and ^{13}C NMR spectra were recorded on either a Varian 400 or 300 MHz machine using residual solvent as internal standards: CHCl_3 at 7.26 ppm, or $\text{C}_3\text{H}_6\text{O}$ at 2.05 ppm, CH_3CN at 2.04 ppm. 2D-EXSY spectra were recorded on a Varian 500 machine. ^{13}C NMR data for catenane **3.1-3.4** were collected from HSQC spectra. Chemical shifts are denoted in ppm and coupling constants in Hertz. Abbreviations for NMR spectra are as follows: s = singlet, d = doublet, t = triplet, q = quartet, m = multiplet. NMR samples were dissolved in CD_3COCD_3 , CD_3CN or CDCl_3 purchased from Cambridge Isotope Laboratories.

Purification of Catenanes³²

After stirring for 3 or 4 days, the catenane solutions were concentrated by removing the solvent acetonitrile via rotary evaporator to give a red residue. The residue was dissolved in minimum volume of methanol/acetone (1:1) and the solution was loaded

on the preparative TLC plate. After drying, the preparative TLC plate was eluted twice with methanol/ethyl acetate (1:1) at 35 °C. Then, the preparative TLC plate was eluted with methanol/2M ammonium chloride/nitromethane (7:2:1). The desired [2]catenanes moved up ($R_f = 0.3-0.5$). The [2]catenanes on the preparative TLC plate appeared orange to red bands. The orange/red band was removed from the plate. The silica gel containing the [2]catenanes was ground and washed with the final eluent-methanol/2M ammonium chloride/nitromethane (7:2:1). An excess of ammonium hexafluorophosphate was added to perform anion exchange. The methanol and nitromethane was removed via rotary evaporator and the red precipitate was suspended in the solution. The solution was filtered and the solid was washed with water several times and allowed to air dry. The obtained solid was dissolved in d_6 -acetone or d_3 -acetonitrile for 1H NMR, ^{13}C NMR and variable temperature NMR.



(3, 5-Dimethoxyphenyl)di-p-tolylmethanol (2.9)

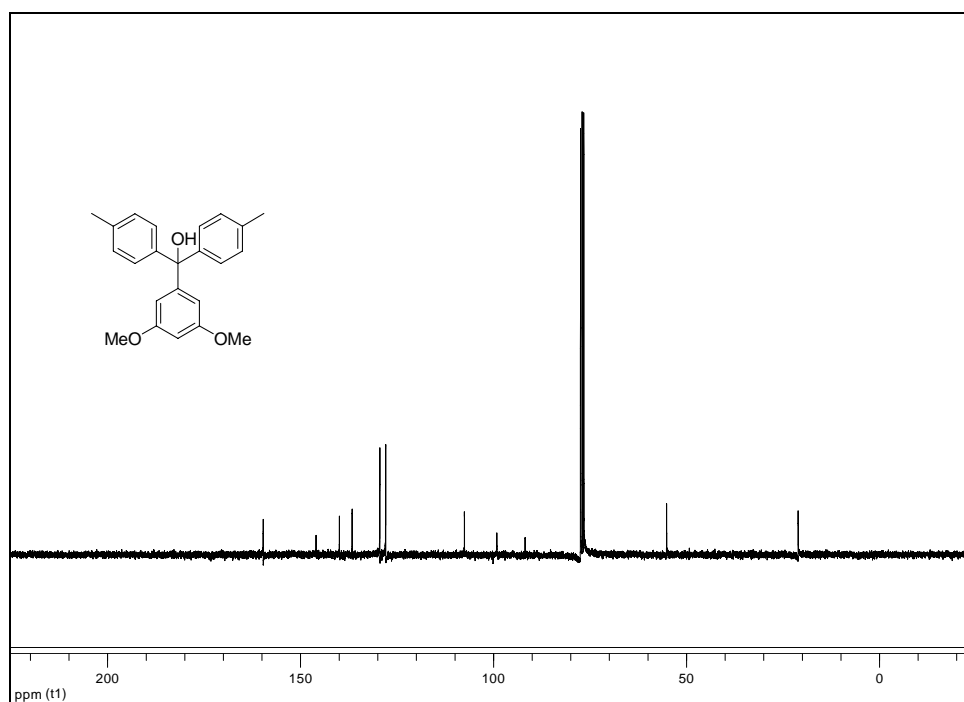
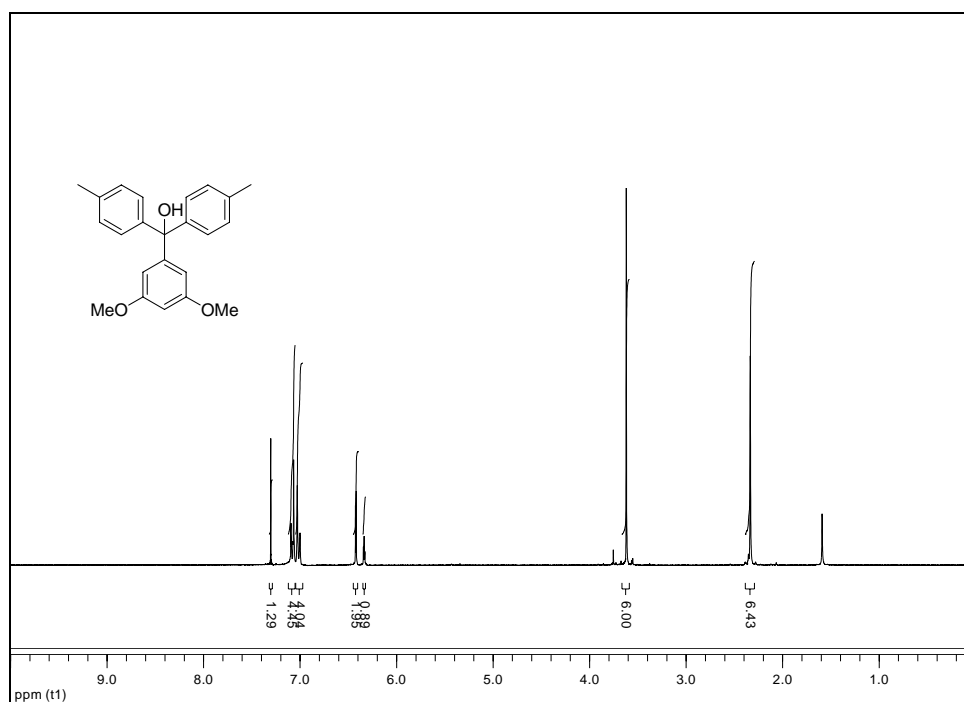
Magnesium turnings (17.5 g, 0.72 mol) were flushed with nitrogen and THF (250 mL) followed by 2 drops of 1,2-dibromoethane were added to a flask equipped with a condenser. 4-Bromotoluene (29.5 mL, 0.240 mol) was added in portion to the mixture in a vigorous exothermic reaction. The mixture was then allowed to stir at room temperature overnight.

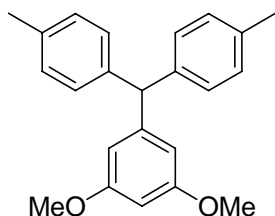
The Grignard reagent was transferred by cannula to a solution of 3, 5-dimethoxybenzoic acid methyl ester (18.8 g, 0.096 mol) in THF (100 mL) at room temperature. The mixture was stirred at room temperature overnight. The reaction was quenched with saturated NH_4Cl (20 mL) and the mixture was extracted with diethyl ether (3×50 mL). The ether layer was washed with water (3×50 mL) and dried with MgSO_4 . The filtrate was evaporated to provide a yellow oil (34 g), which was carried on to the next step without purification.

^1H NMR (CDCl_3 , 300 MHz): δ ppm 7.05 (d, $J=8.2$ Hz, 4H), 6.98 (d, $J=8.2$, 4H), 6.38 (d, $J=2.3$ Hz, 2H), 6.29 (t, $J=2.3$ Hz, 1H), 3.58 (s, 6H), 2.29 (s, 6H).

^{13}C NMR (CDCl_3 , 75 MHz): δ ppm 159.64, 145.95, 139.90, 136.59, 129.41, 127.89, 107.49, 99.09, 91.79, 55.12, 21.03.

MS (ESI): m/z 371.6 ($M+Na^+$) ($M=C_{23}H_{24}O_3$ requires 348.17, Na^+ requires 23).





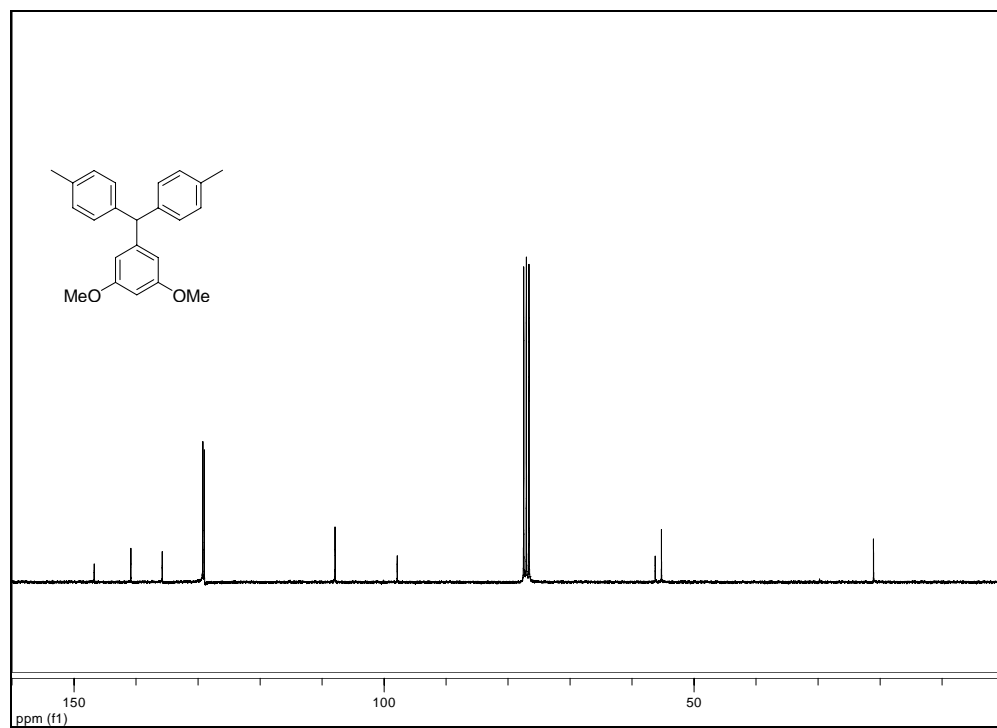
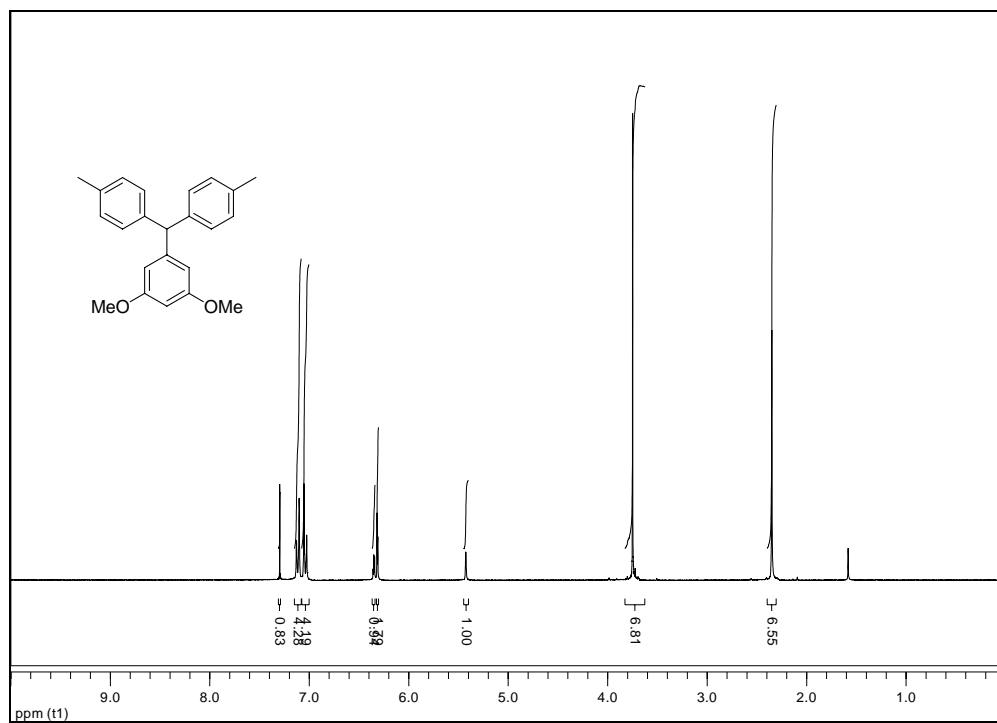
1-Di-p-tolylmethyl-3, 5-dimethoxybenzene (2.10)

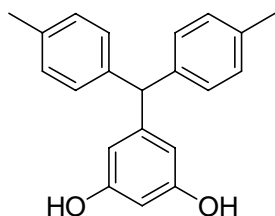
A mixture of (3,5-dimethoxyphenyl)di-p-tolylmethanol (30 g, 0.086 mol), 5% palladium-on-carbon (1.5 g), CH₃OH (30 mL), CH₃COOH (1 mL), CH₂Cl₂ (250 mL) was stirred at room temperature under a balloon of hydrogen for one week. The catalyst was filtered through a pad of Celite and the filtrate was evaporated. The residue was purified by flash chromatography (petroleum ether/methylene chloride (1:1)) to give a yellow oil (16 g, 56%).

¹H NMR (CDCl₃, 300 MHz): δ ppm 7.08 (d, J=8.5 Hz, 4H), 7.00 (d, J=8.2 Hz, 4H), 6.31 (t, J=2.3 Hz, 1H), 6.27 (d, J=2.1 Hz, 2H), 5.39 (s, 1H), 3.71 (s, 6H), 2.31 (s, 6H).

¹³C NMR (CDCl₃, 75 MHz): δ ppm 160.62, 146.76, 140.85, 135.78, 129.23, 128.99, 107.90, 97.87, 56.26, 55.26, 21.05.

MS (ESI): m/z 355.2 (M+Na⁺) (M=C₂₃H₂₄O₂ requires 332.18).





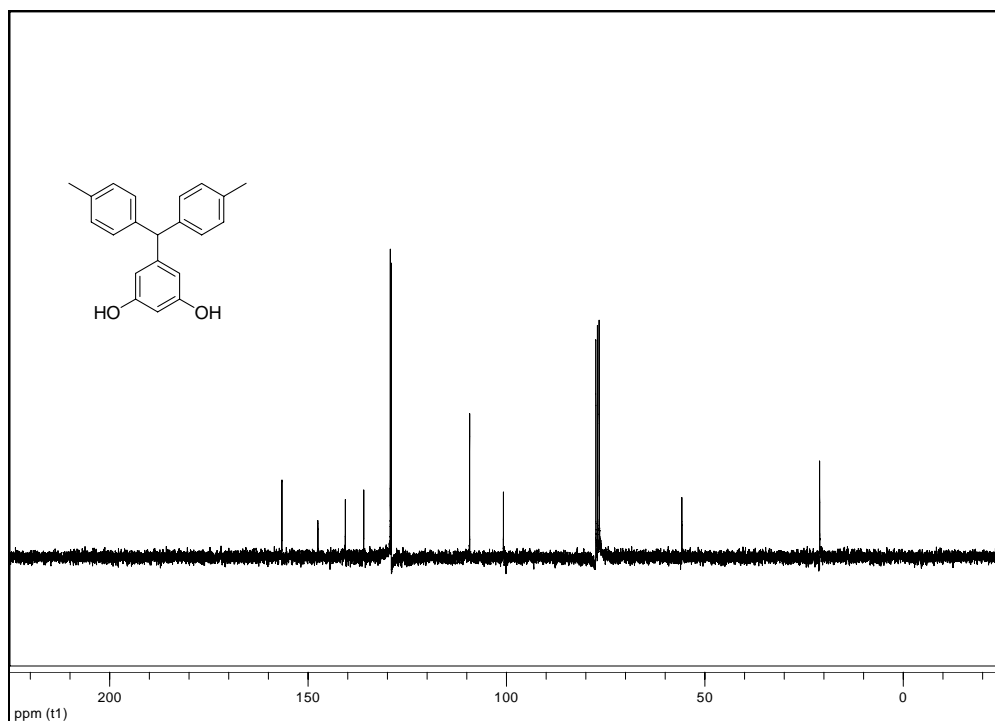
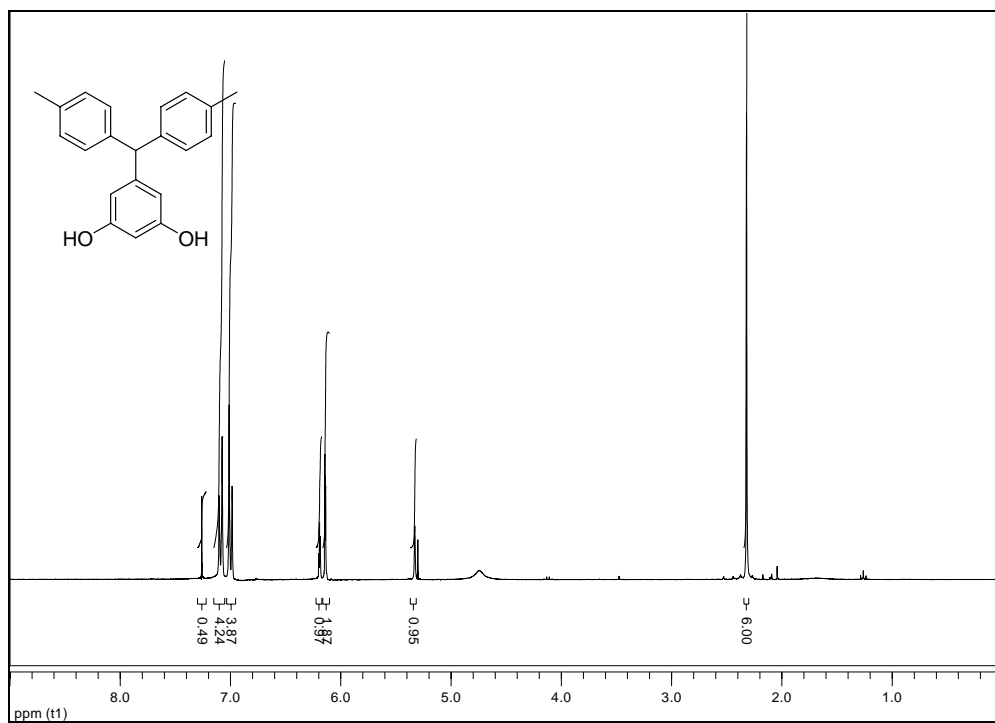
5-Di-p-tolylmethylbenzene-1,3-diol (2.14b)

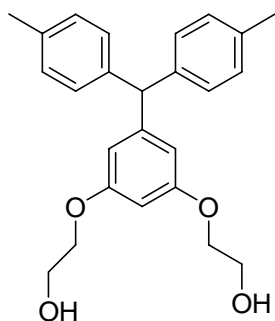
To a solution of 1-di-p-tolylmethyl-3,5-dimethoxybenzene (7.0 g, 0.021 mol) in methylene chloride (80 mL), was added boron tribromide (4.8 mL, 0.0504 mol) at -78 °C. The mixture was allowed to warm to room temperature and stir for 20 h. The reaction was quenched with methanol (80 mL) and ice (80 g). The mixture was extracted with methylene chloride (3 × 50 mL) and the organic layer was washed with water (3 × 50 mL). The extract was dried with MgSO₄, filtered and the filtrate was evaporated to give an orange paste (6.3 g, 98%).

¹H NMR (CDCl₃, 300 MHz): δ ppm 7.09 (d, J=8.2 Hz, 4H), 7.00 (d, J=8.2 Hz, 4H), 6.19 (t, J=2.3 Hz, 1H), 6.14 (d, J=2.3 Hz, 2H), 5.33 (s, 1H), 2.32 (s, 6H).

¹³C NMR (CDCl₃, 75 MHz): δ ppm 156.54, 147.46, 140.54, 135.91, 129.20, 128.99, 109.22, 100.71, 55.73, 20.99.

MS (ESI): m/z 327.5 (M+Na⁺) (M=C₂₁H₂₀O₂ requires 304.15).





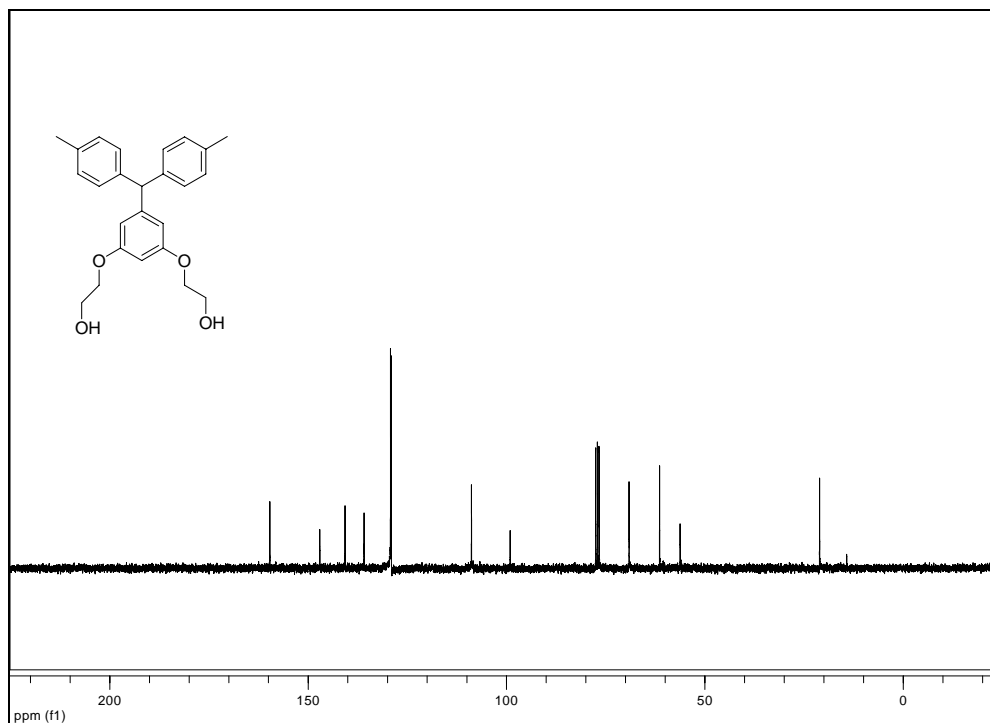
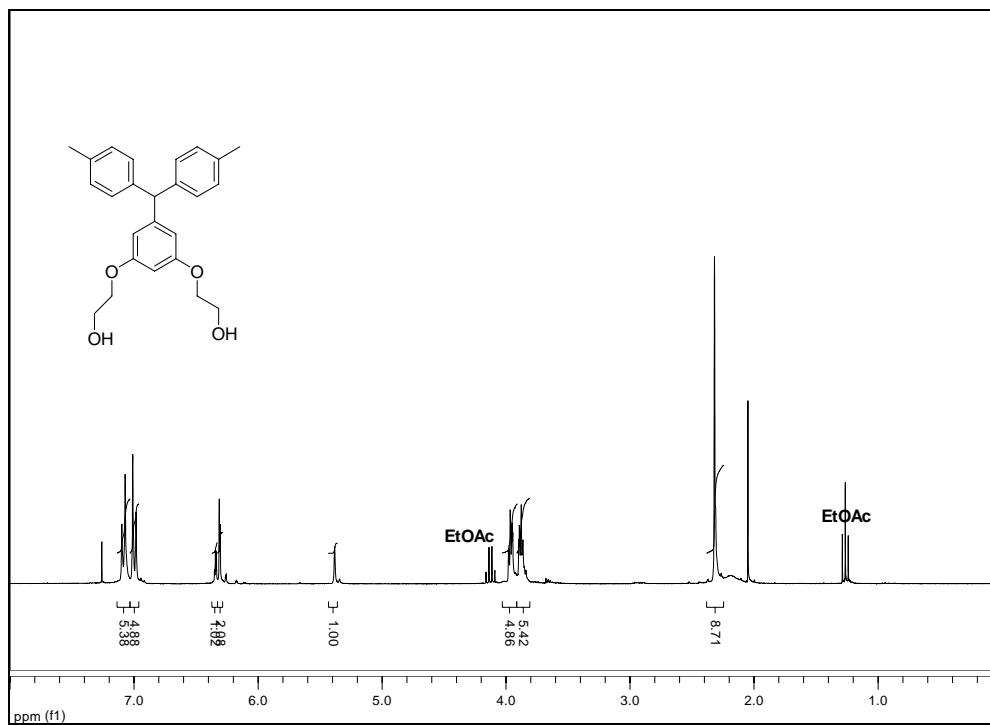
2-[3-Di-p-tolylmethyl-5-(2-hydroxyethoxy)phenoxy]ethanol (2.15b)

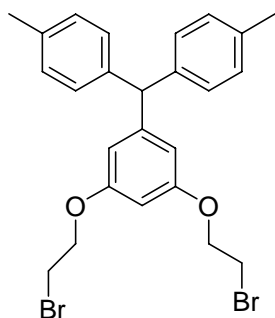
To a solution of 5-di-p-tolylmethylbenzene-1,3-diol (3.2 g, 0.0105 mol) in ethanol (20 mL) was added a solution containing NaOH (1.26 g, 0.0315 mol), ethanol (20 mL), water (7 mL). The mixture was stirred at room temperature for 10 min. 2-Chloroethanol (2.1 mL, 0.0315 mol) was added at room temperature and the reaction mixture was stirred under reflux for 4 days, then allowed to cool and concentrated under reduced pressure. The residue was extracted with ethyl acetate (3 × 30 mL). The organic layer was washed with water (3 × 30 mL) and brines (3 × 30 mL). The organic portion was dried with MgSO₄, filtered and the filtrate was evaporated to give a grey solid (3.85 g, 93%).

¹H NMR (CDCl₃, 300 MHz): δ ppm 7.08 (d, J=7.9 Hz, 4H), 7.00 (d, J=8.2 Hz, 4H), 6.34 (t, J=2.3 Hz, 1H), 6.31 (d, J=2.1 Hz, 2H), 5.38 (s, 1H), 3.96 (td, J=4.7 Hz, 1.8 Hz, 4H), 3.88 (td, J=4.7 Hz, 1.8 Hz, 4H), 2.32 (s, 6H).

¹³C NMR (CDCl₃, 75 MHz): δ ppm 159.56, 146.97, 140.61, 135.81, 129.14, 128.97, 108.74, 98.97, 69.02, 61.32, 56.14, 20.98.

MS (ESI): m/z 415.7 (M+Na⁺) (M=C₂₅H₂₈O₄ requires 392.20).





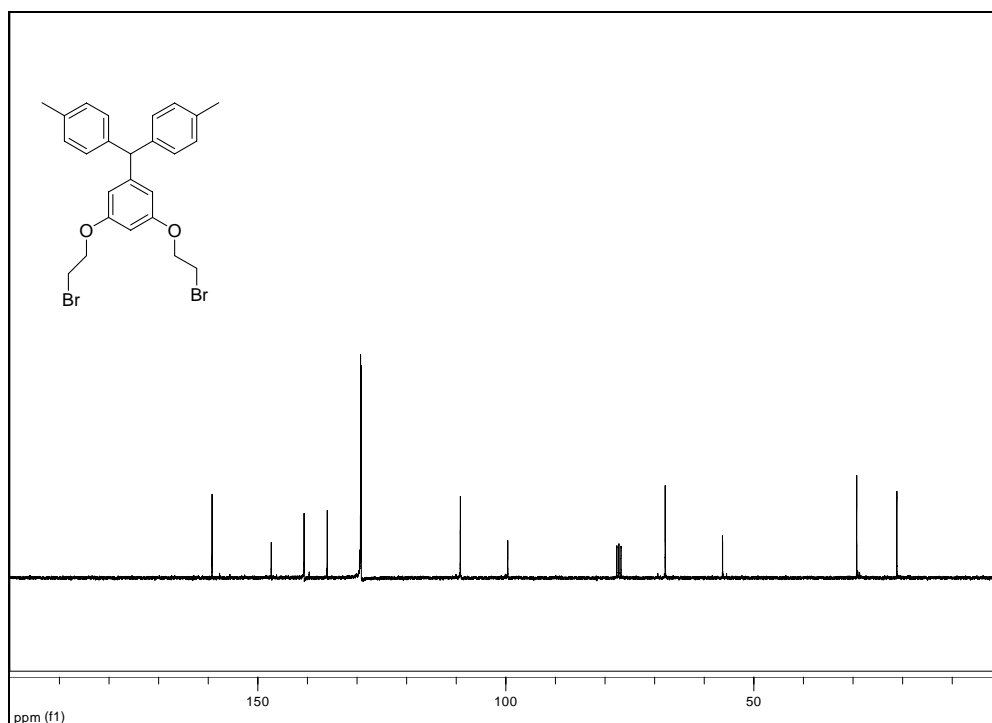
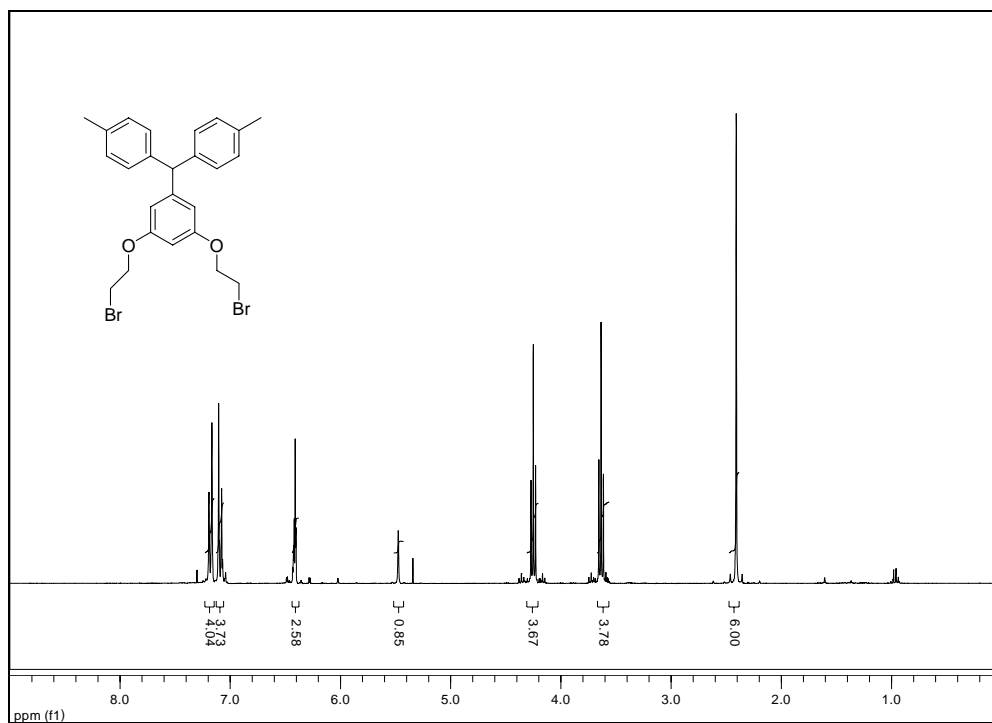
1,3-Bis(2-bromoethoxy)-5-di-p-tolylmethylbenzene (2.16b)

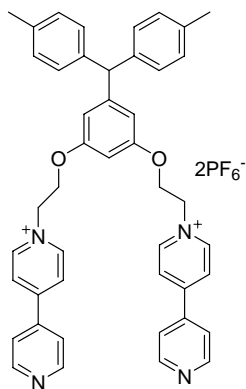
To a suspension of triphenylphosphine (5.84 g, 22.3 mmol) in acetonitrile (25 mL) was added bromine (3.56 g, 22.3 mmol) in acetonitrile (20 mL) dropwise at -10 °C over 1 h. The mixture was allowed to warm to room temperature and 2-[3-di-p-tolylmethyl-5-(2-hydroxyethoxy)phenoxy]ethanol (3.8 g, 9.68 mmol) in acetonitrile (10 mL) were added. The reaction mixture was stirred at room temperature for 24 h. Acetonitrile was removed *in vacuo* and the residue was purified by flash chromatography with methylene chloride to give a brown paste (2.8 g, 56%).

¹H NMR (CDCl₃, 300 MHz): δ ppm 7.18 (d, J=7.9 Hz, 4H), 7.09 (d, J=8.2 Hz, 4H), 6.42 (t, J=2.6 Hz, 1H), 6.41 (d, J=2.1 Hz, 2H), 5.48 (s, 1H), 4.25 (t, J=6.2 Hz, 4H), 3.63 (t, J=6.2 Hz, 4H), 2.41 (s, 6H).

¹³C NMR (CDCl₃, 75 MHz): δ ppm 159.23, 147.28, 140.66, 135.99, 129.28, 129.15, 109.16, 99.60, 67.85, 56.29, 29.24, 21.16.

MS (ESI): m/z 539.1 (M+Na)⁺, 541.1 (M+2+Na)⁺, 543.1 (M+4+Na)⁺ (M= C₂₅H₂₆Br₂O₂ requires 516.03).





**1,3-Bis(2-(4,4'-dipyridinium)ethoxy)-5-di-p-tolylmethylbenzene
dihexafluorophosphate (2.17b)**

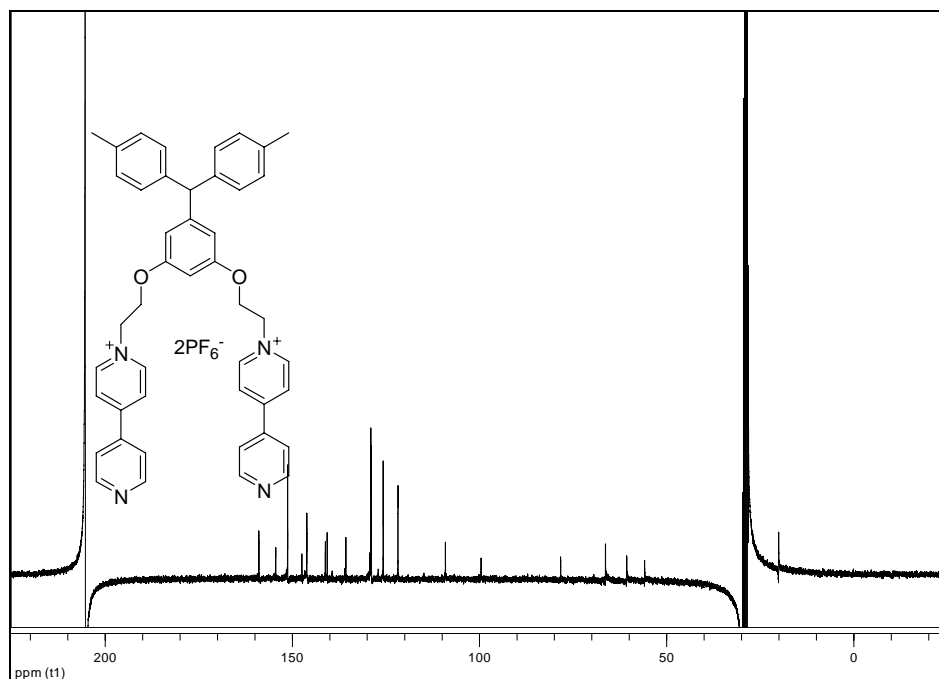
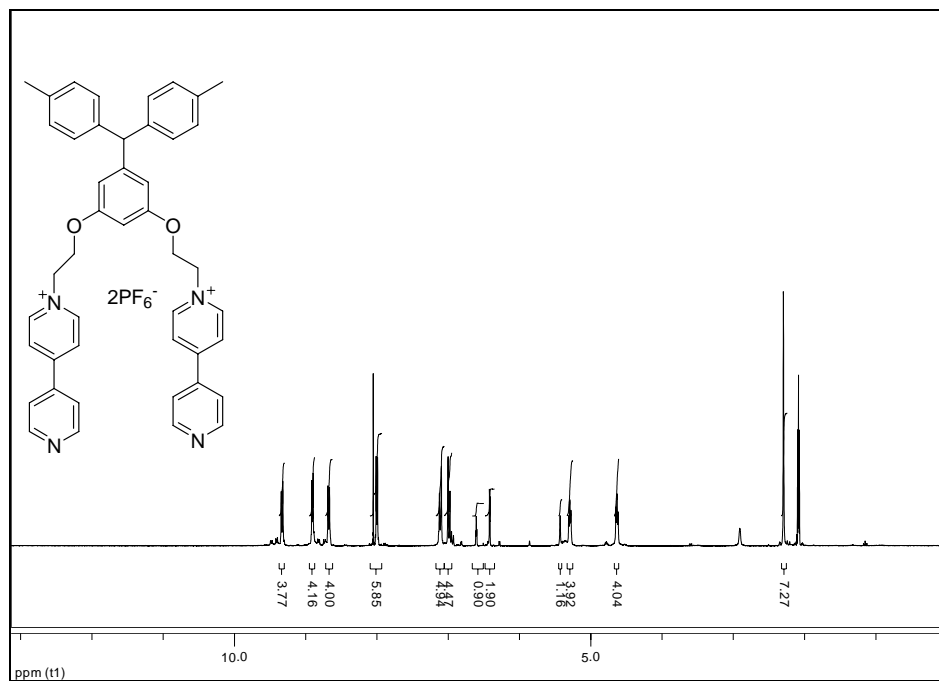
A mixture of 1,3-bis-(2-bromoethoxy)-5-(di-p-tolylmethyl)benzene (1.2 g, 2.31 mmol) and 4,4'-dipyridyl (1.8 g, 11.6 mmol) was stirred at 65 °C for 2 days. The mixture was allowed to cool and concentrated *in vacuo*. The residue was dissolved in hot water and ammonium hexafluorophosphate (0.75 g, 4.62 mmol) was added to the aqueous solution. A brown oil precipitated to the bottom of the flask and the aqueous layer was decanted. The oil was washed with chloroform (6 × 10 mL) to give a brown solid (1.9 g, 86%).

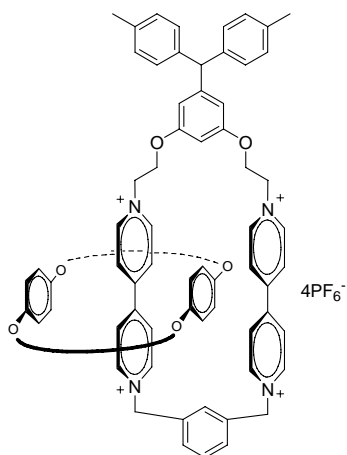
¹H NMR (C₃D₆O, 300 MHz): δ ppm 9.25 (d, J=7.0 Hz, 4H), 8.86 (d, J=5.9 Hz, 4H), 8.61 (d, J=6.7, 4H), 7.95 (d, J=6.1 Hz, 4H), 7.07 (d, J=7.9 Hz, 4H), 6.97 (d, J=8.2 Hz, 4H), 6.57 (t, J=2.1, 1H), 6.40 (d, J=2.1 Hz, 2H), 5.40 (s, 1H), 5.24 (t, J=4.7 Hz, 4H), 4.59 (t, J=4.7 Hz, 4H), 2.25 (s, 6H).

¹³C NMR (C₃D₆O, 75 MHz): δ ppm 159.90, 155.40, 152.20, 148.40, 147.08, 142.14, 141.63, 136.66, 129.99, 129.84, 126.69, 122.74, 110.07, 100.55, 79.28, 67.31, 61.63,

56.84, 21.04.

MS (ESI): m/z 335.2 (M^{2+}), 815.4 ($M+PF_6$)⁺ ($M=C_{45}H_{42}N_4O_2^{2+}$ requires 670.33).





Catenane 2.4 1,3-Bis(2-(4,4'-dipyridinium)ethoxy)-5-(di-p-tolylmethyl)benzene

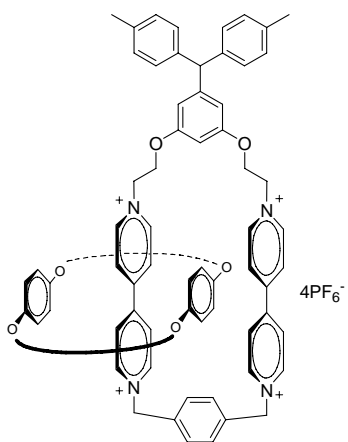
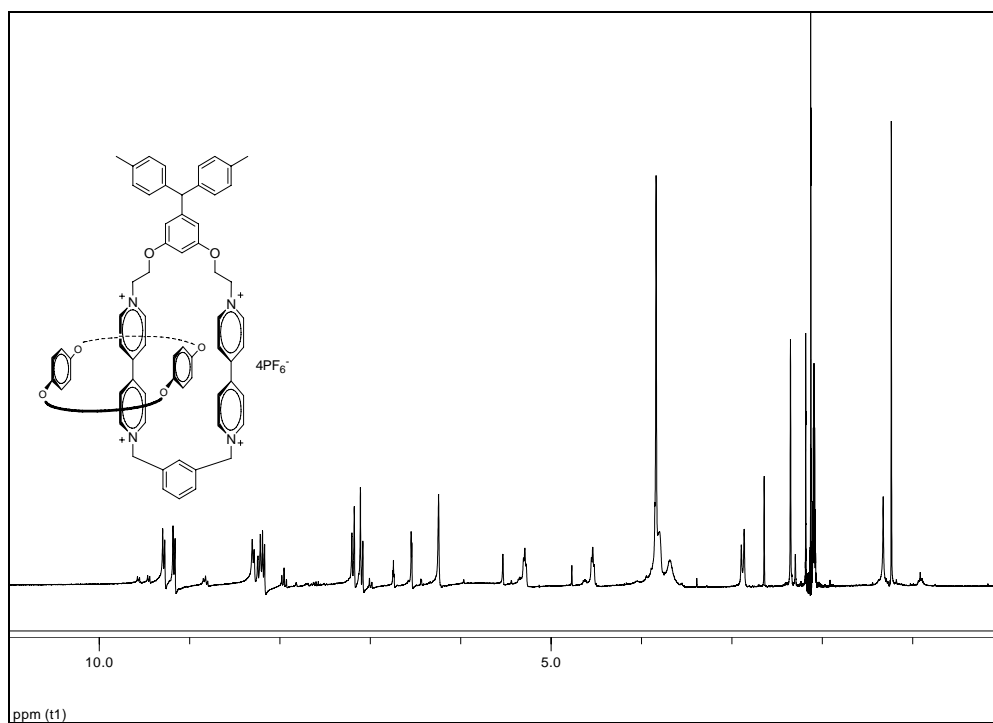
dihexafluorophosphate (**15b**) (0.140 g, 0.146 mmol) and BPP34C10 (0.125 g, 0.233 mmol) were combined and dissolved in CH₃CN (15 mL). This solution was allowed to stir for 10 min at which point α,α' -dibromo-*m*-xylene (0.050 g, 0.190 mmol) was added and the reaction vessel sealed with a septum. This red solution stirred 4 days under ambient conditions after which time the solvent was removed *in vacuo*. The catenane was purified as previously described and after drying, 21 mg (7%) of red solid was recovered.

¹H NMR (C₃D₆O, 300 MHz): δ ppm 9.24 (d, *J*=6.8 Hz, 4H), 9.13 (d, *J*=6.8 Hz, 4H), 8.26~8.13 (m, 12H), 7.15 (d, *J*=8.0 Hz, 4H), 7.05 (d, *J*=8.2 Hz, 4H), 6.71 (t, *J*=2.1 Hz, 1H), 6.50 (d, *J*=2.1 Hz, 2H), 6.20 (s, 4H), 5.49 (s, 1H), 5.25 (t, *J*=4.5 Hz, 4H), 4.50 (t, *J*=4.5 Hz, 4H), 3.80 (br, 32H), 2.31 (s, 6H).

¹³C NMR (C₃D₆O, 75 MHz): δ ppm 158.70, 151.81, 147.48, 146.68, 146.06, 145.71, 140.78, 135.72, 134.25, 133.84, 132.13, 131.01, 129.08, 128.97, 127.62, 127.11, 125.88, 125.53, 114.56, 107.41, 103.32, 70.32, 70.18, 69.80, 67.31, 66.09, 64.34, 60.80, 56.28,

20.12.

MS (ESI): m/z 327.9 (M^{4+}), 485.6 ($M+PF_6$) $^{3+}$, 801.0 ($M+2PF_6$) $^{2+}$ ($M=C_{81}H_{90}N_4O_{12}^{4+}$ requires 1361.65).



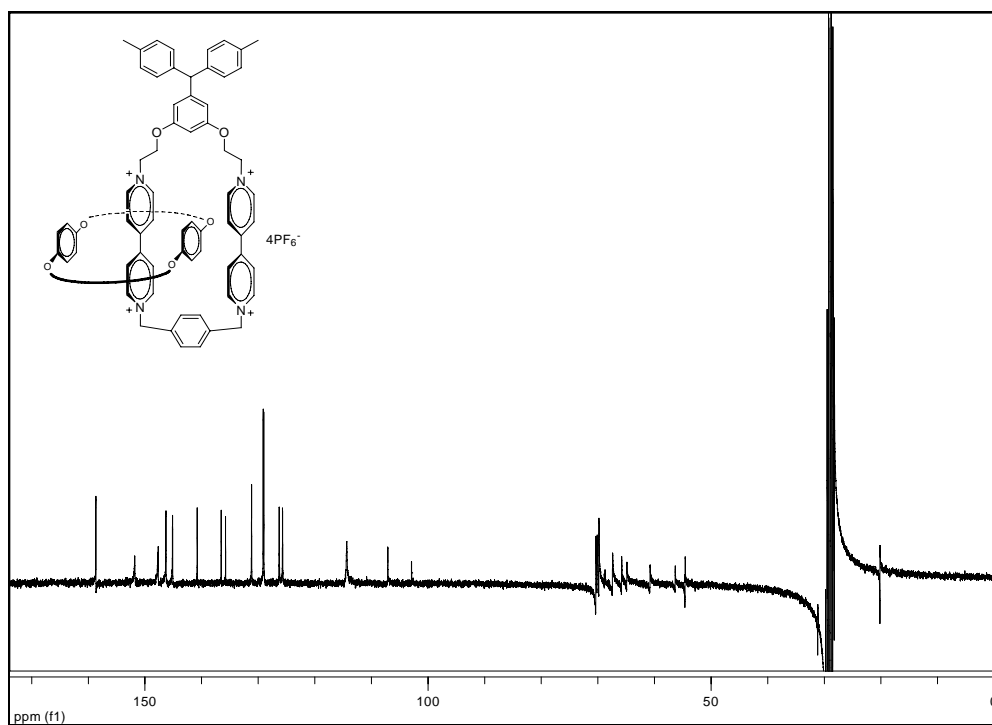
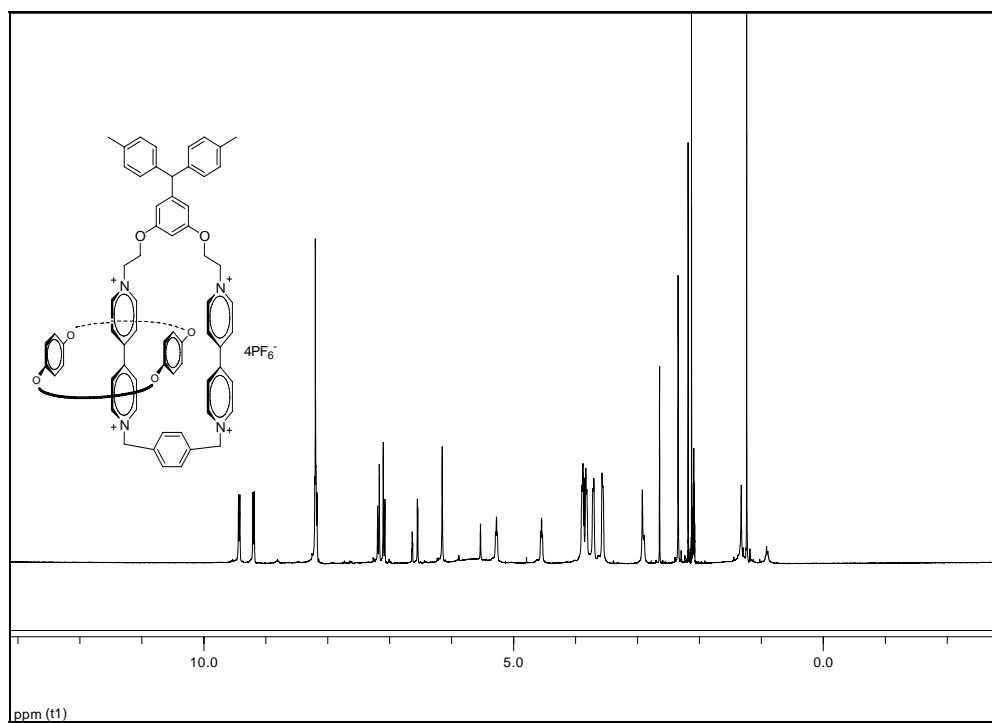
Catenane 2.5 1,3-Bis(2-(4,4'-dipyridinium)ethoxy)-5-(di-p-tolylmethyl)benzene

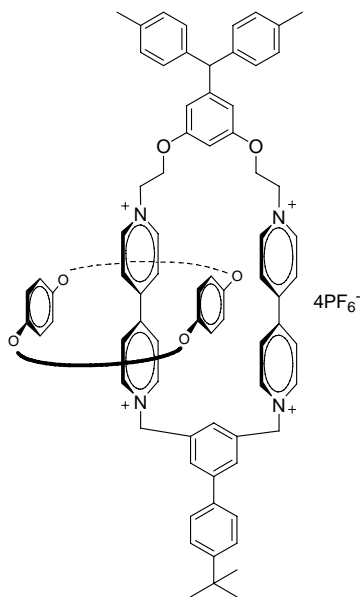
dihexafluorophosphate (**15b**) (0.140 g, 0.146 mmol) and BPP34C10 (0.125 g, 0.233 mmol) were combined and dissolved in CH₃CN (15 mL). This solution was allowed to stir for 10 min at which point α,α' -dibromo-*p*-xylene (0.051 g, 0.192 mmol) was added and the reaction vessel sealed with a septum. This red solution stirred 4 days under ambient conditions after which time the solvent was removed *in vacuo*. The catenane was purified as previously described and after drying, 55 mg (19 %) of red solid was recovered.

¹H NMR (C₃D₆O, 300 MHz): δ ppm 9.39 (d, J=6.7 Hz, 4H), 9.16 (d, J=6.7 Hz, 4H), 8.16 (m, 12H), 7.14 (d, J=7.9 Hz, 4H), 7.05 (d, J=8.2 Hz, 4H), 6.60 (t, J=2.1 Hz, 1H), 6.51 (d, J=2.1 Hz, 2H), 6.11 (s, 4H), 5.49 (s, 1H), 5.24 (t, J=4.2 Hz, 4H), 4.51 (t, J=4.2 Hz, 4H), 3.86~3.52 (m, 32H), 2.30 (s, 6H).

¹³C NMR (C₃D₆O, 75 MHz): δ ppm 158.67, 151.80, 147.76, 146.29, 145.12, 140.77, 136.54, 135.76, 131.17, 129.11, 129.01, 126.29, 125.70, 114.37, 107.11, 102.91, 70.34, 70.13, 69.81, 67.40, 65.80, 64.88, 60.78, 56.34, 54.61, 20.16.

MS (ESI): *m/z* 327.9 (M⁴⁺), 485.6 (M+PF₆)³⁺, 800.9 (M+2PF₆)²⁺ (M=C₈₁H₉₀N₄O₁₂⁴⁺ requires 1361.65).





Catenane 2.6 1,3-Bis(2-(4,4'-dipyridinium)ethoxy)-5-(di-p-tolylmethyl)benzene

dihexafluorophosphate (**15b**) (0.140 g, 0.146 mmol) and BPP34C10 (0.125 g, 0.233

mmol) were combined and dissolved in CH₃CN (15 mL). This solution was allowed to stir for 10 min at which point 5-bis(bromomethyl)-4'-(1,1'-dimethylethyl)-1,1'-

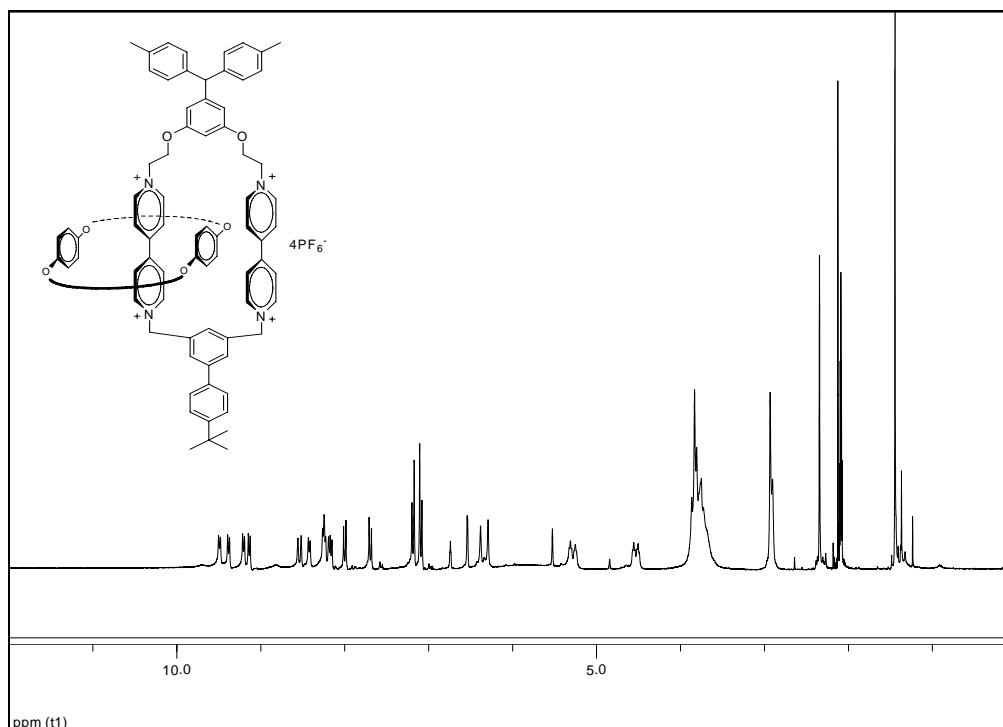
biphenyl (0.050 g, 0.190 mmol) was added and the reaction vessel sealed with a septa.

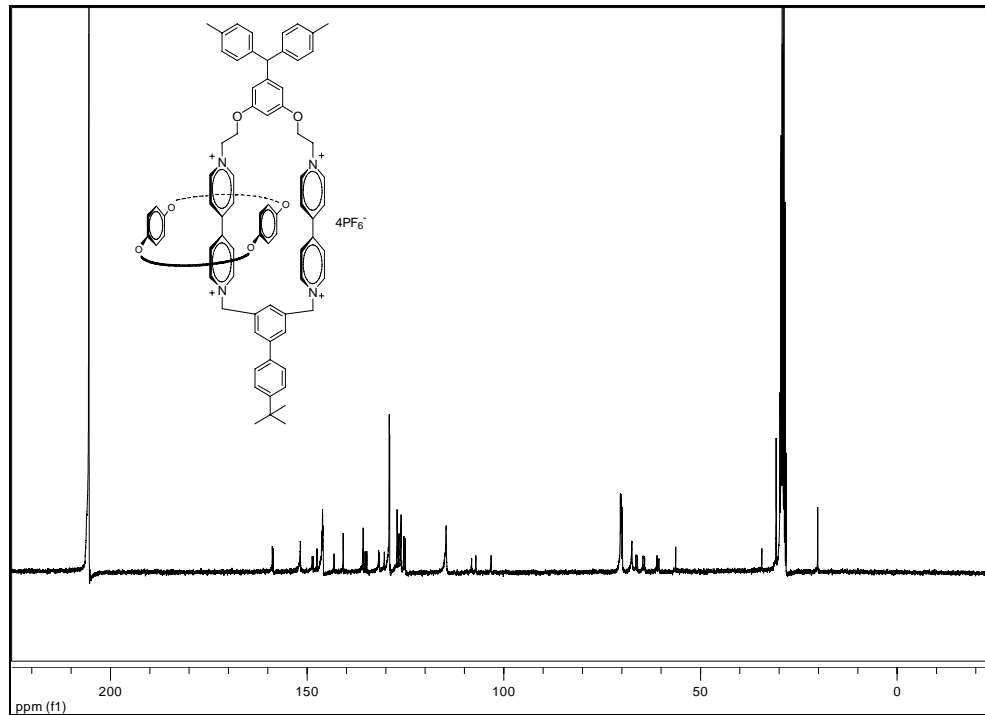
This red solution stirred 4 days under ambient conditions after which time the solvent was removed *in vacuo*. The catenane was then purified as described above to give a red solid.

¹H NMR (C₃D₆O, 300 MHz): δ ppm 9.44 (d, J=6.8 Hz, 2H), 9.35 (d, J=7.0 Hz, 2H), 9.15 (d, J= 6.8 Hz, 2H), 9.10 (d, J=7.0 Hz), 8.48 (d, J=10.0 Hz, 2H), 8.39 (d, J=6.5, 2H), 8.23~8.10 (m, 7H), 7.96 (d, J=8.5 Hz, 2H), 7.66 (d, J=8.8 Hz, 2H), 7.15 (d, J=7.9 Hz, 4H),

7.06 (d, $J=8.2$ Hz, 4H), 6.68 (t, $J=2.1$ Hz, 1H), 6.52 (d, $J=2.1$ Hz, 2H), 6.33 (s, 2H), 6.25 (s, 2H), 5.80 (s, broad, 7H), 5.49 (s, 1H), 5.26 (t, $J=4.7$ Hz, 2H), 5.21 (t, $J=4.7$ Hz, 2H), 4.55 (t, $J=4.7$ Hz, 2H), 4.48 (t, $J=4.7$ Hz, 2H), 3.83~3.67 (m, 32H), 2.31 (s, 6H), 1.42 (s, 9H).

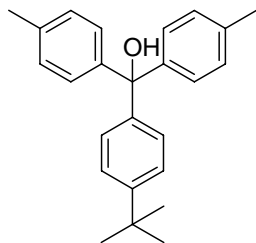
^{13}C NMR ($\text{C}_3\text{D}_6\text{O}$, 75 MHz): δ ppm 158.86, 158.64, 151.73, 148.72, 148.49, 147.50, 146.28, 146.09, 145.97, 143.16, 140.83, 135.89, 135.75, 135.27, 134.80, 131.83, 131.66, 130.38, 129.13, 129.03, 127.12, 126.64, 126.19, 126.10, 125.97, 125.37, 125.03, 114.65, 108.17, 107.10, 103.24, 70.36, 70.20, 69.87, 67.43, 66.39, 66.01, 64.62, 64.19, 61.04, 60.57, 56.29, 34.40, 30.76, 21.18.





Synthesis route of 1,1'-[[4-(1,1-dimethylethyl)phenyl]methylene]bis

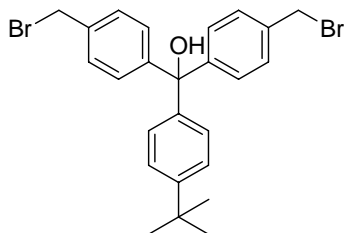
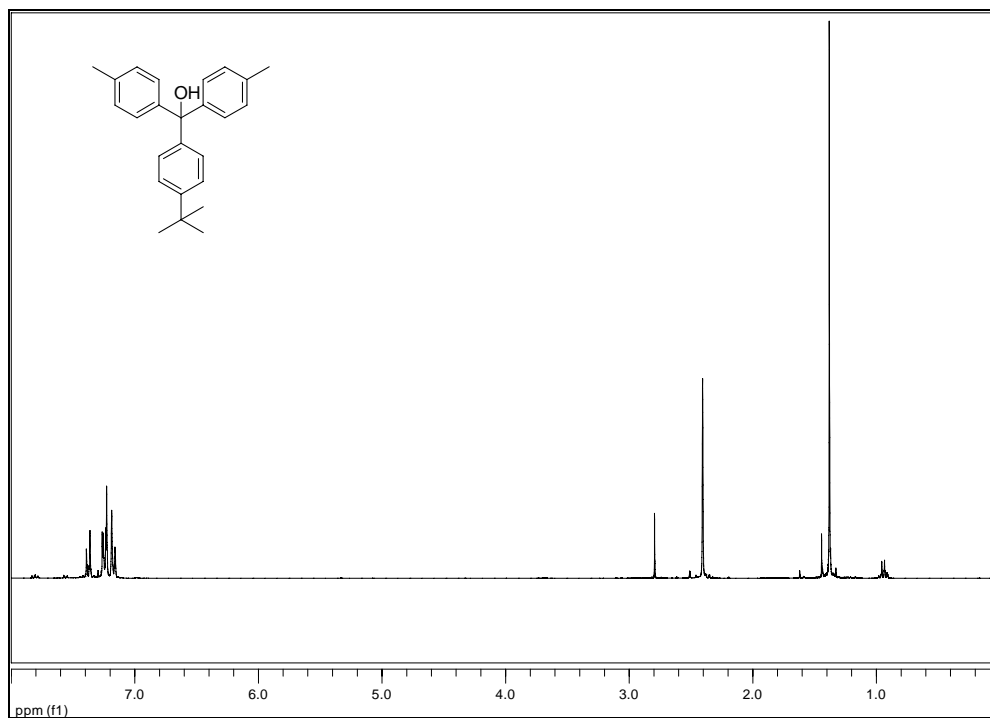
[4-(bromomethyl)]benzene (3.5) in the literature⁴³



(4-tert-Butylphenyl)di-p-tolylmethanol (3.3)⁴³

Magnesium turnings (2.2 g, 0.091 mol) were added to a 3-neck flask. The ports of the 3-neck flask were affixed with a reflux condenser, addition funnel, and rubber septa. The flask was purged with nitrogen and dry THF (50 mL) was added to the flask under

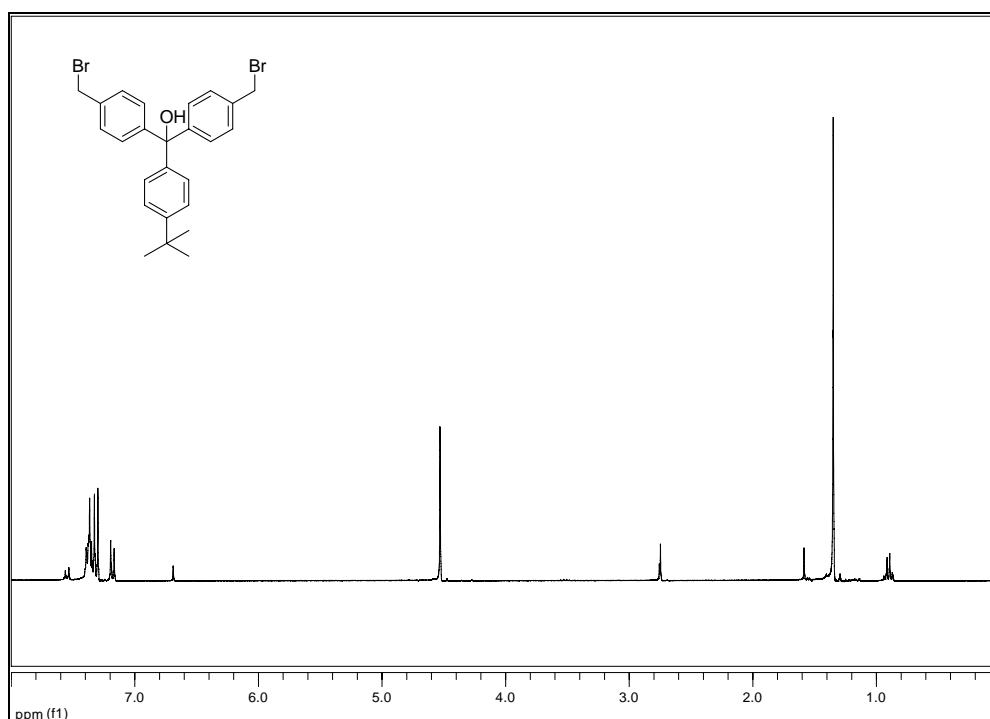
nitrogen via a syringe. Approximately 6 – 10 drops of 1, 2-dibromoethane were added to the reaction flask under nitrogen via a syringe to activate the magnesium. The magnesium/THF mixture was heated to approximately 50 °C via an oil bath. THF (50 mL) and 4-bromotoluene (8 mL, 0.065 mol) were sequentially added to the addition funnel under nitrogen. Methyl-4-tertbutylbenzoate (5.0 mL, 0.026 mol) was added to the reaction flask under nitrogen via a syringe. The 4-bromotoluene/THF mixture was added to the mixture dropwise and the reaction mixture was refluxed at 70 – 80 °C for 20 – 24 h. The reaction mixture was cooled to room temperature and poured into a solution of ice (100 mL) and concentrated H₂SO₄ (3.3 mL) followed by the addition of NH₄Cl (3.3 g) to the aqueous mixture. The aqueous mixture was extracted with diethyl ether (100 mL × 3). The combined organic fractions were washed with 5 wt% NaHCO₃ (100 mL × 3), water (100 mL × 3), dried (MgSO₄) and concentrated *in vacuo* (9.0 g, quantitative crude yield). The crude product was purified via column chromatography [SiO₂ – petroleum ether - CH₂Cl₂ (2:1), v/v] to give pure compound (**3.3**) (3.4 g, 38% yield). The ¹H NMR spectrum of the purified product was consistent with the chemical structure and that reported in the literature.⁴³

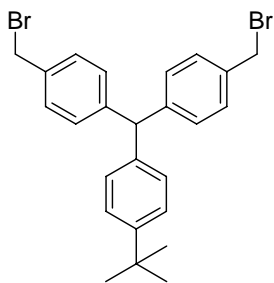


Bis(4-bromomethylphenyl)-(4-tert-butylphenyl)methanol (3.4)⁴³

NBS (1.8 g, 0.01 mol) and benzoyl peroxide (0.1 g, 0.0005 mol) were added to a 50 mL sealed round bottom flask and purged with nitrogen for 30 min. Compound **3.3** (1.7 g, 0.005 mol) and ethyl acetate (17 mL) were added to a separate 50 mL sealed round bottom flask and purged with nitrogen for 10 min. The solution of compound **3.3** and

ethyl acetate was transferred via syringe to the sealed flask containing NBS and benzoyl peroxide at room temperature under nitrogen. The reaction mixture was refluxed via a heat lamp (250 W) for 24 h under a nitrogen atmosphere, cooled to room temperature, and extracted with ethyl acetate (40 mL). The organic fraction was washed with aqueous saturated NaHCO_3 (25 mL \times 3), H_2O (25 mL \times 3), dried (MgSO_4) and concentrated *in vacuo* (1.8 g, 73% crude yield). The ^1H NMR spectrum of crude compound **3.4** was consistent with the chemical structure. A small amount of the over-brominated product was also observed in the ^1H NMR spectrum.





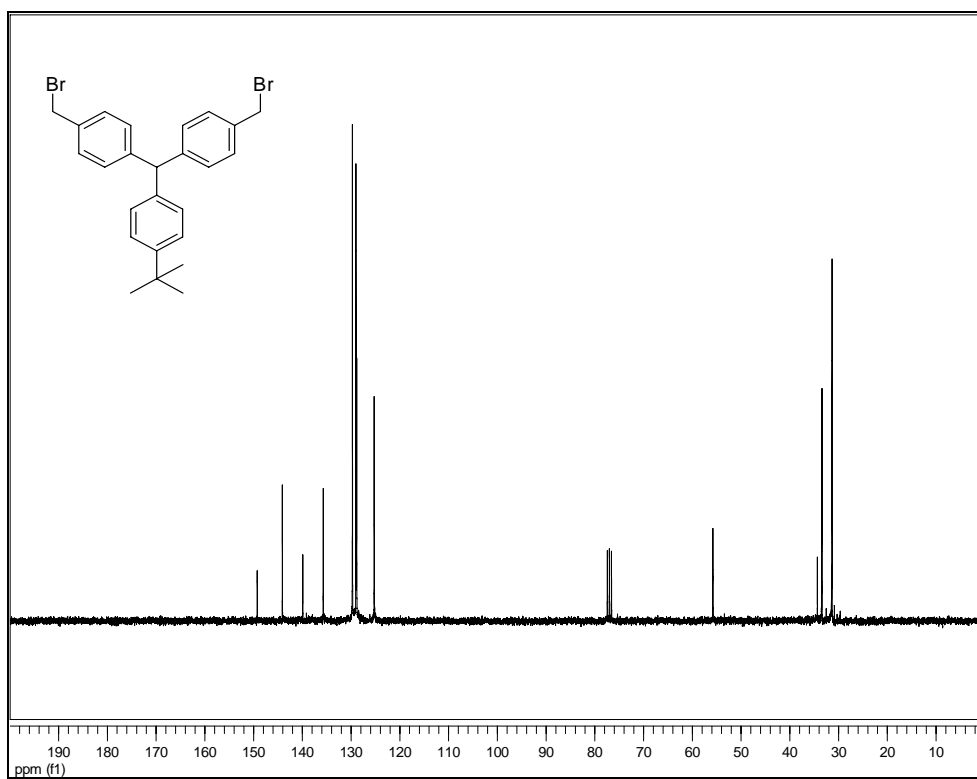
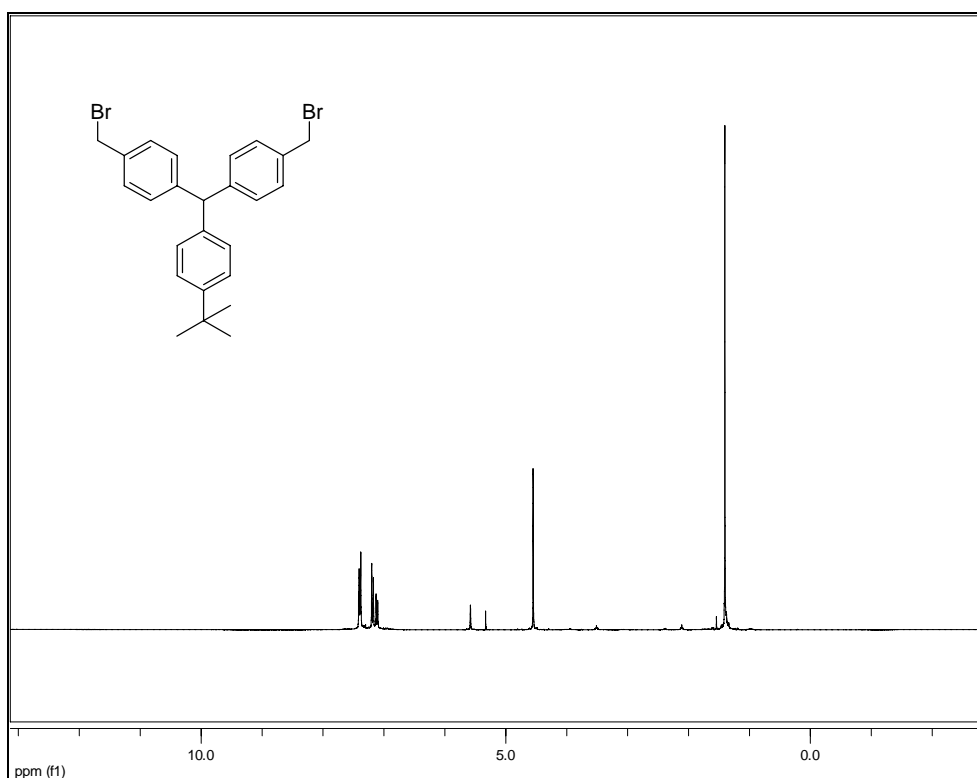
1,1'-[[4-(1,1-dimethylethyl)phenyl]methylene]bis[4-(bromomethyl)]benzene (3.5)⁴³

A mixture of compound **3.4** (2.4 g, 4.8 mmol) and trifluoroacetic acid (72 mL) was cooled to 0 °C in an ice bath under nitrogen. NaBH₄ (1.8 g, 47.8 mmol) was slowly added to the reaction mixture under nitrogen and the reaction mixture was stirred for 5 min at 0 °C. The reaction mixture was concentrated *in vacuo* and the residue was dissolved in water (50 mL) followed by the addition of NaHCO₃ (50 mL). The aqueous mixture was extracted with CH₂Cl₂ (50 mL × 3). The combined organic fractions were dried (Na₂SO₄) and concentrated *in vacuo* (1.5 g, 65% crude yield). The ¹H NMR spectrum of crude compound **3.5** was consistent with the chemical structure and that reported in the literature.⁴³

¹H NMR (CDCl₃, 300 MHz): δ ppm 7.48-7.32 (m, 6H), 7.19 (d, *J* = 8.04 Hz, 4H), 7.11 (d, *J* = 8.18 Hz, 2H), 5.58 (s, 1H), 4.55 (s, 4H), 1.40 (s, 9H)

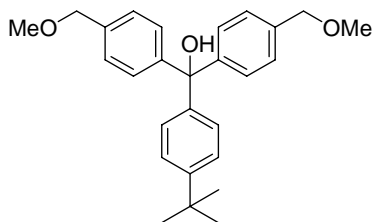
¹³C NMR (CDCl₃, 75 MHz): δ ppm 149.4, 144.3, 135.9, 129.9, 129.2, 129.0, 125.4, 55.9, 34.5, 33.6, 31.5.

MS (EI+DIP): *m/z* 484, 486, 488 (M, M+2, M+4) (M=C₂₅H₂₆Br₂ requires 484.0).



Alternative route A of synthesis of

1,1'-[[4-(1,1-dimethylethyl)phenyl]-methylene]bis-[4-(bromomethyl)]benzene (3.5)



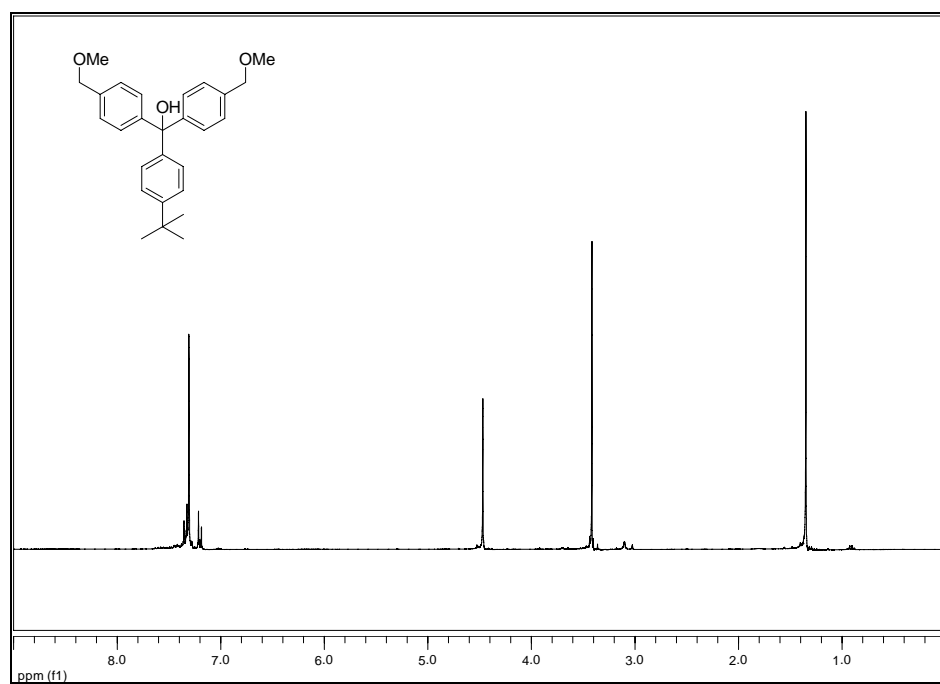
(4-tert-Butyl-phenyl)-bis-(4-methoxymethyl-phenyl)-methanol (3.6)

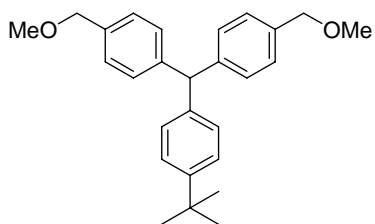
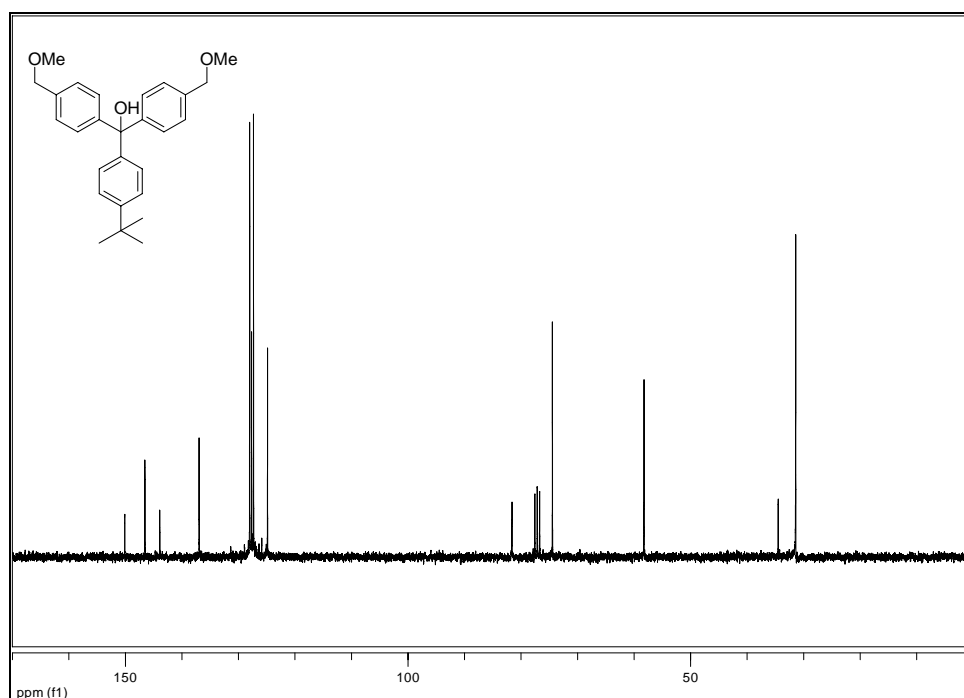
Magnesium turnings (0.822 g, 0.0338 mol) were added to a 3-neck flask equipped with a reflux condenser, addition funnel, and rubber septa. The flask was flushed with nitrogen and dry THF (10 mL) was added to the flask under nitrogen via a syringe. Approximately 5 drops of 1, 2-dibromoethane were added to the reaction flask under nitrogen via a syringe to activate the magnesium. 1-Bromo-4-methoxymethyl-benzene⁴⁴ (3.4 g, 0.0169 mol) in THF (10 mL) was added under nitrogen.

Methyl-4-tertbutylbenzoate (1.3 g, 0.00676 mol) was added to the reaction flask under nitrogen via a syringe. The reaction mixture was stirred overnight. Then the reaction mixture was quenched by saturated NH_4Cl (20 mL). The aqueous mixture was extracted with diethyl ether (30 mL \times 3). The combined organic fractions were washed with 5 wt% NaHCO_3 (30 mL \times 3), water (30 mL \times 3), dried (MgSO_4) and concentrated *in vacuo*. The crude product was purified via column chromatography [SiO_2 – petroleum ether – Ethyl ether (1:1), v/v] to give pure compound **3.6** (0.780 g, 28% yield).

¹H NMR (CDCl₃, 300 MHz) δ ppm 7.39-7.20 (m, 12H), 4.54 (s, 4H), 3.51 (s, 6H), 1.45 (s, 9H).

¹³C NMR (CDCl₃, 75 MHz): δ ppm 150.09, 146.60, 143.95, 136.91, 128.03, 127.70, 127.34, 124.85, 81.59, 74.44, 58.20, 34.49, 31.40.



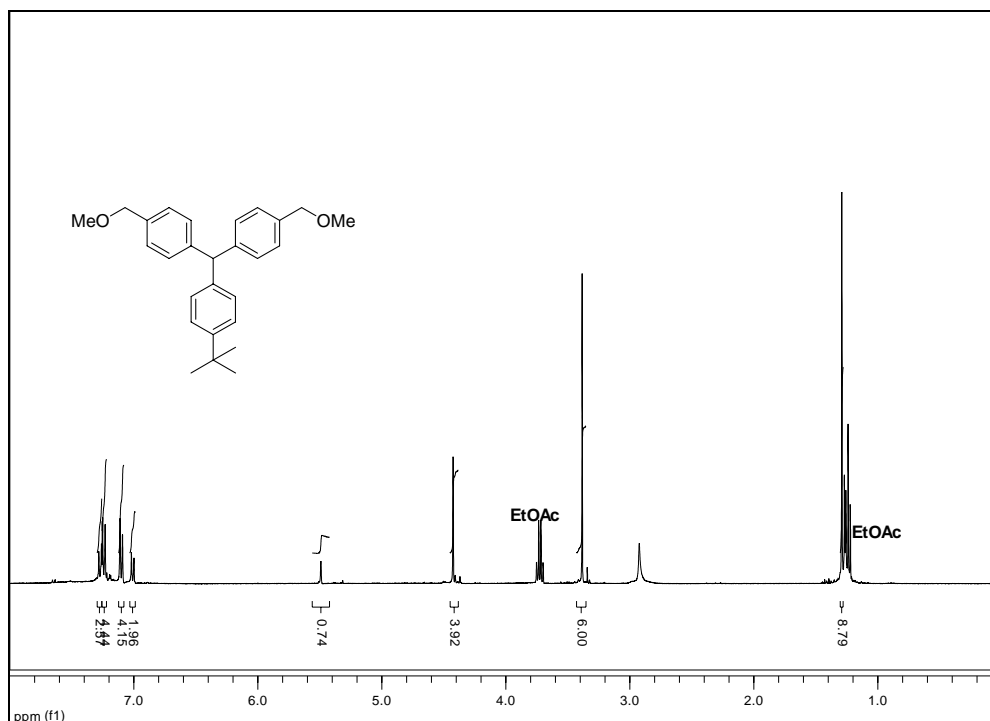


Bis-(4-methoxymethylphenyl)-(4-tert-butylphenyl)methane (3.7)³⁵

(4-tert-Butylphenyl)bis(4-methoxymethylphenyl)methanol **3.6** (0.780 g, 1.92 mmol) was dissolved in TFA (15 mL) to give a green solution at room temperature. The mixture was cooled to 0 °C and NaBH₄ (0.73 g, 19.2 mmol) was slowly added in portion under nitrogen. The reaction mixture was stirred at 0 °C for 30 min and concentrated *in vacuo*. The residue was dissolved in water and extracted with Et₂O (3 × 10 mL). The organic layer was washed with NaHCO₃ and water and dried (MgSO₄) to give **3.7** as a yellow oil

(0.710 g, 95 %).

¹H NMR (CDCl₃, 300 MHz) δ ppm 7.29-7.22 (m, 6H), 7.10 (d, J = 7.91 Hz, 4H), 7.01 (d, J = 8.56 Hz, 2H), 5.49 (s, 1H), 4.42 (s, 4H), 3.38 (s, 6H), 1.31 (s, 9H).



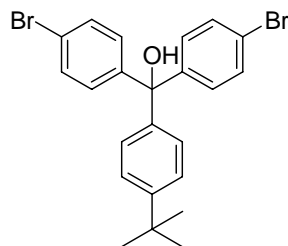
1,1'-[[4-(1,1-dimethylethyl)phenyl]-methylene]bis-[4-(bromomethyl)]benzene (3.5)

Bis-(4-methoxymethylphenyl)-(4-tert-butylphenyl)methane **3.7** (0.710 g, 1.83 mmol) was flushed with nitrogen for 30 min followed by addition of methylene chloride (15 mL). The mixture was cooled down to -78 °C and BBr₃ (0.5 mL, 5.48 mmol) was added under nitrogen via syringe. The mixture was allowed to warm to room temperature and remained overnight. The reaction was quenched by methanol (10 mL) and ice water (10 mL). The mixture was extracted with ethyl ether (10 mL \times 3) and washed with water (10

mL \times 3). The organic layer was dried with MgSO_4 and concentrated *in vacuo*. The crude product was purified via column chromatography [SiO_2 – petroleum ether – CH_2Cl_2 (1:1), v/v] to give pure compound **3.5** (0.400g, 45 %). The ^1H NMR spectrum of the pure compound was consistent with the chemical structure and that reported in the literature.⁴³

Alternative route B of synthesis of

1,1'-[[4-(1,1-dimethylethyl)phenyl]-methylene]bis-[4-(bromomethyl)]benzene (**3.5**)



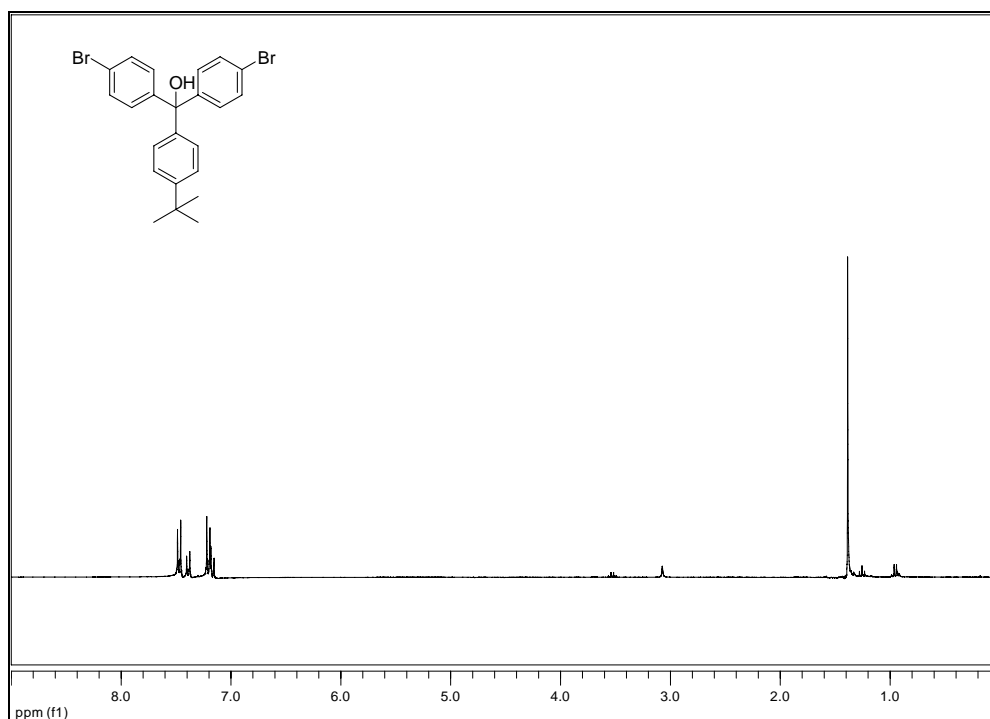
Bis-(4-bromophenyl)-(4-tert-butylphenyl)methanol (**3.9**)

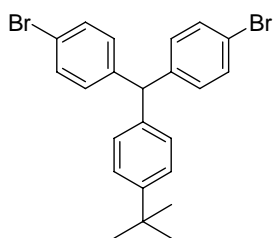
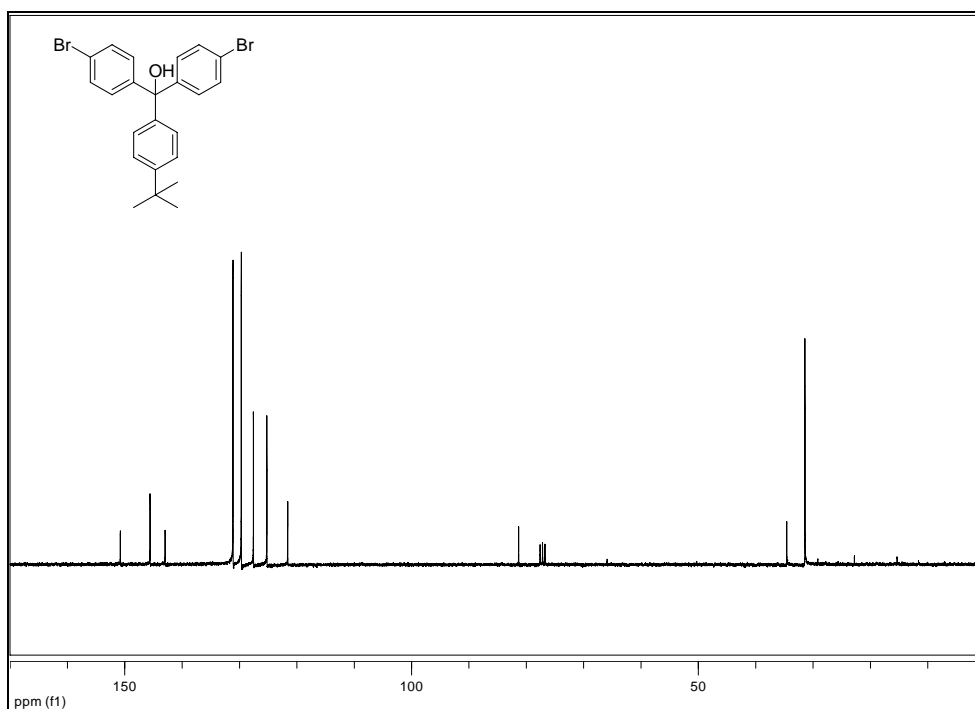
1,4-Dibromobenzene (1.85 g, 7.8 mmol) was flushed under nitrogen for 30 min and THF (10 mL) followed by $n\text{-BuLi}$ (3.0 M, 2.6 mL) was added at $-78\text{ }^\circ\text{C}$. The mixture was stirred at $-78\text{ }^\circ\text{C}$ for 30 min and 4-tert-Butyl-benzoic acid methyl ester (0.5 g, 2.6 mmol) was added via syringe. The reaction mixture was stirred at room temperature overnight. The reaction was quenched by water (10 mL) and extracted with Et_2O ($3 \times 10\text{ mL}$) and water ($3 \times 10\text{ mL}$). The organic layer was dried (MgSO_4) and concentrated *in vacuo*. The yellow crude product was purified via column chromatography to give pure compound **3.9** (1.2 g, quantitatively %).

^1H NMR (CDCl_3 , 300 MHz) δ ppm 7.47 (d, $J=8.7$ Hz, 4H), 7.39 (d, 8.7 Hz, 2H), 7.21 (d, 8.7 Hz, 4H), 7.17 (d, $J=8.7$ Hz, 2H), 1.39 (s, 9H).

^{13}C NMR (CDCl_3 , 75 MHz): δ ppm 150.78, 145.56, 142.98, 131.14, 129.69, 127.58, 125.24, 121.60, 81.33, 34.59, 31.41.

MS (ESI): m/z 495.0 ($\text{M}+\text{Na}^+$), 497.0 ($\text{M}+2+\text{Na}^+$), 499.0 ($\text{M}+4+\text{Na}^+$) ($\text{M}=\text{C}_{23}\text{H}_{22}\text{Br}_2\text{O}$ requires 472.00).





Bis-(4-bromophenyl)-(4-tert-butylphenyl)methane (3.10)³⁵

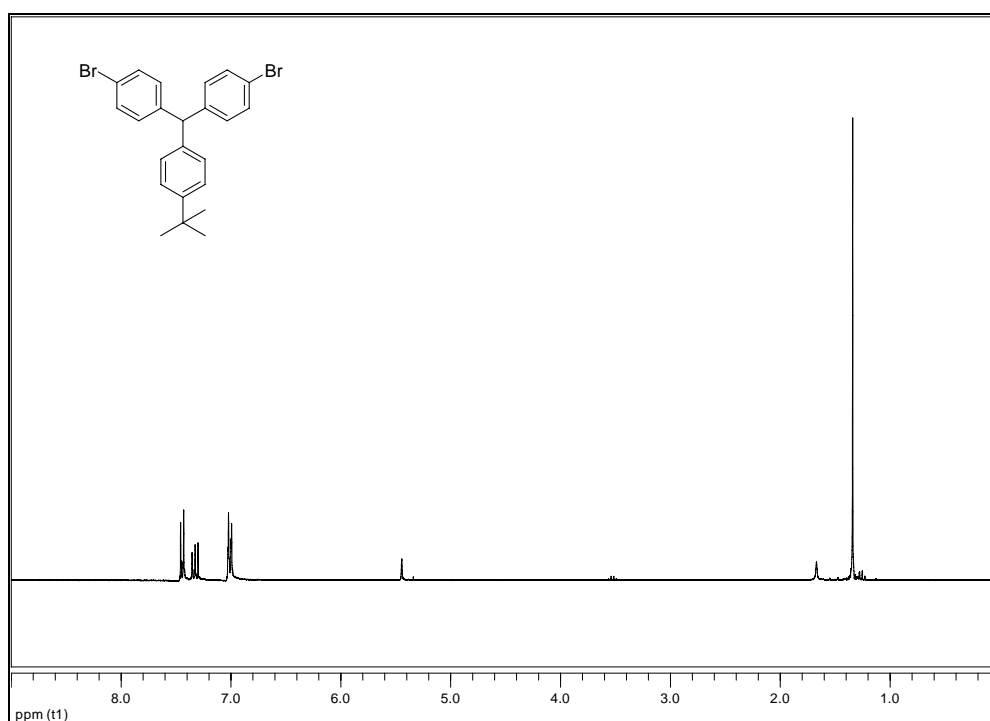
Bis-(4-bromophenyl)-(4-tert-butylphenyl)methanol **3.9** (1.2 g, 2.6 mmol) was dissolved in TFA (15 mL) to give a green solution at room temperature. The mixture was cooled to 0 °C and NaBH₄ (0.98 g, 26 mmol) was slowly added in portion under nitrogen. The reaction mixture was stirred at 0 °C for 30 min and concentrated *in vacuo*. The residue was dissolved in water and extracted with Et₂O (3×10 mL). The organic layer was washed with NaHCO₃ and water and dried (MgSO₄) to give **3.10** as a yellow oil (1.2 g,

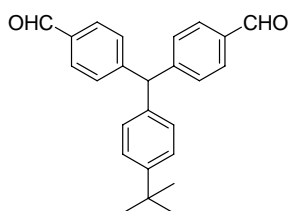
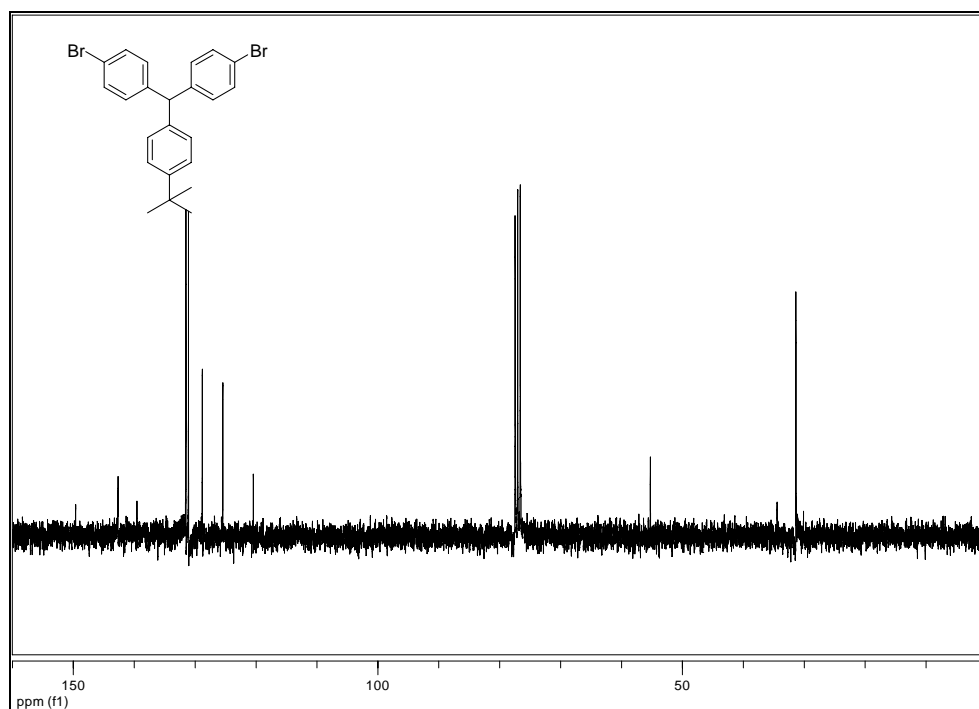
quantitatively %).

^1H NMR (CDCl_3 , 300 MHz) δ ppm 7.44 (d, $J=8.4$ Hz, 4H), 7.34 (d, $J=8.4$ Hz, 2H), 7.01 (m, 6H), 5.45 (s, 1H), 1.34 (s, 9H).

^{13}C NMR (CDCl_3 , 75 MHz): δ ppm 149.63, 142.67, 139.55, 131.51, 131.09, 128.83, 125.44, 120.45, 55.26, 34.47, 31.37.

MS (EI and DIP): m/z 456 (M), 458 (M+2), 460 (M+4) (M= $\text{C}_{23}\text{H}_{22}\text{Br}_2$ requires 456.01)





4''-tert-butyl-4,4'-(phenylmethylene)bisbenzaldehyde (3.11)

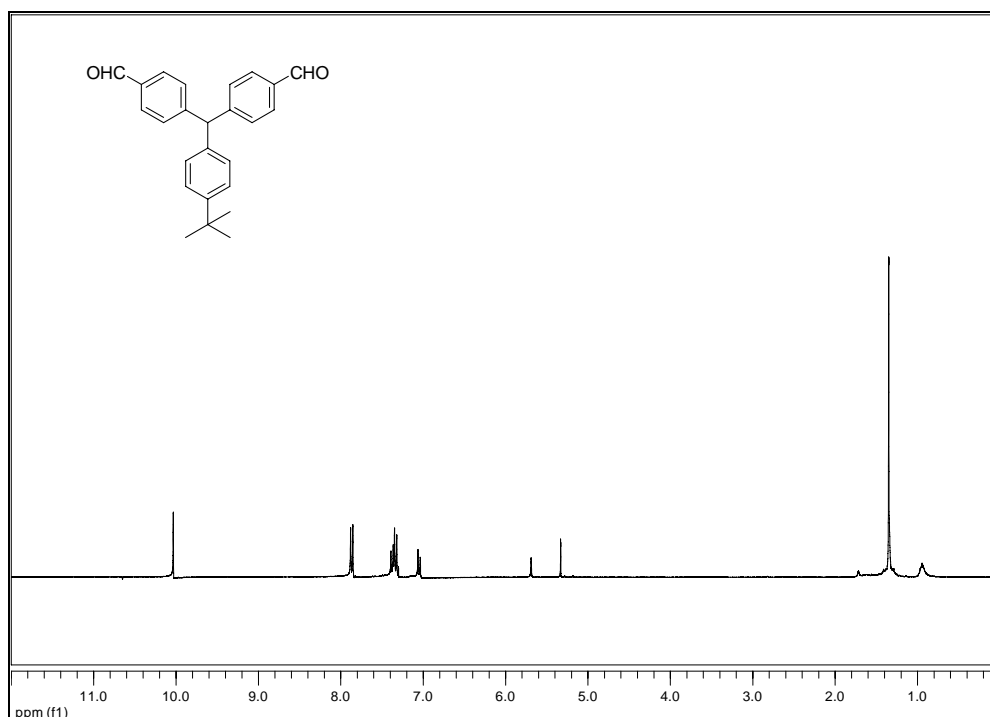
Compound **3.10** (5.0 g, 10.9 mmol) was flushed under nitrogen for 30 min and THF (25 mL) followed by n-BuLi (3.0 M, 18 mL) was added via syringe at -78 °C. The dry DMF (4.2 mL, 54.6 mmol) was added slowly to the reaction flask under nitrogen.⁴⁵ The reaction mixture was allowed to room temperature and stirred overnight. The reaction was quenched by 3N HCl (30 mL) and extracted with Et₂O (3×30 mL) and water (3×20 mL). The organic layer was dried and concentrated *in vacuo*. The crude product was purified via column chromatography [SiO₂ – petroleum ether – CH₂Cl₂ (1:1), v/v] to give

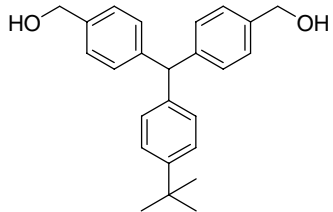
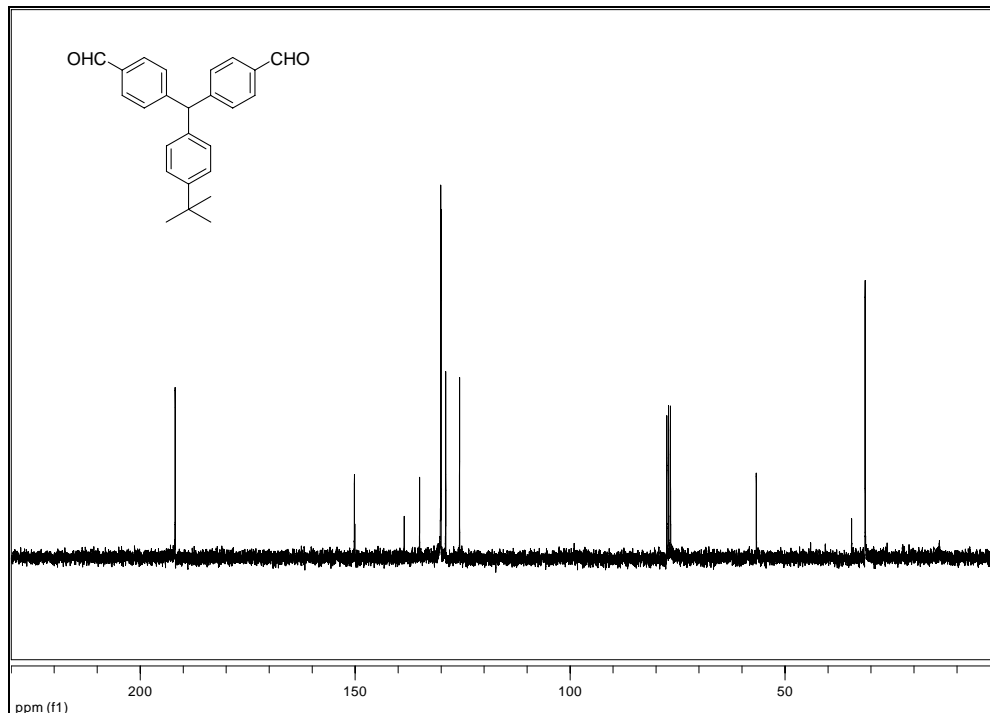
pure compound **3.11** (1.9 g, 49 % yield).

¹H NMR (CDCl₃, 300 MHz) δ ppm 10.03 (s, 2H), 7.87 (d, J=8.1 Hz, 4H), 7.38 (d, J=8.4 Hz, 2H), 7.33 (d, J=8.1 Hz, 4H), 7.05 (d, J=8.4 Hz, 2H), 5.69 (s, 1H), 1.35 (s, 9H).

¹³C NMR (CDCl₃, 75 MHz): δ ppm 191.87, 150.17, 150.09, 138.58, 135.01, 130.11, 130.01, 128.93, 125.71, 56.68, 34.52, 31.36.

MS (ESI): m/z 379.2 (M+Na⁺) (M=C₂₅H₂₄O₂ requires 356.18).





{4-[(4-tert-Butylphenyl)-(4-hydroxymethylphenyl)methyl]phenyl}methanol (3.12**)**

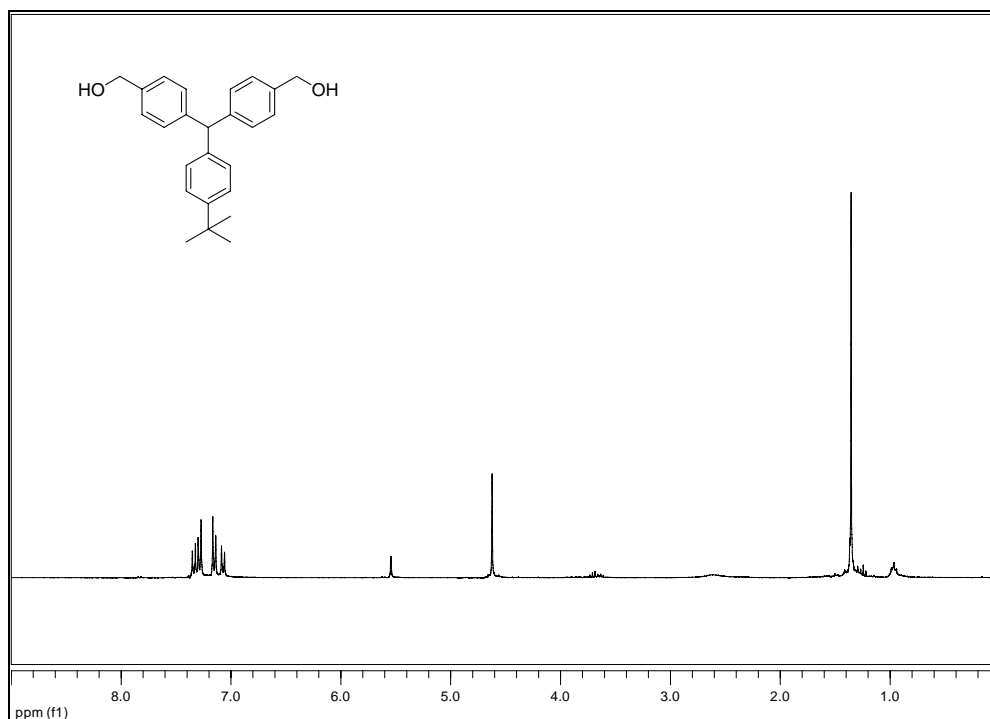
Compound **3.11** (1.9 g, 5.33 mmol) was dissolved in ethanol (40 mL). NaBH₄ (0.604 g, 16 mmol) was added at 0 °C and the reaction mixture was stirred at room temperature for 5 h. The reaction was quenched with water and extracted with Et₂O (3 × 20 mL) and water (3 × 20 mL). The organic layer was dried (MgSO₄) and concentrated *in vacuo* to give pure compound **3.12** (1.8 g, 94 % yield).

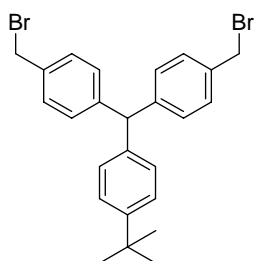
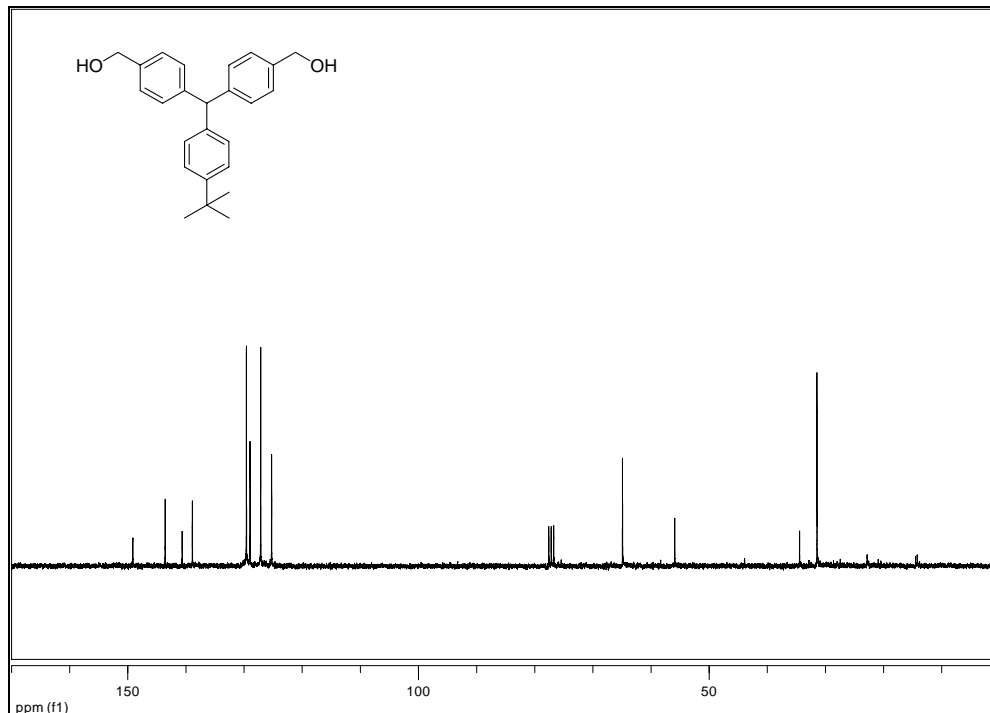
¹H NMR (CDCl₃, 300 MHz) δ ppm 7.34 (d, J=8.1 Hz, 2H), 7.29 (d, J=7.8 Hz, 4H), 7.15

(d, $J=7.8$ Hz, 4H), 7.07 (d, $J=8.1$ Hz, 2H), 5.54 (s, 1H), 4.62 (s, 4H), 1.36 (s, 9H). ^{13}C

NMR (CDCl_3 , 75 MHz): δ ppm 149.15, 143.58, 140.66, 138.90, 129.61, 128.98, 127.14, 125.27, 64.91, 55.92, 34.44, 31.46.

MS (ESI): 383.2 ($\text{M}+\text{Na}^+$) ($\text{M}=\text{C}_{25}\text{H}_{28}\text{O}_2$ requires 360.21)

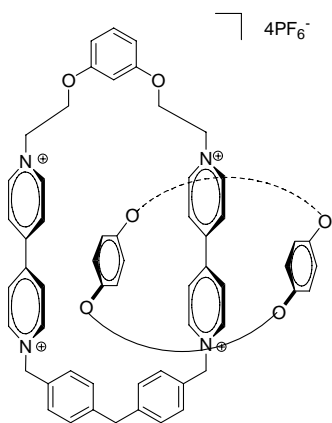




1,1'-[[4-(1,1-dimethylethyl)phenyl]methylene]bis[4-(bromomethyl)phenyl]benzene (3.5)

Triphenylphosphine (3.0 g, 11.5 mmol) was dissolved in acetonitrile (10 mL) and bromine (1.84 g, 11.5 mmol) was added dropwise at 0 °C in 30 min. The mixture was allowed to warm to room temperature and {4-[(4-tert-butylphenyl)-(4-hydroxymethylphenyl)methyl]phenyl}methanol **3.12** (1.8 g, 4.99 mmol) was added. The reaction mixture was stirred at room temperature overnight.

Acetonitrile was removed *in vacuo* and the residue was purified by flash chromatography [SiO₂ – petroleum ether – CH₂Cl₂ (1:1), v/v] to give **3.5** as a white solid (1.7 g, 70 %). The ¹H NMR spectrum of the pure compound was consistent with the chemical structure and that reported in the literature.³⁵



Catenane 3.1

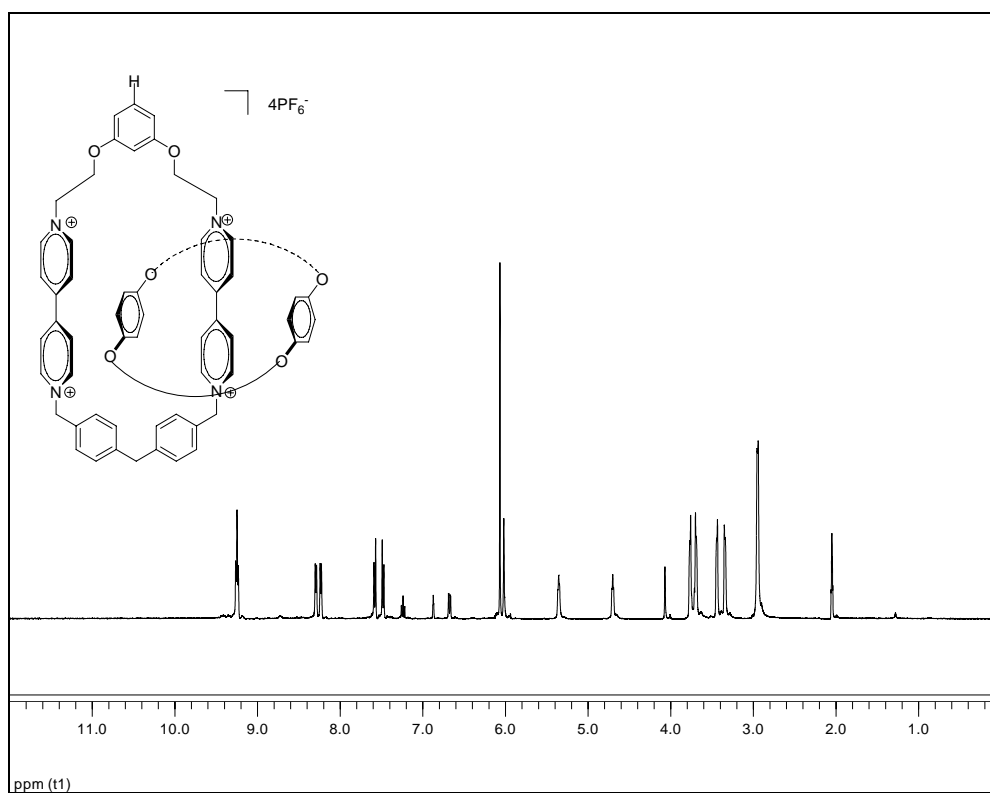
1, 3-Di(2-(4,4'-dipyridinium)ethoxy)benzene dihexafluorophosphate (**2.17a**) (0.123 g, 0.16 mmol), bis(4-bromomethylphenyl)methane (**3.1**) (0.068 g, 0.192 mmol) and BPP34C10 (0.223 g, 0.416 mmol) were combined and dissolved in CH₃CN (20 mL). The reaction vessel was sealed with a septum. This red solution stirred 4 days under ambient conditions after which time the solvent was removed *in vacuo*. The catenane was purified as described above and after removal of solvent *in vacuo*, 0.063 g (22 %) of catenane **3.1** as a red solid was obtained.

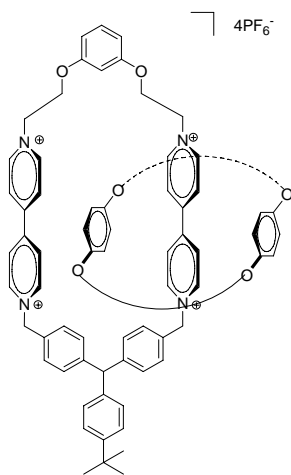
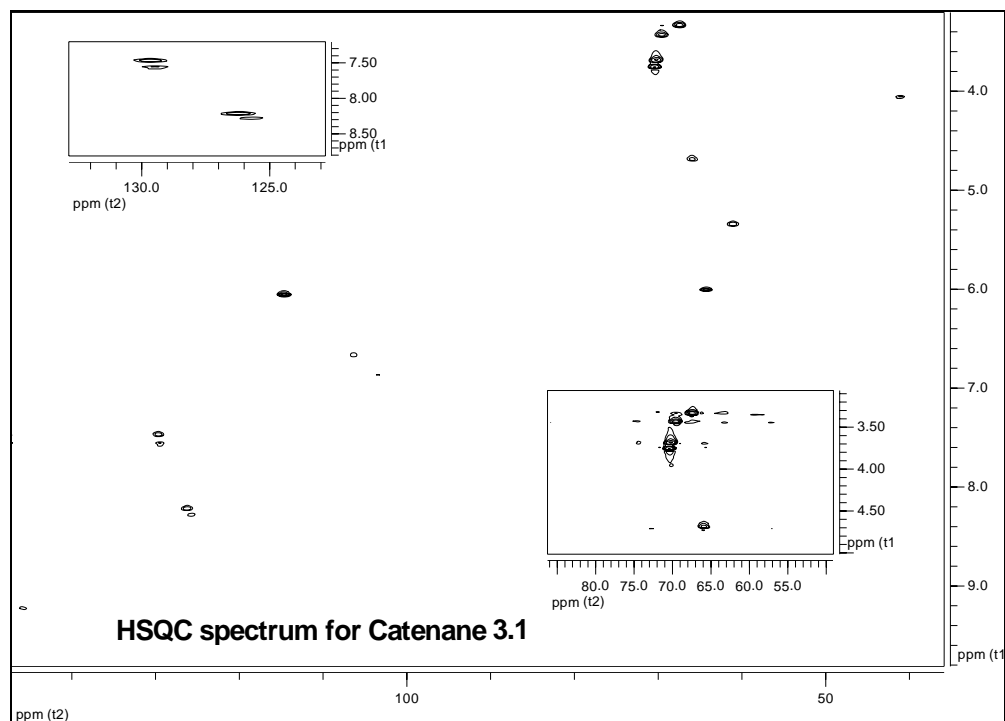
¹H NMR (C₃D₆O, 300 MHz at 20 °C): δ ppm 9.25 (m, J=6.1, 6.5 Hz, 8H), 8.29 (d, J=6.4 Hz, 4H), 8.23 (d, J=6.3 Hz, 4H), 7.58 (d, J=7.8 Hz, 4H), 7.48 (d, J=8.0 Hz, 4H), 7.24 (t,

J=8.4, 1H), 6.87 (t, J=2.1 Hz, 1H), 6.67 (dd, J=8.4, 2.1 Hz, 2H), 6.07 (s, 8H), 6.02 (s, 4H), 5.36 (t, J=4.1 Hz, 4H), 4.76 (t, J=4.1 Hz, 4H), 4.07 (s, 2H), 3.76~3.35 (m, 32H).

^{13}C NMR ($\text{C}_3\text{D}_6\text{O}$, 100 MHz): δ , ppm 145.9, 130.5, 129.9, 129.5, 126.3, 125.9, 11.8, 106.6, 103.5, 70.3, 69.9, 69.4, 67.2, 65.8, 63.9, 60.9, 40.8.

MS (ESI): m/z 450.5 ($\text{M}^{4+}\text{PF}_6^-$), 748.3 ($\text{M}^{4+} 2\text{PF}_6^-$) ($\text{M}^{4+}=\text{C}_{73}\text{H}_{82}\text{N}_4\text{O}_{12}^{4+}$ requires 1206.59)





Catenane 3.2

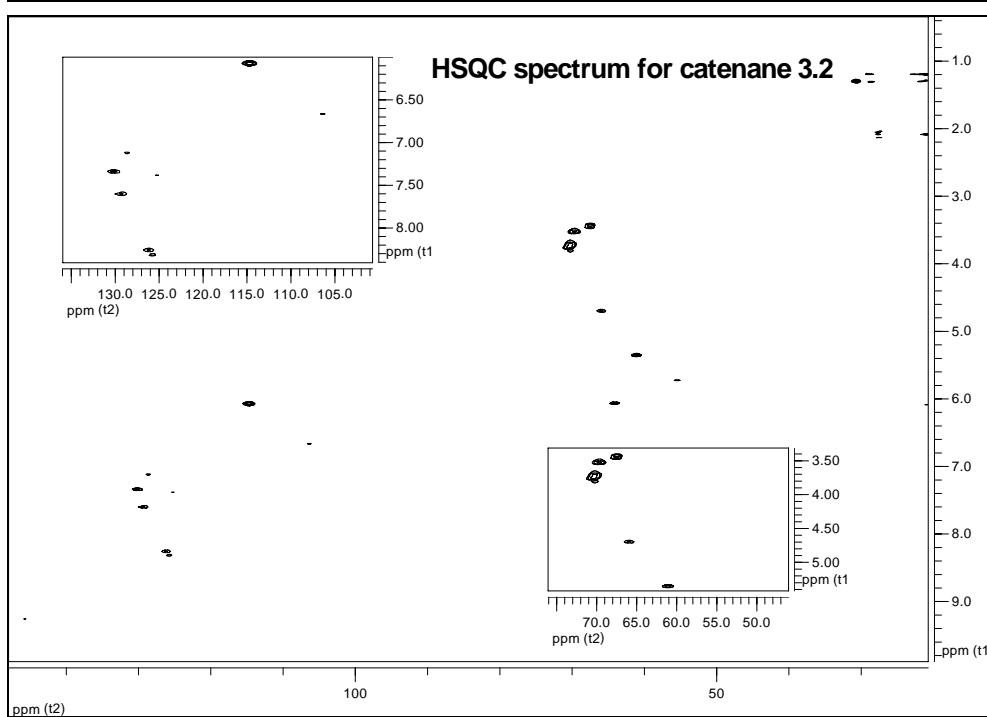
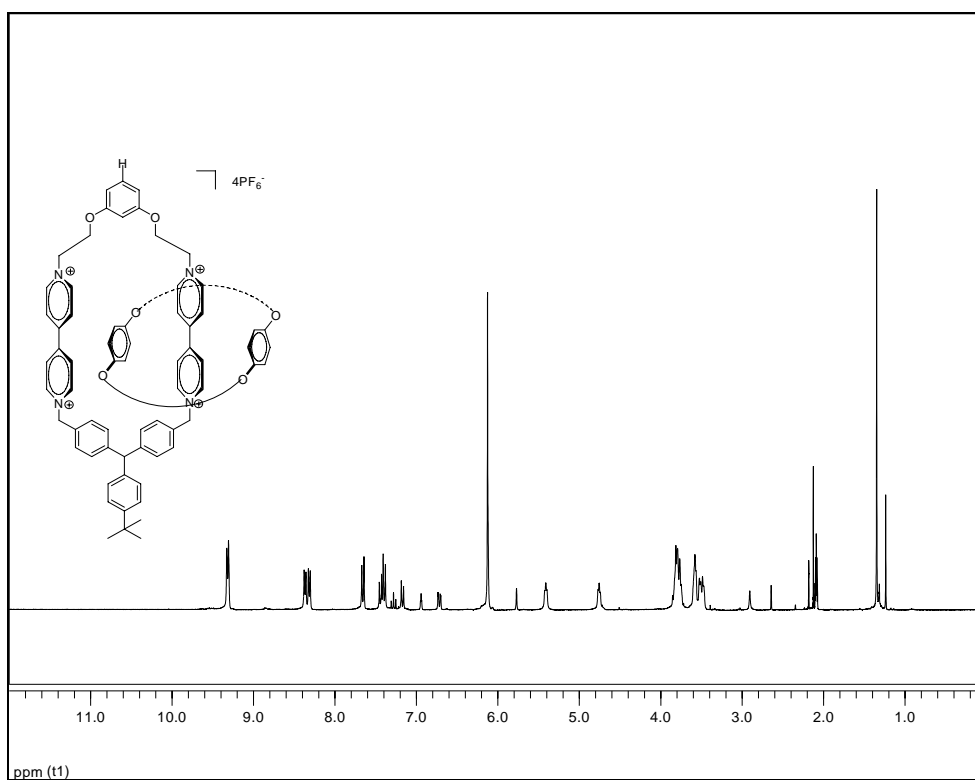
1,3-Di(2-(4,4'-dipyridinium)ethoxy)benzene dihexafluorophosphate (**2.17a**) (0.092 g, 0.120 mmol), 1,1'-[[4-(1,1-dimethylethyl)phenyl]methylene]-bis[4-(bromomethyl)benzene (**3.5**) (0.076 g, 0.156 mmol) and BPP34C10 (0.103 g, 0.192

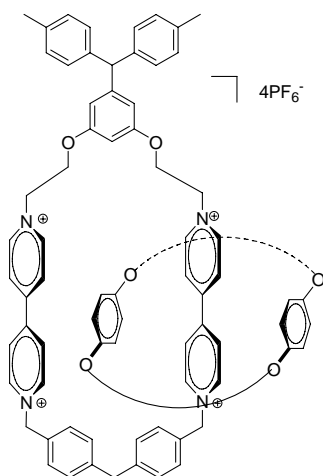
mmol) were combined and dissolved in CH₃CN (20 mL). The reaction vessel was sealed with a septum. This red solution stirred 4 days under ambient conditions after which time the solvent was removed *in vacuo*. The catenane was purified as described above and after removal of solvent *in vacuo*, 0.055 g (24 %) of catenane **3.2** as a red solid was obtained.

¹H NMR (C₃D₆O, 300 MHz at 20 °C): δ ppm 9.31 (d, J=5.9 Hz, 8H), 8.37 (d, J=6.7 Hz, 4H), 8.31 (d, J=6.7 Hz, 4H), 7.66 (d, J=8.2 Hz, 4H), 7.44 (d, J=8.5 Hz, 2H), 7.39 (d, J=8.0 Hz, 4H), 7.28 (t, J=8.5 Hz, 1H), 7.17 (d, J=8.2 Hz, 2H), 6.94 (t, J=2.3 Hz, 1H), 6.72 (dd, J=8.5, 2.3 Hz, 2H), 6.13 (s, 12H), 5.77 (s, 1H), 5.44 (t, J=3.8 Hz, 4H), 4.76 (t, J=4.1 Hz, 4H), 3.85~3.47 (m, 32H), 1.32 (s, 9H).

¹³C NMR (C₃D₆O, 100 MHz): δ ppm 145.7, 130.3, 130.2, 129.1, 128.7, 126.3, 125.7, 125.2, 114.7, 106.4, 103.4, 70.4, 70.0, 69.6, 67.4, 65.8, 64.0, 60.8, 55.35, 30.6.

MS (ESI): m/z 494.9 (M⁴⁺PF₆⁻), 814.3(M⁴⁺ 2PF₆⁻) (M⁴⁺=C₈₃H₉₄N₄O₁₂⁴⁺ requires 1338.68).





Catenane **3.3**

1,3-Bis-(2-(4,4'-dipyridinium)ethoxy)-5-(di-p-tolylmethyl)benzene

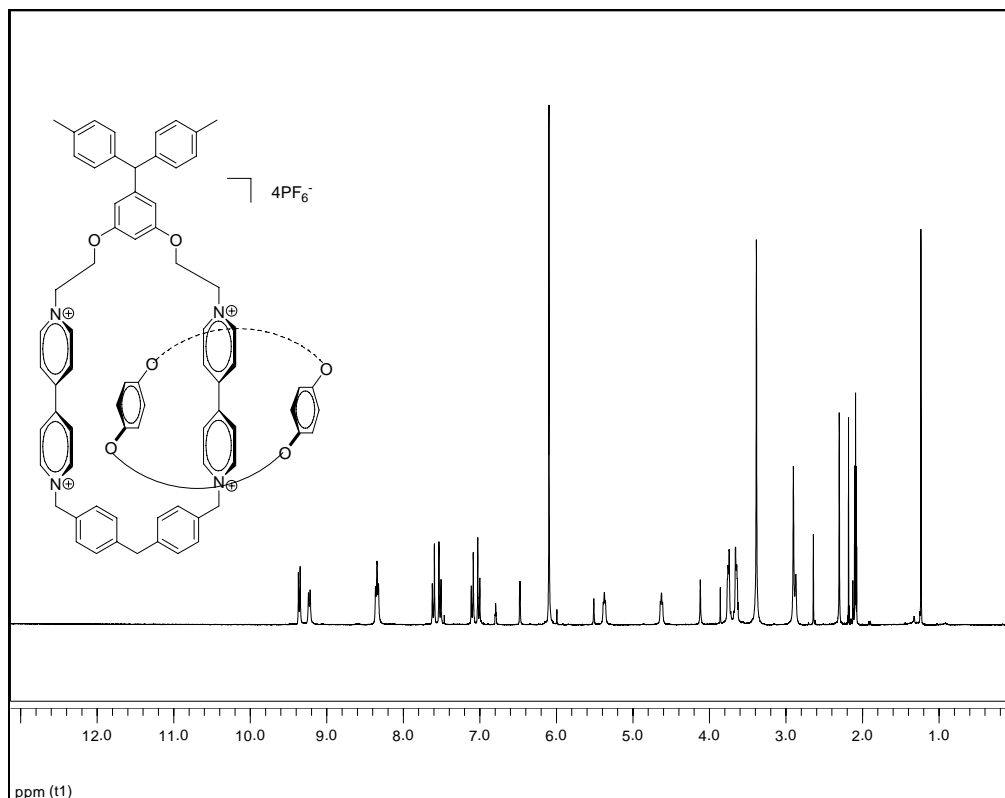
dihexafluorophosphate (**2.17b**) (0.158 g, 0.164 mmol), bis(4-bromomethylphenyl)

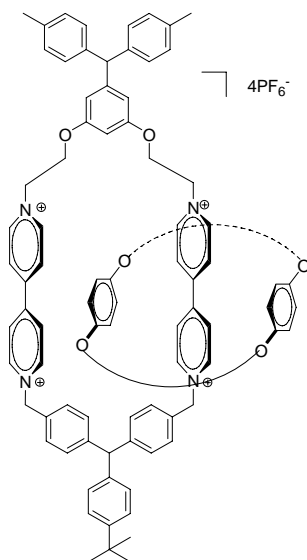
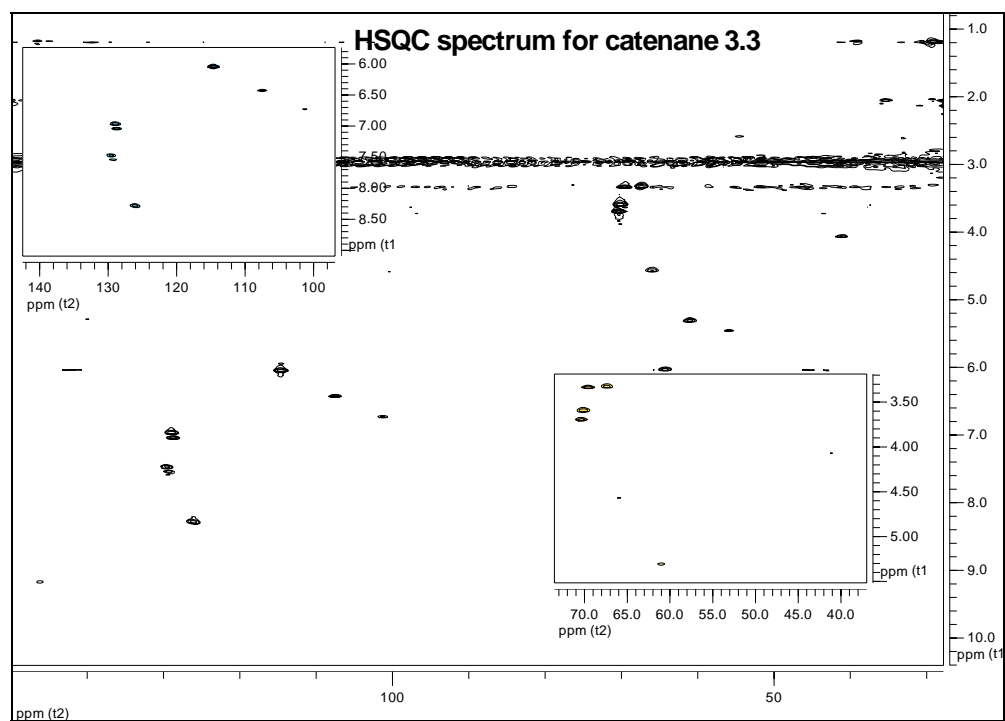
methane (**3.1**) (0.075 g, 0.213 mmol) and BPP34C10 (0.141 g, 0.263mmol) were combined and dissolved in CH₃CN (20 mL). The reaction vessel was sealed with a septum. This red solution stirred 4 days under ambient conditions after which time the solvent was removed *in vacuo*. The catenane was purified as described above and after removal of solvent *in vacuo*, 0.058 g (18 %) of catenane **3.3** as a red solid was obtained.

¹H NMR (C₃D₆O, 400 MHz at 20 °C): δ ppm 9.36 (d, J=7.0 Hz, 4H), 9.23 (d, J=6.7 Hz, 4H), 8.34 (m, J=6.5, 5.3 Hz, 8H), 7.61 (d, J=8.5 Hz, 4H), 7.52 (d, J=8.2 Hz, 4H), 7.10 (d, J=8.5 Hz, 4H), 7.01 (d, J=8.2 Hz, 4H), 6.80 (t, J=2.1 Hz, 1H), 6.47 (d, J=2.1 Hz, 2H), 6.10 (s, 12H), 5.51 (s, 1H), 5.37 (t, J=4.1 Hz, 4H), 4.61 (t, J=4.1 Hz, 4H), 4.12 (s, 2H), 3.76~3.39 (m, 32H), 2.30 (s, 6H).

^{13}C NMR ($\text{C}_3\text{D}_6\text{O}$, 100 MHz): δ ppm 146.2, 146.0, 129.5, 129.2, 128.9, 128.8, 125.9, 114.6, 107.6, 101.3, 70.3, 69.9, 69.5, 67.1, 65.8, 64.1, 61.0, 55.9, 40.9, 27.5.

MS (ESI): m/z 515.2 ($\text{M}^{4+}\text{PF}_6^-$), 845.8($\text{M}^{4+} 2\text{PF}_6^-$) ($\text{M}^{4+}=\text{C}_{88}\text{H}_{96}\text{N}_4\text{O}_{12}^{4+}$ requires 1400.70).





Catenane 3.4

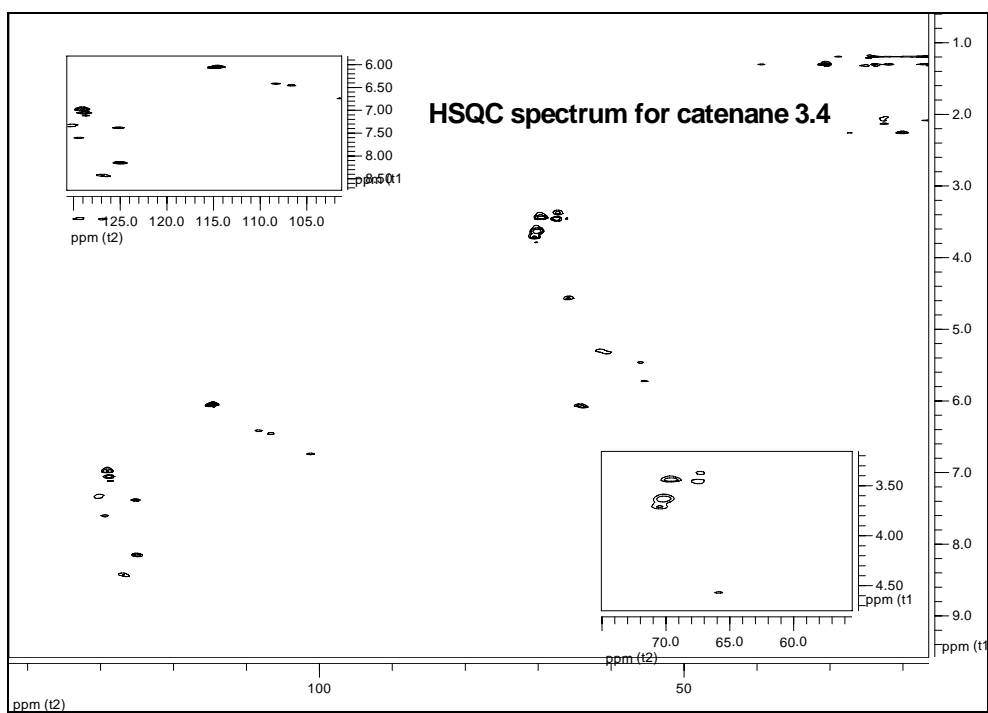
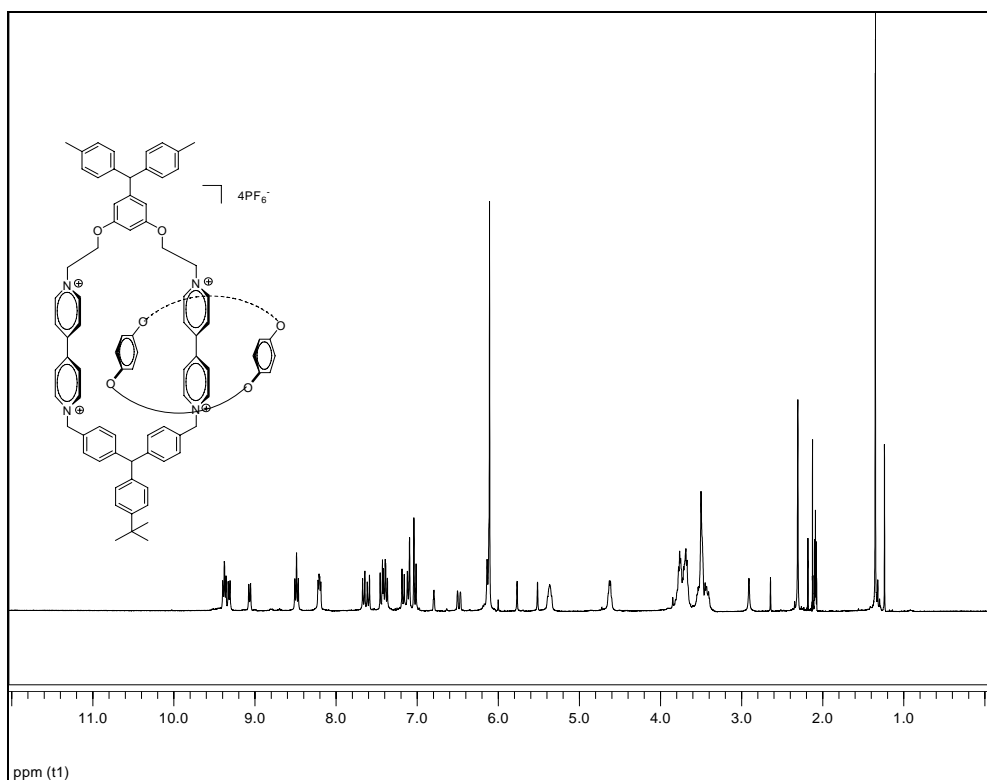
1,3-Bis-(2-(4,4'-dipyridinium)ethoxy)-5-(di-p-tolylmethyl)benzene

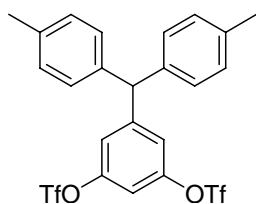
dihexafluorophosphate (**2.17b**) (0.140 g, 0.146 mmol), 1,1'-[[4-(1,1-dimethylethyl)phenyl]methylene]bis[4-(bromomethyl)benzene (**3.5**) (0.092 g, 0.190 mmol) and BPP34C10 (0.125 g, 0.233 mmol) were combined and dissolved in CH₃CN (20 mL). The reaction vessel was sealed with a septum. This red solution stirred 4 days under ambient conditions after which time the solvent was removed *in vacuo*. The catenane was purified as described above and after removal of solvent *in vacuo*, 0.057 g (19 %) of catenane **3.4** as a red solid was obtained.

¹H NMR (C₃D₆O, 400 MHz at 20 °C): δ ppm 9.38 (m, J=6.7, 5.6 Hz, 4H), 9.32 (d, J=7.0 Hz, 2H), 9.07 (d, J=6.7 Hz, 2H), 8.49 (m, J=6.8, 6.5 Hz, 4H), 8.21 (dd, J=6.7, 2.1 Hz, 4H), 7.66 (d, J=8.2 Hz, 2H), 7.60 (d, J=8.2 Hz, 2H), 7.44 (d, J=8.5 Hz, 2H), 7.40 (d, J=7.9 Hz, 2H), 7.38 (d, J=8.2 Hz, 2H), 7.17 (d, J=8.2 Hz, 2H), 7.11 (d, J=7.9 Hz, 4H), 7.03 (d, J=8.2 Hz, 4H), 6.79 (t, J=2.1 Hz, 1H), 6.48 (dd, J=10.9, 2.1 Hz, 2H), 6.14~6.10 (m, 12H), 5.77 (s, 1H), 5.52 (s, 1H), 5.36 (m, 4H), 4.62 (m, 4H), 3.79~3.41 (m, 32H), 2.31 (s, 6H), 1.35 (s, 9H).

¹³C NMR (C₃D₆O, 100 MHz): δ ppm 146.3, 146.2, 145.6, 130.4, 130.0, 129.3, 129.0, 128.9, 128.7, 126.7, 125.3, 125.0, 114.7, 108.3, 106.6, 101.2, 70.3, 70.0, 69.5, 67.3, 67.2, 68.9, 64.3, 63.8, 61.5, 60.4, 55.9, 55.4, 30.7, 20.0.

MS (ESI): m/z 911.9(M⁴⁺ 2PF₆⁻) (M⁴⁺=C₉₈H₁₀₈N₄O₁₂⁴⁺ requires 1532.79).





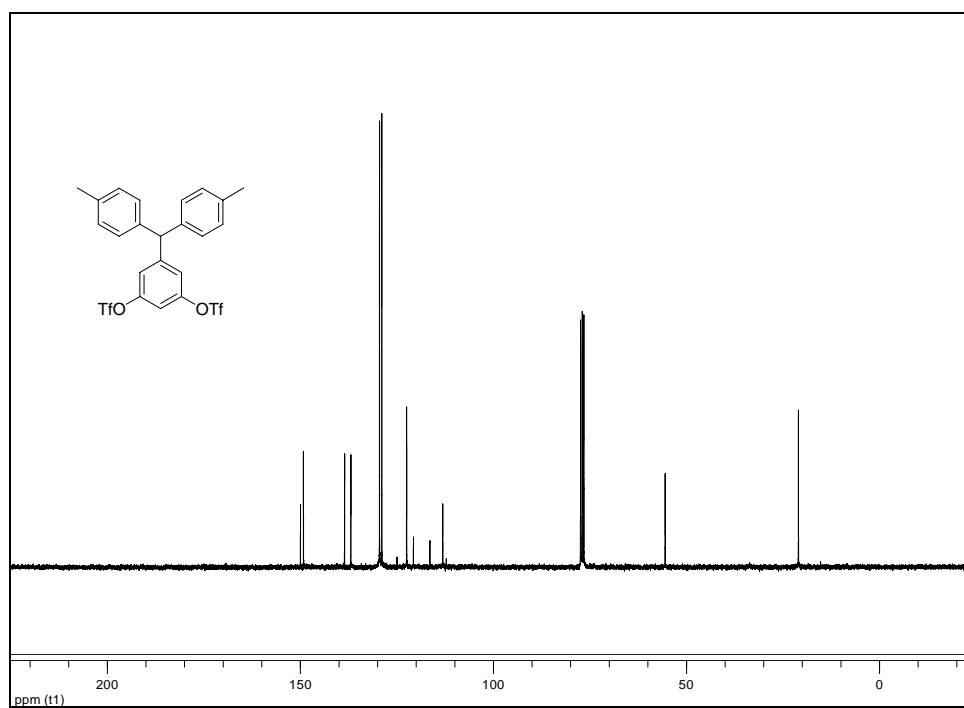
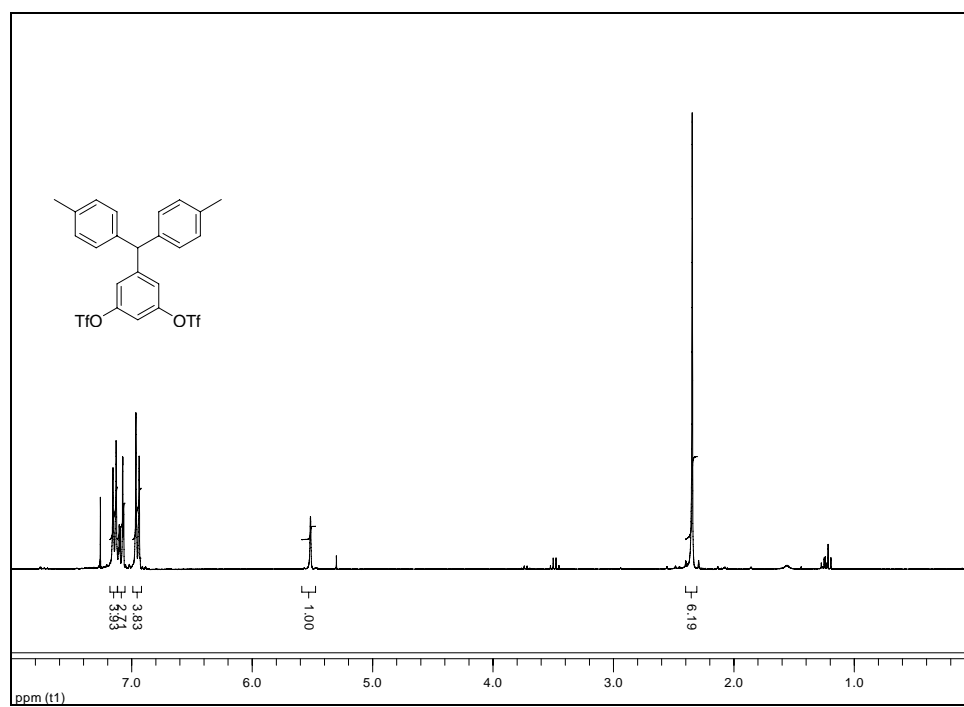
Trifluoromethanesulfonic acid 3-di-p-tolylmethyl-5-trifluoromethanesulfonyloxy-phenyl ester (4.1)

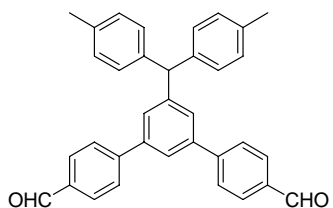
5-Di-p-tolylmethylbenzene-1,3-diol (1.0 g, 3.3 mmol) and 4-(N,N'-dimethylamino)pyridine (DMAP) (0.161 g, 1.32 mmol) were flushed with nitrogen for 30 min followed by addition of dry methylene chloride (13 mL) and 2,6-lutidine (0.96 mL, 8.25 mmol).⁴⁸ The mixture was cooled down to -20 °C and Tf₂O (1.4 mL, 8.25 mmol) was added under nitrogen via syringe. The reaction mixture was stirred at 0 °C for 1 h and was allowed to warm to room temperature overnight. The reaction was quenched with water (20 mL) and extracted with ethyl ether (20 mL × 3). The organic layer was washed sequentially with 1 M HCl (20 mL × 3), water (20 mL × 3) and brines (20 mL × 3). The organic layer was dried with MgSO₄ and concentrated *in vacuo* to give the product **4.1** (1.6 g, 85 %).

¹H NMR (CDCl₃, 300 MHz): δ ppm 7.16 (d, *J* = 7.76 Hz, 4H), 7.12-7.05 (m, 3H), 6.96 (d, *J* = 7.89 Hz, 4H), 5.52 (s, 1H), 2.34 (s, 6H).

¹³C NMR (CDCl₃, 75 MHz): δ ppm 149.98, 149.20, 138.54, 136.92, 129.52, 128.91, 124.91, 122.48, 120.71, 116.46, 113.12, 112.21, 55.51, 21.00.

MS (ESI): *m/z* = 591.8 (M+Na⁺) (M = C₂₃H₁₈F₆O₆S₂ requires 568.04).





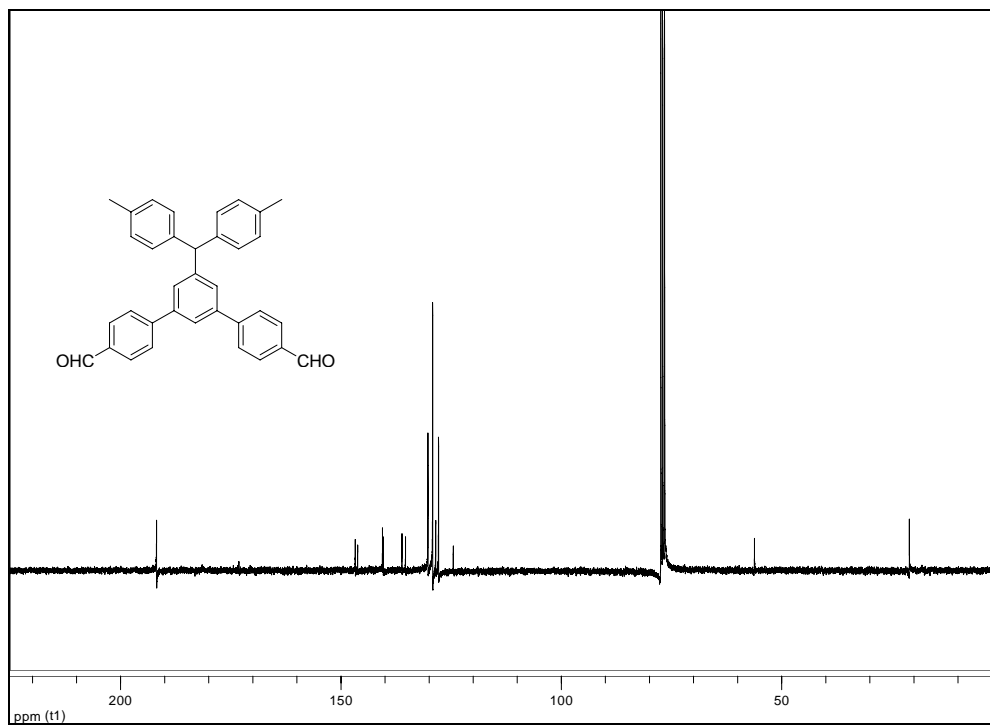
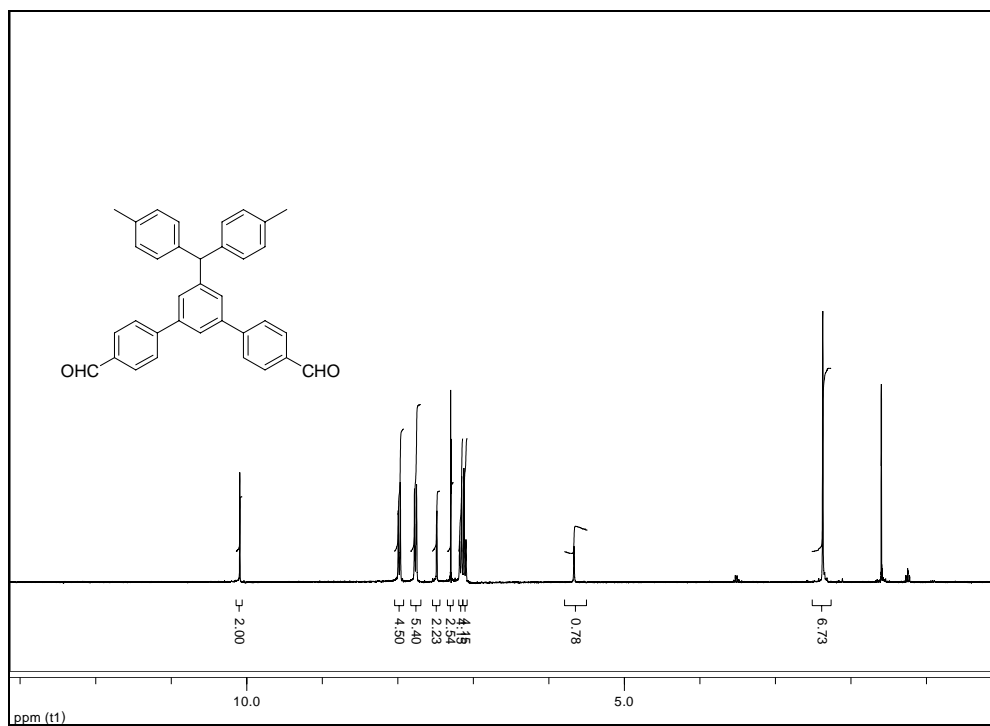
Compound 4.2

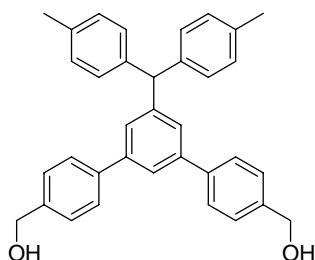
4-Formylbenzeneboronic acid⁵⁰ (1.01 g, 6.75 mmol), and CsCO₃ (4.6 g, 14.05 mmol) were added to a three-neck round bottom flask with a reflux condenser, rubber septa and flushed with nitrogen for 30 min. In a nitrogen glovebox, Pd₂(dba)₃ (0.077 g, 0.0843 mmol), PPh₃ (0.088 g, 0.337 mmol) was added to the flask.⁴⁹ Taking the flask out, trifluoromethanesulfonic acid 3-di-p-tolylmethyl-5-trifluoromethanesulfonyloxyphenyl ester (**4.1**) (1.6 g, 2.81 mmol) in THF (25 mL) were added under nitrogen via syringe. The temperature was raised to 60 °C and the mixture remained at this temperature for 36 h. The reaction was cooled down to room temperature and quenched with water (20 mL) and extracted with ethyl ether (30 mL × 3). The organic layer was washed with water (30 mL × 3) and dried with MgSO₄ and concentrated *in vacuo* to give the compound 4.2 (1.2 g, 89 %).

¹H NMR (CDCl₃, 300 MHz): δ ppm 10.09 (s, 2H), 7.98 (d, *J* = 8.09 Hz, 4H), 7.77 (d, *J* = 8.09 Hz, 4H), 7.48 (t, *J* = 1.58 Hz, 1H), 7.30 (d, *J* = 1.58 Hz, 2H), 7.17 (d, *J* = 8.07 Hz, 4H), 7.11 (d, *J* = 8.07 Hz, 4H), 5.67 (s, 1H), 2.36 (s, 6H)

¹³C NMR (CDCl₃, 75 MHz): δ ppm 191.84, 146.74, 146.21, 140.56, 140.41, 136.15, 135.35, 130.25, 129.19, 128.50, 127.85, 124.50, 56.17, 21.03.

MS (ESI): $m/z=503.3$ ($M+Na^+$) ($M= C_{35}H_{28}O_2$ requires 480.21)



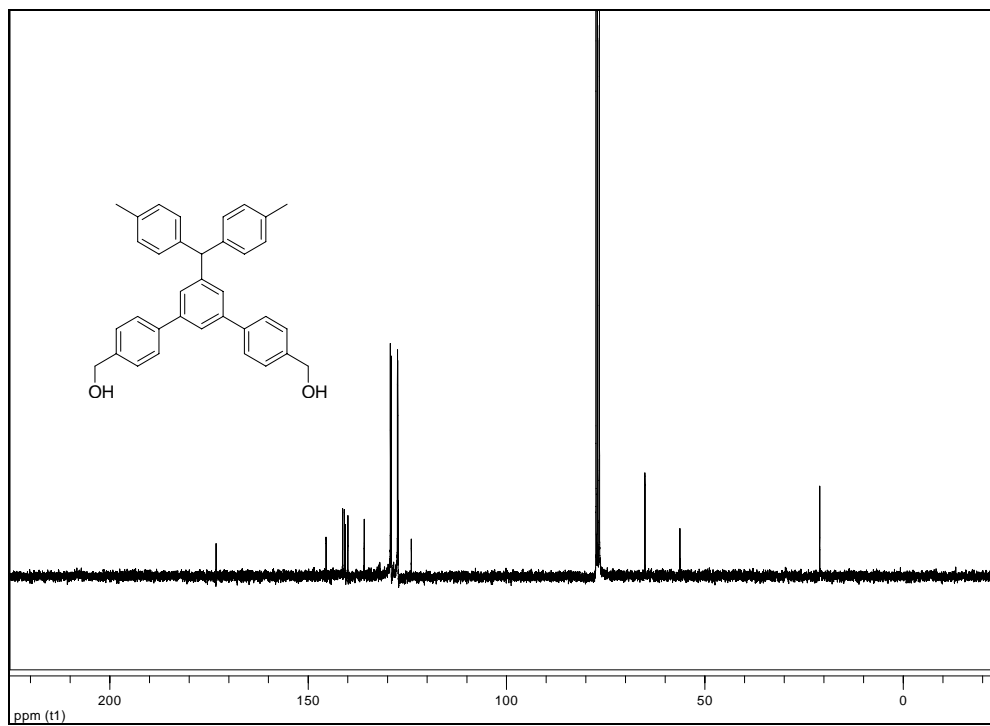
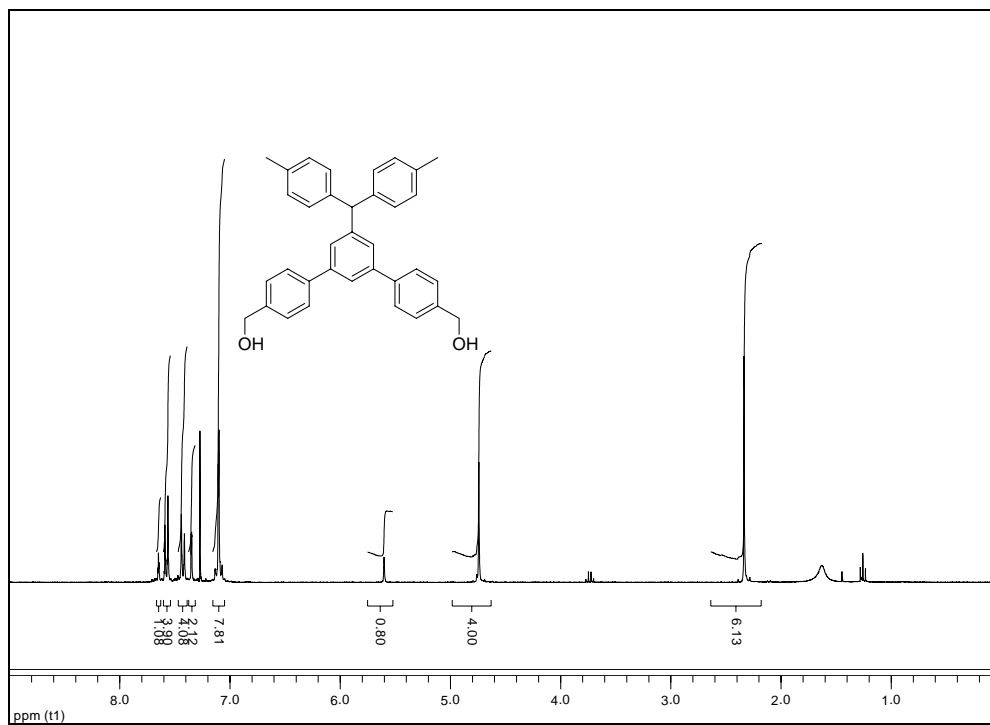


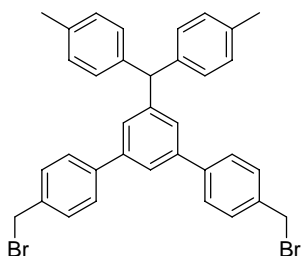
(5'-Di-p-tolylmethyl-4''-hydroxymethyl-[1,1';3',1'']terphenyl-4-yl)methanol (4.3)

Compound **4.2** (0.33 g, 0.69 mmol) was dissolved in ethanol (5 mL) followed by addition of sodium borohydride (0.078 g, 2.07 mmol) at 0 °C. The reaction mixture was stirred at room temperature for 2 h. The reaction was quenched with water (30 mL) and the mixture was extracted with ethyl ether (20 mL \times 3). The organic layer was washed with water (20 mL \times 3) and dried with MgSO₄ and concentrated *in vacuo* to give the product **4.3** (0.290 g, 87 %).

¹H NMR (CDCl₃, 300 MHz): δ ppm 7.65 (t, J = 1.66 Hz, 1H), 7.58 (d, J = 8.44 Hz, 4H), 7.43 (d, J = 8.44 Hz, 4H), 7.35 (d, J = 1.66 Hz, 2H), 7.15-7.05 (m, 8H), 5.60 (s, 1H), 4.75 (s, 3H), 2.34 (s, 6H).

¹³C NMR (CDCl₃, 75 MHz): δ ppm 145.48, 141.30, 140.87, 140.60, 139.97, 135.87, 129.27, 129.08, 127.48, 127.42, 127.33, 123.99, 65.10, 56.28, 21.04.



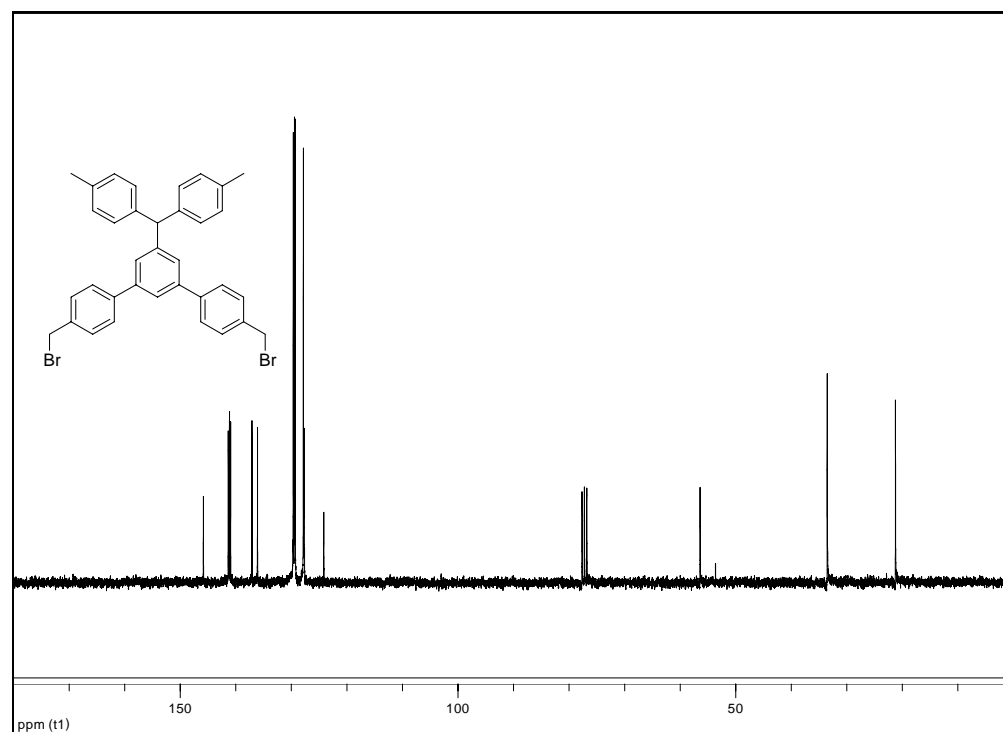
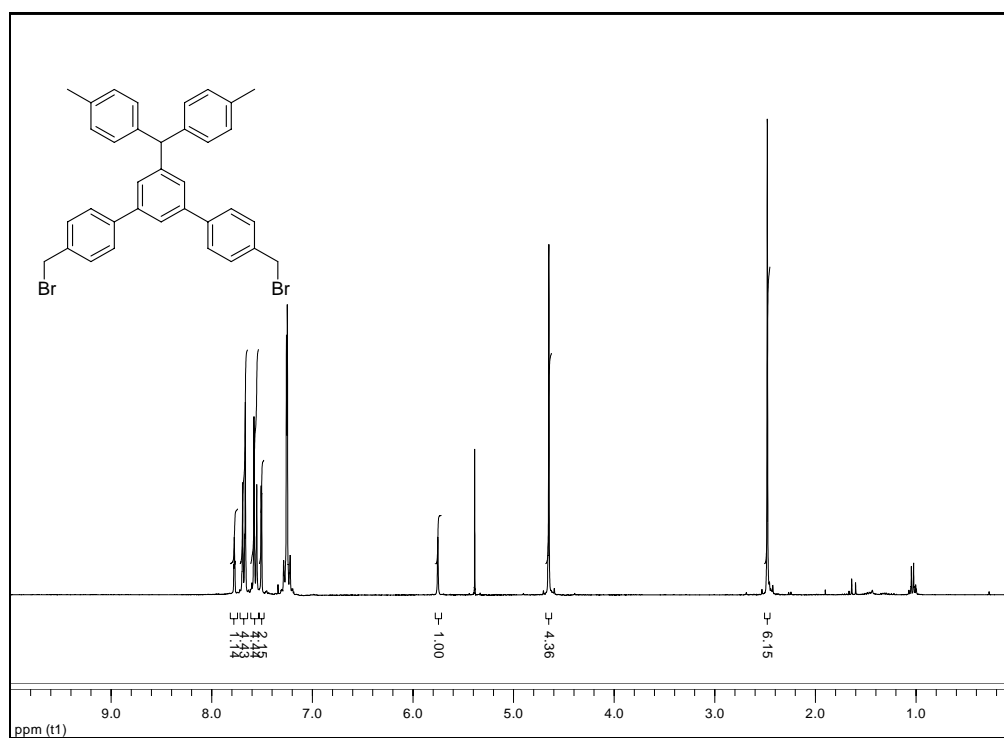


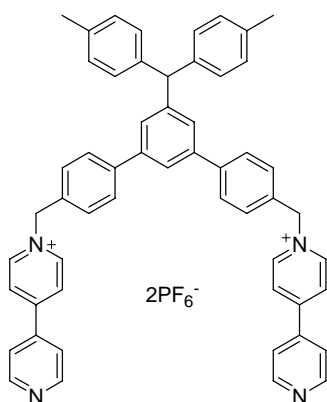
Compound 4.4

Triphenylphosphine (0.362 g, 1.38 mmol) was dissolved in acetonitrile (1.5 mL) and bromine (0.220 g, 1.38 mmol) was added dropwise at 0 °C over 30 min. The mixture was allowed to warm to room temperature and (5'-di-p-tolylmethyl-4''-hydroxymethyl-[1,1';3',1'']terphenyl-4-yl)methanol (**4.3**) (0.290 g, 0.60 mmol) was added. The reaction mixture was stirred at room temperature overnight. Acetonitrile was removed *in vacuo* and the residue was purified by flash chromatography [SiO₂ – petroleum ether – CH₂Cl₂ (1:1), v/v] to give a yellow solid (0.270 g, 74 %).

¹H NMR (CDCl₃, 300 MHz): δ ppm 7.77 (t, *J* = 1.63 Hz, 1H), 7.69 (m, m 4H), 7.57 (m, 4H), 7.51 (d, *J* = 1.63 Hz, 1H), 7.28-7.22 (m, 8H) 5.75 (s, 1H), 4.65 (s, 4H), 2.47 (s, 6H).

¹³C NMR (CDCl₃, 75 MHz): δ ppm 145.82, 141.34, 141.13, 140.92, 137.07, 136.08, 129.63, 129.42, 129.29, 127.82, 127.68, 124.16, 56.40, 33.48, 21.23.





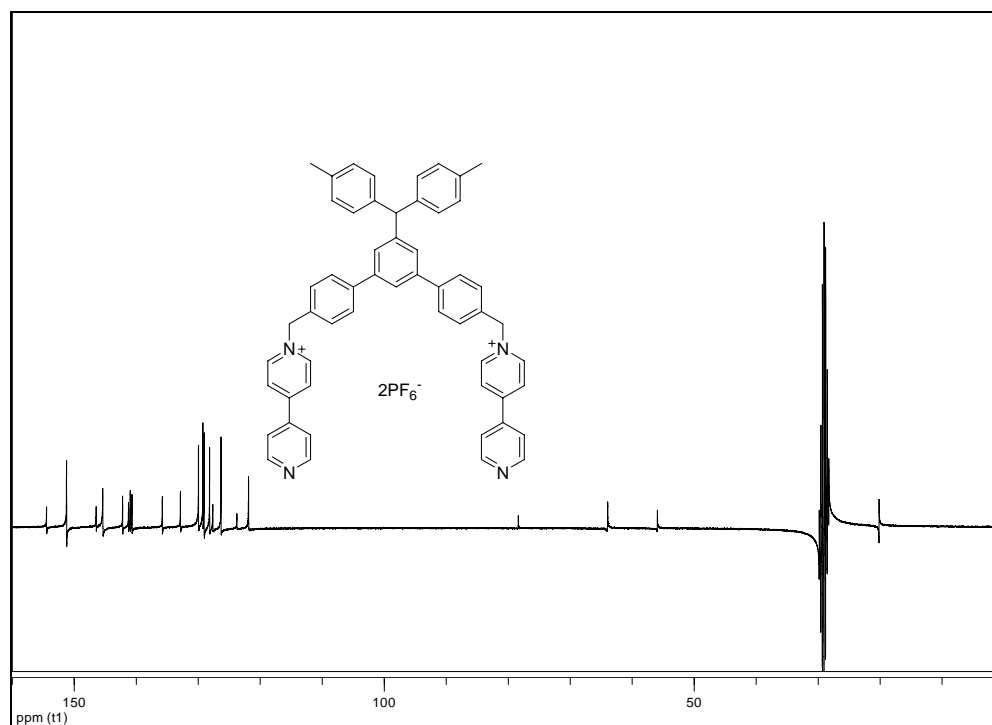
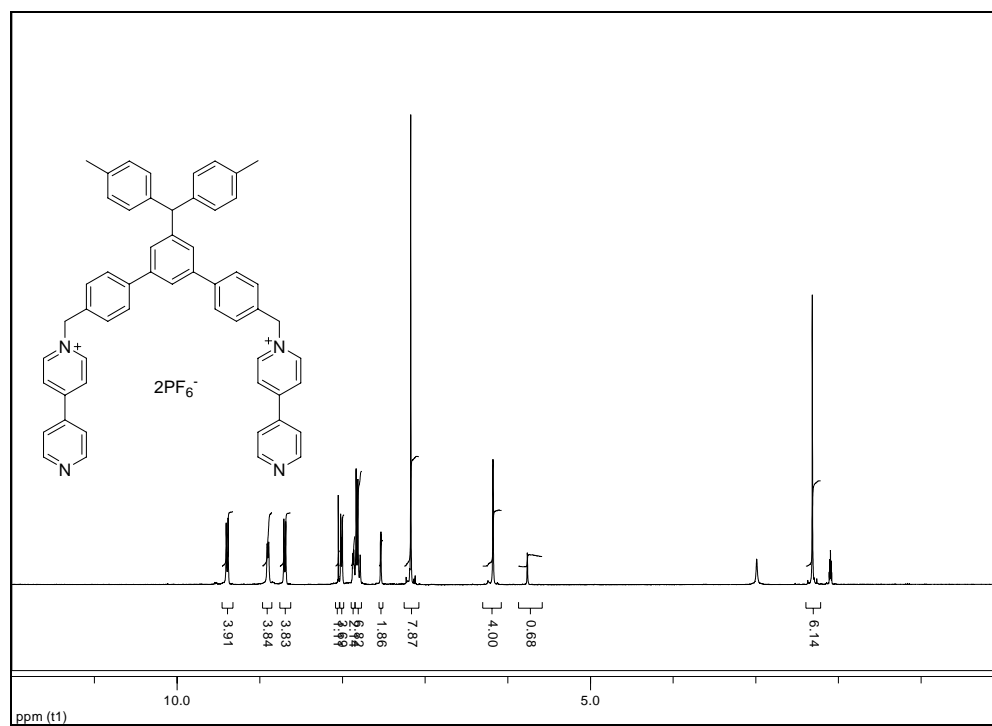
Compound 4.5

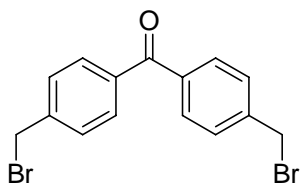
A mixture of compound **4.4** (0.270 g, 0.44 mmol) and 4,4'-dipyridyl (0.55 g, 3.5 mmol) was stirred at 65 ° C for 2 days. The mixture was allowed to cool and concentrate *in vacuo*. The residue was dissolved in hot water and ammonium hexafluorophosphate (0.143 g, 0.88 mmol) were added to the aqueous solution. A yellow oil precipitated to the bottom of the flask and the aqueous layer was decanted. The oil was washed with chloroform (6 × 10 mL) to give a yellow solid (0.270 g, 58%).

¹H NMR (C₃D₆O, 300 MHz): δ ppm 9.39 (d, *J* = 6.95 Hz, 4H), 8.90 (d, *J* = 5.80 Hz, 4H), 8.70 (d, *J* = 6.95 Hz, 4H), 8.01 (dd, *J* = 4.51, 1.66 Hz, 4H), 7.89-7.85 (m, 1H), 7.85-7.77 (m, 8H), 7.54 (d, *J* = 1.54 Hz, 2H), 7.25-7.07 (m, 8H), 6.18 (s, 4H), 5.76 (s, 1H), 2.32 (s, 6H).

¹³C NMR (C₃D₆O, 75 MHz): δ ppm 155.35, 152.12, 147.34, 146.27, 143.08, 142.13, 141.84, 141.56, 136.67, 133.74, 130.83, 130.13, 129.93, 129.04, 128.52, 127.19, 124.64, 122.76, 79.24, 64.83, 56.81, 21.04.

MS (ESI): $m/z=381.3$ (M^{2+}) ($M^{2+}=C_{55}H_{46}N_4^{2+}$ requires 762.37)





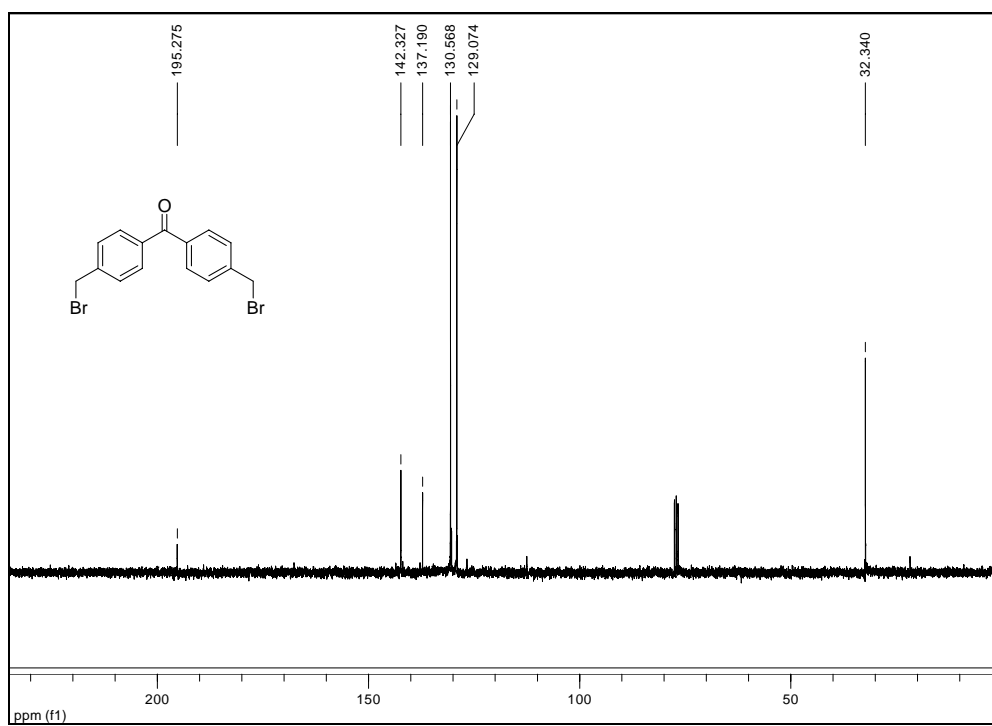
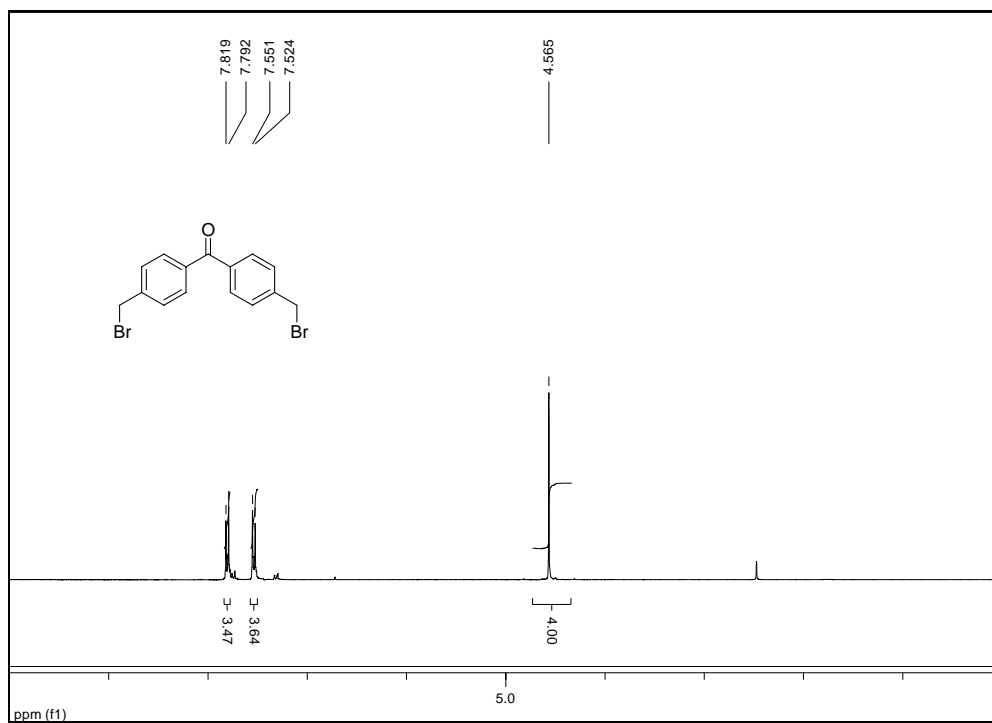
Bis-(4-bromomethylphenyl)methanone (4.7)^{51b}

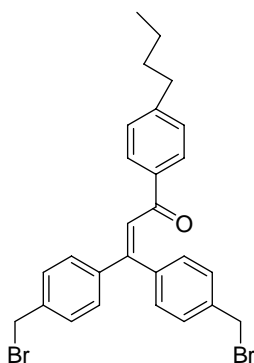
NBS (3.5 g, 200 mmol) and benzoyl peroxide (0.2300 g, 9.5 mmol) were added to a 50 mL round bottom flask and the flask was flushed with nitrogen for 30 minutes. 4,4'-Dimethylbenzophenone (2.0 g, 95.1 mmol) and ethyl acetate (20 mL) were added to a second flask and flushed with nitrogen for 5 minutes. The 4,4'-dimethylbenzophenone in ethyl acetate was transferred to the flask containing NBS and benzoyl peroxide via syringe under nitrogen. The reaction mixture was refluxed via a heat lamp for 24 hours under a nitrogen atmosphere. The reaction mixture was cooled to room temperature, extracted with ethyl acetate (50 mL), washed with saturated aqueous NaHCO_3 (25 mL \times 3) and H_2O (25 mL \times 3), dried with anhydrous Na_2SO_4 and concentrated under reduced pressure to give the crude product (3.4 g, quantitative crude yield).

^1H NMR (CDCl_3 , 300 MHz): δ ppm 7.80 (d, $J=8.1$ Hz, 4H), 7.53 (d, $J=8.1$ Hz, 4H), 4.54 (s, 4H).

^{13}C NMR (CDCl_3 , 75 MHz): δ ppm 195.27, 142.33, 137.19, 130.53, 129.11, 32.48.

MS (ESI): m/z 388.92 ($\text{M}+\text{Na}^+$), 390.91 ($\text{M}+2+\text{Na}^+$), 392.91 ($\text{M}+4+\text{Na}^+$) ($\text{M}=\text{C}_{15}\text{H}_{12}\text{Br}_2\text{O}$ requires 365.93).





3,3-Bis-(4-bromomethylphenyl)-1-(4-butylphenyl)propenone (**4.9b**)

1-Butyl-4-ethynylbenzene (0.86 g, 5.4 mmol) was flushed under nitrogen for 30 min and THF (30 mL) followed by addition of n-BuLi (3.0 M, 1.8 mL) at -78 °C. Bis-(4-bromomethylphenyl)methanone (**4.7**) (2.0 g, 5.4 mmol) in THF (10 mL) was added dropwise over 10 min and the reaction mixture was stirred at -78 °C for 4 h and was allowed to warm to room temperature overnight. The reaction was quenched by water and extracted with diethyl ether (3 × 20 mL) and water (3 × 20 mL). The organic layer was dried (MgSO₄) and was concentrated *in vacuo*. A brown oil was obtained without further purification for the next step.

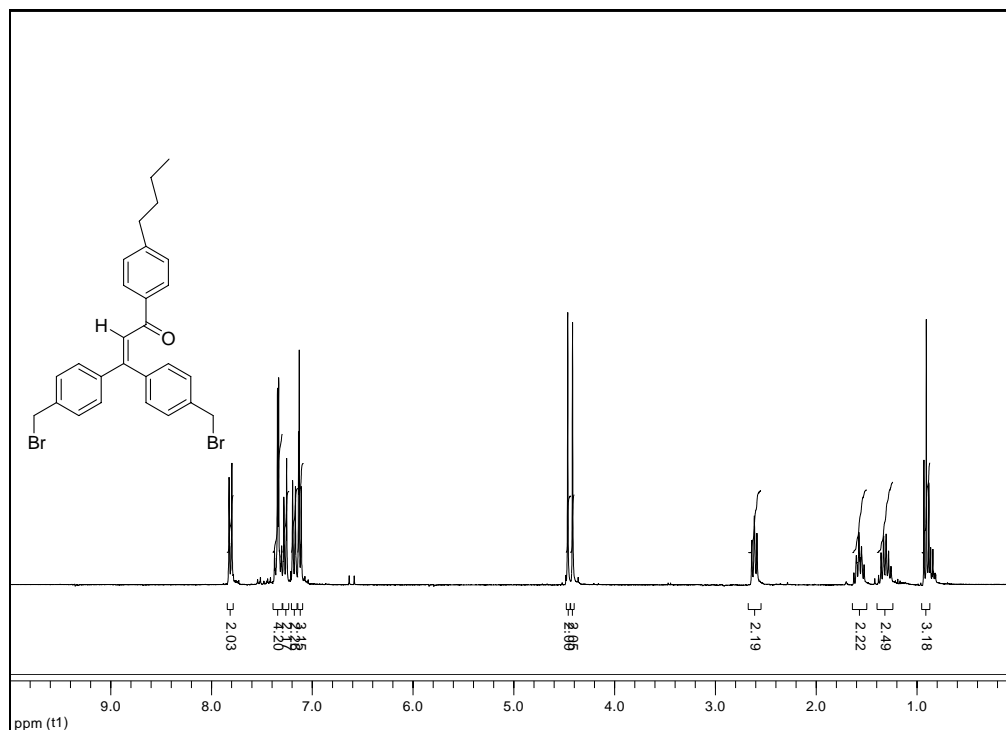
To the brown oil acetic acid (40 mL) was added followed by a few drops of sulfuric acid. The reaction mixture was stirred at room temperature overnight. The reaction was quenched by water and extracted with CH₂Cl₂ (3 × 20 mL) and water (3 × 20 mL). The organic layer was dried (MgSO₄) and was concentrated *in vacuo*. The crude product was purified via column chromatography [SiO₂ – petroleum ether – Et₂O (10:1), v/v] to give

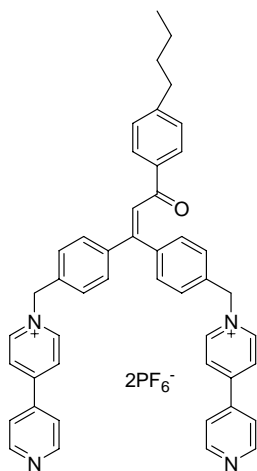
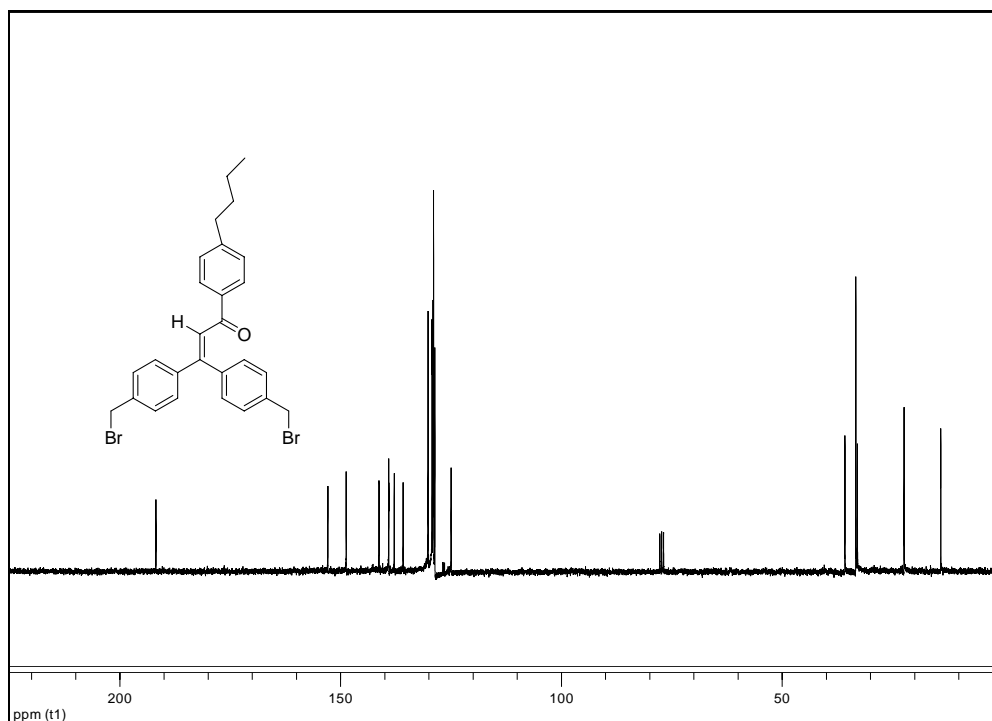
pure compound (1.1 g, 39% yield).

^1H NMR (CDCl_3 , 300 MHz): δ ppm 7.81 (d, $J=8.1$ Hz, 2H), 7.34 (m, 4H), 7.27 (d, $J=8.4$ Hz, 2H), 7.18 (d, $J=8.4$ Hz, 2H), 7.13 (s, 1H), 7.12 (d, $J=8.4$ Hz, 2H), 4.47 (s, 2H), 4.42 (s, 2H), 2.61 (t, $J=7.8$ Hz, 2H), 1.56 (m, 2H), 1.31 (m, 2H), 0.91 (t, $J=7.2$ Hz, 3H).

^{13}C NMR (CDCl_3 , 75 MHz): δ ppm 191.83, 152.90, 148.75, 141.31, 139.12, 139.10, 137.86, 135.85, 130.20, 129.31, 129.08, 128.95, 128.67, 124.98, 35.79, 33.32, 32.98, 22.41, 14.08.

MS (ESI): m/z 547.0 ($\text{M}+\text{Na}^+$), 549.1 ($\text{M}+2+\text{Na}^+$), 551.0 ($\text{M}+4+\text{Na}^+$) ($\text{M}=\text{C}_{27}\text{H}_{26}\text{Br}_2\text{O}$ requires 524.04).





Compound 4.10b

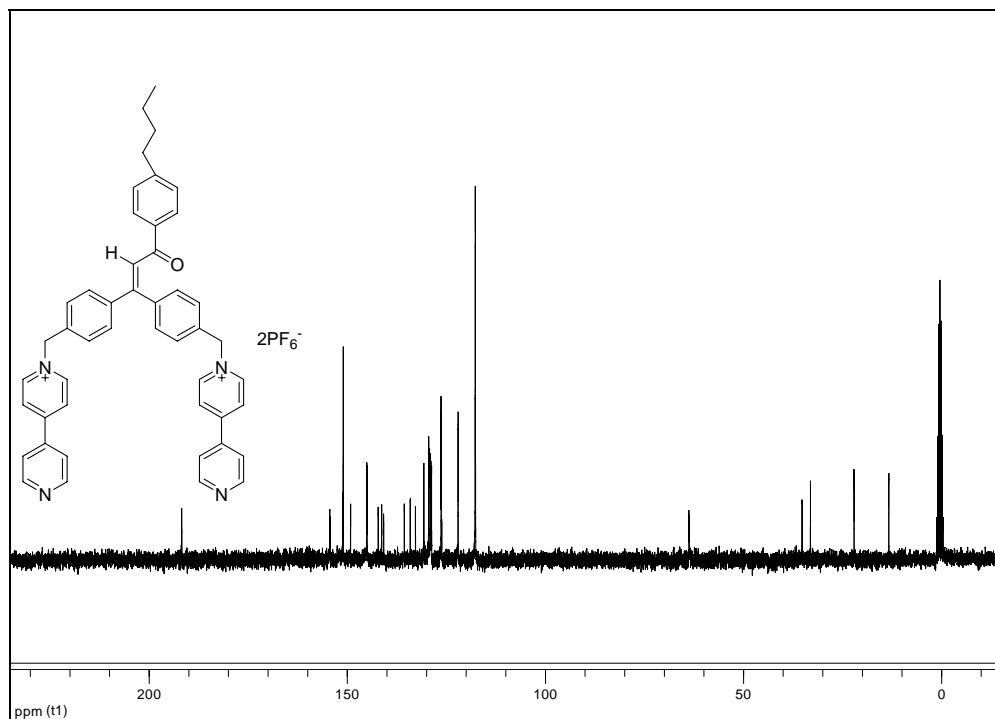
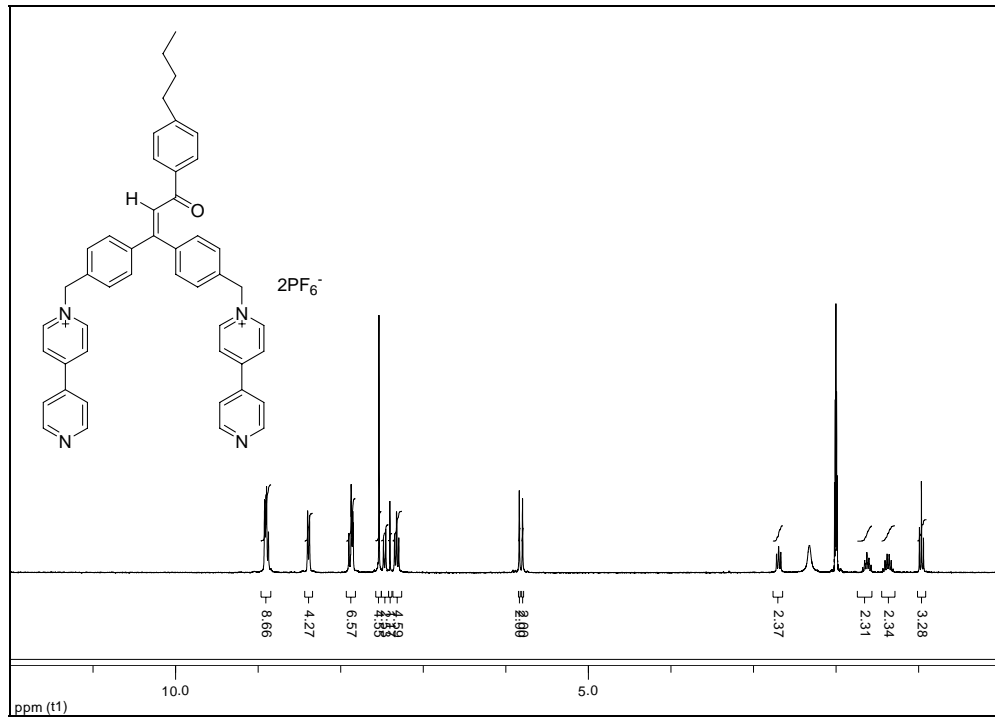
A mixture of 3,3-bis-(4-bromomethylphenyl)-1-(4-butylphenyl)propenone (1.1 g, 2.18 mmol) and 4,4'-dipyridyl (2.73 g, 17.5 mmol) in acetonitrile (50 mL) was stirred at 40 °C and 55 °C for 1 day, respectively. The mixture was concentrated *in vacuo* and the residue

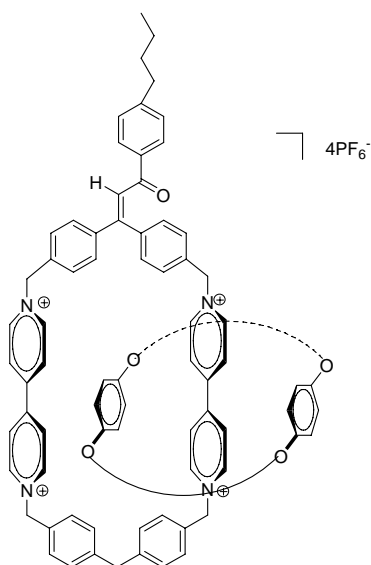
was washed with EtOAc to remove the excess 4,4'-dipyridyl. The solid (0.99 g) was dissolved in methanol and ammonium hexafluorophosphate (0.385 g, 2.36 mmol) in water (10 mL) was added. The methanol was evaporated and the off-white solid (0.99 g, 54 % yield) was obtained from the aqueous phase by filtration.

¹H NMR (CD₃CN, 300 MHz): δ ppm 8.90 (m, 8H), 8.39 (d, J=6.9 Hz, 4H), 7.87 (m, 6H), 7.54 (s, 4H), 7.47(d, J=7.8 Hz, 2H), 7.40 (s, 1H), 7.32 (m, 4H), 5.84 (s, 2H), 5.80 (s, 2H), 2.70 (t, J=7.6 Hz, 2H), 1.63 (m, 2H), 1.38 (m, 2H), 0.97 (t, J=7.2 Hz).

¹³C NMR (CD₃CN, 75 MHz): δ ppm 191.79, 154.43, 154.34, 151.16, 151.03, 149.18, 145.08, 144.99, 142.21, 141.37, 141.32, 140.82, 135.62, 134.12, 132.80, 130.69, 129.45, 129.40, 129.06, 128.91, 128.74, 126.34, 126.27, 126.17, 122.04, 63.78, 63.68, 35.21, 33.10, 22.09, 13.32.

MS (ESI): m/z 339.16 (M²⁺), 823.42 (M²⁺PF₆⁻) (M²⁺= C₄₇H₄₂N₄O²⁺ requires 678.33).





Catenane 4.3

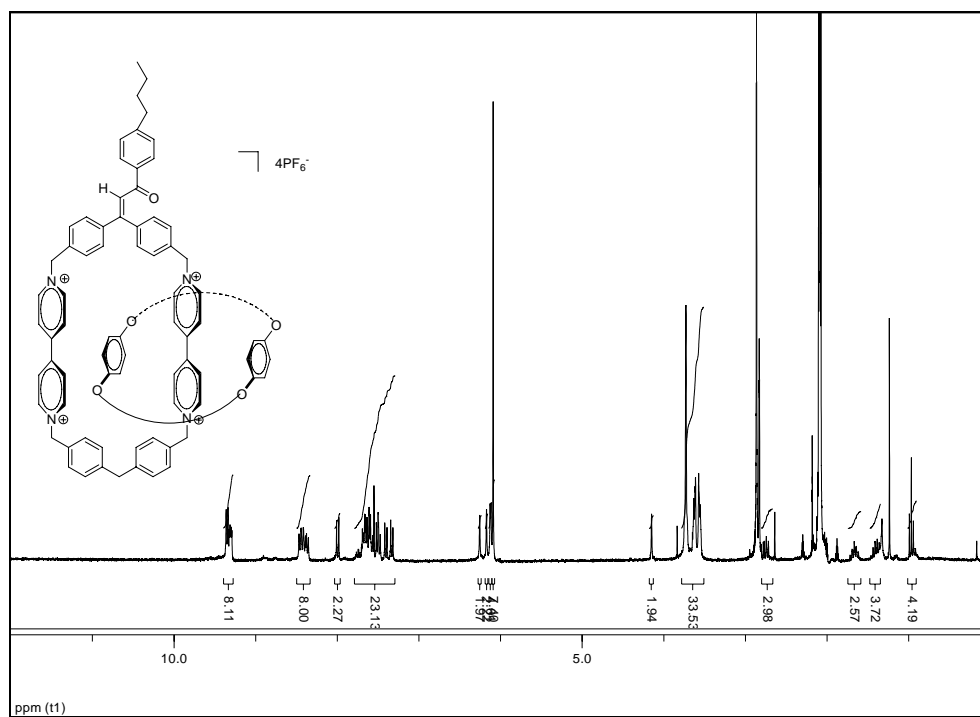
Compound **4.10b** (0.116 g, 0.120 mmol), bis(4-bromomethylphenyl)methane (**3.1**)

(0.055 g, 0.156 mmol) and BPP34C10 (0.102 g, 0.191mmol) were combined and dissolved in CH₃CN (20 mL). The reaction vessel was sealed with a septum. This red solution stirred 4 days under ambient conditions after which time the solvent was removed *in vacuo*. The catenane was purified via two preparative TLC as described in the general catenane purification method and after removal of solvent *in vacuo*, 0.003 g (1.25 %) of red solid was obtained.

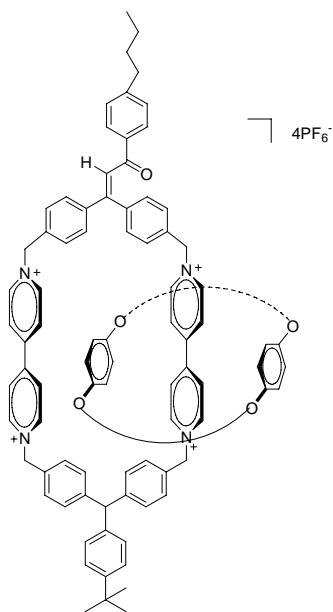
¹H NMR (CD₃CN, 300 MHz): δ ppm 9.39-9.27 (m, 8H), 8.43 (m, 8H), 7.99 (d, *J* = 8.39 Hz, 2H), 7.69-7.32 (m, 18H) 6.25 (s, 2H), 6.17 (s, 2H), 6.12 (s, 2H), 6.09 (s, 2H), 4.15 (s, 2H), 3.78-3.51 (m, 32H), 2.80-2.66 (m, 2H), 0.97 (t, *J* = 7.31, 7.31 Hz, 1H).

MS (ESI): *m/z* 518.26 (M⁴⁺PF₆⁻)³⁺, 849.36 (M⁴⁺2PF₆⁻)²⁺ (M⁴⁺=C₉₀H₉₆N₄O₁₁)⁴⁺ requires

1408.71).



Catenane 4.4

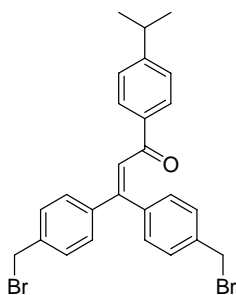
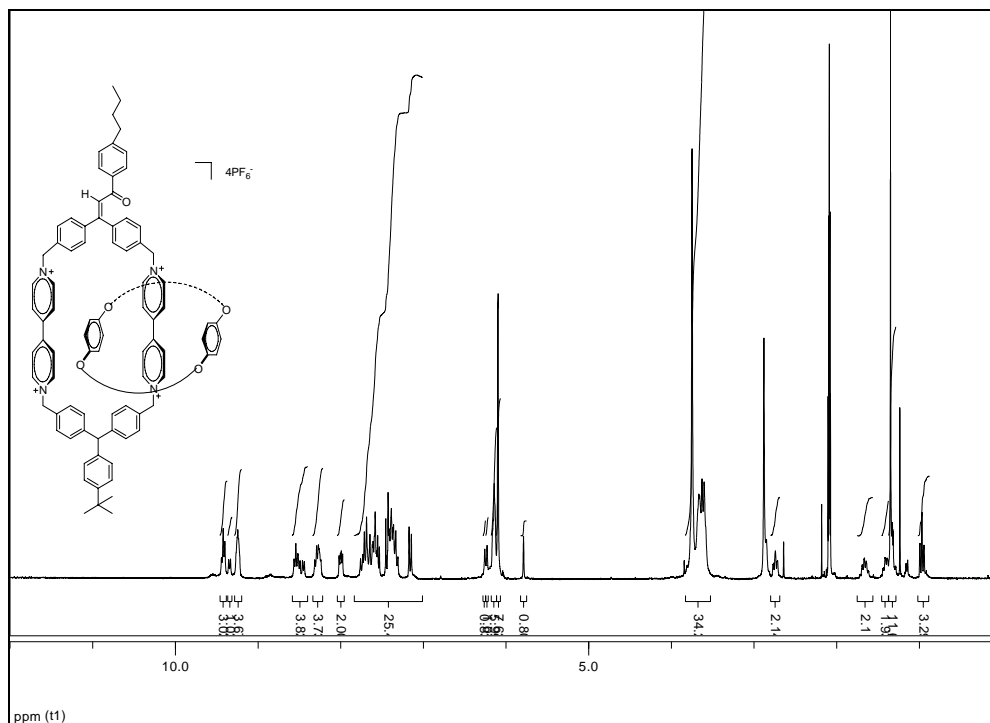


Compound **4.10b** (0.122 g, 0.126 mmol),

1,1'-[[4-(1,1-dimethylethyl)phenyl]methylene]bis[4-(bromomethyl)benzene] (**3.5**) (0.077 g, 0.164 mmol) and BPP34C10 (0.108 g, 0.201 mmol) were combined and dissolved in CH₃CN (20 mL). The reaction vessel was sealed with a septum. This red solution stirred 4 days under ambient conditions after which time the solvent was removed *in vacuo*. The catenane was purified as described in the general catenane purification method and after removal of solvent *in vacuo*, 0.015 g (5.6 %) of red solid was obtained.

¹H NMR (CD₃CN, 300 MHz): δ ppm 9.42 (m, 3H), 9.37-9.32 (m, 1H), 9.25 (m, 4H), 8.58-8.40 (m, 4H), 8.34-8.22 (m, 4H), 8.04-7.96 (m, 2H), 7.76-7.31 (m, 21H), 6.28-6.25 (m, 4H), 6.24-6.22 (m, 4H), 6.18-6.11 (m, 4H), 6.10 (s, 8H), 5.79 (s, 1H), 3.83-3.53 (m, 32H), 2.80-2.69 (m, 2H), 1.75-1.56 (m, 2H), 1.37-1.28 (m, 2H), 0.97 (t, *J* = 7.2 Hz, 3H).

MS (ESI): *m/z* 561.90 (M⁴⁺PF₆⁻)³⁺, 915.45 (M⁴⁺2PF₆⁻)²⁺ (M⁴⁺=C₁₀₀H₁₀₈N₄O₁₁)⁴⁺ requires 1540.80).



3,3-Bis-(4-bromomethylphenyl)-1-(4-isopropylphenyl)propenone (4.9c)

1-Ethynyl-4-isopropylbenzene⁵² (0.141, 0.98 mmol) was flushed under nitrogen for 30 min and THF (4 mL) followed by addition of n-BuLi (1.37 M, 0.7 mL) at -78 °C. Bis-(4-bromomethylphenyl)methanone (0.3 g, 0.82 mmol) in THF (2 mL) was added dropwise over 5 min and the reaction mixture was stirred at -78 °C for 4 h and was

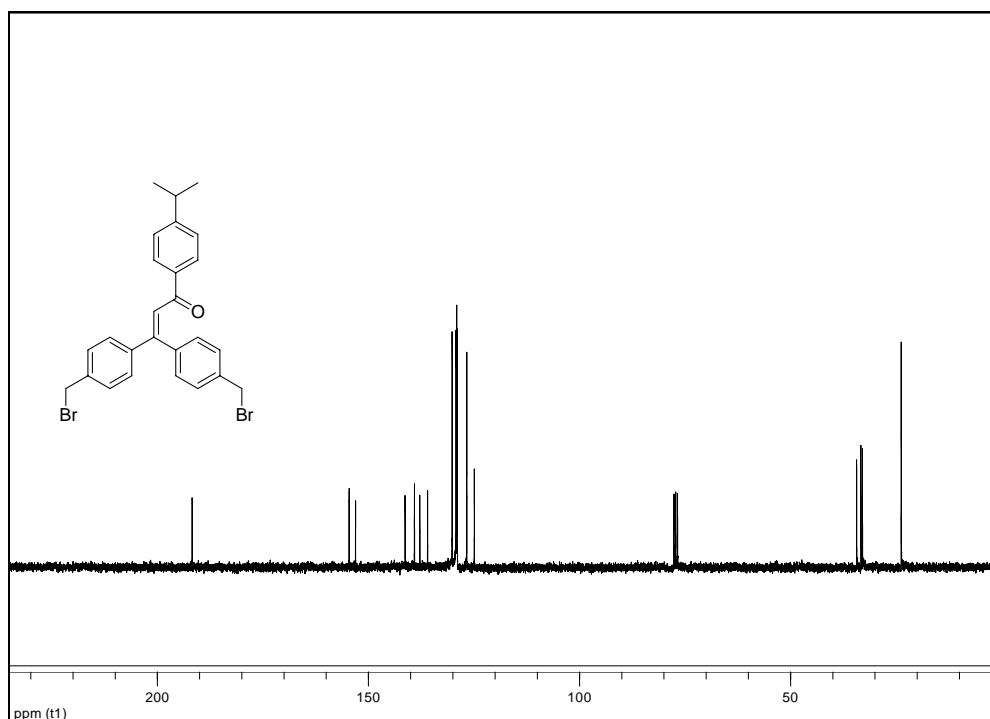
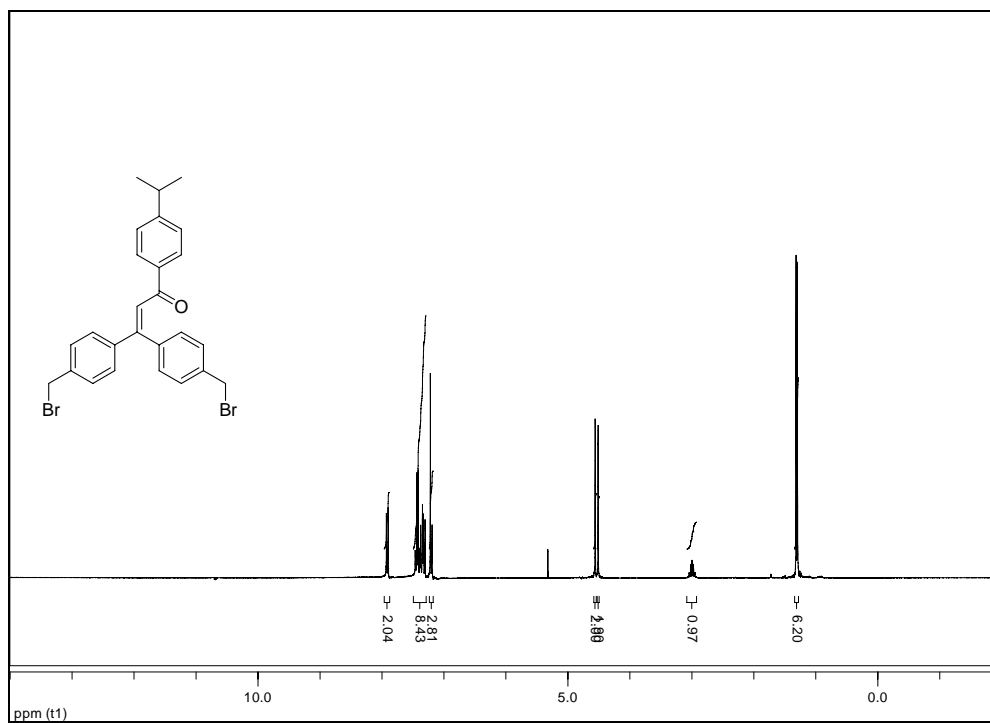
allowed to warm to 0 °C and stirred for 3 h. The reaction was quenched by water and extracted with diethyl ether (3×10 mL) and water (3×10 mL). The organic layer was dried (MgSO₄) and was concentrated *in vacuo*. A brown oil was obtained and a yellow oil (crude, 0.300 g) was collected via flash chromatography [SiO₂ – petroleum ether – Et₂O (1:1), v/v].

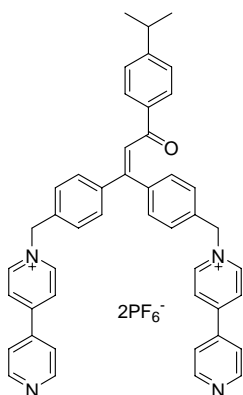
To the yellow oil acetic acid (10 mL) was added followed by a few drops of sulfuric acid. The reaction mixture was stirred at room temperature overnight. The reaction was quenched by water and extracted with CH₂Cl₂ (3×10 mL) and water (3×10 mL). The organic layer was dried (MgSO₄) and was concentrated *in vacuo*. The crude product was purified via column chromatography [SiO₂ – petroleum ether – Et₂O (10:1), v/v] to give pure compound (0.166 g, 38% yield).

¹H NMR (CDCl₃, 300 MHz): δ ppm 7.91 (d, J=8.7 Hz, 2H), 7.43 (m, 4H), 7.36 (d, J=8.4 Hz, 2H), 7.32 (d, J=8.4 Hz, 2H), 7.22 (s, 1H), 7.20 (d, J=8.1 Hz, 2H), 4.56 (s, 2H), 4.51 (s, 2H), 2.99 (m, J=6.6 Hz, 1H), 1.31 (d, J=6.6 Hz, 6H).

¹³C NMR (CDCl₃, 75 MHz): δ ppm 191.77, 154.59, 153.06, 141.32, 139.11, 137.84, 135.99, 130.17, 129.30, 129.09, 129.05, 128.95, 126.70, 124.92, 34.34, 33.32, 32.96, 23.79.

MS (ESI): m/z 533.04 (M+Na⁺), 535.02 (M+2+Na⁺), 537.01 (M+4+Na⁺) (M=C₂₆H₂₄Br₂O requires 510.02).





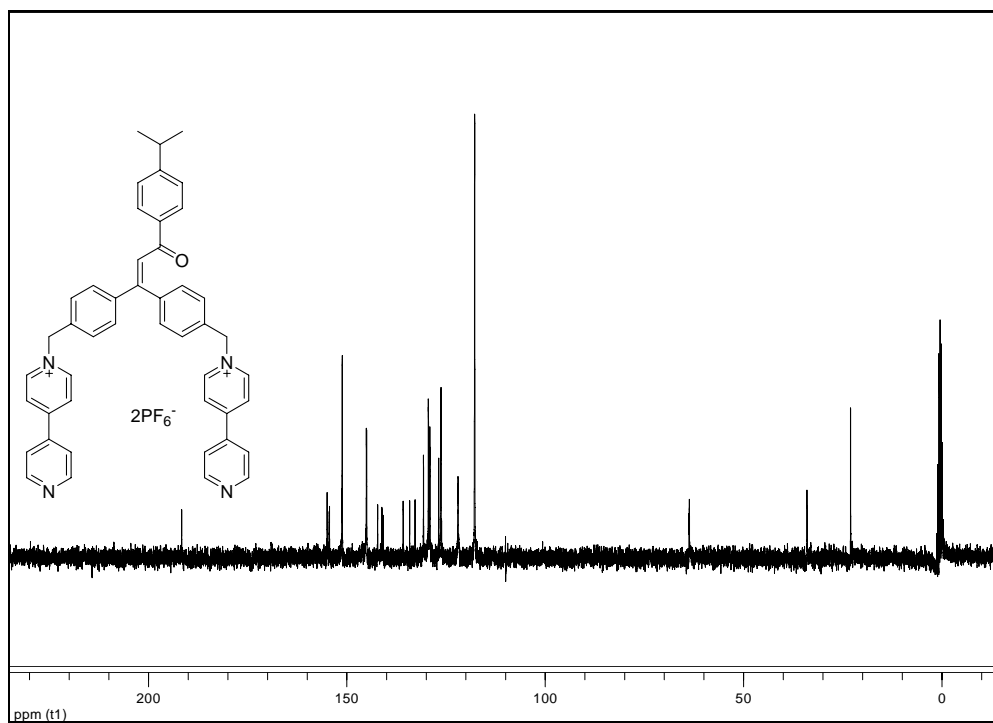
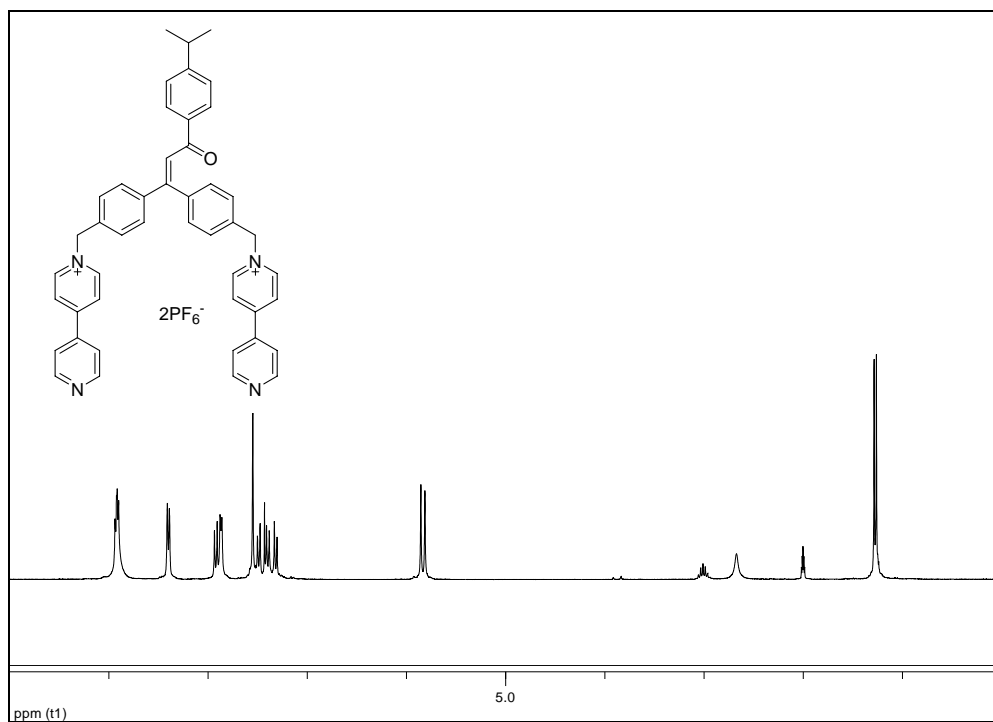
Compound 4.10c

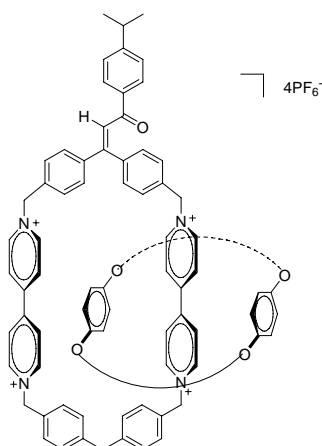
A mixture of 3,3-bis-(4-bromomethylphenyl)-1-(4-isopropylphenyl)propenone (0.073 g, 0.14 mmol) and 4,4'-dipyridyl (0.178 g, 1.14 mmol) in acetonitrile (10 mL) was stirred at 40 °C and 55 °C for 1 day, respectively. The mixture was concentrated *in vacuo* and the residue was washed with EtOAc to remove the excess 4,4'-dipyridyl. The solid (0.70 g) was dissolved in methanol and ammonium hexafluorophosphate (0.045 g, 0.28 mmol) in water (10 mL) was added. The methanol was evaporated and the off-white solid (0.81 g, 61 % yield) was obtained from the aqueous phase by filtration.

¹H NMR (CD₃CN, 300 MHz): δ ppm 8.91 (m, 8H), 8.40 (d, J=6 Hz, 4H), 7.92 (d, J=8.1 Hz, 2H), 7.87 (d, 5.1 Hz, 4H), 7.55 (s, 4H), 7.49 (d, J=8.4 Hz, 2H), 7.43 (s, 1H), 7.40 (d, J=8.4 Hz, 2H), 7.32 (d, J=8.1 Hz, 2H), 5.85 (s, 2H), 5.81 (s, 2H), 3.01 (m, 1H), 1.27 (d, J=6.9 Hz, 6H).

¹³C NMR (CD₃CN, 75 MHz): δ ppm 191.64, 154.98, 154.47, 154.39, 151.30, 151.18, 145.09, 145.02, 142.25, 141.15, 140.86, 135.82, 134.18, 132.83, 130.69, 129.47, 129.09, 126.85, 126.33, 126.27, 121.99, 63.78, 63.69, 34.02, 23.05.

MS (ESI): m/z 332.16 (M^{2+}) ($M^{2+} = C_{46}H_{40}N_4O^{2+}$ requires 664.32).





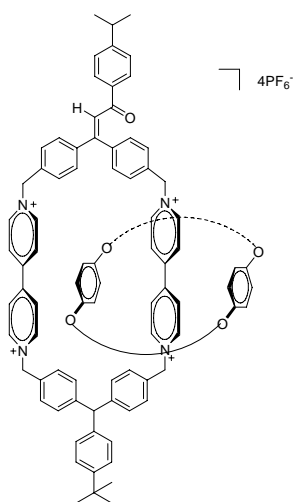
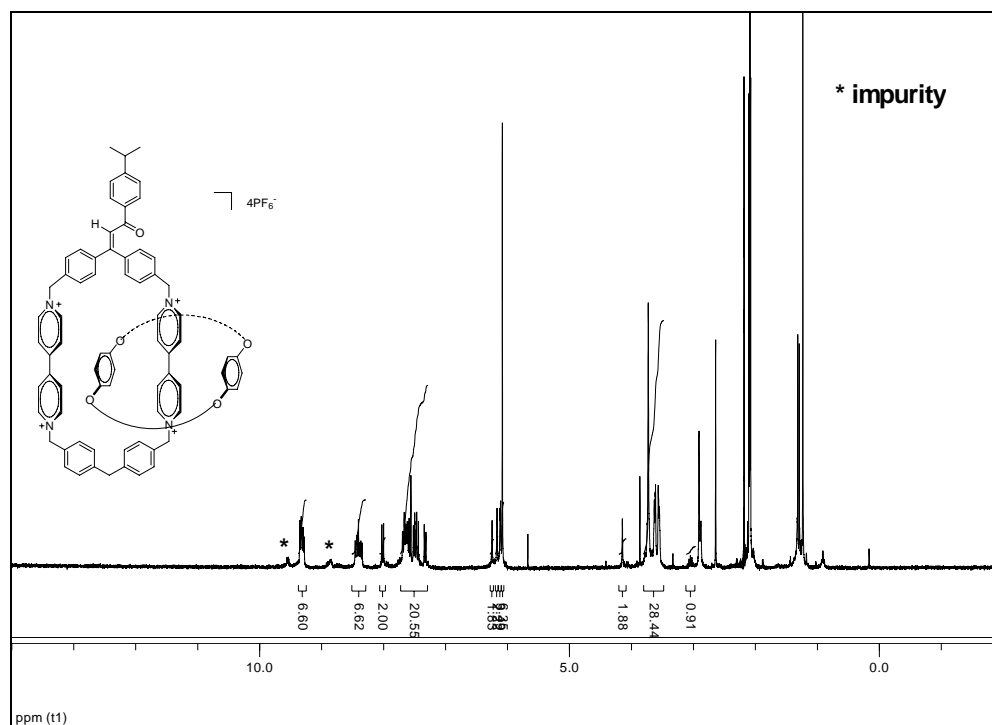
Catenane 4.5

Compound **4.10c** (0.111 g, 0.116 mmol), bis(4-bromomethylphenyl)methane (**3.1**)

(0.054 g, 0.151 mmol) and BPP34C10 (0.100 g, 0.186mmol) were combined and dissolved in CH₃CN (20 mL). The reaction vessel was sealed with a septum. This red solution stirred 4 days under ambient conditions after which time the solvent was removed *in vacuo*. The catenane was purified via two preparative TLC as described in the general catenane purification method and after removal of solvent *in vacuo*, 0.003 g (1.3 %) of red solid was obtained.

¹H NMR (CD₃CN, 300 MHz): δ ppm 9.38-9.25 (m, 8H), 8.41 (m, 8H), 8.01 (d, *J* = 8.35 Hz, 2H), 7.72-7.29 (m, 19H), 6.25 (s, 2H), 6.17 (s, 2H), 6.12 (s, 2H), 6.11 (s, 2H), 6.08 (s, 8H), 4.15 (s, 2H), 3.80-3.48 (m, 32H), 3.12-2.98 (m, 1H), 1.36-1.27 (d, *J* = 6.90 Hz 6H).

MS (ESI): *m/z* 842.13 (M⁴⁺2PF₆⁻)²⁺, 1830.27(M⁴⁺3PF₆⁻)⁺ (M⁴⁺=C₈₉H₉₄N₄O₁₁⁴⁺ requires 1394.69).



Catenane 4.6

Compound **4.10c** (0.122 g, 0.126 mmol),

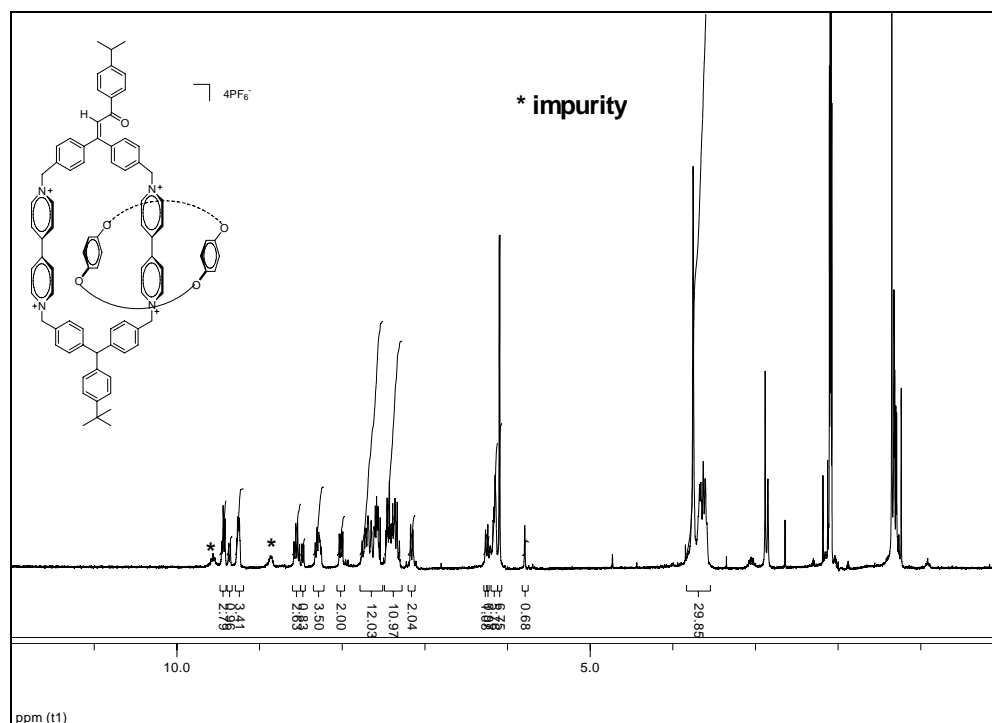
1,1'-[[4-(1,1-dimethylethyl)phenyl]methylene]bis[4-(bromomethyl)benzene (**3.5**) (0.077 g, 0.164 mmol) and BPP34C10 (0.108 g, 0.201 mmol) were combined and dissolved in CH₃CN (20 mL). The reaction vessel was sealed with a septum. This red solution stirred

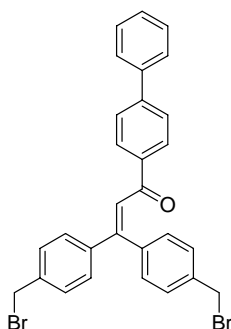
4 days under ambient conditions after which time the solvent was removed *in vacuo*. The catenane was purified via one preparative TLC plates as described in the general catenane purification method and after removal of solvent *in vacuo*, 0.011 g (6.1 %) of red solid was obtained.

^1H NMR (CD_3CN , 300 MHz): δ ppm 9.43 (m, 3H), 9.39-9.33 (m, 1H), 9.29-9.19 (m, 4H), 8.55 (m, 4H), 8.50-8.45 (m, 1H), 8.30 (m, 4H), 8.01 (m, 4H), 7.78-7.51 (m, 12H), 7.49-7.28 (m, 11H), 7.16 (d, $J = 7.96$ Hz, 2H), 6.27 (s, 2H), 6.24 (s, 2H), 6.20-6.12 (m, 4H), 6.10 (s, 8H), 5.79 (s, 1H), 3.83-3.55 (m, 32H), 3.04 (m, 1H).

MS (ESI): m/z 381.80 (M^{4+}), 557.40 ($\text{M}^{4+}\text{PF}_6^-$) $^{3+}$, 908.27 ($\text{M}^{4+}2\text{PF}_6^-$) $^{2+}$

($\text{M}^{4+}=\text{C}_{99}\text{H}_{106}\text{N}_4\text{O}_{11}$ requires 1526.78).





1-Biphenyl-4-yl-3,3-bis-(4-bromomethyl-phenyl)-propenone (4.9d)

4-Ethynylbiphenyl⁵⁴ (0.220 g, 1.24 mmol) was flushed under nitrogen for 30 min and THF (9 mL) followed by addition of n-BuLi (1.37 M, 1 mL) at -78 °C. The mixture was allowed to warm up to room temperature and stirred for 4 h. The mixture was cooled down to -78 °C. Bis-(4-bromomethylphenyl)methanone (0.455 g, 1.24 mmol) in THF (4 mL) was added dropwise in 5 min and the reaction mixture was stirred at -78 °C for 4 h and was allowed to warm to 0 °C and stirred for 4 h. The reaction was quenched by water and extracted with ethyl acetate (3 × 10 mL) and washed with water (3 × 10 mL). The organic layer was dried (MgSO₄) and was concentrated *in vacuo*. A yellow oil (crude, 0.220 g) was collected via flash chromatography [SiO₂ – petroleum ether – Et₂O (1:1), v/v].

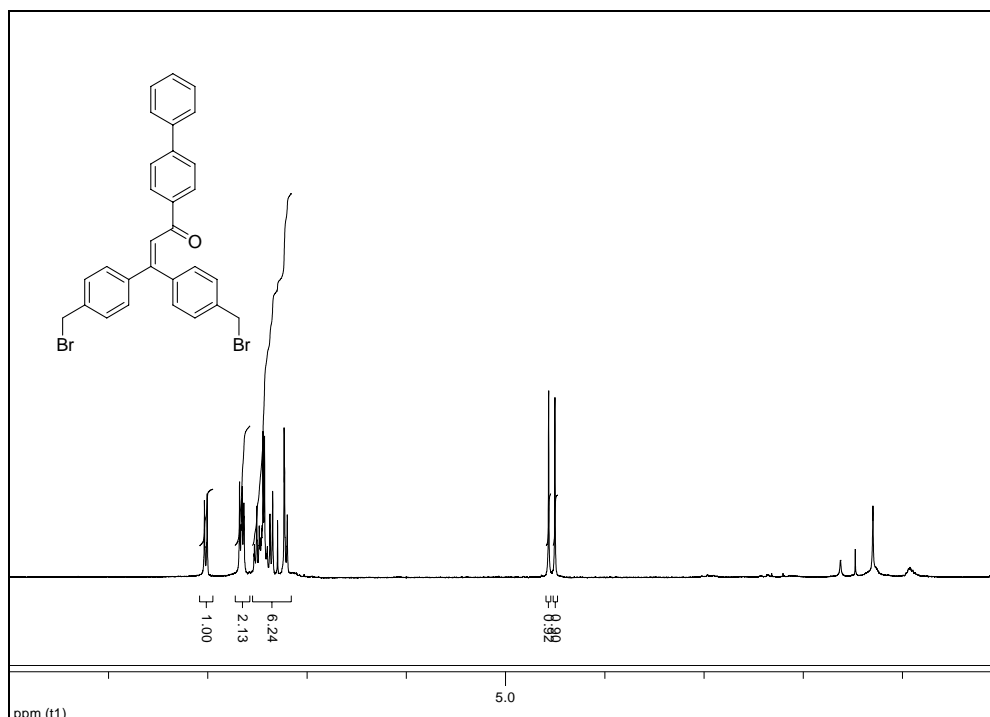
To the yellow oil acetic acid (10 mL) was added followed by a few drops of sulfuric acid. The reaction mixture was stirred at room temperature overnight. The reaction was quenched by water and extracted with ethyl acetate (3 × 10 mL) and washed water (3 × 10 mL), saturated NaHCO₃ (3 × 10 mL), water (3 × 10 mL). The organic layer was dried

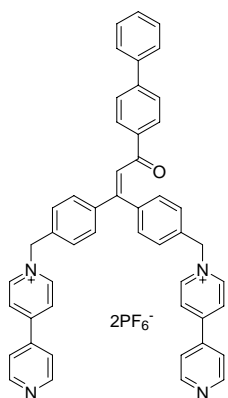
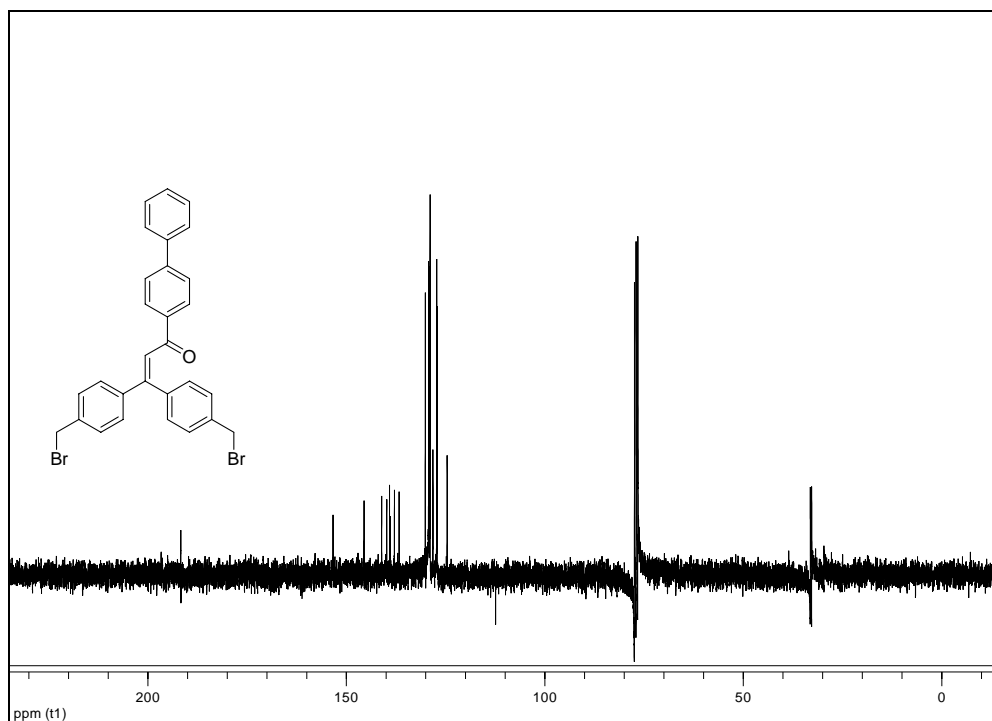
(MgSO₄) and was concentrated *in vacuo*. The crude product was purified via column chromatography [SiO₂ – petroleum ether – Et₂O (10:1), v/v] to give pure compound **4.9d** (0.210 g, 31 % yield).

¹H NMR (CDCl₃, 300 MHz): δ ppm 8.08 (d, J=8.4 Hz, 2H), 7.74-7.60 (m, 4H), 7.56-7.17 (m, 12H), 4.57 (s, 2H), 4.50 (s, 2H).

¹³C NMR (CDCl₃, 75 MHz): δ ppm 191.71, 153.34, 145.53, 141.10, 139.81, 139.11, 138.88, 137.89, 136.70, 130.09, 129.22, 128.92, 128.18, 127.16, 124.60, 33.10, 32.76.

MS (ESI): m/z 567.00 (M+Na⁺), 568.99 (M+2+Na⁺), 570.99 (M+4+Na⁺) (M=C₂₉H₂₂Br₂O requires 544.00).





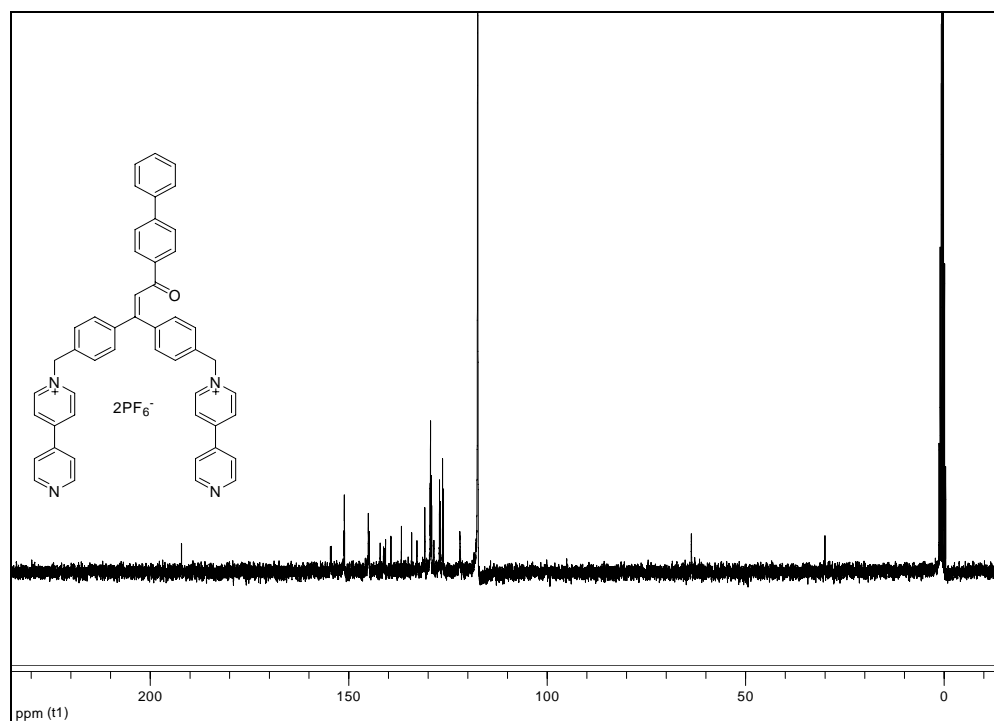
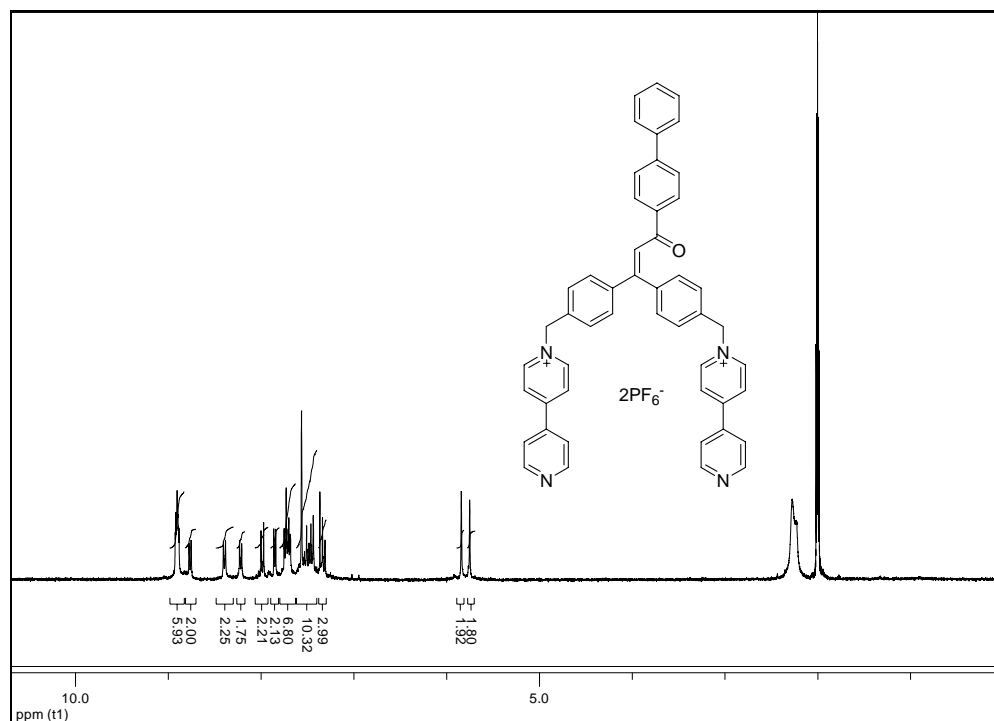
Compound 4.10d

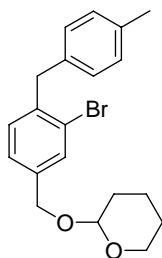
A mixture of 1-biphenyl-4-yl-3,3-bis-(4-bromomethylphenyl)propenone (**4.9d**) (0.090 g, 0.16 mmol) and 4,4'-dipyridyl (0.206 g, 1.32 mmol) in acetonitrile (15 mL) was stirred at 40 °C and 55 °C for 1 day, respectively. The mixture was concentrated *in vacuo* and the

residue was washed with EtOAc to remove the excess 4,4'-dipyridyl. The solid was dissolved in methanol and ammonium hexafluorophosphate (0.052 g, 0.32 mmol) in water (5 mL) was added. The methanol was evaporated and the off-white solid **4.10** (0.112 g, 71 % yield) was obtained from the aqueous phase by filtration.

¹H NMR (CD₃CN, 300 MHz): δ ppm 8.90 (m, 6H), 8.75 (d, *J* = 6.9 Hz, 2H), 8.38 (d, *J* = 6.9 Hz, 2H), 8.23 (d, *J* = 6.9 Hz, 2H), 7.99 (d, *J* = 8.4 Hz, 2H), 7.85 (m, 2H), 7.75-7.68 (m, 6H), 7.62-7.40 (m, 9H), 7.38-7.30 (m, 2H), 5.84 (s, 2H), 5.75 (s, 2H). **¹³C NMR** (CD₃CN, 75 MHz): δ ppm 192.11, 154.60, 154.41, 151.19, 151.10, 151.06, 145.04, 145.01, 144.79, 142.06, 141.24, 141.07, 140.72, 139.35, 136.71, 134.13, 132.80, 130.81, 129.47, 129.39, 129.17, 129.08, 128.53, 127.18, 127.13, 126.91, 126.35, 126.13, 121.98, 63.67, 63.64, 30.01.

MS (ESI): *m/z* 349.18 (M²⁺), 843.31 (M²⁺PF₆)⁺ (M²⁺ = C₄₉H₃₈N₄O²⁺ requires 698.30).



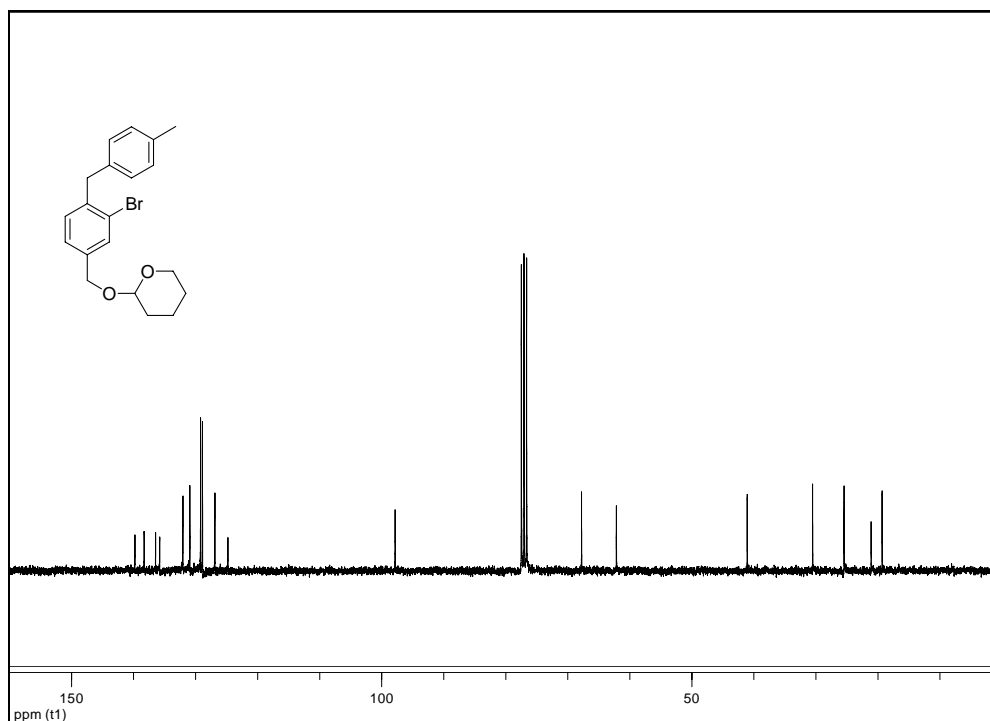
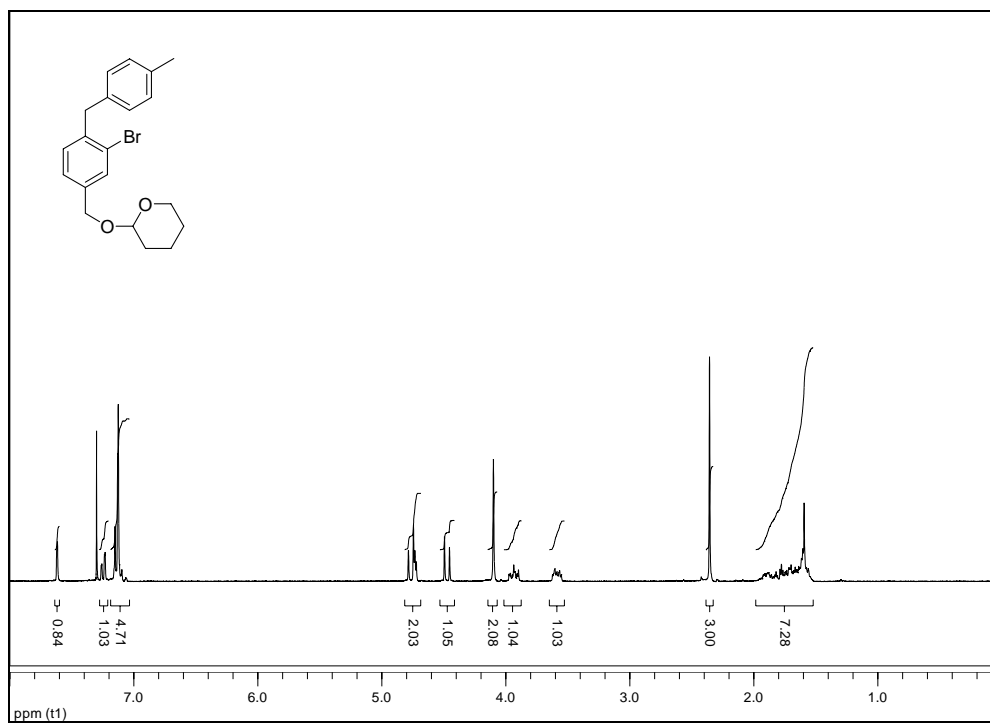


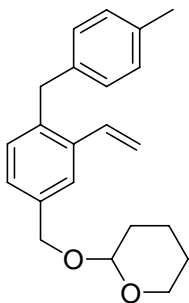
2-[3-Bromo-4-(4-methylbenzyloxy)benzyloxy]tetrahydropyran (**5.9**)

2-(3-Bromo-4-bromomethyl-benzyloxy)tetrahydropyran (**5.8**) (0.52 g, 1.43 mmol), copper(I) cyanide (0.013 g, 0.143 mmol), 2,2'-dipyridyl (0.022 g, 0.143 mmol) and were added to a 15 mL flask and flushed with nitrogen for 30 min. Dry THF (3 mL) was added via syringe followed by addition of 4-methylphenylmagnesium bromide solution (2.2 mL, 1 M) at -78°C . The mixture was allowed to room temperature and stirred overnight. The reaction was quenched with water. The orange suspension was filtered with Celite. The organic layer was extracted with Et_2O (3×10 mL) and washed with water (3×10 mL). The organic layer was dried (MgSO_4) and concentrated *in vacuo*. The crude product was purified with column chromatography [SiO_2 – petroleum ether – CH_2Cl_2 (1:1), v/v] to give pure compound **5.9** (0.36 g, 67 % yield).

^1H NMR (CDCl_3 , 300 MHz): δ ppm 7.62 (d, $J = 1.48$ Hz, 1H), 7.25 (dd, $J = 7.80, 1.48$ Hz, 4H), 7.17-7.11 (m, 5H), 4.78-4.73 (m, 2H), 4.47 (d, $J = 12.17$ Hz, 1H), 4.10 (s, 2H), 4.00-3.87 (m, 1H), 3.65-3.49 (m, 1H), 2.36 (s, 3H), 1.99-1.51 (m, 6H).

^{13}C NMR (CDCl_3 , 75 MHz): δ ppm 139.77, 138.29, 136.44, 135.79, 132.04, 130.92, 129.19, 128.88, 126.88, 124.78, 97.82, 67.77, 62.16, 41.07, 30.52, 25.46, 21.09, 19.32.





2-[4-(4-Methylbenzyl)-3-vinylbenzyloxy]tetrahydropyran (**5.10**)

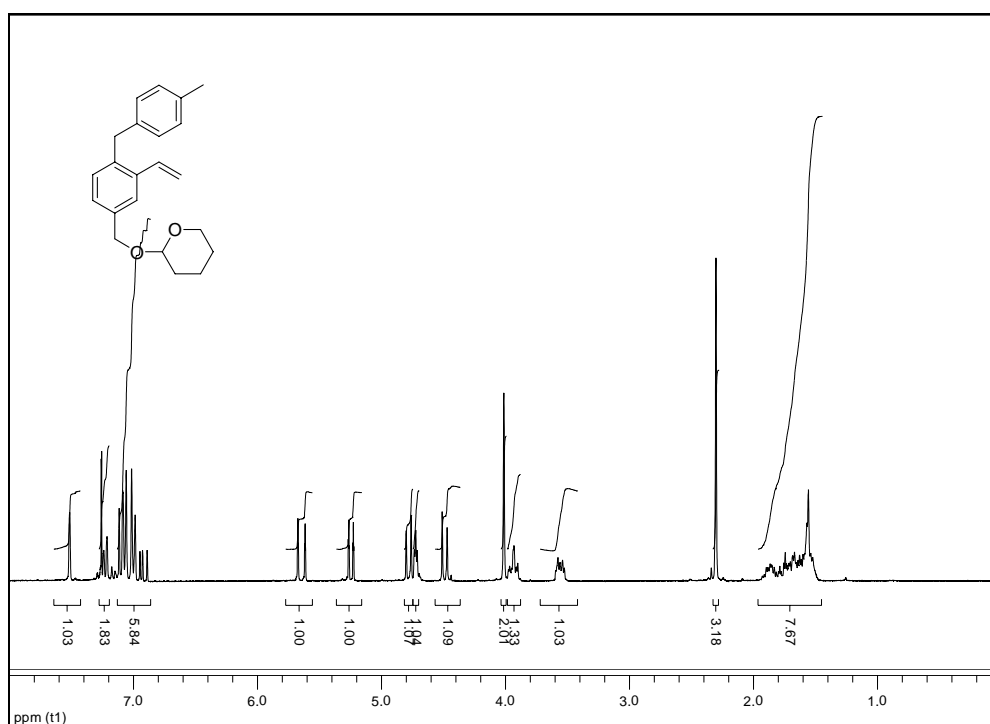
$\text{PdCl}_2(\text{dppf})$ (0.435 g, 0.532 mmol) was added to a 100 mL three-neck flask with a condenser. The flask was flushed with nitrogen for 30 min. Dry THF (25 mL) followed by 2-[3-Bromo-4-(4-methylbenzyl)benzyloxy]tetrahydropyran (**5.9**) (4.0 g, 10.66 mmol) in THF (20 mL) was added to the flask.⁵⁷ The mixture was cooled down to $-78\text{ }^\circ\text{C}$ and vinylmagnesium bromide (22 mL, 1.0 M) was added slowly. The reaction mixture was allowed to warm to room temperature in 2 h and refluxed for 24 h. The reaction was quenched with water (20 mL) and the aqueous mixture was extracted with Et_2O (20 mL \times 3) and washed with water (20 mL \times 3). The organic layer was dried (MgSO_4) and concentrated *in vacuo*. The crude product was purified with column chromatography [SiO_2 – petroleum ether – CH_2Cl_2 (1:1), v/v] to give pure compound **5.10** (3.0 g, 88 % yield).

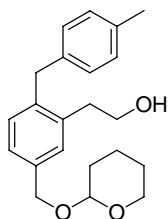
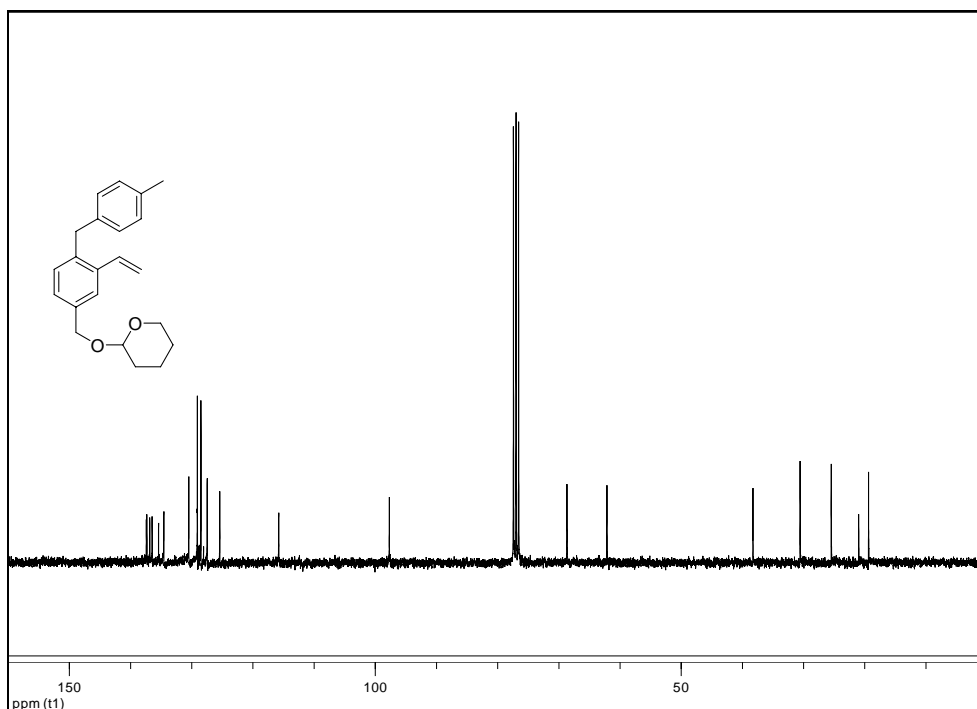
$^1\text{H NMR}$ (CDCl_3 , 300 MHz): δ ppm 7.52 (s, 1H), 7.34-6.85 (m, 8H), 5.65 (td, $J = 17.37$, 1.19 Hz, 1H), 5.25 (td, $J = 10.98$, 1.19 Hz, 1H), 4.78 (d, $J = 11.82$ Hz, 1H), 4.72 (t, $J = 3.52$ Hz, 1H), 4.49 (d, $J = 11.82$ Hz, 1H), 4.01 (s, 2H), 3.97-3.90 (m, 1H), 3.57-3.52 (m,

1H), 2.31 (s, 3H), 1.95-1.47 (m, 6H).

^{13}C NMR (CDCl_3 , 75 MHz): δ ppm 137.38, 136.86, 136.47, 135.42, 134.55, 130.47, 129.09, 128.79, 128.49, 127.47, 125.41, 115.78, 97.70, 68.67, 62.13, 38.27, 30.56, 25.47, 20.98, 19.37.

MS (ESI): m/z 345.19 ($\text{M}+\text{Na}^+$) ($\text{M}=\text{C}_{22}\text{H}_{26}\text{O}_2$ requires 322.19).





2-[2-(4-Methylbenzyl)-5-(tetrahydropyran-2-yloxymethyl)phenyl]ethanol (5.11**)**

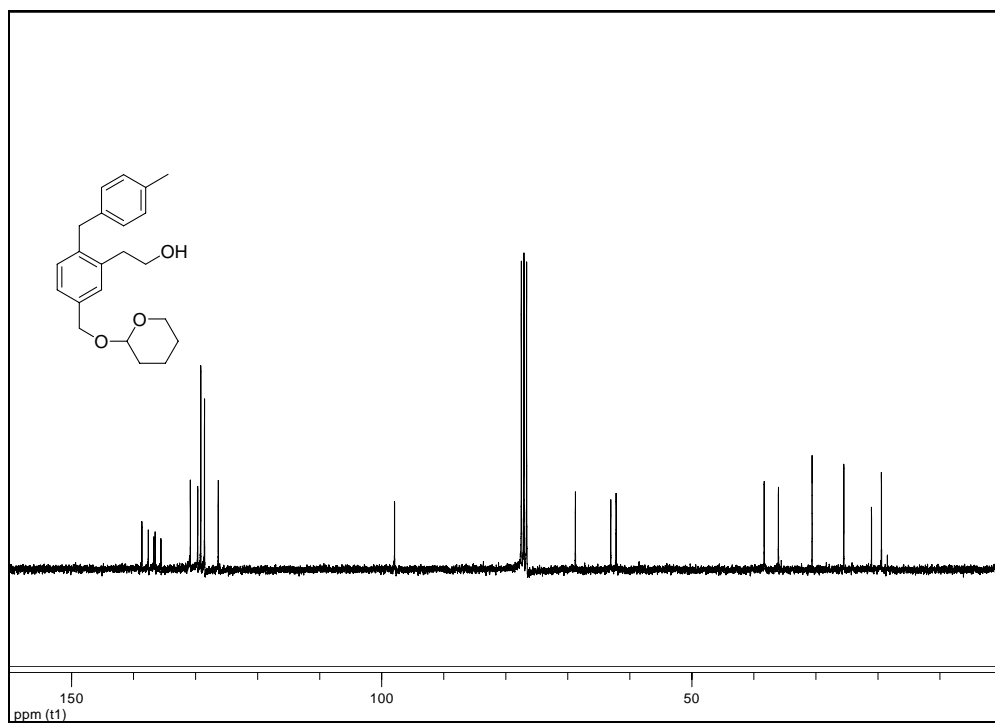
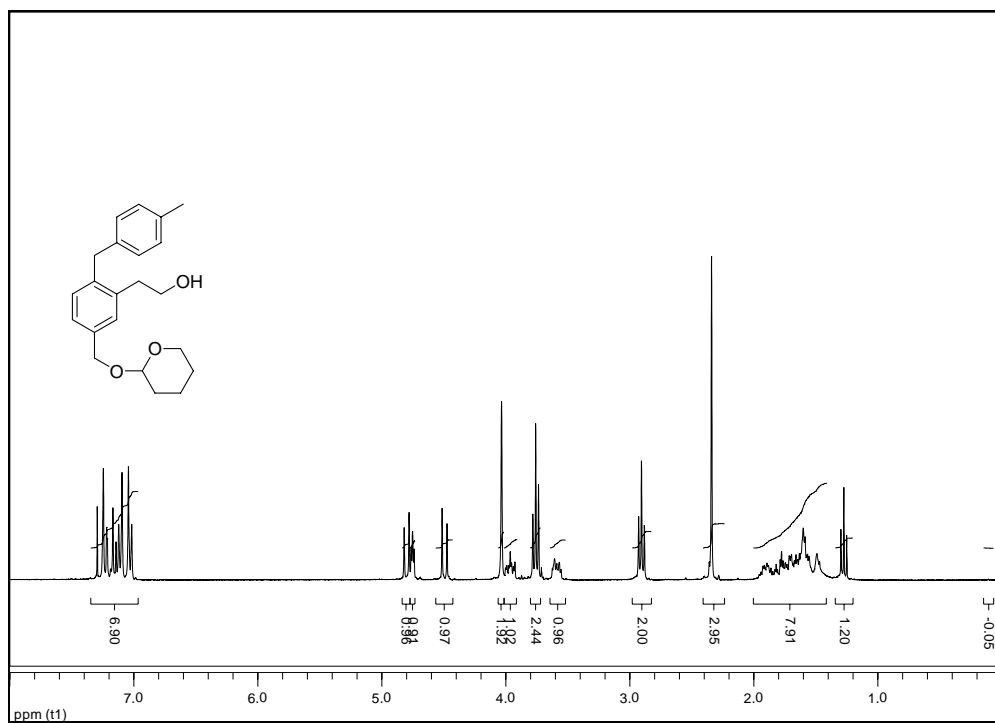
BH₃.THF (7.3 mL, 1.0 M) was added to a 50 mL flask via syringe and cooled down to 0 °C, followed by addition of cyclohexene (1.5 mL, 14.5 mmol).⁵⁸ The mixture was stirred for 1 h at 0 °C. 2-[4-(4-Methylbenzyl)-3-vinylbenzyloxy]tetrahydropyran (**5.10**) (1.8 g, 5.58 mmol) in THF (10 mL) was added and the reaction mixture was allowed to warm to room temperature and stirred overnight. NaOH (10 mL, 3N) and H₂O₂ (10 mL, 30 %) were added sequentially and the mixture continued to stir for 3 h. The reaction mixture

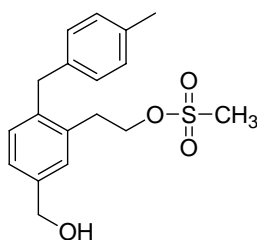
was extracted with Et₂O (20 mL × 3) and washed with water (20 mL × 3). The organic layer was dried (MgSO₄) and concentrated *in vacuo* to give crude product. The crude product was purified with column chromatography [SiO₂ – petroleum ether – Et₂O (10:1), v/v] to give pure compound **5.11** (1.6 g, 84 % yield).

¹H NMR (CDCl₃, 300 MHz): δ ppm 7.35-6.96 (m, 7H), 4.80 (d, *J* = 11.83 Hz, 1H), 4.75 (t, *J* = 3.48 Hz, 1H), 4.49 (d, *J* = 11.83 Hz, 1H), 4.03 (s, 2H), 3.96 (m, 1H), 3.76 (t, *J* = 6.90 Hz, 2H), 3.60 (m, 1H), 2.91 (t, *J* = 6.90 Hz, 2H), 2.35 (s, 3H), 2.00-1.41 (m, 6H).

¹³C NMR (CDCl₃, 75 MHz): δ ppm 138.64, 137.61, 136.71, 136.51, 135.58, 130.83, 129.65, 129.15, 128.56, 126.33, 97.92, 68.77, 63.06, 62.20, 38.33, 36.04, 30.60, 25.49, 21.03, 19.42.

MS (ESI): *m/z* 363.22 (M+Na⁺) (M= C₂₂H₂₈O₃ requires 340.20).





Methanesulfonic acid 2-[5-hydroxymethyl-2-(4-methylbenzyl)phenyl]ethyl ester (5.13)

2-[2-(4-Methylbenzyl)-5-(tetrahydropyran-2-yloxymethyl)phenyl]ethanol (**5.11**) (2.2 g, 6.46 mmol) was flushed with nitrogen for 30 min. CH_2Cl_2 (35 mL) followed by Et_3N (2.7 mL, 19.4 mmol) was added.^{59,60} The mixture was cooled down to 0 °C and methanesulfonyl chloride (1.8 mL, 12.9 mmol) was added via syringe. The solution was stirred at 0 °C for 1 h and at room temperature for 2 h, respectively. The reaction was quenched with water (40 mL). The aqueous mixture was extracted with CH_2Cl_2 (3×40 mL) and washed with water (3×40 mL). The organic layer was dried (MgSO_4) and concentrated *in vacuo* to give crude product - methanesulfonic acid 2-[2-(4-methylbenzyl)-5-(tetrahydropyran-2-yloxymethyl)phenyl]ethyl ester (**5.12**) without further purification.

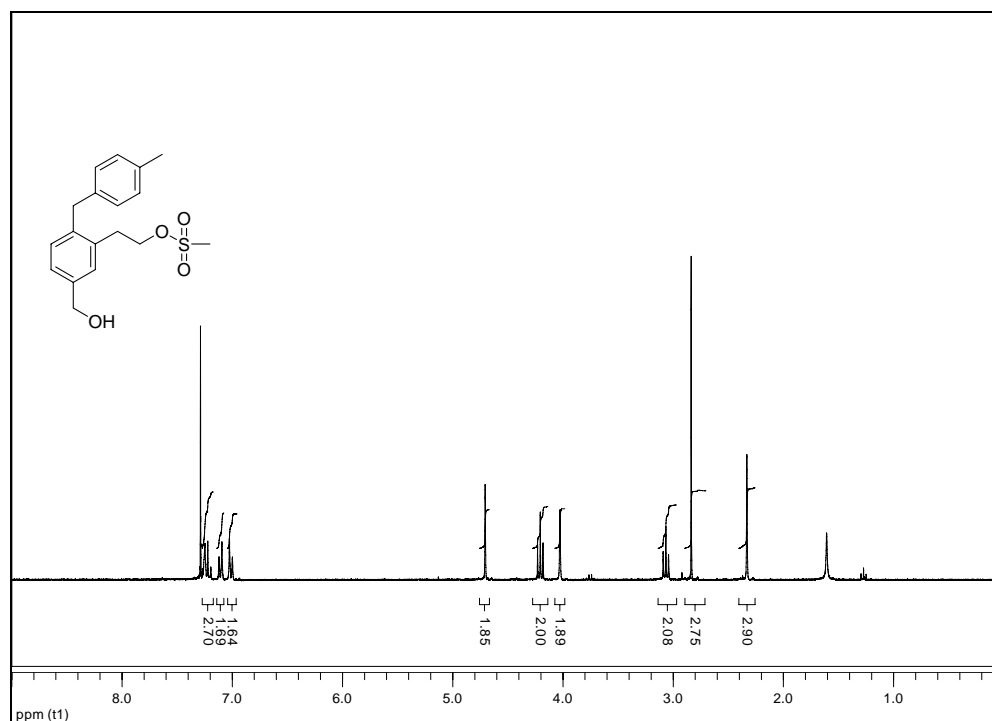
The crude methanesulfonic acid 2-[2-(4-methylbenzyl)-5-(tetrahydropyran-2-yloxymethyl)phenyl]ethyl ester (**5.12**), methanol (20 mL), TsOH (20 mg) were stirred at room temperature for 4 h. The reaction mixture was dilute with water. The aqueous mixture was extracted with CH_2Cl_2 (3×40 mL) and water(3×40 mL). The organic layer was dried (MgSO_4) and concentrated *in vacuo*. The crude product was purified via

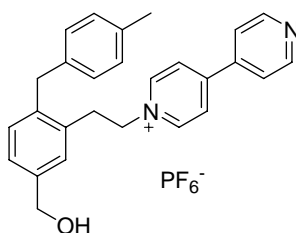
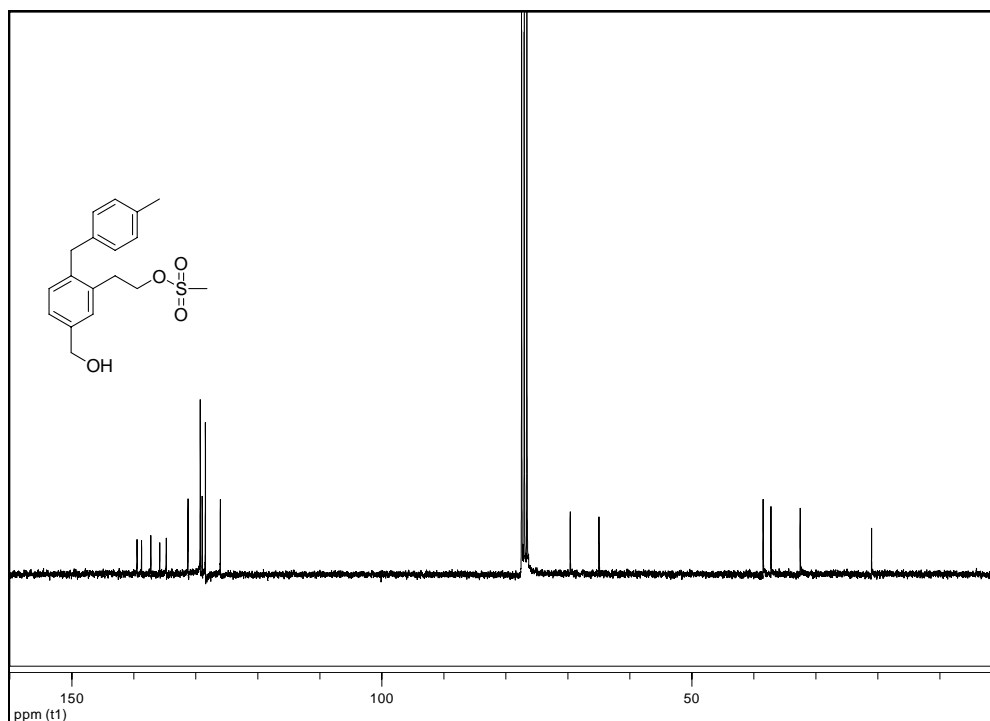
column chromatography [SiO_2 – petroleum ether – Et_2O (1:2), v/v] to give pure compound **5.13** (1.76 g, 81 % yield for two steps).

^1H NMR (CDCl_3 , 300 MHz): δ ppm 7.27-7.17 (m, 3H), 7.11 (d, $J = 7.86$ Hz, 2H), 7.01 (d, $J = 7.86$ Hz, 2H), 4.71 (s, 2H), 4.21 (t, $J = 7.34$ Hz, 2H), 4.03 (s, 2H), 3.07 (t, $J = 7.34$ Hz, 2H), 2.84 (s, 3H), 2.33 (s, 3H).

^{13}C NMR (CDCl_3 , 75 MHz): δ ppm 139.47, 138.75, 137.25, 135.82, 134.76, 131.25, 129.28, 128.96, 128.45, 126.04, 69.60, 64.97, 38.50, 37.23, 32.52, 21.00.

MS (ESI): m/z 357.1 ($\text{M}+\text{Na}^+$) ($\text{M} = \text{C}_{18}\text{H}_{22}\text{O}_4\text{S}$ requires 334.12).





**1-{2-[5-Hydroxymethyl-2-(4-methylbenzyl)phenyl]ethyl}-[4,4']bipyridinium
hexafluorophosphate (5.1a)**

Methanesulfonic acid 2-[5-hydroxymethyl-2-(4-methylbenzyl)phenyl]ethyl ester (**5.13**) (1.7 g, 5.1 mmol) and 4,4'-dipyridyl (6.4 g, 41 mmol) was stirred in acetonitrile (60 mL) at 65 °C for 5 days. Then the solvent was removed *in vacuo*. The residue was dissolved in water (10 mL) and NH_4PF_6^- (0.831 g, 5.1 mmol) in water (10 mL) was added to perform

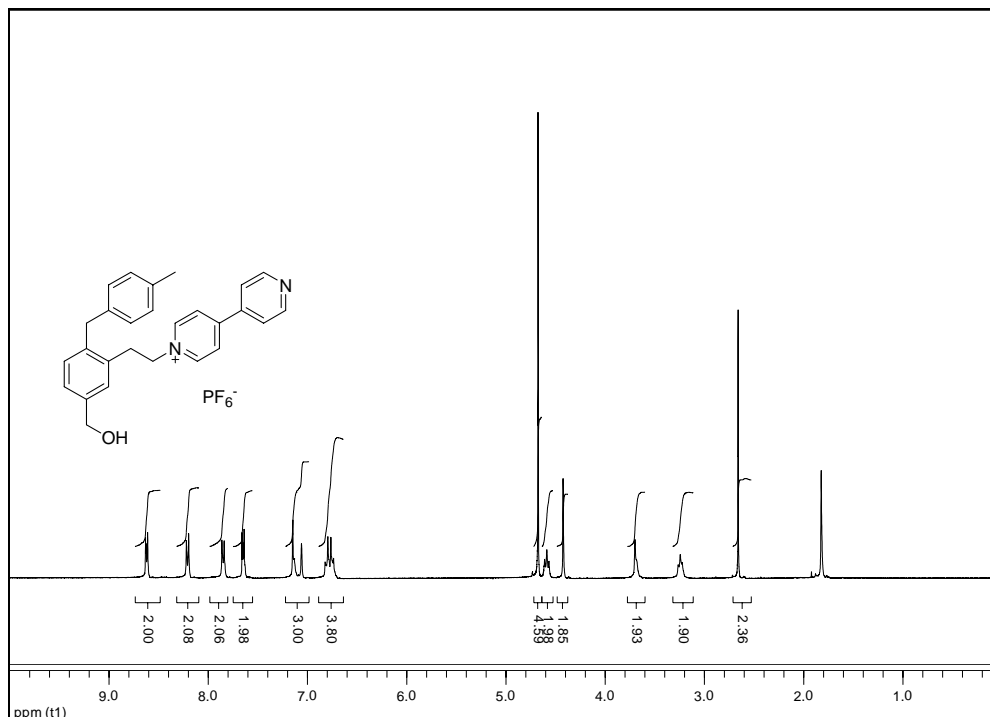
ion exchange. White precipitate appeared and blue oil residue was formed after overnight.

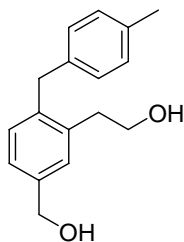
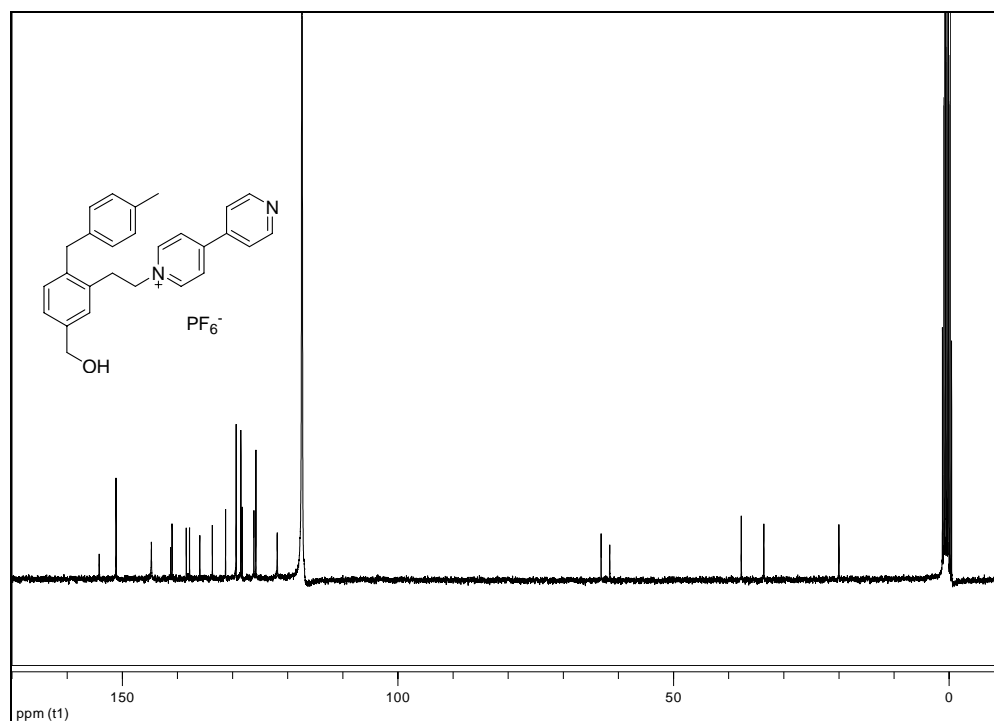
The water was decanted and a blue residue was obtained (2.2 g, 84 % yield).

¹H NMR (CD₃CN, 300 MHz): δ ppm 8.62 (m, 2H), 8.21 (m, 2H), 7.89 (m, 2H), 7.65 (m, 2H), 7.22-6.98 (m, 3H), 6.89-6.64 (m, 4H), 4.60 (t, *J* = 7.3 Hz, 2H), 4.42 (s, 2H), 4.01 (s, 2H), 3.25 (t, *J* = 7.3 Hz, 2H), 2.66 (s, 3H).

¹³C NMR (CD₃CN, 75 MHz) δ ppm 154.20, 151.14, 144.73, 141.22, 140.97, 138.39, 137.80, 135.93, 133.66, 131.26, 129.34, 128.49, 128.28, 126.12, 125.76, 121.89, 63.14, 61.57, 37.71, 33.62, 20.00.

MS (ESI): *m/z* 395.1 (*M*⁺) (*M*⁺ = C₂₇H₂₇N₂O⁺ requires 395.21).



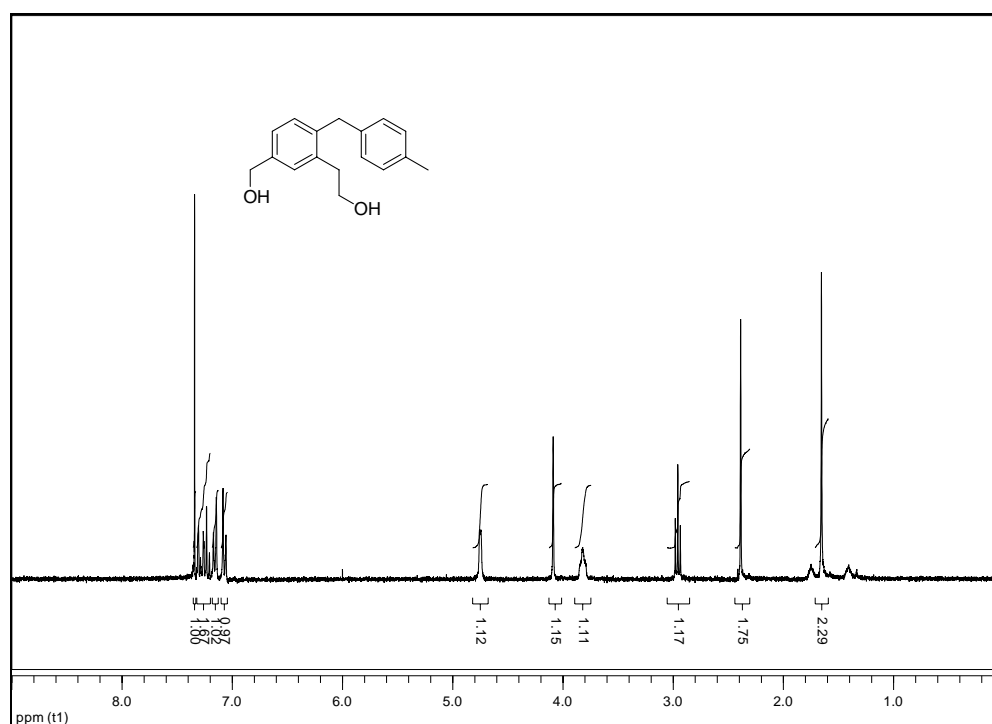


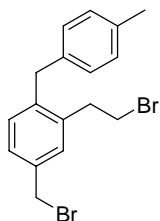
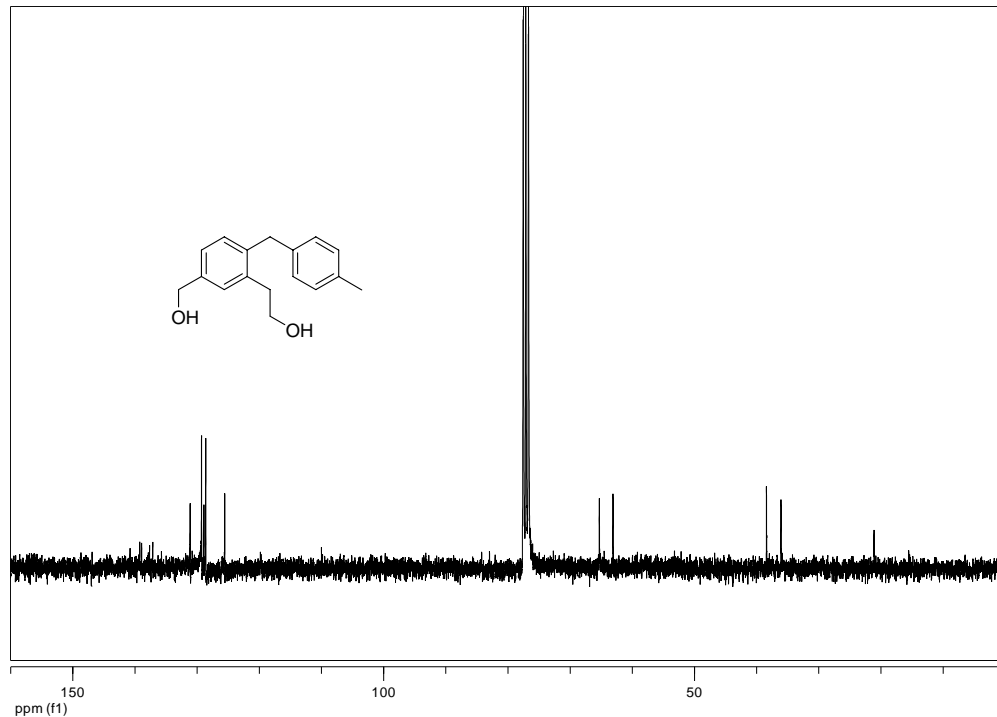
2-[5-Hydroxymethyl-2-(4-methylbenzyl)phenyl]ethanol (5.14)

2-[2-(4-Methylbenzyl)-5-(tetrahydropyran-2-yloxymethyl)phenyl]ethanol (**5.11**) (3.0 g, 8.81 mmol), and TsOH (35 mg) were dissolved in methanol (40 mL) and stirred for 4 h.⁶⁰ The reaction mixture was diluted with water and extracted with CH₂Cl₂ (40 mL × 3). The organic layer was treated with saturated NaHCO₃ (3 × 30 mL) and washed with water (3 × 30 mL). The organic portion was dried (MgSO₄) and concentrated *in vacuo* to give the colorless oil (2.3 g, quantitative %).

^1H NMR (CDCl_3 , 300 MHz): δ ppm 7.32-7.20 (m, 3H), 7.16 (d, $J = 7.80$ Hz, 2H), 7.07 (d, $J = 7.8$ Hz, 2H), 4.75 (s, 2H), 4.09 (s, 2H), 3.82 (t, $J = 6.80$ Hz, 2H), 2.96 (t, $J = 6.80$ Hz, 2H), 2.39 (s, 3H).

^{13}C NMR (CDCl_3 , 75 MHz): δ ppm 140.80, 139.24, 138.93, 137.66, 137.14, 131.13, 129.29, 128.91, 128.62, 125.56, 65.30, 63.10, 38.41, 36.08, 21.11.





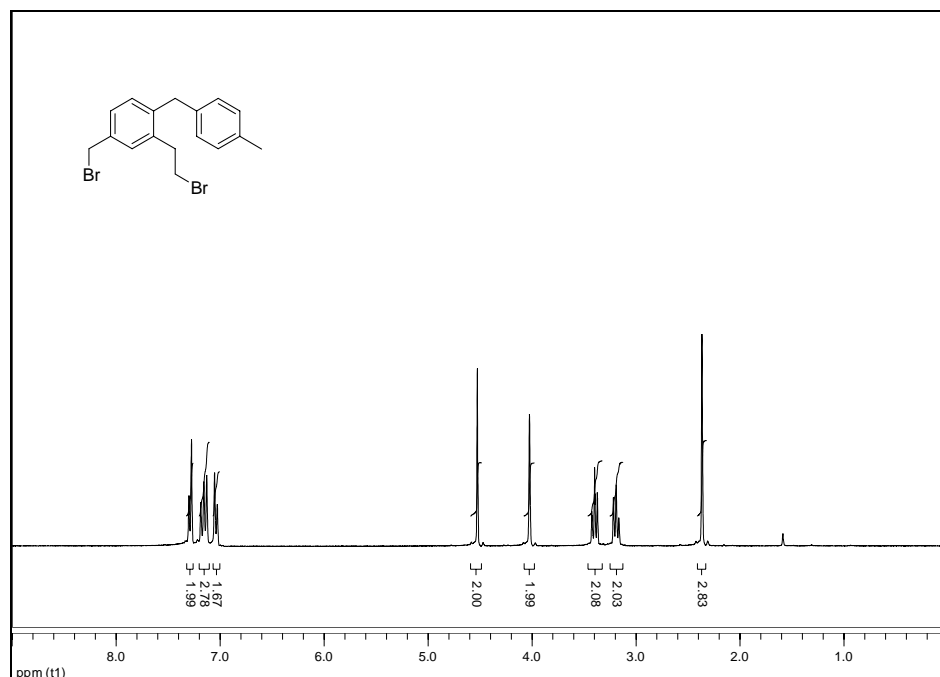
2-(2-Bromoethyl)-4-bromomethyl-1-(4-methylbenzyl)benzene (5.15)

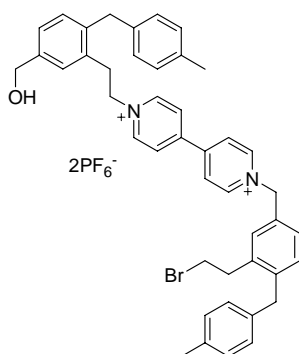
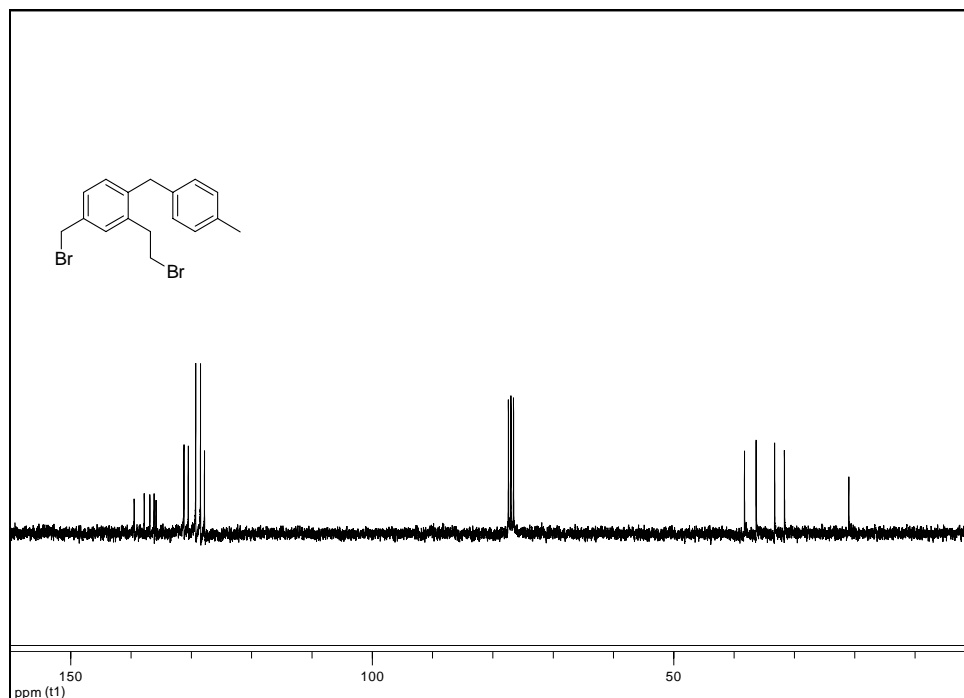
To a 100 mL flask was added PPh₃ (5.6 g, 21.5 mmol) followed by acetonitrile (20 mL). The mixture was cooled down to 0 °C and Br₂ (3.4 g, 21.5 mmol) in acetonitrile (10 mL) was added dropwise in 30 min until the solution maintained yellow for a while. The solution was allowed to warm up to room temperature. 2-[5-Hydroxymethyl-2-(4-methylbenzyl)phenyl]ethanol (**5.14**) (2.4 g, 9.36 mmol) was

added and minimum amount of acetonitrile (1 mL) was used to rinse the residue and added to the flask. The reaction mixture was stirred at room temperature overnight. Then the reaction mixture was filtered and the liquid was concentrated *in vacuo* to give a brown oil. The liquid was concentrated *in vacuo* to give the crude product. The crude product was purified with column chromatography [SiO₂ – petroleum ether – CH₂Cl₂ (1:1), v/v] to give the pure compound **5.15** (2.7 g, 75 %).

¹H NMR (CDCl₃, 300 MHz): δ ppm 7.32-7.25 (m, 3H), 7.20-7.11 (m, 2H), 7.04 (d, *J* = 7.84 Hz, 2H), 4.53 (s, 2H), 4.02 (s, 2H), 3.39 (t, *J* = 7.73 Hz, 2H), 3.19 (t, *J* = 7.73 Hz, 2H), 2.38 (s, 3H)

¹³C NMR (CDCl₃, 75 MHz): δ ppm 137.79, 136.86, 136.16, 135.84, 131.21, 130.49, 129.26, 128.47, 127.81, 38.28, 36.35, 33.29, 31.66, 20.99.





Compound 5.16

1-{2-[5-Hydroxymethyl-2-(4-methylbenzyl)phenyl]ethyl}-[4,4']bipyridinium

hexafluorophosphate (**5.1a**) (0.800 g, 1.63 mmol) and

2-(2-bromoethyl)-4-bromomethyl-1-(4-methylbenzyl)benzene (**5.15**) (1.24 g, 3.25 mmol)

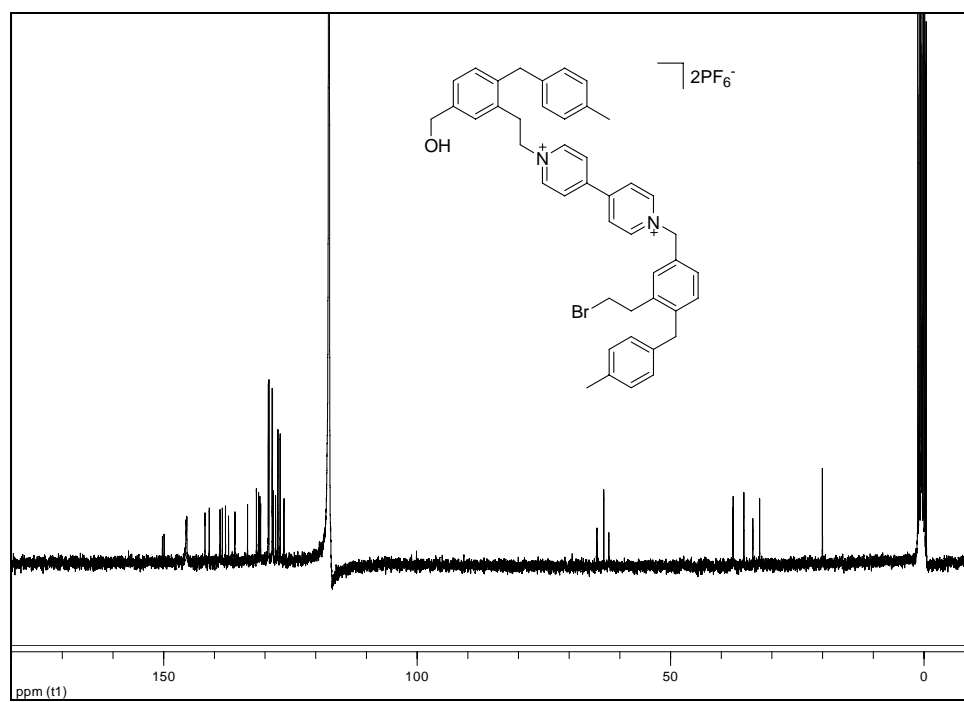
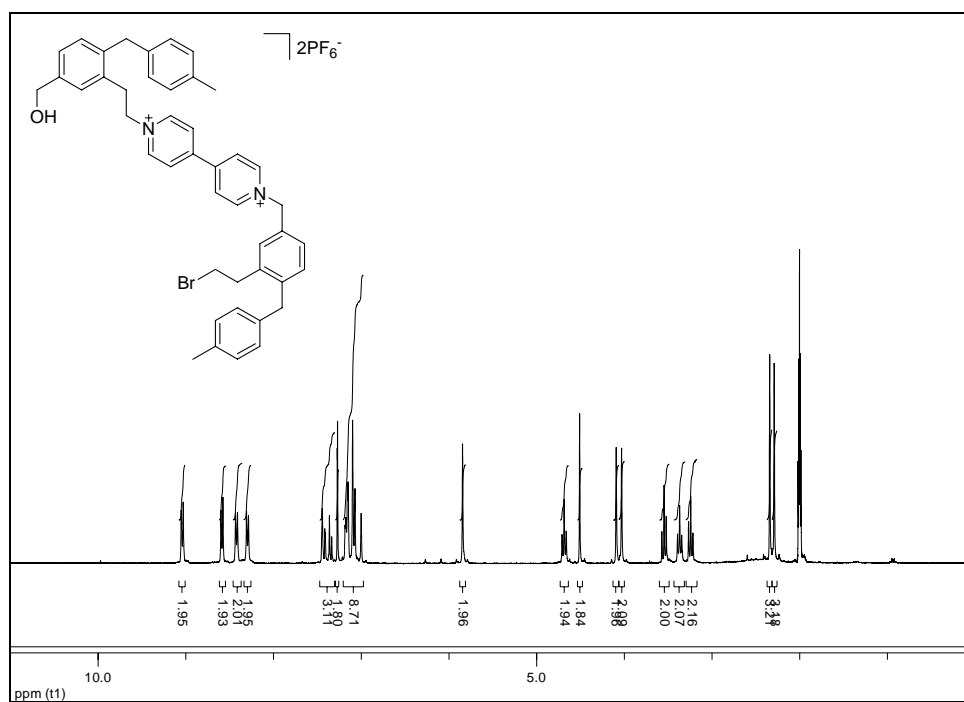
was dissolved in acetonitrile (30 mL). The mixture was heated at 40 °C for 1 day and at

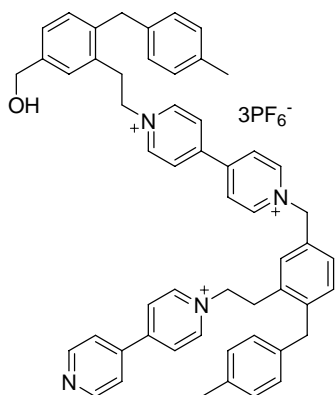
55 °C for 1 day. The solvent was removed *in vacuo*. The excess **5.15** was removed with petroleum ether a few times. The residue was dissolved in methanol (5 mL) and NH_4PF_6^- (0.531 g, 3.26 mmol) in water (5 mL) was added to perform anion exchange. The methanol was removed *in vacuo* and the yellow solid was obtained from the aqueous portion by filtration (0.81 g, 96 %).

^1H NMR (CD_3CN , 300 MHz): δ ppm 9.04 (d, $J = 6.90$ Hz, 2H), 8.59 (d, $J = 6.90$ Hz, 2H), 8.42 (d, $J = 6.90$ Hz, 1H), 8.30 (d, $J = 6.90$ Hz, 2H), 7.47-7.30 (m, 3H), 7.27 (d, $J = 1.02$ Hz, 2H), 7.20-6.98 (m, 9H), 5.84 (s, 2H), 4.69 (t, $J = 7.17$ Hz, 2H), 4.51 (s, 2H), 4.09 (s, 2H), 4.03 (s, 2H), 3.55 (t, $J = 7.41, 7.41$ Hz, 2H), 3.36 (t, $J = 7.17$ Hz, 2H), 3.24 (t, $J = 7.41$ Hz, 1H), 2.33 (s, 3H), 2.30 (s, 3H).

^{13}C NMR (CD_3CN , 75 MHz): δ ppm 150.24, 149.91, 145.60, 145.57, 145.48, 145.46, 145.43, 141.84, 141.01, 138.87, 138.42, 137.80, 137.19, 135.97, 135.93, 133.44, 131.69, 131.27, 131.00, 130.87, 129.35, 129.23, 128.58, 128.53, 128.37, 127.91, 127.45, 127.01, 126.26, 64.50, 63.16, 62.16, 37.69, 37.63, 35.52, 33.75, 32.41, 20.03.

MS (ESI): m/z 841.2 ($\text{M} + \text{PF}_6^-$) $^+$, 843.2 ($\text{M} + 2 + \text{PF}_6^-$) $^+$, 348.1 (M) $^{2+}$ ($\text{M} = \text{C}_{44}\text{H}_{45}\text{BrN}_2\text{O}^{2+}$ requires 696.27).





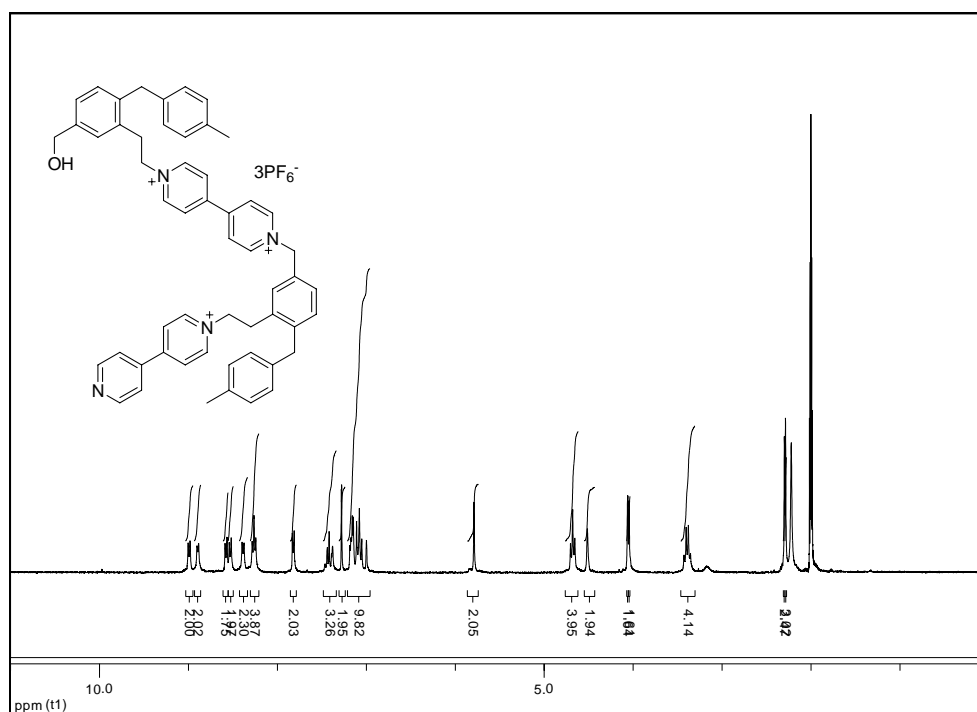
Compound 5.17

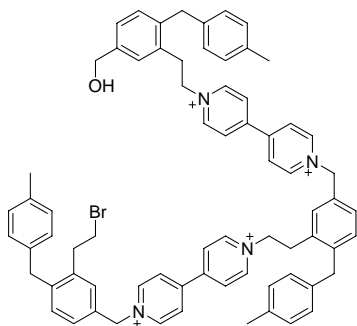
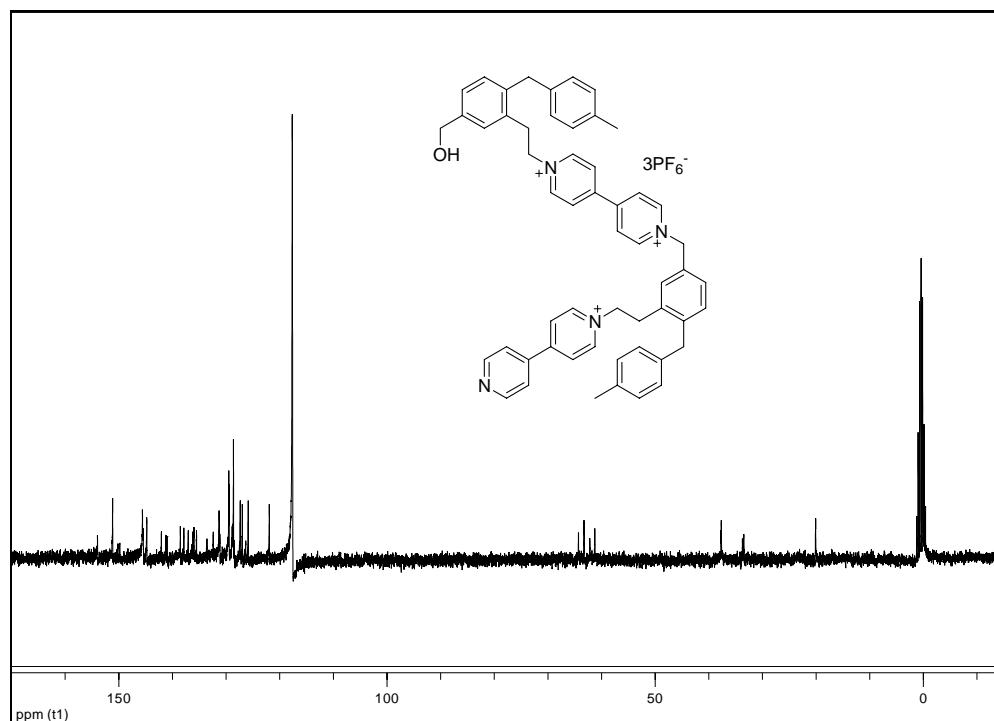
Compound **5.16** (0.470 g, 0.476 mmol), sodium iodide (0.143 g, 0.952 mmol) and 4,4'-dipyridyl (1.1 g, 7.14 mmol) were dissolved in acetonitrile (30 mL). The mixture was heated at 60 °C for 5 days. The reaction mixture was cooled down to room temperature and the solvent was removed *in vacuo*. The excess 4,4'-dipyridyl was removed with EtOAc a few times until no trace of 4,4'-dipyridyl was found in the ^1H NMR spectrum. The solid was dissolved in methanol/acetone (1:1, 10 mL) and NH_4PF_6^- (0.232 g, 1.43 mmol) in water (5 mL) was added to perform anion exchange. The brown precipitate was collected by filtration (0.410 g, 71 %).

^1H NMR (CD_3CN , 300 MHz): δ ppm 8.99 (d, $J = 6.52$ Hz, 2H), 8.90 (d, $J = 5.89$ Hz, 2H), 8.58 (d, $J = 6.66$ Hz, 2H), 8.53 (d, $J = 6.79$ Hz, 2H), 8.39 (d, $J = 6.59$ Hz, 2H), 8.26 (t, $J = 6.17$ Hz, 2H), 7.82 (m, 2H), 7.41 (m, 3H), 7.28 (d, $J = 1.00$ Hz, 2H), 7.21-6.96 (m, 9H), 5.79 (s, 2H), 4.68 (t, $J = 7.06$ Hz, 2H), 4.52 (s, 2H), 4.06 (s, 2H), 4.05 (s, 2H), 3.39 (m, 2H), 2.30 (s, 3H), 2.29 (s, 3H).

^{13}C NMR (CD_3CN , 75 MHz): δ ppm 153.97, 151.15, 150.16, 149.82, 145.59, 144.78, 142.06, 141.20, 140.96, 138.52, 137.87, 137.05, 136.21, 135.99, 135.51, 133.57, 132.39, 131.30, 131.15, 129.49, 129.42, 128.86, 128.48, 127.36, 126.97, 126.33, 125.87, 121.94, 64.30, 63.26, 62.18, 61.25, 37.67, 33.74, 33.47, 20.07.

MS (ESI): m/z 257.85 (M) $^{3+}$, 459.20 ($\text{M}+\text{PF}_6^-$) $^{2+}$ ($\text{M}=\text{C}_{54}\text{H}_{53}\text{N}_4\text{O}^{3+}$ requires 773.42).





Compound 5.18

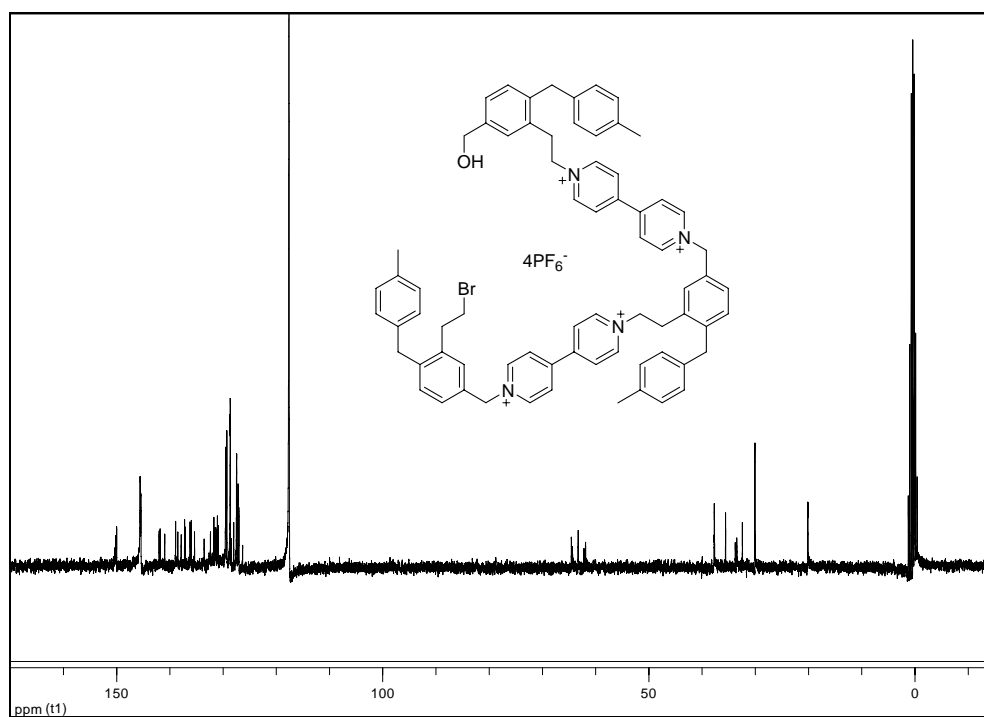
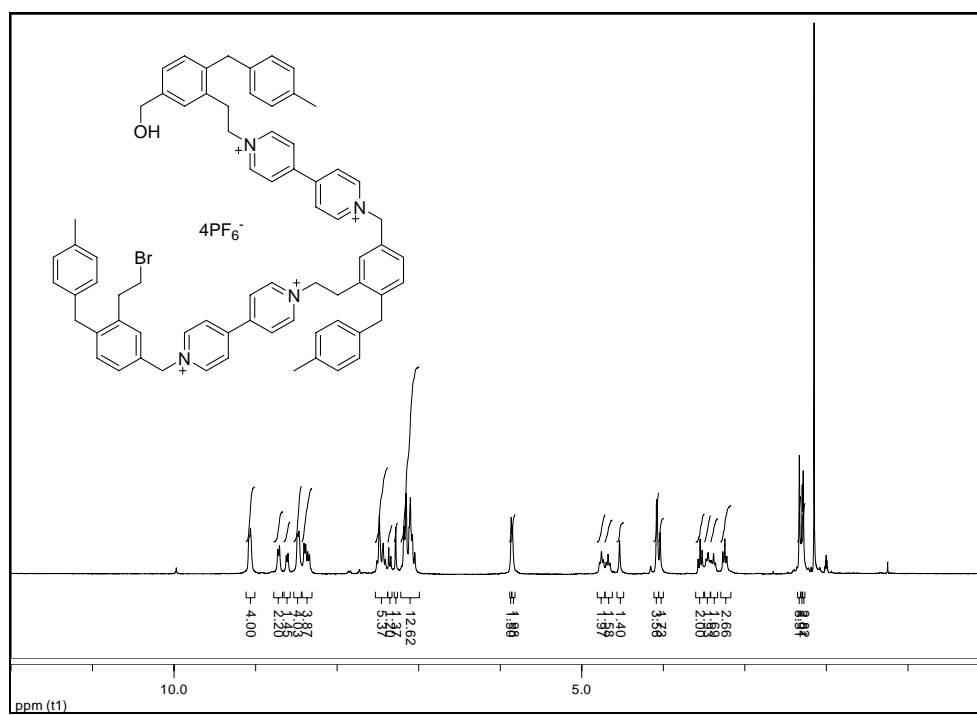
Compound **5.17** (0.200 g, 0.165 mmol) and 2-(2-bromoethyl)-4-bromomethyl-1-(4-methylbenzyl)benzene (**5.15**) (0.126 g, 0.330 mmol) was dissolved in acetonitrile (10 mL). The reaction mixture was heated at 40 °C for 1 day and at 55 °C for 1 day. The solvent was removed *in vacuo*. The excess **5.15** was removed with petroleum ether **for** a few times. The residue was dissolved in methanol (5

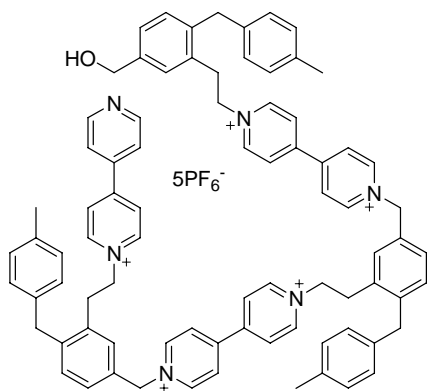
mL) and NH_4PF_6^- (0.531 g, 3.26 mmol) in water (3 mL) was added to perform anion exchange. The methanol was removed *in vacuo* and the brown solid was isolated by filtration from the aqueous portion (0.220 g, 81 %).

^1H NMR (CD_3CN , 300 MHz): δ ppm 9.07 (m, 4H), 8.72 (d, $J = 6.34$ Hz, 2H), 8.61 (d, $J = 6.45$ Hz, 2H), 8.48 (m, 4H), 8.37 (m, 4H), 7.46 (m, 5H), 7.35 (d, $J = 7.77$ Hz, 1H), 7.28 (s, 1H), 7.22-6.99 (m, 12H), 5.86 (s, 1H), 5.86 (s, 2H), 5.84 (s, 2H), 4.76 (t, $J = 7.31$ Hz, 2H), 4.68 (t, $J = 7.08$ Hz, 2H), 4.54 (s, 2H), 4.08 (s, 2H), 4.07 (s, 2H), 4.04 (s, 2H), 3.55 (t, $J = 7.47$ Hz, 2H), 3.45 (t, $J = 7.47$ Hz, 2H), 3.38 (t, $J = 7.11$ Hz, 2H), 3.25 (t, $J = 7.47$ Hz, 2H), 2.33 (s, 1H), 2.30 (s, 3H), 2.29 (s, 3H), 2.28 (s, 3H).

^{13}C NMR (CD_3CN , 75 MHz): δ ppm 150.19, 150.01, 145.60, 145.45, 142.02, 141.82, 140.97, 138.92, 138.51, 137.87, 137.24, 137.10, 136.21, 135.97, 135.37, 133.56, 132.38, 131.73, 131.47, 131.33, 131.07, 130.92, 129.50, 129.43, 129.30, 128.65, 128.62, 128.46, 128.01, 127.45, 127.20, 127.03, 126.34, 64.56, 64.37, 63.29, 62.19, 61.90, 37.71, 35.58, 33.77, 33.48, 32.44, 30.07, 20.15.

MS (ESI): m/z 407.21 ($\text{M} + \text{PF}_6^-$) $^{3+}$, 682.31 ($\text{M} + 2\text{PF}_6^-$) $^{2+}$ ($\text{M} = \text{C}_{71}\text{H}_{71}\text{BrN}_4\text{O}^{4+}$ requires 1074.48).





Compound 5.2b

Compound **5.18** (0.220 g, 0.133 mmol), sodium iodide (0.040 g, 0.266 mmol) and 4,4'-dipyridyl (0.317 g, 1.995 mmol) were dissolved in acetonitrile (15 mL). The mixture was heated at 60 °C for 4 days. The reaction mixture was cooled down to room temperature and the solvent was removed *in vacuo*. The excess 4,4'-dipyridyl was removed with EtOAc a few times until no trace of 4,4'-dipyridyl was found in the ^1H NMR spectrum. The solid was dissolved in methanol/acetone (1:1, 5 mL) and NH_4PF_6^- (0.108 g, 0.665 mmol) in water (3 mL) was added to perform anion exchange. The brown precipitate was collected by filtration (0.200 g, 84 %).

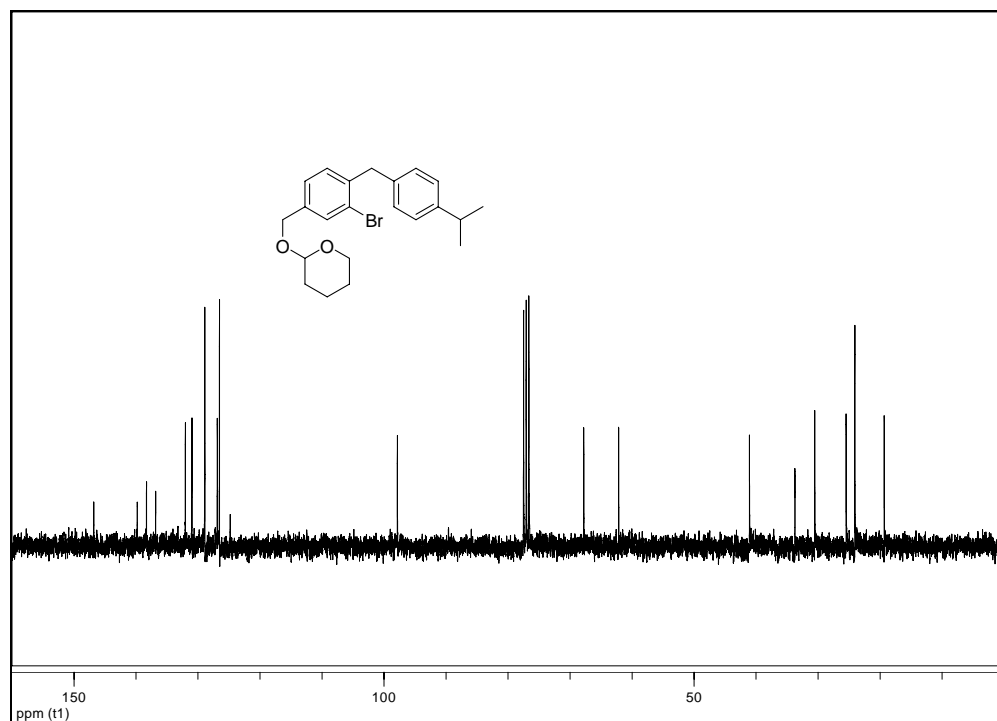
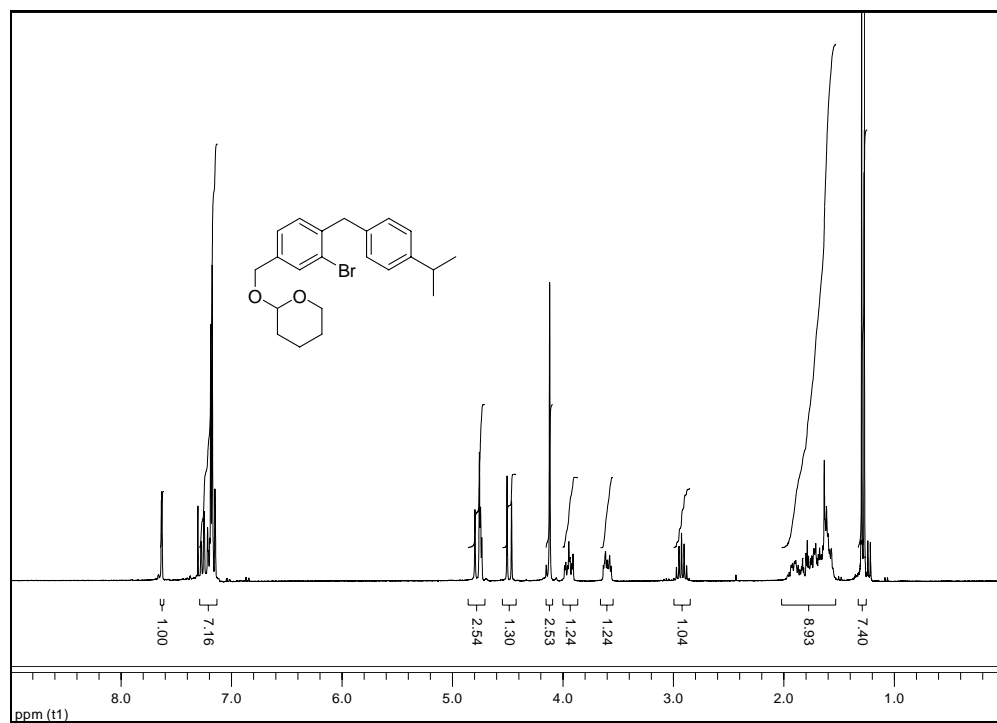
^1H NMR (CD_3CN , 300 MHz): δ ppm 9.03 (d, $J = 7.07$ Hz, 2H), 9.00 (d, $J = 7.07$ Hz, 2H), 8.87 (dd, $J = 4.42, 1.71$ Hz, 2H), 8.72 (d, $J = 6.95$ Hz, 2H), 8.57 (d, $J = 7.07$ Hz, 2H), 8.51 (d, $J = 7.07$ Hz, 2H), 8.42 (dd, $J = 6.95, 2.83$ Hz, 4H), 8.35 (d, $J = 6.95$ Hz, 2H), 8.30 (d, $J = 6.95$ Hz, 2H), 8.24 (d, $J = 6.95$ Hz, 2H), 7.81 (dd, $J = 4.42, 1.71$ Hz, 2H), 7.50-7.32 (m, 7H), 7.27 (d, $J = 1.05$ Hz, 2H), 7.20-7.03 (m, 11H), 6.91 (s, 1H), 5.83

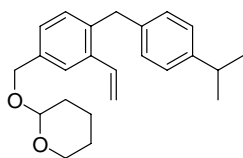
15 mL flask and flushed with nitrogen for 30 min. Dry THF (5 mL) was added via syringe followed by addition of isopropylphenylmagnesium bromide solution (4 mL, 0.5 M) at -78 °C. The mixture was allowed to warm to room temperature and stirred overnight. The reaction was quenched with water. The orange suspension was filtered with Celite. The organic layer was extracted with Et₂O (3 × 10 mL) and washed with water (3 × 10 mL). The organic layer was dried (MgSO₄) and concentrated *in vacuo*. The crude product was purified with column chromatography [SiO₂ – petroleum ether – CH₂Cl₂ (1:1), v/v] to give pure compound **5.20** (0.36 g, 60 % yield).

¹H NMR (CDCl₃, 300 MHz): δ ppm 7.63 (d, *J* = 1.4 Hz, 1H), 7.29-7.11 (m, 6H), 4.76 (m, 2H), 4.49 (d, *J* = 12.2 Hz, 1H), 4.12 (s, 2H), 3.95 (m, 1H), 3.60 (m, 1H), 2.93 (m, 1H), 2.03-1.52 (m, 6H), 1.30 (d, *J* = 6.9 Hz, 6H).

¹³C NMR (CDCl₃, 75 MHz): δ ppm 146.81, 139.78, 138.30, 136.82, 132.02, 130.96, 128.89, 126.88, 126.54, 124.80, 97.84, 67.78, 62.15, 41.06, 33.73, 30.53, 25.46, 24.06, 19.32.

MS (ESI): *m/z* 425.1 (M+Na⁺), 427.1 (M+2+Na⁺) (M= C₂₂H₂₇BrO₂ require 402.12).





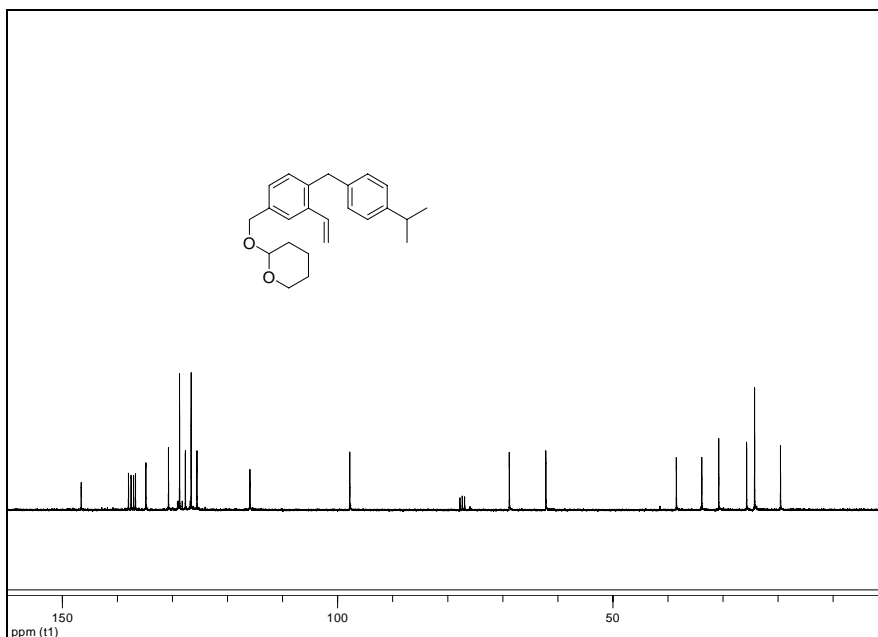
2-[4-(4-Isopropylbenzyl)-3-vinylbenzyloxy]tetrahydropyran (5.21)

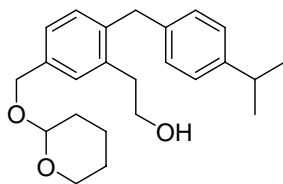
PdCl₂(dppf) (0.857 g, 1.05 mmol) was added to a 250 mL three-neck flask with a condenser. The flask was flushed with nitrogen for 30 min. Dry THF (100 mL) followed by 2-[3-bromo-4-(4-isopropylbenzyl)benzyloxy]tetrahydropyran (8.5 g, 21 mmol) in THF (30 mL) was added to the flask.⁵⁷ The mixture was cooled down to -78 °C and vinylmagnesium bromide (42 mL, 1.0 M) was added slowly. The reaction mixture was allowed to warm to room temperature in 2 h and refluxed for 24 h. The reaction was quenched with water (50 mL) and the aqueous mixture was extracted with Et₂O (3 × 50 mL) and washed with water (3 × 50 mL). The organic layer was dried (MgSO₄) and concentrated *in vacuo*. The crude product was purified with column chromatography [SiO₂ – petroleum ether – CH₂Cl₂ (1:1), v/v] to give pure compound **5.21** (6.1 g, 83 % yield).

¹H NMR (CDCl₃, 300 MHz): δ ppm 7.72 (d, *J* = 1.29 Hz, 1H), 7.49-7.19 (m, 6H), 7.13 (dd, *J* = 17.4, 11.0 Hz, 1H), 5.83 (dd, *J* = 17.4, 1.3 Hz, 1H), 5.41 (dd, *J* = 11.0, 1.3 Hz, 1H), 4.96 (d, *J* = 11.9 Hz, 1H), 4.90 (m, 1H), 4.66 (d, *J* = 11.9 Hz, 1H), 4.18 (s, 2H), 4.11 (m, 1H), 3.71 (m, 1H), 3.01 (m, 1H), 2.12-1.61 (m, 6H), 1.39 (d, *J* = 6.9 Hz, 6H).

¹³C NMR (CDCl₃, 75 MHz): δ ppm 146.57, 137.98, 137.50, 137.05, 136.71, 134.82,

MS (ESI): m/z 373.2 (M+Na⁺) (M= C₂₄H₃₀O₂ requires 350.22).



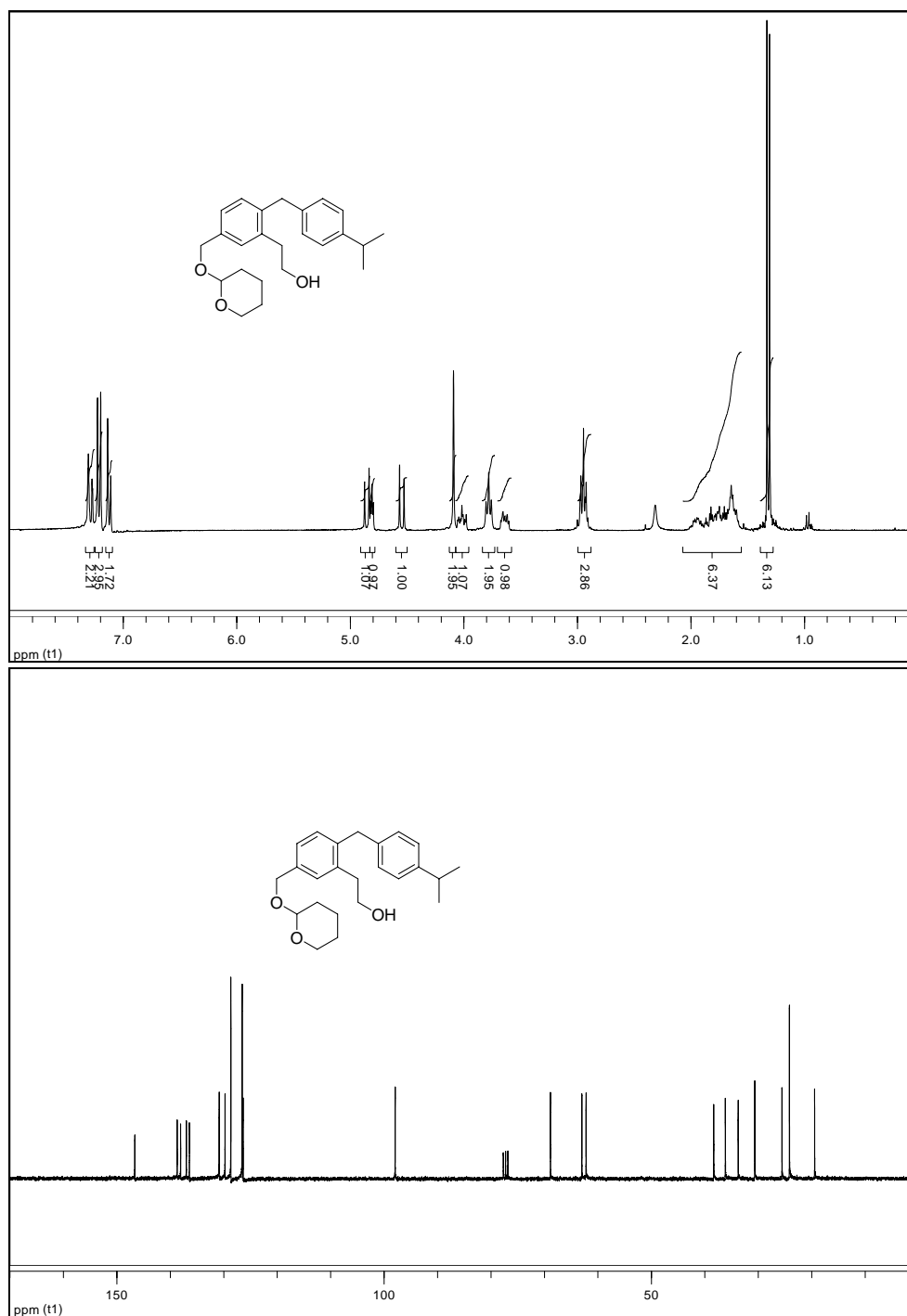


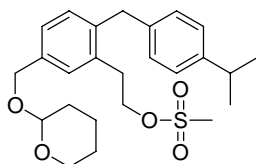
2-[2-(4-Isopropylbenzyl)-5-(tetrahydropyran-2-yloxymethyl)phenyl]ethanol (5.22)

BH₃.THF (27.6 mL, 1.0 M) was added to a 100 mL flask via syringe and cooled down to 0 °C, followed by cyclohexene (5.6 mL, 55.2 mmol). The mixture was stirred for 1 h at 0 °C. 2-[4-(4-Isopropylbenzyl)-3-vinylbenzyloxy]tetrahydropyran (6.1 g, 17.4 mmol) in THF (30 mL) was added and the reaction mixture was allowed to warm to room temperature and stirred overnight. NaOH (30 mL, 3N) and H₂O₂ (25 mL, 30 %) were added sequentially and the mixture continued to stir for 3 h. The reaction mixture was extracted with Et₂O (3 × 50 mL) and washed with water (3 × 50 mL). The organic layer was dried (MgSO₄) and concentrated *in vacuo* to give crude product (10.8 g). A portion of crude product (2.9 g) was purified with column chromatography [SiO₂ – petroleum ether – Et₂O (10:1), v/v] to give pure compound **5.22** (1.4 g, 81 % yield).

¹H NMR (CDCl₃, 300 MHz): δ ppm 7.36-7.06 (m, 7H), 4.85 (d, *J* = 11.8 Hz, 1H), 4.81 (m, 1H), 4.55 (d, *J* = 11.8 Hz, 1H), 4.09 (s, 1H), 4.02 (m, 1H), 3.78 (t, *J* = 6.9 Hz, 2H), 3.64 (m, 1H), 3.01-2.89 (m, 3H), 2.05-1.55 (m, 6H), 1.32 (d, *J* = 6.9 Hz, 6H). **¹³C NMR** (CDCl₃, 75 MHz): δ ppm 146.63, 138.69, 138.06, 136.97, 136.41, 130.84, 129.75, 128.66, 126.55, 126.37, 97.92, 68.88, 63.00, 62.21, 38.33, 36.16, 33.75, 30.65, 25.56, 24.17, 19.45.

MS (ESI): m/z 391.2 ($M+Na^+$) ($M = C_{24}H_{32}O_3$ requires 368.24).





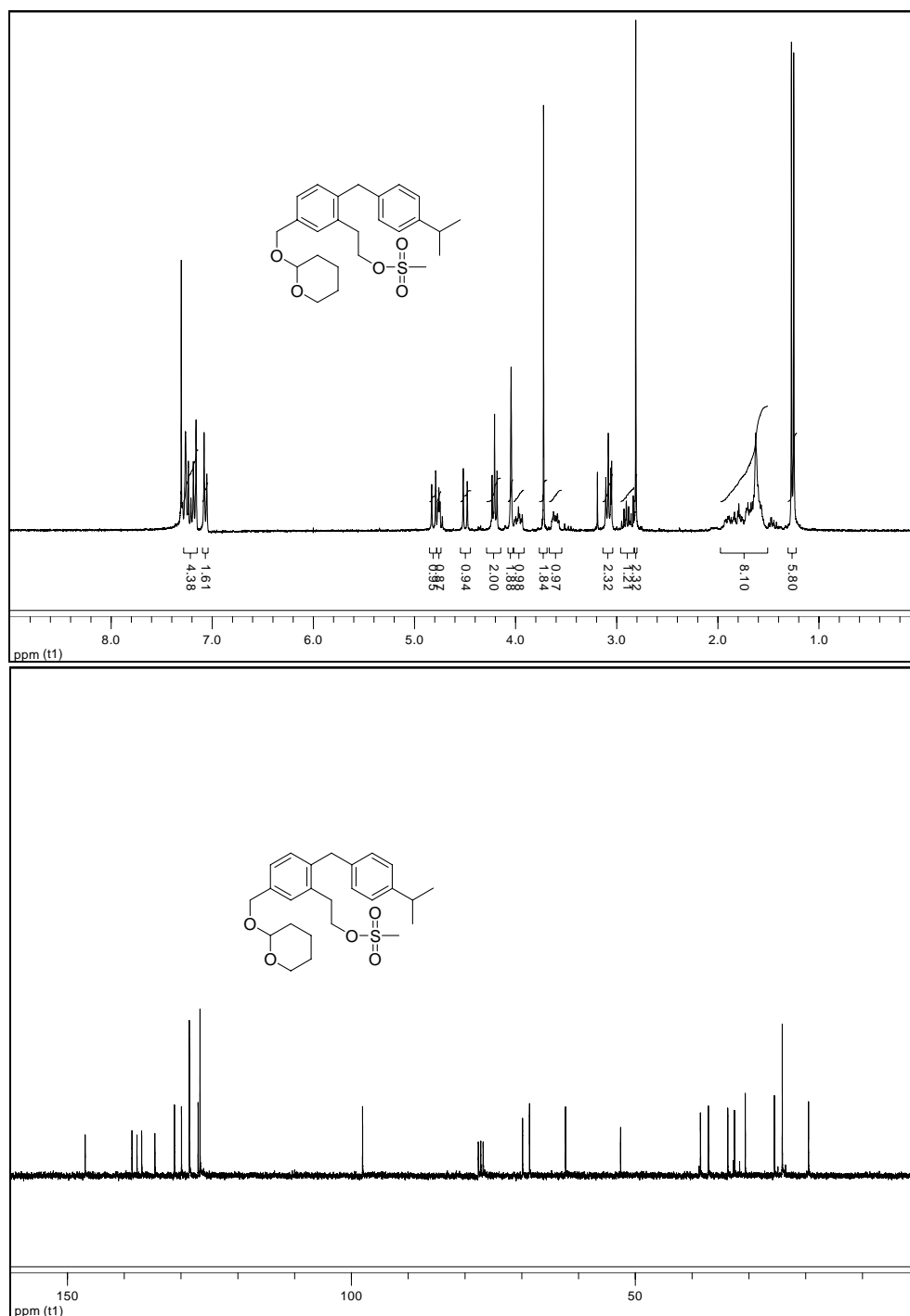
Methanesulfonic acid 2-[2-(4-isopropylbenzyl)-5-(tetrahydropyran-2-yloxymethyl)phenyl]ethyl ester (5.23)

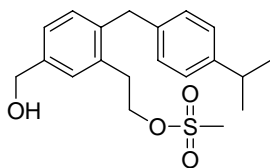
2-[2-(4-Isopropylbenzyl)-5-(tetrahydropyran-2-yloxymethyl)phenyl]ethanol (1.2 g, 3.26 mmol) was flushed with nitrogen for 30 min. CH_2Cl_2 (18 mL) followed by Et_3N (1.4 mL, 9.77 mmol) was added.⁵⁹ The mixture was cooled down to 0 °C and methanesulfonyl chloride (0.9 mL, 6.51 mmol) was added via syringe. The solution was stirred at 0 °C for 1 h and at room temperature for 2 h, respectively. The reaction was quenched with water (20 mL). The aqueous mixture was extracted with CH_2Cl_2 (3×20 mL) and washed with water (3×20 mL). The organic layer was dried (MgSO_4) and concentrated *in vacuo* to give crude product without further purification (1.4 g, 96%).

^1H NMR (CDCl_3 , 300 MHz): δ ppm 7.28-7.20 (m, 3H), 7.17 (d, $J = 8.1$ Hz, 2H), 7.07 (d, $J = 8.1$ Hz, 2H), 4.81 (d, $J = 11.8$ Hz, 1H), 4.76 (m, 1H), 4.50 (d, $J = 11.8$ Hz, 1H), 4.21 (t, $J = 7.31$ Hz, 2H), 4.04 (s, 2H), 4.01-3.92 (m, 1H), 3.65-3.55 (m, 1H), 3.07 (t, $J = 7.31$ Hz, 2H), 2.90 (m, 1H), 2.81 (s, 3H), 1.98-1.51 (m, 6H), 1.26 (d, $J = 6.9$ Hz, 6H).

^{13}C NMR (CDCl_3 , 75 MHz): δ ppm 146.88, 138.63, 137.75, 136.92, 134.60, 131.15, 129.91, 128.53, 126.98, 126.65, 98.02, 69.85, 68.63, 62.29, 52.59, 38.53, 37.12, 33.71, 32.52, 30.63, 25.50, 24.11, 19.49.

MS (ESI): m/z 469.2 ($M+Na^+$) ($M=C_{25}H_{34}O_5S$ requires 446.21).





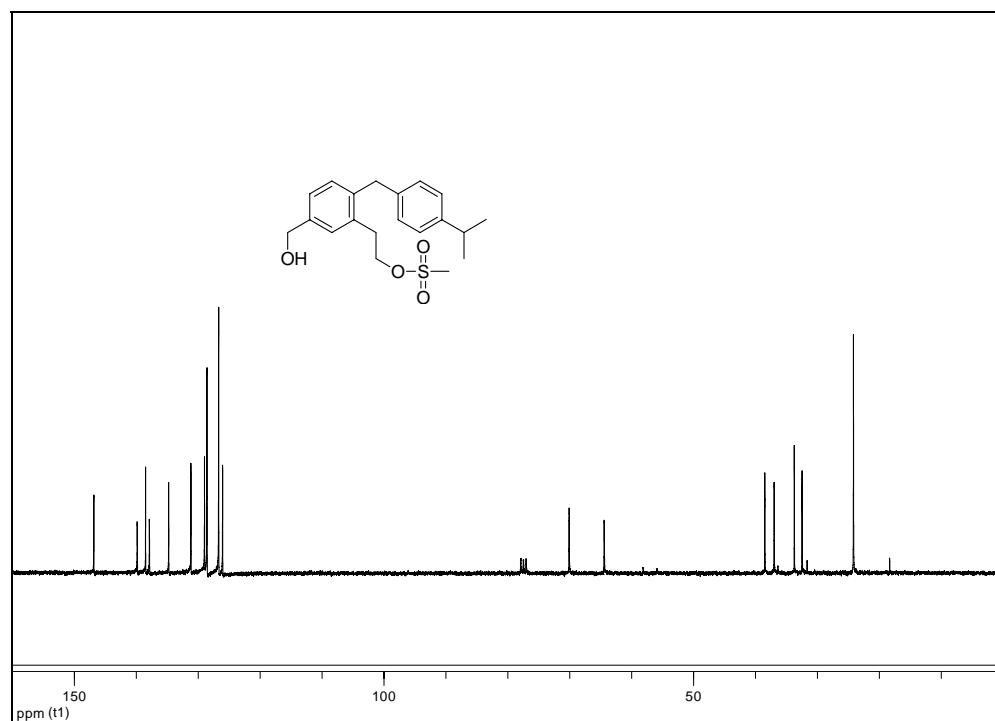
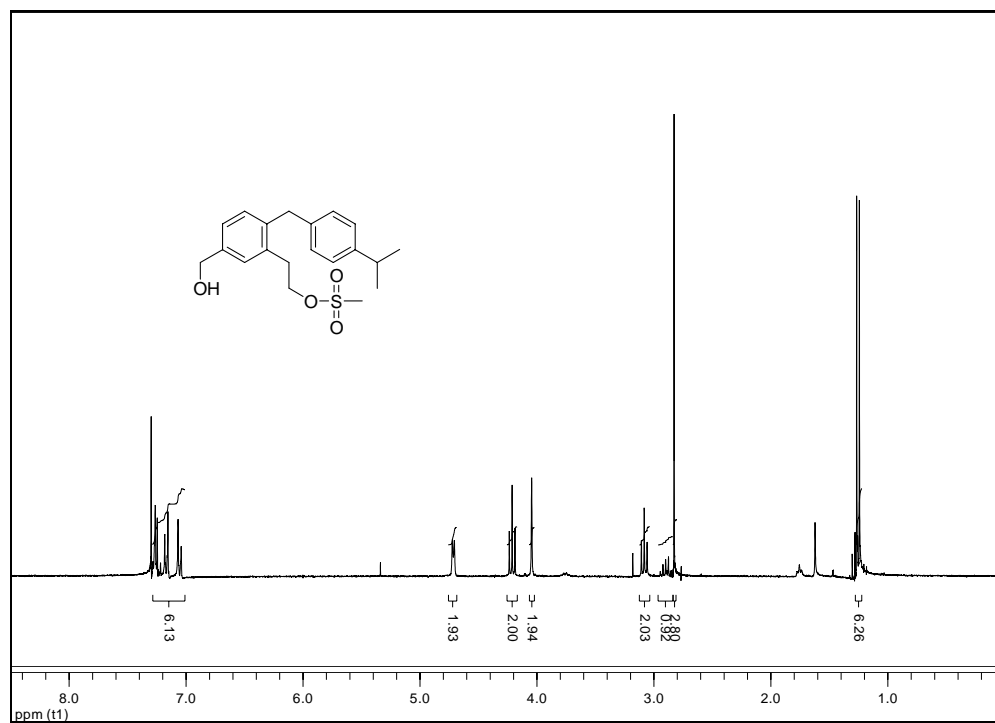
Methanesulfonic acid 2-[5-hydroxymethyl-2-(4-isopropylbenzyl)phenyl]ethyl ester
(5.24)

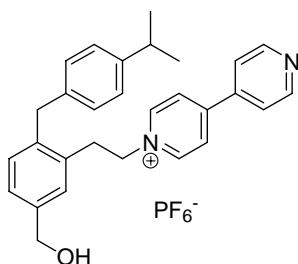
Methanesulfonic acid 2-[2-(4-isopropylbenzyl)-5-(tetrahydropyran-2-yloxymethyl)-phenyl] ethyl ester (1.4 g, 3.13 mmol), methanol (20 mL), TsOH (15 mg) were stirred for 4 h at room temperature.⁶⁰ The reaction mixture was dilute with water. The aqueous mixture was extracted with CH₂Cl₂ (3 × 20 mL) and water (3 × 20 mL). The organic layer was dried and concentrated *in vacuo*. The crude product was purified via column chromatography [SiO₂ – petroleum ether – Et₂O (1:2), v/v] to give pure compound **5.24** (0.84 g, 74 % yield).

¹H NMR (CDCl₃, 300 MHz): δ ppm 7.29-7.21 (m, 3H), 7.17 (d, *J* = 8.3 Hz, 2H), 7.05 (d, *J* = 8.3 Hz, 2H), 4.71 (d, *J* = 5.1 Hz, 2H), 4.21 (t, *J* = 7.3 Hz, 2H), 4.04 (s, 1H), 3.08 (t, *J* = 7.3 Hz, 2H), 2.98-2.85 (m, 1H), 2.82 (s, 3H), 1.29-1.20 (d, *J* = 6.9 Hz 6H).

¹³C NMR (CDCl₃, 75 MHz): δ ppm 146.86, 139.86, 138.50, 137.89, 134.77, 131.18, 128.98, 128.59, 126.75, 126.06, 70.10, 64.44, 38.49, 36.99, 33.73, 32.47, 24.17.

MS (ESI): *m/z* 385.2 (M+Na⁺) (M= C₂₀H₂₆O₄S requires 362.16).





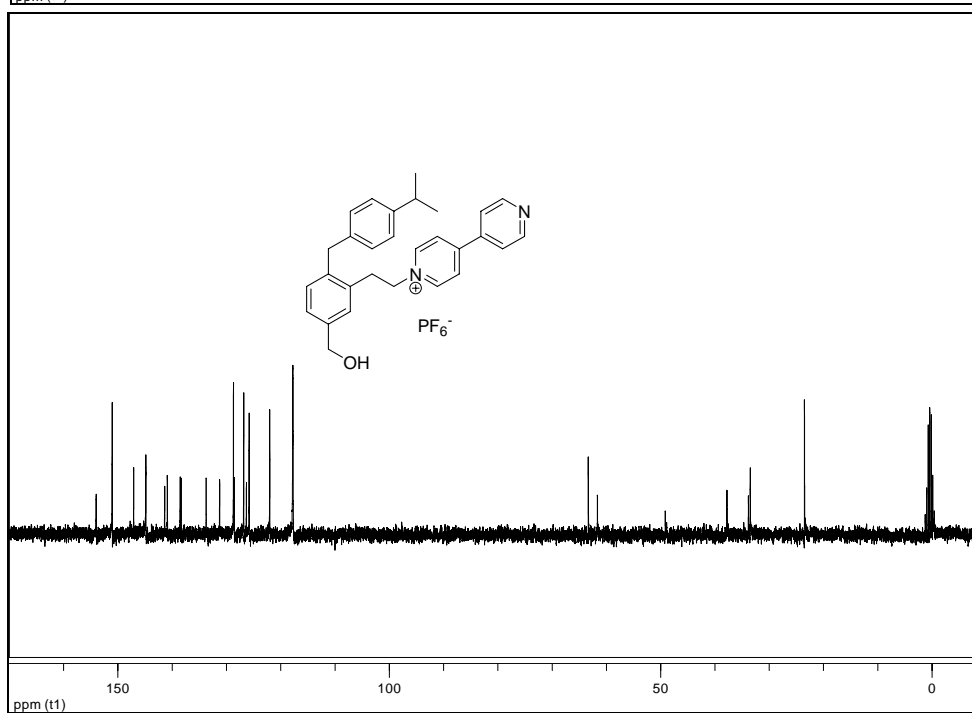
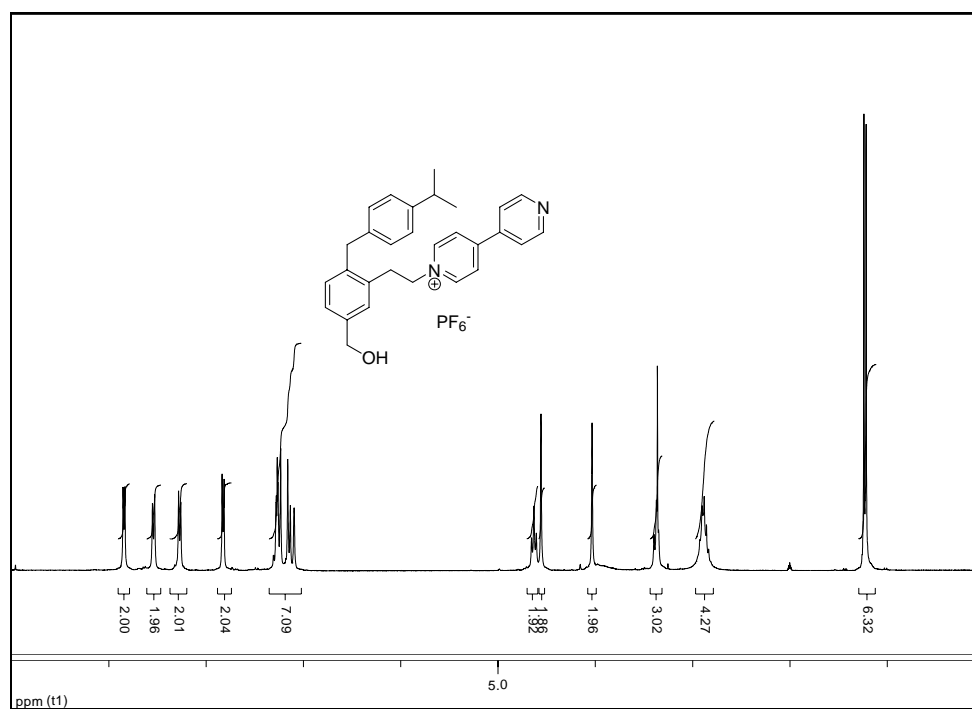
Compound 5.1b

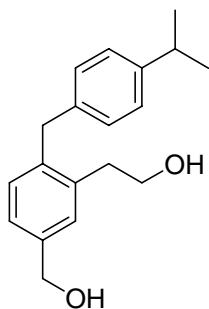
Methanesulfonic acid 2-[5-hydroxymethyl-2-(4-isopropylbenzyl)phenyl]ethyl ester (0.84 g, 2.32 mmol) and 4,4'-dipyridyl (2.9 g, 18.5 mmol) was stirred in acetonitrile (30 mL) at 65 °C for 5 days. Then the solvent was removed *in vacuo*. The residue was dissolved in methanol and NH_4PF_6^- (0.378 g, 2.32 mmol) in water (10 mL) was added to perform ion exchange. The methanol was removed and light yellow solid was obtained by filtration. The solid was recrystallized with methanol and water three times to give pure compound **5.1b** (1.0 g, 75 % yield).

^1H NMR (CD_3CN , 300 MHz): δ ppm 8.84 (d, J = 6.1 Hz, 2H), 8.54 (d, J = 6.7 Hz, 2H), 8.27 (d, J = 6.7 Hz, 2H), 7.83 (dd, J = 4.6, 1.6 Hz, 2H), 7.31-7.14 (m, 7H), 4.63 (t, J = 7.3 Hz, 2H), 4.56 (s, 2H), 4.03 (s, 2H), 3.32 (t, J = 7.3 Hz, 2H), 2.88 (m, 1H), 1.24 (d, J = 6.30 Hz, 6H).

^{13}C NMR (CD_3CN , 75 MHz): δ ppm 154.02, 151.06, 147.10, 144.86, 141.39, 140.89, 138.53, 138.33, 133.75, 131.27, 128.72, 128.58, 126.83, 126.33, 125.83, 122.04, 63.33, 61.65, 49.14, 37.79, 33.83, 33.48, 23.49.

MS (ESI): m/z 423.18 (M^+) ($\text{M}^+ = \text{C}_{29}\text{H}_{31}\text{N}_2\text{O}^+$ requires 423.24).





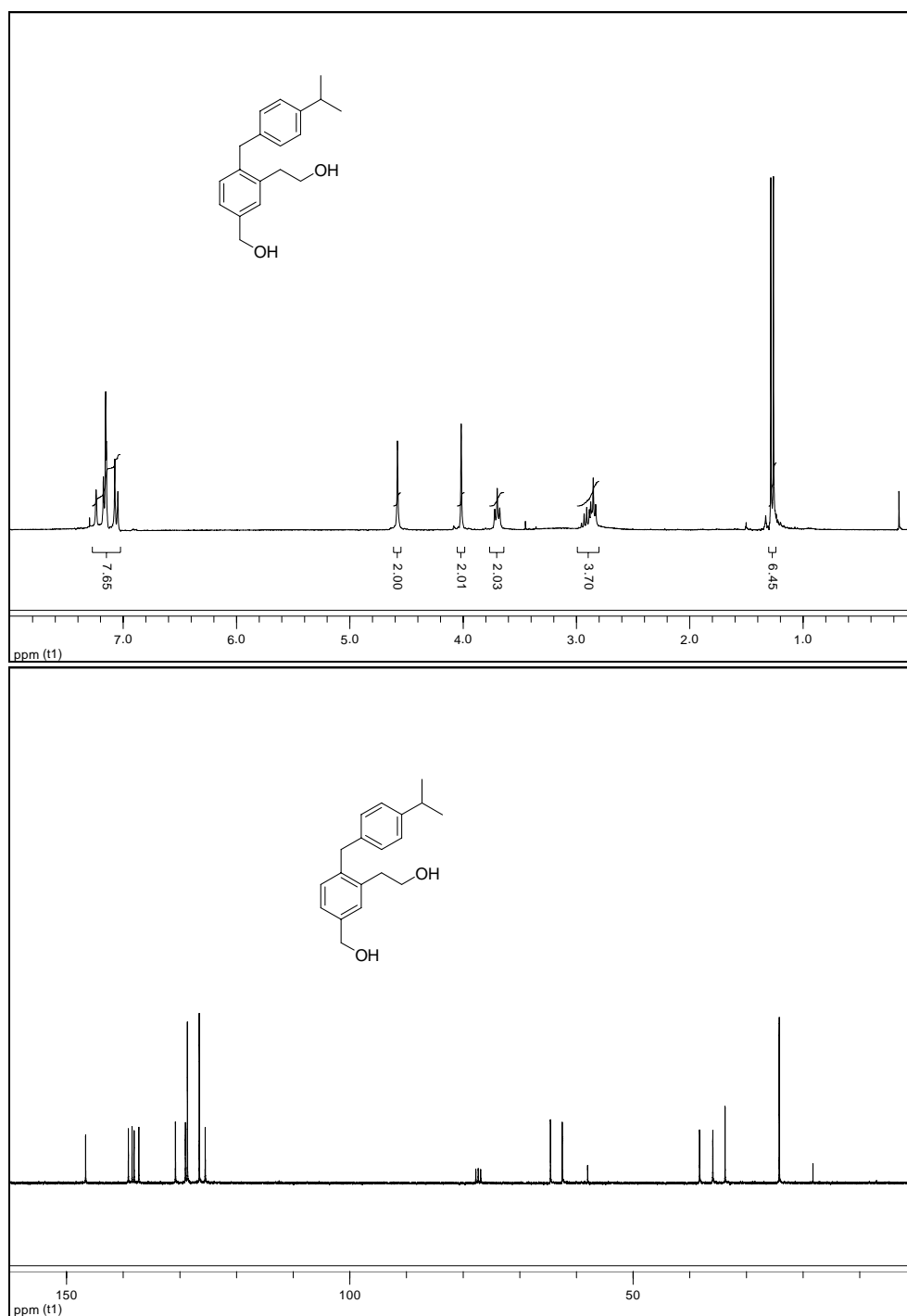
2-[5-Hydroxymethyl-2-(4-isopropylbenzyl)phenyl]ethanol (5.25)

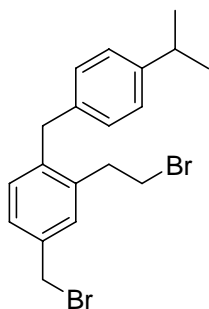
2-[2-(4-Isopropylbenzyl)-5-(tetrahydropyran-2-yloxymethyl)phenyl]ethanol (0.095 g, 0.26 mmol), and TsOH (15 mg) were dissolved in methanol (10 mL) and stirred for 4 h.⁶⁰ The reaction mixture was diluted with water and extracted with CH₂Cl₂ (3 × 10 mL). The organic layer was treated with saturated NaHCO₃ (3 × 10 mL) and washed with water (3 × 10 mL). The organic portion was dried (MgSO₄) and concentrated *in vacuo* to give the colorless oil (0.071 g, 97 %).

¹H NMR (CDCl₃, 300 MHz): δ ppm 7.28-7.01 (m, 7H), 4.58 (s, 2H), 4.02 (s, 2H), 3.70 (t, *J* = 6.6 Hz, 2H), 2.89 (m, 3H), 1.27 (d, *J* = 6.9 Hz, 6H).

¹³C NMR (CDCl₃, 75 MHz): δ ppm 146.63, 139.08, 138.43, 138.07, 137.24, 130.78, 129.02, 128.67, 126.57, 125.52, 64.59, 62.51, 38.27, 35.93, 33.77, 24.21.

MS (ESI): *m/z* 307.13 (M+Na⁺) (M=C₁₉H₂₄O₂ requires 284.18).





2-(2-Bromoethyl)-4-bromomethyl-1-(4-isopropylbenzyl)benzene (5.26)

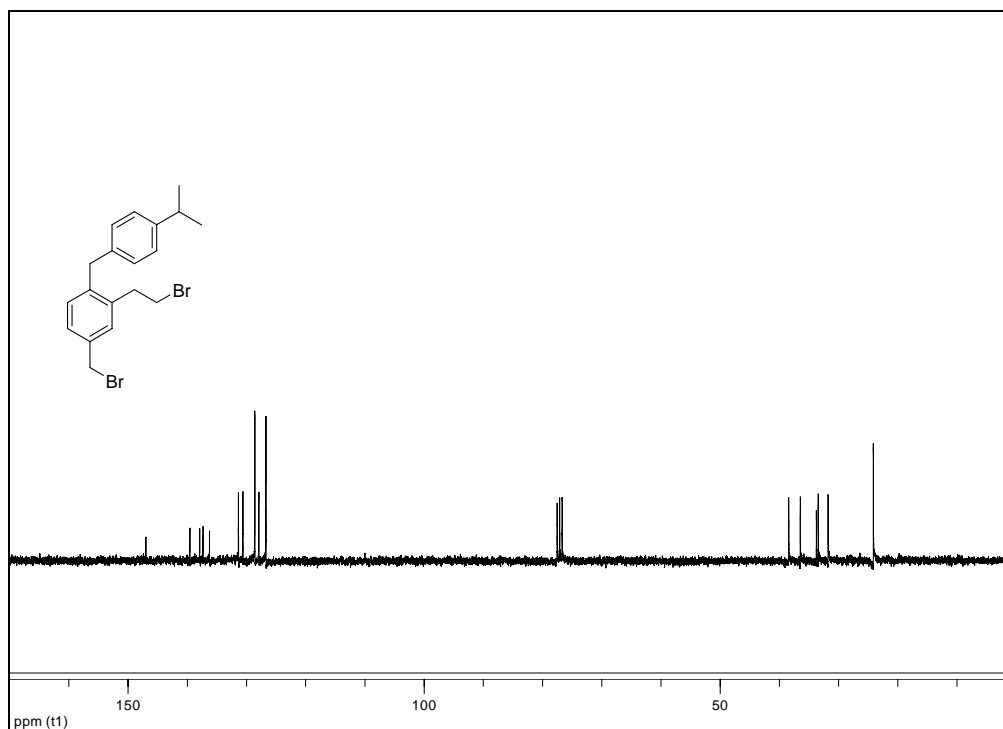
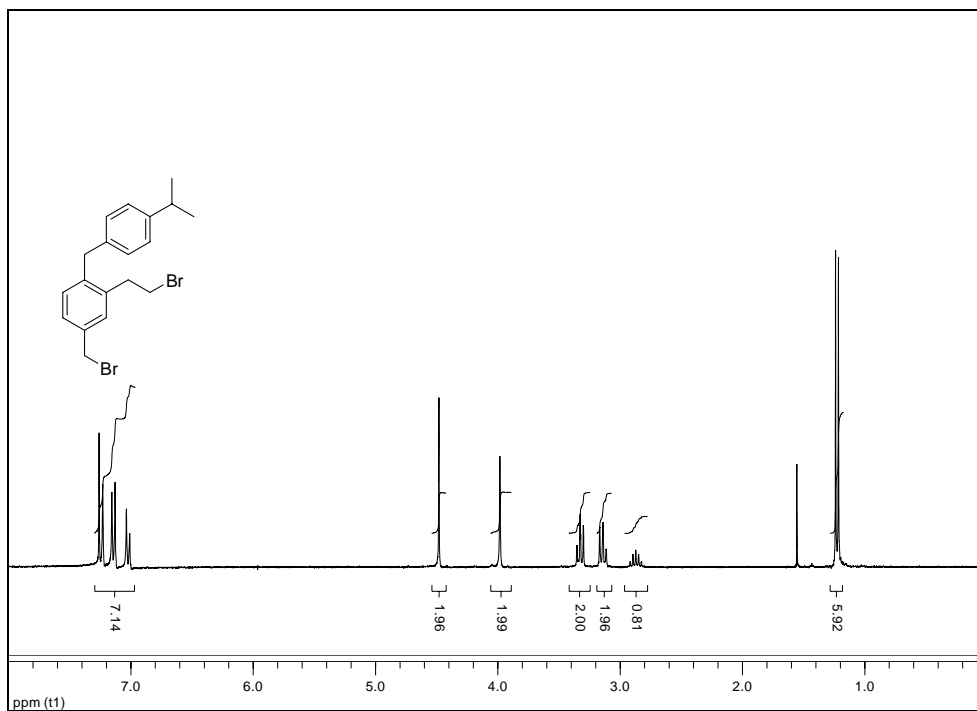
To a 100 mL flask was added PPh_3 (5.7 g, 21.84 mmol) followed by acetonitrile (20 mL). The mixture was cooled down to 0 °C and Br_2 (3.5 g, 21.84 mmol) in acetonitrile (10 mL) was added dropwise in 30 min until the solution maintained yellow. The solution was allowed to warm to room temperature. 2-[5-Hydroxymethyl-2-(4-isopropylbenzyl)phenyl]ethanol (2.7 g, 9.49 mmol) was added and minimum amount of acetonitrile (1 mL) was used to rinse the residue and added to the flask. The reaction mixture was stirred at room temperature overnight. Then the reaction mixture was filtered and the liquid was concentrated *in vacuo* to give a brown oil. The liquid was concentrated *in vacuo* to give the crude product. The crude product was purified with column chromatography [SiO_2 – petroleum ether – CH_2Cl_2 (1:1), v/v] to give the pure compound (3.2 g, 82 %).

^1H NMR (CDCl_3 , 300 MHz): δ ppm 7.30-6.97 (m, 7H), 4.48 (s, 2H), 3.98 (s, 2H), 3.33 (t, $J=8.1$ Hz, 2H), 3.13 (t, $J=8.1$ Hz, 1H), 2.96-2.78 (m, 1H), 1.21 (d, $J=6.9$ Hz, 6H).

^{13}C NMR (CDCl_3 , 75 MHz): δ ppm 146.99, 139.56, 137.90, 137.34, 136.24, 131.35,

130.60, 128.58, 127.90, 126.70, 38.41, 36.45, 33.73, 33.42, 31.76, 24.11.

MS (EI+GC): 407.8 (M), 409.9 (M+2), 411.7 (M+4) (M= C₁₉H₂₂Br₂ requires 408.01).



References

1. Credi, A. *J. Phys.: Condens. Matter* **2006**, *18*(33), S1779-S1795.
2. a) Flood, A. H.; Ramirez, R. J. A.; Deng, W.; Muller, R. P.; Goddard, W. A., III; Stoddart, J. F. *Aust. J. Chem.* **2004**, *57*(4), 301-322. b) Balzani, V.; Credi, A.; Ferrer, B.; Silvi, S.; Venturi, M. Artificial Molecular Motors and Machines: Design Principles and Prototype Systems. In *Molecular Machines*, Ed. Kelly T.R.; Springer publishers, 2005; pp 1-27.
3. a) http://nobelprize.org/nobel_prizes/chemistry/laureates/1997/press.html b) Feynman, R. P. in *Miniaturization* ; Gilbert, H. D. Ed.; Reinhold: New York, 1961; Chapter 16, pp 282-296.
4. Hernandez J. V; Kay E. R; Leigh D. A. *Science*, **2004**, *306*(5701), 1532-7.
5. Mandl, C. P.; Koenig, B. *Angew. Chem. Int.Ed.* **2004**, *43*(13), 1622-1624.
6. Mavroidis, C.; Dubey, A.; Yarmush, M. L. *Ann. Rev. Biomed. Eng.* **2004**, *6*, 363-395.
7. http://en.wikipedia.org/wiki/Image:Atpsynthase_nobelfoundation.jpg; This copyrighted image has been released by a company or organization.
8. Balzani, V.; Credi, A.; Raymo, F. M.; Stoddart, J. F. *Angew. Chem. Int.Ed.* **2000**, *39*(19), 3348-3391.
9. Kelly, T.R.; Silva D. H.; Silva R. A. *Nature*, **1999**, *401*, 150-152.

10. Kelly, T. R. *Acc. Chem. Res.* **2001**, *34*, 514-522.
11. Kelly, T. R.; Cai, X.; Damkaci, F.; Panicker, S. B.; Tu, B.; Bushell, S. M.; Cornella, I.; Piggott, M. J.; Salives, R.; Caverio, M.; Zhao, Y.; Jasmin, S. *J. Am. Chem. Soc.* **2007**, *129*(2), 376-386.
12. Koimura N.; Zijlstra R. W. J.; Van Delden R. A.; Harada N.; Feringa B. L. *Nature*, **1999**, *401*, 152-155.
13. a) Koumura, N.; Geertsema, E. M.; Meetsma, A.; Feringa, B.L. *J. Am. Chem. Soc.* **2000**, *122*, 12005-12006. b) Koumura, N.; Geertsema, E. M.; van Gelder, M. B.; Meesma, A.; Feringa, B. L. *J. Am. Chem. Soc.* **2002**, *124*, 5037-5051. c) Van Delden R. A.; Koumura N.; Schoevaars A.; Meetsma A.; Feringa B. L. *Org. Biomol. Chem.* **2003**, *1*(1), 33-5 d) Van Delden, R. A.; Hurenkamp, J. H.; Feringa, B. L. *Chem. Eur. J.* **2003**, *9*(12), 2845-2853. d) Feringa, B. L.; Van Delden, R. A.; Ter Wiel, M. K. J. *Pure Appl. Chem.* **2003**, *75*(5), 563-575.
14. Ter Wiel, M. K. J.; van Delden, R. A.; Meetsma, A.; Feringa, B. L. *J. Am. Chem. Soc.* **2003**, *125*, 15076-15086.
15. Eelkema, R.; Pollard, M. M.; Vicario, J.; Katsonis, N.; Serrano Ramon, B.; Bastiaansen, C. W. M.; Broer, D. J.; Feringa, B. L. *Nature* 2006, *440*, 163.
16. Leigh, D. A.; Wong, J. K. Y.; Dehez, F.; Zerbetto, F. *Nature* **2003**, *424*(6945), 174-179.

17. Hernandez J. V; Kay E. R; Leigh D. A. *Science*, **2004**, 306(5701), 1532-7.
18. Sauvage, J.-P; Dietrich-Buchecker, C. (ed.) *Catenane, Rotaxanes, and Knots*; Wiley-VCH publishers: Weinheim, 1999.
19. Arico, F.; Badjic, J. D.; Cantrill, S. J.; Flood, A. H.; Leung, K. C.-F.; Liu, Y.; Stoddart, J. F. Templated synthesis of interlocked molecules. In *Templates in Chemistry II*, Ed. Schalley C. A.; Vogtle F.; Dotz K. H., Springer publishers, 2005; pp 203-259.
20. a) Bonnet, S.; Collin, J. P.; Koizumi, M.; Mobian, P.; Sauvage, J. P. *Adv. Mater.* **2006**, 18(10), 1239-1250. b) Sauvage, J.-P. *Acc. Chem. Res.* **1998**, 31, 611-619. c) Sauvage, J.-P. *Acc. Chem. Res.* **1990**, 23, 319-327.
21. a) Kay, E. R.; Leigh, D. A. Hydrogen Bond-assembled Synthetic Molecular Motors and Machines. In *Templates in Chemistry II*, Ed. Schalley C. A.; Vogtle F.; Dotz K. H., Springer publishers, 2005; 133-177. b) Leigh, D. A.; Venturini, A.; Wilson, A. J.; Wong, J. K. Y.; Zerbetto, F. *Chem. Eur. J.* **2004**, 10(20), 4960-4969. c) Leigh, D. A.; Lusby, P. J.; Slawin, A. M. Z.; Walker, D. B. *Angew. Chem. Inter. Ed.* **2005**, 44(29), 4557-4564.
22. Raymo, F. M.; Stoddart, J. F. Templated Synthesis of Catenanes and Rotaxanes. In *Templated Organic Synthesis* Eds. Diederich, F.; Stang, P. J. ; Wiley-VCH Publishers, 2000: Weinheim, Germany; pp 75-104.

23. Dietrich-Buchecker, C. O.; Sauvage, J. P.; Kintzinger, J. P. *Tetrahedron Lett.* **1983**, 24(46), 5095-8.
24. Hunter, C. A. *J. Am. Chem. Soc.* **1992**, 114, 5303-11.
25. Johnston, A. G.; Leigh, D. A.; Murphy, A.; Smart, J. P.; Deegan, M. D. *J. Am. Chem. Soc.* **1996**, 118, 10662-10663.
26. a) Lane, A. S.; Leigh, D. A.; Murphy, A. *J. Am. Chem. Soc.* **1997**, 119, 11092-11093.
b) Leigh, D. A.; Murphy, A.; Smart, J. P.; Slawin, A. M. Z. *Angew. Chem., Int. Ed.* **1997**, 36, 728-732.
27. Gatti, F. G.; Leigh, D. A.; Nepogodiev, S. A.; Slawin, A. M. Z.; Teat, S. J.; Wong, J. K. Y. *J. Am. Chem. Soc.* **2001**, 123, 5983-5989.
28. Raehm, L.; Hamilton, D. G.; Sanders, J. K. M. *Synlett* **2002**, 11, 1743-1761.
29. Odell, B.; Reddington, M. V.; Slawin, A. M. Z.; Spencer, N.; Stoddart, J. F.; Williams, D. J. *Angew. Chem.* **1988**, 100, 1605-1608.
30. D'Acerno, C.; Doddi, G.; Ercolani, G.; Mencarelli, P. *Chem. Eur. J.* **2000**, 6(19), 3540-3546.
31. Stoddart, J. F.; Williams, D. J.; Amabilino, D. B.; Anelli, P.-L.; Ashton, P. R.; Brown, G. R.; Cordova, E.; Godinez, L. A.; Hayes, W. *J. Am. Chem. Soc.* **1995**, 117(45), 11142-70.
32. Martyn D. E. Ph.D dissertation, University of Oklahoma, Norman, 2006.

33. a) Halterman, R. L.; Martyn, D. E.; Pan, X.; Ha, D. B.; Frow, M.; Haessig, K. *Org. Lett.* **2006**, 8, 2119-2121. b) Halterman, R. L.; Martyn, D. E.; Pan, X. *Abstr 230th ACS Meeting 2005*, ORGN-307.
34. Brockmann, H.; Kluge, F.; Muxfeldt, H. *Chem. Ber.* **1957**, 90, 2302-18.
35. Gribble, G. W.; Leese, R. M.; Evans, B. E.; *Synthesis*, **1977**, 61, 172-176.
36. Punna, S.; Meunier, S.; Finn, M. G; *Org. Lett.* **2004**, 6, 2777-2779.
37. Muller, W.; Lowe, D. A.; Neijt, H.; Urwyler, S.; Herrling, P. L.; Blaser, D; Seebach, D. *Helv. Chim. Acta* **1992**, 75, 855-864.
38. Friebolin, H. Dynamic NMR Spectroscopy. In Basic One- and Two-Dimensional NMR Spectroscopy; Wiley-VCH publishers: Weinheim, 2005; pp 305-329.
39. Ashton, P. R.; Boyd, S. E.; Menzer, S.; Pasini, D.; Raymo, F. M.; Spencer, N.; Stoddart, J. F.; White, A. J. P.; Williams, D. J.; Wyatt, P. G. *Chem. Eur. J.* **1998**, 4(2), 299-310.
40. Amabilino, D. B.; Ashton, P. R.; Perez-Garcia, L.; Stoddart, J. F. *Angew. Chem. Inter. Ed.* **1995**, 34(21), 2378-80.
41. Hamilton, D. G.; Davies, J. E.; Prodi, L.; Sanders, J. K. M. *Chem. Eur. J.* **1998**, 4(4), 608-620.
42. Steinberg, H.; Cram, D. J. *J. Am. Chem. Soc.* **1952**, 74, 5388-5391.
43. Staab, H. A.; Ruland, A.; Kuo-chen, C. *Chem. Ber.* **1982**, 115, 1755-1764.

44. Stuhr-Hansen, N.; Sorensen, J. K.; Moth-Poulsen, K.; Christensen, J. B.; Bjornholm, T.; Nielsen, M. B. *Tetrahedron* **2005**, *61*(52), 12288-12295.
45. Chen, L. S.; Chen, G. J.; Tamborski, C. J. *J. Organomet. Chem.* **1980**, *193*(3), 283-92.
46. Ashton, P. R.; Baldoni, V.; Balzani, V.; Claessens, C. G.; Credi, A.; Hoffmann, H. D. A.; Raymo, F. M. ; Stoddart, J. F.; Venturi, M.; White, A. J. P.; Williams, D. J. *Eur. J. Org. Chem.* **2000**, 1121-1130.
47. Halterman R. L., Pan X., Martyn D. E., Moore J. L., Long A. *accepted*.
48. Forbus, T. R., Jr.; Taylor, S. L.; Martin, J. C. *J. Org. Chem.* **1987**, *52*(19), 4156-9.
49. Miyaura, N.; Suzuki, A. *Chem. Rev.* **1995**, *95*(7), 2457-83.
50. Feulner, H.; Linti, G.; Noeth, H. *Chem. Ber.* **1990**, *123*(9), 1841-3.
51. a) Givens, R. S.; Venkatramanan, M. K.; Figard, J. *Tetrahedron Lett.* **1984**, *25*(21), 2187-90. b) Gruetzmacher, H. F.; Husemann, W. *Tetrahedron* **1987**, *43*, 3205-11.
52. Corey, E. J.; Fuchs, P. L. *Tetrahedron Lett.* **1972**, *13*, 3769-3772.
53. Edens, M.; Boerner, D.; Chase C. R.; Nass D.; Schiavelli M. D. *J. Org. Chem.* **1977**, *42*, 3403.
54. Barrett, A. G. M.; Hopkins, B. T.; Love, A. C.; Tedeschi, L. *Org. Lett.* **2004**, *6*(5), 835-837.
55. Fleifel, A. M. *J. Org. Chem.* **1960**, *25*, 1024-5.
56. a) Curran, D. P.; Yang, F.; Cheong, J. *J. Am. Chem. Soc.* **2002**, *124*, 14993-15000. b)

- Sekine, M.; Aoyagi, M.; Ushioda, M.; Ohkubo, A.; Seio, K. *J. Org. Chem.* **2005**, *70*, 8400-8408.
57. Bumagin, N. A.; Luzikova, E. V. *J. Organomet. Chem.* **1997**, *532*, 271-273.
58. Kabalka, G. W.; Yu, S.; Li, N. *Tetrahedron Lett.* **1997**, *38*(31), 5455-5458.
59. Albrecht, S.; Defoin, A.; Tarnus, C. *Synthesis* **2006**, *10*, 1635-1638.
60. Bongini, A.; Cardillo, G.; Orena, M.; Sandri, S. *Synthesis* **1979**, *8*, 618-20.